

UNCLASSIFIED

AD NUMBER

ADB004736

LIMITATION CHANGES

TO:

Approved for public release; distribution is unlimited.

FROM:

Distribution authorized to U.S. Gov't. agencies only; Administrative/Operational Use; MAR 1975. Other requests shall be referred to Federal Aviation Administration, Supersonic Transport Office, 800 Independence Avenue, SW, Washington, DC 20590. This document contains export-controlled technical data.

AUTHORITY

faa ltr, 26 apr 1977

THIS PAGE IS UNCLASSIFIED

THIS REPORT HAS BEEN DELIMITED
AND CLEARED FOR PUBLIC RELEASE
UNDER DOD DIRECTIVE 5200.20 AND
NO RESTRICTIONS ARE IMPOSED UPON
ITS USE AND DISCLOSURE.

DISTRIBUTION STATEMENT A

APPROVED FOR PUBLIC RELEASE;
DISTRIBUTION UNLIMITED.

Report No. FAA-SS-73-11-9

**SST Technology
Follow-On Program—Phase II
NOISE SUPPRESSOR/NOZZLE DEVELOPMENT
VOLUME IX**

**PERFORMANCE TECHNOLOGY—ANALYSIS OF THE
LOW-SPEED PERFORMANCE OF MULTITUBE
SUPPRESSOR/EJECTOR NOZZLES (O-167 KN)**

D. B. Morden, R. S. Armstrong

**Boeing Commercial Airplane Company
P.O. Box 3707
Seattle, Washington 98124**



D6-42319

March 1975

FINAL REPORT

Task III

Approved for U.S. Government only. This document is exempted from public availability because of restrictions imposed by the Export Control Act. Transmittal of this document outside the U.S. Government must have prior approval of the Supersonic Transport Office.

**Prepared for
FEDERAL AVIATION ADMINISTRATION
Supersonic Transport Office
800 Independence Avenue, S.W.
Washington, D.C. 20590**



AD B 0 0 4 7 3 6

**AD No. _____
DDC FILE COPY**

The contents of this report reflect the views of the Boeing Commercial Airplane Company, which is responsible for the facts and the accuracy of the data presented herein. The contents do not necessarily reflect the official views or policy of the Department of Transportation. This report does not constitute a standard, specification, or regulation.

EXHIBIT NO.	
FILE	DATE RECD <input type="checkbox"/>
DATE	DATE DUE <input checked="" type="checkbox"/>
APPROVALS	<input type="checkbox"/>
REMARKS	
BY	
SIGNATURE/INITIALS	
DATE	
REV. DATE	
13	

TECHNICAL REPORT STANDARD TITLE PAGE

18 19 1. Report Number FAA-SS-73-11-9 6	2. Government Accession No.	3. Recipient's Catalog No. 12 143 p.	
4. Title and Subtitle SST Technology Follow-On Program—Phase II. Noise Suppressor/Nozzle Development, Volume IX. Performance Technology—Analysis of the Low Speed Performance of Multitube Suppressor/Ejector Nozzles (0-167 kn).		5. Date Mar 75	6. Performing Organization Code
7. Author(s) D. B. Morden R. S. Armstrong		8. Performing Organization Report No. D6-42319	10. Work Unit No.
9. Performing Organization Name and Address Boeing Commercial Airplane Company P.O. Box 3707 Seattle, Washington 98124		11. Contract or Grant No. DOT-FA-72WA-2893	
12. Sponsoring Agency Name and Address Federal Aviation Administration Supersonic Transport Office 800 Independence Avenue S.W. Washington, D.C. 20590		13. Type of Report and Period Covered Final Report Task III	
15. Supplementary Notes S. Blatt, DOT/SST Technical Monitor			
16. Abstract The effects of geometric variables on the performance of multitube suppressor/ejector nozzles are described and quantified for static and low forward velocity cases. The bulk of the investigation concentrates on configurations compatible with supersonic transport engine exhaust systems. Experimental results are presented for 28 related, model-scale suppressor/ejector configurations tested at nozzle pressure ratios from 2 to 4 over a range of velocities from 0 to 167 kn. High static performance and minimum lapse rate are shown to be compatible through the proper selection of suppressor/ejector geometry and the optimum ejector inlet area.			
17. Key Words Suppressor nozzle Forward velocity effects Multitube suppressor/ejector Nozzle performance Base ventilation SST Ejector performance		18. Distribution Statement Approved for U.S. Government only. This document is exempted from public availability because of restrictions imposed by the Export Control Act. Transmittal of this document outside the U.S. Government must have prior approval of the Supersonic Transport Office.	
19. Security Classif. (of this report) Unclassified	20. Security Classif. (of this page) Unclassified	21. No. of Pages 143	22. Price

Form DOT F 1700 7 (8-69)

390 145 ✓

mt

PREFACE

This is one of a series of final reports on noise and propulsion technology submitted by the Boeing Commercial Airplane Company, Seattle, Washington, 98124, in fulfillment of Task III of Department of Transportation Contract DOT-FA-72WA-2893, dated 1 February 1972.

To benefit utilization of technical data developed by the noise suppressor and nozzle development program, the final report is divided into 10 volumes covering key technology areas and a summary of total program results. The 10 volumes are issued under the master title, "Noise Suppressor/Nozzle Development." Detailed volume breakdown is as follows:

		Report No.
Volume I	— Program Summary	FAA-SS-73-11-1
Volume II	— Noise Technology	FAA-SS-73-11-2
Volume III	— Noise Technology—Backup Data Report	FAA-SS-73-11-3
Volume IV	— Performance Technology Summary	FAA-SS-73-11-4
Volume V	— Performance Technology—The Effect of Initial Jet Conditions on a 2-D Constant Area Ejector	FAA-SS-73-11-5
Volume VI	— Performance Technology—Thrust and Flow Characteristics of a Reference Multitube Nozzle With Ejector	FAA-SS-73-11-6
Volume VII	— Performance Technology—A Guide to Multitube Suppressor Nozzle Static Performance: Trends and Trades	FAA-SS-73-11-7
Volume VIII	— Performance Technology—Multitube Suppressor/Ejector Interaction Effects on Static Performance (Ambient and 1150° F Jet Temperature)	FAA-SS-73-11-8
Volume IX	— Performance Technology—Analysis of the Low-Speed Performance of Multitube Suppressor/Ejector Nozzles (0-167 kn)	FAA-SS-73-11-9
Volume X	— Advanced Suppressor Concepts and Full-Scale Tests	FAA-SS-73-11-10

This report is volume IX of the series and was prepared by the Propulsion Research Staff of the Boeing Commercial Airplane Company.

FOREWORD

This document extends the investigation of bare multitube suppressor performance¹ and suppressor/ejector interaction effects² to include the effects of low forward velocity on the performance of these exhaust systems. The noise suppression characteristics of the same hardware are presented in reference 3. The work was accomplished under Task III of the DOT/SST Follow-On Technology Phase II Contract Number DOT-FA72WA-2893.

TABLE OF CONTENTS

	Page
1.0 SUMMARY.....	1
1.1 Introduction	1
1.2 Results	1
1.3 Summary of Findings	1
2.0 INTRODUCTION.....	7
3.0 PARAMETERS AND DEFINITIONS.....	11
3.1 Range of Variables	11
3.1.1 Flow Variables	11
3.1.2 Suppressor and Ejector Variables.....	11
3.2 Constraints	12
3.2.1 Suppressor Constraints	12
3.2.2 Ejector Constraints	12
3.3 Definitions for Nozzle Area Ratio, Ejector Area Ratio, and Setback.....	12
3.3.1 Nozzle Area Ratio (NAR).....	14
3.3.2 Effective Nozzle Area Ratio	14
3.3.3 Ejector Area Ratio (EAR).....	14
3.3.4 Effective Ejector Area Ratio.....	14
3.3.5 Setback.....	14
4.0 TEST DESCRIPTION.....	15
4.1 Facility Description and Data Acquisition.....	15
4.2 Description of Nozzles	15
4.2.1 General	15
4.2.2 Round Convergent Reference Nozzle (R/C)	20
4.2.3 Suppressor Ramp Shapes.....	20
4.2.3.1 Elliptical Ramp.....	20
4.2.3.2 Circular Arc Ramp	20
4.2.3.3 Contoured Ramp.....	23
4.2.4 Tube Length	23
4.2.5 Close-Packed Arrays (Four) with Elliptical Ramps and Tubes: 19-, 37-, and 61-Tubes	24
4.2.6 R/37: 37-Tube, NAR-3.3 Suppressor with Contoured Ramp	24
4.2.7 37-Tube, NAR-3.3, Close-Packed Array with Elliptical Ramp and R/C Tubes	24
4.2.8 Radial Array Suppressors	24
4.2.9 Summary of Suppressor Specifications	30
4.3 Ejectors.....	30
4.3.1 General	30
4.3.2 Summary of Ejector Specifications.....	32

CONTENTS—Continued

	Page
5.0 EXPERIMENTAL PERFORMANCE RESULTS.....	35
5.1 Introduction	35
5.2 List of Performance Curves.....	36
5.3 Summary Curves for Performance as a Function of Pressure Ratio and Velocity	37
6.0 ANALYSIS.....	73
6.1 Introduction	73
6.2 The Pressure Ratio Dependence on Forward Velocity Effect	73
6.2.1 Bare Suppressor Performance	73
6.2.2 Suppressor/Ejector Performance	73
6.2.2.1 Preamble	73
6.2.2.2 Ejector Lip Suction.....	75
6.2.2.3 Suppressor Afterbody Drag.....	75
6.2.2.4 Ejector Drag	75
6.2.2.5 Ram Drag Penalty	75
6.2.2.6 Resulting Performance	75
6.2.2.7 Crossover Velocity	77
6.2.2.8 Behavior of Restricted Inlets.....	77
6.3 Forward Velocity Effects (Constant Pressure Ratio).....	83
6.3.1 Introduction	83
6.3.2 Ideal Thrust.....	83
6.3.3 Discharge Coefficient	83
6.3.4 Bare Suppressor Performance	84
6.3.5 Suppressor/Ejector Performance: An Example Suppressor with Various Area Ratio Ejectors	87
6.3.5.1 Base Drag	87
6.3.5.2 Ramp Drag	89
6.3.5.3 Afterbody Drag.....	89
6.3.5.4 Ejector Lip Suction.....	89
6.3.5.5 Gross Thrust Coefficient	92
6.3.6 Suppressor Geometry Effects	95
6.3.6.1 Nozzle Area Ratio.....	95
6.3.6.2 Ramp Shape	97
6.3.6.3 Tube Number	101
6.3.6.4 Tube Shape.....	104
6.3.6.5 Tube Length	104
6.3.6.6 Tube Array	104
6.3.7 Ejector Geometry Effects	104
6.3.7.1 Ejector Drag	104
6.3.7.1.1 Pressure Drag.....	104
6.3.7.1.2 Skin Friction Losses	109

CONTENTS—Continued

	Page
6.3.7.2 Secondary Air Handling	109
6.3.7.3 Inlet Flow Model	111
6.3.7.4 Inlet Geometry	114
6.3.7.5 Ejector Length and Area Ratio	122
6.3.8 Temperature Effects on Performance	123
7.0 CONCLUSIONS AND RECOMMENDATIONS	127
REFERENCES	129

FIGURES

No.		Page
1	Effect of Velocity on the Performance of Suppressors Without Ejectors.	2
2	Comparison of Performance and Lapse Rate and Crossover Velocity for 37-Tube, NAR-3.3 Close-Packed Array, Bare and With EAR-3.7 Ejector	4
3	Effect of Ejector Inlet Area on the Performance of Suppressor/Ejectors.	5
4	General Behavior of Bare Suppressor Performance as a Function of Pressure Ratio and Velocity	6
5	Application of Stowable Suppressor to an Advanced SST Exhaust System.	8
6	Suppressor/Ejector-Schematic	11
7	Definition of Suppressor and Ejector Area Ratio	13
8	Test Installation	16
9	Forward Velocity Effects-9- by 9-ft Wind Tunnel Test	17
10	Oil Flow on Forebody and Boundary Layer Suction.	18
11	Temperature and Pressure Profile at Charging Station.	19
12	Round-Convergent Reference Nozzle	20
13	Elliptical Ramps	21
14	37-Tube, NAR-3.3, Close-Packed Array With Circular Arc Ramp; EAR = 3.1 and SB/D _{eq} = 0.25	22
15	Contoured Ramp.	23
16	19- and 61-Tube Area-Ratio-3.3 Suppressors.	25
17	37-Tube, Close-Packed Suppressors NAR = 2.75 and 3.3	26
18	Comparison of 37-Tube, Area-Ratio-3.3 Nozzles.	27
19	37-Tube, Area-Ratio-3.3, Close-Packed Arrays With Various Ramps and Tube Shapes.	28
20	Radial Array Nozzles.	29
21	Area Ratio 2.6 and 3.1 Flight Lip Ejectors	31
22	View of Ejector Inlet: 19-Tube, NAR-3.3, Close-Packed Array With Elliptical Ramp; EAR 3.1 Ejector, Zero Setback.	32
23	Ejector Dimension Definition Sketch	32
24	Area Ratio (EAR) 3.7 Flight Ejectors L _E /D _{eq} = 2 and 6	33
25	General Form of Performance Carpet Plots for Bare Suppressors	35
26	General Form of Carpet Plots for Suppressor/Ejector Performance.	36
27	Gross Thrust Coefficient for the Round Convergent Reference Nozzle, No Ejector.	38
28	Gross Thrust Coefficient for 19-Tube, NAR = 3.3, Close-Packed Array Without Ejector.	39
29	Gross Thrust Coefficient for 19-Tube, NAR = 3.3, Close-Packed Array With EAR = 3.1 Ejector (Setback 0.25)	40
30	Gross Thrust Coefficient for 19-Tube, NAR = 3.3, Close-Packed Array With EAR = 3.7 Ejector	41
31	Gross Thrust Coefficient for 19-Tube, NAR = 3.3, Close-Packed Array With EAR = 3.7 Ejector (Setback 0.25)	42

FIGURES—Continued

No.		Page
32	Gross Thrust Coefficient for 37-Tube, NAR = 2.75, Close-Packed Array With EAR = 2.6 Ejector (Setback 0.25)	43
33	Gross Thrust Coefficient for 37-Tube, NAR = 2.75, Close-Packed Array With EAR = 3.1 Ejector	44
34	Gross Thrust Coefficient for 37-Tube, NAR = 2.75, Close-Packed Array With EAR = 3.1 Ejector (Setback 0.25)	45
35	Gross Thrust Coefficient for 37-Tube, NAR = 2.75, Close-Packed Array With EAR = 3.7 Ejector	46
36	Gross Thrust Coefficient for 37-Tube, NAR = 2.75, Close-Packed Array With EAR = 3.7 Ejector (Setback 0.25)	47
37	Gross Thrust Coefficient for 37-Tube, NAR = 2.75, Close-Packed Array With EAR = 3.7 Ejector ($L_T/D_{eq} = 6.0$)	48
38	Gross Thrust Coefficient for 37-Tube, NAR = 3.3, Close-Packed Array Without Ejector.	49
39	Gross Thrust Coefficient for 37-Tube, NAR = 3.3, Close-Packed Array With EAR = 3.1 Ejector	50
40	Gross Thrust Coefficient for 37-Tube, NAR = 3.3, Close-Packed Array With EAR = 3.1 Ejector (Setback 0.25)	51
41	Gross Thrust Coefficient for 37-Tube, NAR = 3.3, Close-Packed Array, With EAR = 3.7 Ejector	52
42	Gross Thrust Coefficient for 37-Tube, NAR = 3.3, Close-Packed Array ($L_T/D_{eq} = 0.75$) With EAR = 3.1 Ejector	53
43	Gross Thrust Coefficient for 37-Tube, NAR = 3.3, Close-Packed Array ($L_T/D_{eq} = 0.75$) With EAR = 3.1 Ejector (Setback 0.125)	54
44	Gross Thrust Coefficient for 37-Tube, NAR = 3.3, Close-Packed Array ($L_T/D_{eq} = 0.75$) With EAR = 3.1 Ejector (Setback 0.250)	55
45	Gross Thrust Coefficient for 37-Tube, NAR = 3.3, Close-Packed Array, Circular Arc Ramp Without Ejector	56
46	Gross Thrust Coefficient for 37-Tube, NAR = 3.3, Close-Packed Array, Circular Arc Ramp With EAR = 3.1 Ejector (Setback 0.25)	57
47	Gross Thrust Coefficient for 37-Tube, NAR = 3.3, Close-Packed Array With $L_T/D_{eq} = 0.75$ Round Convergent Tubes Without Ejector	58
48	Gross Thrust Coefficient for 37-Tube, NAR = 3.3, Close-Packed Array With $L_T/D_{eq} = 0.75$, Round Convergent Tubes With EAR = 3.1 Ejector (Zero and 0.25 Setback)	59
49	Gross Thrust Coefficient for 37-Tube, NAR = 3.3, Close-Packed Array: Round Convergent Tubes, Contoured Ramp With EAR = 3.1 Ejector	60
50	Gross Thrust Coefficient for 37-Tube, NAR = 3.3, Close-Packed Array: Round Convergent Tubes, Contoured Ramp With EAR = 3.7 Ejector	61
51	Gross Thrust Coefficient for 61-Tube, NAR = 3.3, Close-Packed Array Without Ejector.	62
52	Gross Thrust Coefficient for 61-Tube, NAR = 3.3, Close-Packed Array With EAR = 3.1 Ejectors	63

FIGURES—Continued

No.		Page
53	Gross Thrust Coefficient for 61-Tube, NAR = 3.3, Close-Packed Array With EAR = 3.1 Ejector (Setback 0.25).....	64
54	Gross Thrust Coefficient for 31-Tube, NAR = 2.75 Radial Array Without Ejector.....	65
55	Gross Thrust Coefficient for 31-Tube, NAR = 2.75 Radial Array With EAR = 2.6 Ejector.....	66
56	Gross Thrust Coefficient for 31-Tube, NAR = 2.75 Radial Array With EAR = 2.6 Ejector (Setback 0.25).....	67
57	Gross Thrust Coefficient for 31-Tube, NAR = 2.75 Radial Array With EAR = 3.1 Ejector.....	68
58	Gross Thrust Coefficient for 31-Tube, NAR = 2.75 Radial Array With EAR = 3.1 Ejector (Setback 0.25).....	69
59	Gross Thrust Coefficient for 31-Tube, NAR = 2.75 Radial Array With EAR = 3.7 Ejector.....	70
60	Gross Thrust Coefficient for 31-Tube, NAR = 2.75 Radial Array ($L_T/D_{eq} = 0.75$) With EAR = 3.1 Ejector.....	71
61	General Behavior of Bare Suppressor Performance as a Function of Pressure Ratio and Velocity.....	74
62	Ejector Inlet Area A_A and A_S	76
63	Comparison of Performance and Lapse Rate and Crossover Velocity for 37-Tube, NAR-3.3, Close-Packed Array, Bare and With EAR 3.7 Ejector.....	78
64	37-Tube, NAR = 3.3, Close-Packed EAR = 3.1 Ejector With Zero Setback.....	80
65	Performance Carpets for Different Setbacks of the EAR 3.1 Ejector on a 37-Tube, NAR-3.3, Close-Packed Array With Tube Length Equal $0.5 D_{eq}$	81
66	Schematic of Performance Versus Setback.....	82
67	Effect of Velocity on the Performance of Suppressors Without Ejectors.....	85
68	Effect of Velocity on Base Drag as a Percentage of Ideal Thrust for NAR-3.3 Suppressor With Various Numbers of Tubes (No Ejectors).....	86
69	Base Drag as a Percentage of Ideal Thrust for Various Ejectors on the 31-Tube, NAR-2.75 Radial Array Suppressor.....	88
70	Afterbody Drag Versus Velocity for a 31-Tube, NAR = 2.75, Radial Array With Various Ejectors.....	90
71	Lip Suction Versus Velocity for 31-Tube, NAR = 2.75 Radial Array With Various Ejectors.....	91
72	Effect of Ejector Area Ratio on Performance at Forward Velocity.....	93
73	Effect of Velocity on the Performance of Constant Suppressor With Various Ejectors.....	94
74	Effect of Suppressor Nozzle Area Ratio on Performance With Forward Velocity.....	96
75	Ramp Shapes.....	97
76	Superposition of Circular Arc and Elliptical Ramps on a 37-Tube, NAR-3.3 Suppressor With EAR 3.1 Ejector (Zero Setback).....	98
77	Effect of Ramp Shape on Performance With Forward Velocity.....	99

FIGURES--Continued

No.		Page
78	Ramp Drag as a Percentage of Ideal Thrust Versus Velocity for the 31-Tube, NAR-2.75 Radial Array With Various Ejectors	100
79	Base and Afterbody Drags as a Function of Velocity for the 61-Tube, NAR-3.3, Close-Packed Suppressor With and Without Ejector	102
80	Effect of Suppressor Tube Number on Performance With Forward Velocity . . .	103
81	Effect of Tube Shape on Performance With Forward Velocity	105
82	Effect of Tube Length on Performance With Forward Velocity	106
83	Effect of Tube Array on Performance With Velocity	107
84	Ejector Pressure Drag	108
85	Primary Weight Flow as a Function of Velocity (Constant $P_{Tp}/P_{T\infty}$).	109
86	$W_S \sqrt{T_{TS}/W_P} \sqrt{T_{Tp}}$ Versus Velocity, for Constant $P_{Tp}/P_{T\infty}$ *	110
87	Lip Suction Versus Velocity for Constant $P_{Tp}/P_{T\infty}$	110
88	Lip Force Versus Velocity for the 31-Tube, NAR-2.75 Radial Array With EAR 3.1 Ejector (Zero Setback).	111
89	Ejector Inlet Area A_A and A_S	112
90	Schematic for Suppressor/Ejector Inlet Flow Field.	113
91	Effect of Setback and Velocity on Performance (Other Parameters Constant) . .	115
92	Variation of Performance as a Function of Setback and Velocity for the 37-Tube, NAR-3.3, Close-Packed Array with EAR = 3.1 (EAR/NAR = 0.94). . .	116
93	Performance as a Function of Setback and Velocity for a 61-Tube, NAR-3.3 Suppressor With EAR = 3.1 Ejector (EAR/NAR = 0.94).	117
94	Performance as a Function of Setback and Velocity for the 37-Tube, NAR-2.75 Suppressor With EAR 3.1 Ejector (EAR/NAR = 1.12)	119
95	Performance as a Function of Setback and Velocity for the 19-Tube, NAR 3.3 Suppressor With EAR = 3.7 Ejector (EAR/NAR = 1.12).	120
96	Performance as a Function of Setback and Velocity for the 37-Tube, NAR 2.75 Suppressor With EAR 3.7 Ejector (EAR/NAR = 1.34)	121
97	C_{f_p} Versus Setback Showing Optimum Setback as a Function of Velocity	122
98	Effect of NAR and Ejector Length on Performance With Forward Velocity . . .	124
99	Lip Suction as a Function of Forward Velocity for Ambient and 1150° F Jet Temperatures.	126

SYMBOLS AND ABBREVIATIONS

A_p	Geometric flow area (in square inches) of primary nozzle, measured at 70°F
A_B	Suppressor base area in square inches: $A_p(AR + 1)$
A_{eff}	Effective suppressor exit area: $C_D \cdot A_p$
A_{PH}	Geometric flow area of the nozzle including temperature induced area growth
A_A	Minimum annular area between the ejector lip and the exits of the outer row tubes
A_S	Measured area, in square inches, between the tubes in the outer row of a suppressor
A_V	Total ventilation area. A_S + the calculated area between plumes of the jets in the outer row of a suppressor
BL	Boundary layer
C_D	Discharge coefficient, accounting for temperature induced nozzle area growth, calculated as follows:

$$C_D = \frac{A_{PH} \cdot PR \cdot P_{amb}}{\sqrt{T_{TP}}} \cdot \frac{WP}{\left[\frac{2\gamma}{R(\gamma-1)} \left(PR^{-2/\gamma} - PR^{-(\gamma+1/\gamma)} \right) \right]^{1/2}}$$

For this equation, if

$$PR \geq \left(\frac{\gamma+1}{2} \right)^{\gamma/\gamma-1} \quad \text{let} \quad PR = \left(\frac{\gamma+1}{2} \right)^{\gamma/\gamma-1}$$

C_f	Skin friction coefficient
C_{fg}	Gross thrust coefficient (measured suppressor and ejector thrust-drag) (in VIP_0)
C.P.	Close-packed—An arrangement of tubes with approximately the same distance between any two adjacent tubes
Crossover velocity	The forward velocity above which a suppressor/ejector configuration has a smaller C_{fg} than the same suppressor would have without an ejector
$C_{V_{int}}$	Nozzle internal velocity coefficient

SYMBOLS AND ABBREVIATIONS—Continued

D_{aft}	Afterbody drag: sum of the base-plate and ramp drags
D_B or D_{base}	Baseplate drag in pounds, calculated from static pressure measurements taken at area-weighted taps on the baseplate
D_B/FID	Baseplate drag expressed as a percentage of ideal thrust
D_{eq}	The exit diameter, in inches, of a single round convergent nozzle with area equal to the total effective flow area of a multitube nozzle
D_{ramp}	Drag in pounds calculated on the nozzle ramp using static pressure measured at area-weighted taps
EAR	Ejector area ratio: geometric area at ejector throat divided by A_p
Effective EAR	Geometric area of the ejector divided by $(C_D \cdot A_p)$
FID	Ideal thrust in pounds; measured primary mass flow rate multiplied by the ideal, fully expanded velocity in VIP
Lapse Rate	Rate of decrease in gross thrust coefficient with increasing velocity calculated using the values at the desired end points

$$C_{f_g} @ V_1 - C_{f_g} @ V_2$$

L_A	● Axial distance in inches between ejector throat and exit
L_B	Axial distance in inches from ejector hilite to ejector throat
L_E	Ejector length: distance in inches from the flightlip hilite to the ejector exit measured with zero setback
L_E/d	Ejector length divided by individual tube diameter
LIP	The absolute value of the lip suction force calculated from area-weighted static pressure on the lip
LIP/FID	The absolute value of the lip force expressed as a percentage of ideal thrust (FID)
L_T	Tube length measured on the outside of the tube: distance in inches from tube exit to the baseplate
\dot{m}	Measured mass flow rate: WP/g
N	Total number of tubes in a suppressor

SYMBOLS AND ABBREVIATIONS—Continued

NAR	Nozzle area ratio: area inside a circle circumscribed around the outside of the outermost tubes (where they meet baseplate), divided by A_p
Effective NAR	Area inside a circle tangent to the outside of the outer row jets, at the exit plane, divided by the effective flow area ($C_D \cdot A_p$)
P_{amb}	Ambient pressure
P_B	The average static pressure in PSIA obtained at area weighted taps on the nozzle baseplate
PR	Nozzle pressure ratio: P_{T0}/P_{amb}
psig	Gauge pressure: pounds per square inch of pressure above atmosphere
P_{T0} or P_{Tp}	The charging total pressure, i.e., total pressure PSIA at a station upstream of the tube entrances
q	Dynamic pressure = $1/2 \rho V^2$
R	Radius in inches of the inlet to a tube
Radial Array	An arrangement of tubes in radial lines to maximize ventilation
Re	Reynolds number
R_{ej}	Radius from the ejector centerline to the throat, in inches
R_p	Radius from the nozzle centerline to the outside of the outer tubes, in inches
R_H	Radius in inches from ejector centerline to the flightlip hilite
R_{in}	Radius in inches from the nozzle centerline to the outside of a $C_D = 1$ jet issuing from the suppressor measured at the nozzle exit plane (see fig. 7)
R_o	Radius in inches from the centerline to the outermost portion of ejector
R/C	Round convergent reference nozzle with 10° internal half-angle
Setback	A method of altering the secondary air inlet area of a fixed ejector suppressor geometry by repositioning the ejector along the centerline of the suppressor/ejector system. Positive setback is measured as the axial distance from the suppressor exit plane to the flightlip hilite of the ejector.

SYMBOLS AND ABBREIVATIONS—Continued

SB/D_{eq} The amount of setback nondimensionalized by the equivalent diameter of a jet having the same effective flow area as the total flow of the given configuration

T_T, T_{TP} Average total temperature of the primary flow (Fahrenheit unless otherwise noted)

VIP, VIP₀ Ideal primary jet velocity expanded to ambient pressure.

$$\left\{ 2 g R \left(\frac{\gamma}{\gamma - 1} \right) T_{TP} \left[1 - (PR)^{-(\gamma - 1)/\gamma} \right] \right\}^{1/2}$$

V_∞ Forward velocity in knots

WA Measured weight flow rate of air in pounds/second

WP Measured weight flow rate of fuel and air in pounds/second

α Internal half-angle of the round convergent portion of the tube in degrees

γ Ratio of specific heats

1.0 SUMMARY

1.1 INTRODUCTION

Jet noise suppression, a major problem in the development of supersonic transports, has experienced a substantial technology change since the termination of the U.S. SST program. Particular emphasis has been placed on the noise generated by the high pressure ratio jet exhaust flow. A critical factor in the development of jet noise suppression devices for exhaust nozzle systems is the maintenance of acceptable levels of thrust performance over the flight regime. Application to advanced supersonic aircraft demands that the suppressor cause little or no performance loss at cruise conditions. This constraint generally means that the suppressor must be retracted out of the jet stream at other than takeoff and approach flight modes, and this in turn severely limits the range of suppressor hardware parameters that can be considered for practical configurations.

This document presents a portion of the DOT-sponsored program to advance technology and establish a performance design capability within mechanical constraints and acoustic criteria for new noise multitube suppressor exhaust systems. The investigation extends the study of bare multitube suppressor performance (ref. 1) and suppressor/ejector interaction effects (ref. 2) to include the effects of low forward velocity on the performance of these exhaust systems. Noise suppression characteristics are presented on reference 3. For suppressor/ejector nozzles, the level of performance is largely a result of the tradeoff between ejector lip suction and nozzle base drag. As the system is subjected to forward velocity, a ram drag penalty produces a decrease in lip suction that is proportional to the amount of secondary air handled. Thus, to maximize the usefulness of the system over a range of velocities, the present study examines the mechanisms available to allow high static performance and minimize the performance lapse rate while also maintaining the noise suppression and installation constraints.

Results are presented from a systematic, model-scale experimental program which investigated the effects of six suppressor and three ejector parameters over a range of velocities from 0 to 167 kn and pressure ratios from 2 to 4.

1.2 RESULTS

The analysis of the experimental work includes discussion of the dependence of pressure ratio effects on velocity as well as an individual treatment of each of the geometric variables. A summary plot of performance as a function of pressure ratio and velocity is presented for each configuration tested. High static performance and minimum lapse rates are shown to be compatible through the proper selection of suppressor/ejector geometry and ejector inlet area.

1.3 SUMMARY OF FINDINGS

Over the range of variables investigated, variations in geometry produce much larger changes in the level of performance than in the rate of change of performance with velocity. An example of this is shown on figure 1 for various bare suppressor nozzles. To minimize

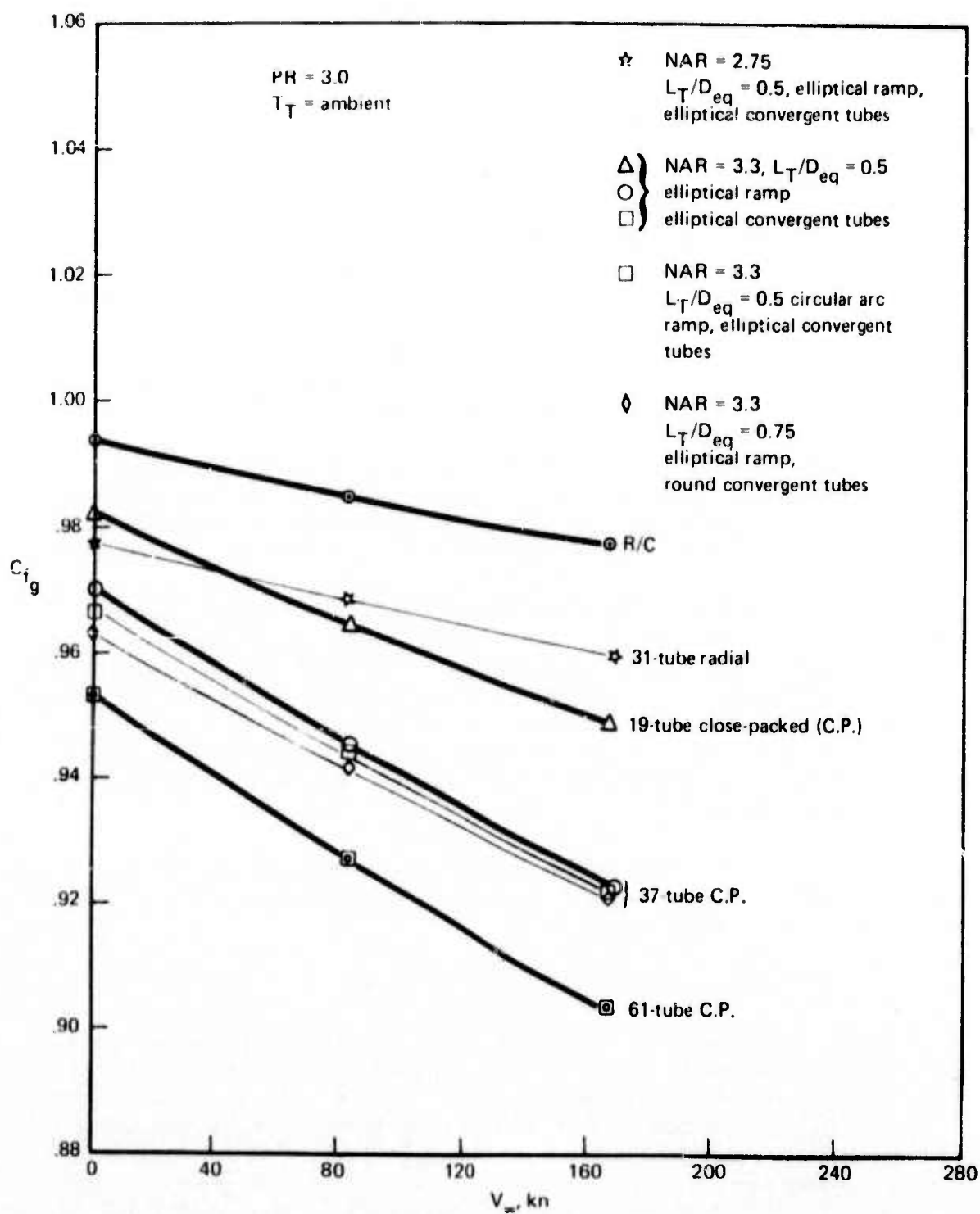


Figure 1. Effect of Velocity on the Performance of Suppressors Without Ejectors

suppressor drag, the use of a radial tube placement and elliptical convergent tubes is recommended. The number of tubes should be held at the minimum consistent with suppression requirements.

Large area ratio ejectors, while producing large static thrust augmentation, also have large lapse rates. The choice of ejector area ratio should include consideration of the performance over the desired range of velocities.

The maximum overall performance during takeoff is provided by configurations which minimize the afterbody drag through the appropriate selection of suppressor variables and effective ejector inlet area.

Figure 2 shows an example of the performance of a suppressor with and without an ejector. The ejector case has higher static performance and greater lapse rate, producing a crossover velocity beyond which the ejector becomes a performance handicap.

The best performance results are obtained when the ejector length is on the order of 12 to 15 individual jet diameters for ejector area ratio < 3.7 and $EAR/NAR < 1.3$. Increased ejector length should be considered if either the ejector area ratio or the EAR/NAR ratio is greater than these values.

The majority of the secondary air entering the ejector appears to pass through the annular area between the ejector lip and the outer row tubes. Only a small percentage of the flow passes between the tubes into the recirculation region. The annular area (and hence the majority of the effective inlet area) is established by the EAR/NAR ratio and the ejector setback.

Ejector inlet area plays a major role in determining the tradeoff between lip suction and base drag. An optimum ejector inlet area exists for each operating condition (jet temperature, pressure ratio, and freestream velocity) as illustrated in figure 3.

Large performance losses are observed as the area is decreased from the optimum. In the limit, the secondary air chokes at the ejector, producing shock-induced flow instabilities and ejector vibration. Increases in ejector inlet areas beyond the optimum cause relatively small performance losses for the range tested.

Typical performance trends for a multitube bare nozzle are shown in figure 4.

At any fixed velocity, afterbody drag is a decreasing percentage of ideal primary thrust as pressure ratio increases. For a fixed pressure ratio, the base drag increases linearly with velocity, and the ramp drag increases in proportion to velocity squared.

Maximum static performance occurs between pressure ratio 2.5 and 3.0. Lapse rate, $|\Delta C_{f_p}| @ \Delta V_\infty$, decreases as pressure ratio increases. Thus, the peak performance decreases and shifts to a higher pressure ratio as velocity increases. For a constant pressure ratio and nozzle area ratio, the level of performance varies strongly with geometry but the lapse rate is nearly constant.

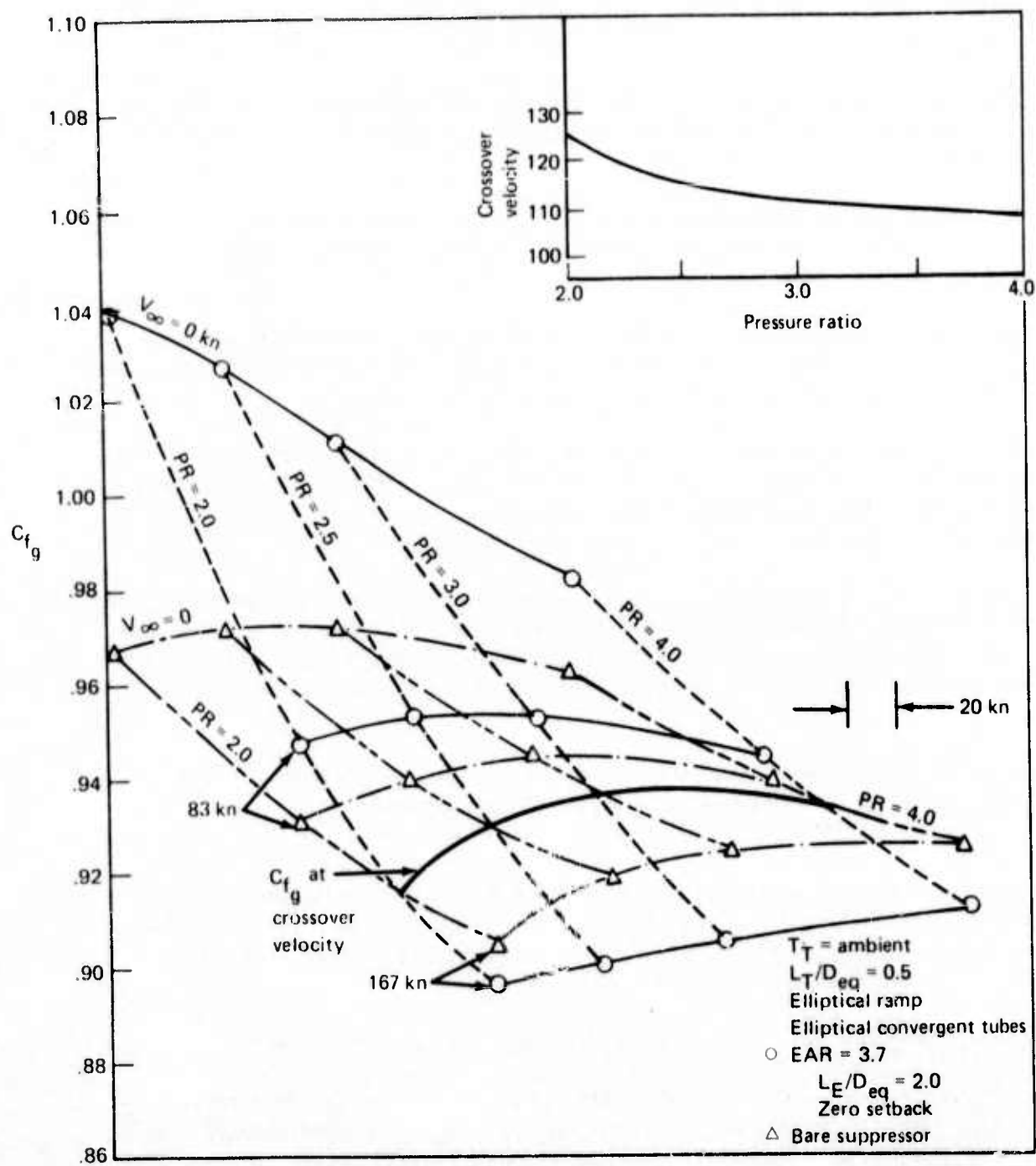


Figure 2.—Comparison of Performance and Lapse Rate and Crossover Velocity for 37-Tube, NAR-3.3 Close-Packed Array, Bare and With EAR-3.7 Ejector

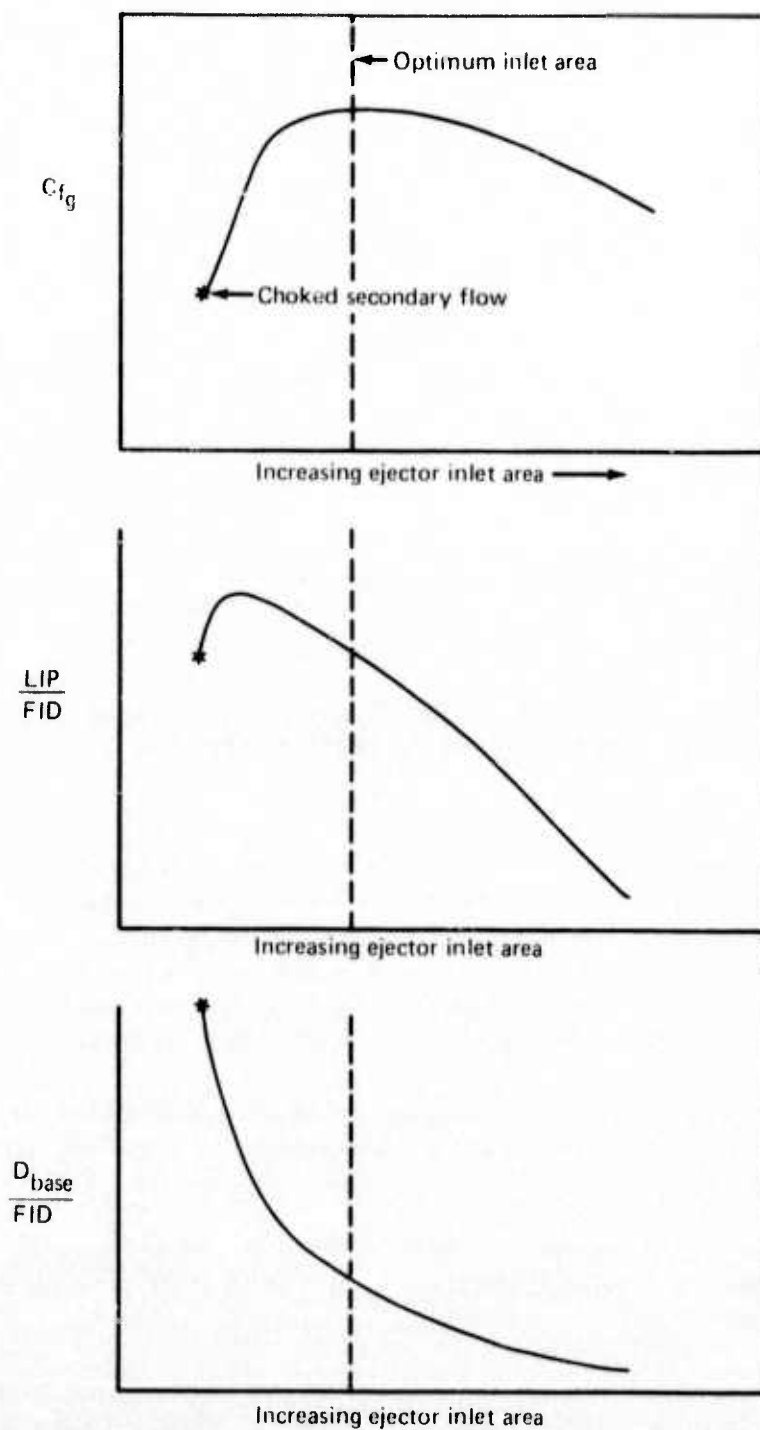


Figure 3.—Effect of Ejector Inlet Area on the Performance of Suppressor/Ejectors

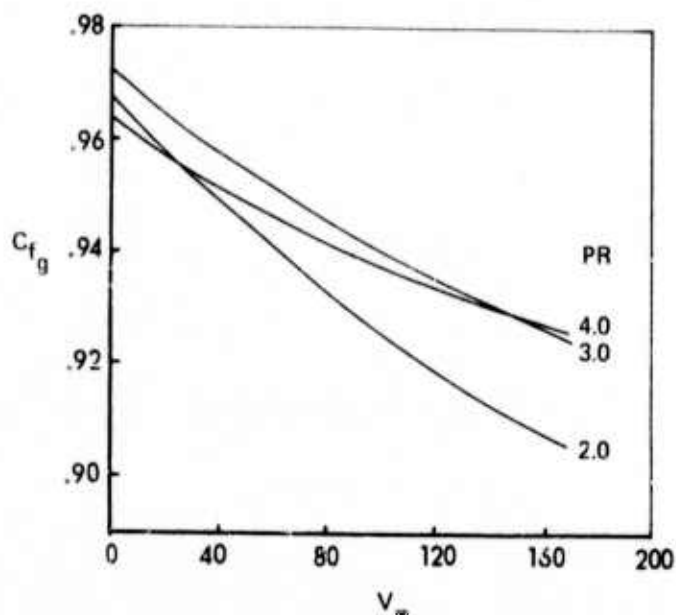


Figure 4.—General Behavior of Bare Suppressor Performance as a Function of Pressure Ratio and Velocity

Typical trends for suppressor/ejector nozzles were studied. Over the range of pressure ratios investigated (2–4), the maximum static performance was found to occur at or near pressure ratio = 2. The lapse rate, while still decreasing with increasing pressure ratio, is much larger with ejectors than for similar bare suppressor cases. Thus, as the velocity increases (relative to a bare suppressor), the rate of performance decrease is greater and the pressure ratio at which the peak performance occurs moves to a higher value for the ejector case.

Both lip suction and base drag become decreasing percentages of ideal thrust as either pressure ratio or velocity increases. The lip suction is more strongly dependent on pressure ratio than is base drag.

The geometric suppressor parameters of tube number, tube shape, length, and array greatly affect static performance but do not contribute substantially to the rate of change in performance due to forward velocity.

Typically, static performance decreases as temperatures increase because of decreased secondary air handling. The reduced air handling results in lower ram drag penalty and thus, lower lapse rate with forward velocity.

For the type of suppressor/ejector system investigated, an ejector area ratio of approximately 3.1 and EAR/NAR of 1.2 are recommended as providing the best performance tradeoffs. Very little setback would be needed for such a configuration, and the setback could be used to "fine tune" the system over the range of velocity.

2.0 INTRODUCTION

Aircraft designed for supersonic cruise require engines with a high thrust-to-frontal-area ratio and high exhaust jet velocities. Noise suppression is essential during takeoff, initial climb-out, and landing. The noise associated with the high velocity jet can be reduced substantially by placing hardware into the primary exhaust flow to break the jet into small elements. However, the extreme sensitivity of the supersonic aircraft mission to nozzle performance during supersonic cruise dictates that the suppressor hardware, with its inherent thrust loss, be retracted from the jet during cruise. SST technology (ref. 4) demonstrated high suppression values for multitube suppressor nozzles that could be stowed into the divergent portion of a high-performance con-di nozzle during transonic acceleration and supersonic cruise (fig. 5). At low speeds the divergent portion of the cruise nozzle could be moved outward to form a nearly constant area ejector.

By providing an inlet for ambient (secondary) air to be accelerated into the ejector by the entrainment of the high velocity primary jets, a static pressure reduction is created which produces a thrust force on the ejector lip. The amount of air entrained by the primary is a function of the ejector area and length, among other things. On the order of twelve individual jet diameters are required to provide sufficient mixing length to entrain the maximum amount of secondary air and obtain maximum ejector lip suction. The use of a multitube suppressor makes the required ejector length feasible from an installation and weight point of view.

The static pressure reduction at the ejector inlet also produces an increase in the afterbody drag on the suppressor nozzle. References 1 and 2 demonstrate that the overall suppressor/ejector performance is strongly influenced by the lower-than-ambient pressure acting on the base area between the tubes. The amount of base drag is a function of both the ventilation provided by the suppressor geometry and the static pressure reduction due to the secondary air inlet velocity.

Provided the inlet area is large enough, the net effect of the partially counteracting ejector lip suction and suppressor afterbody drag is a static performance augmentation due to the secondary air handled by the ejector. Given sufficient ejector length, the amount of secondary air handled—and hence the static performance—continues to increase with increasing ejector area ratio.

As the ejector/suppressor is subjected to forward velocity, a ram drag performance penalty must be paid for the secondary air. This penalty, though a real component of the momentum equation, is manifested as a reduction in lip suction with forward velocity. The larger the amount of secondary air handled statically, the greater the decrease in lip suction with velocity. Thus, to properly evaluate the performance of a suppressor/ejector system, maximizing the static performance is not sufficient to produce the best exhaust system for take-off and climb-out.

The present investigation described and quantifies the mechanisms available to allow high static performance and minimize the rate of decrease in performance with increasing velocity (lapse rate) while maintaining the noise suppression and installation constraints.

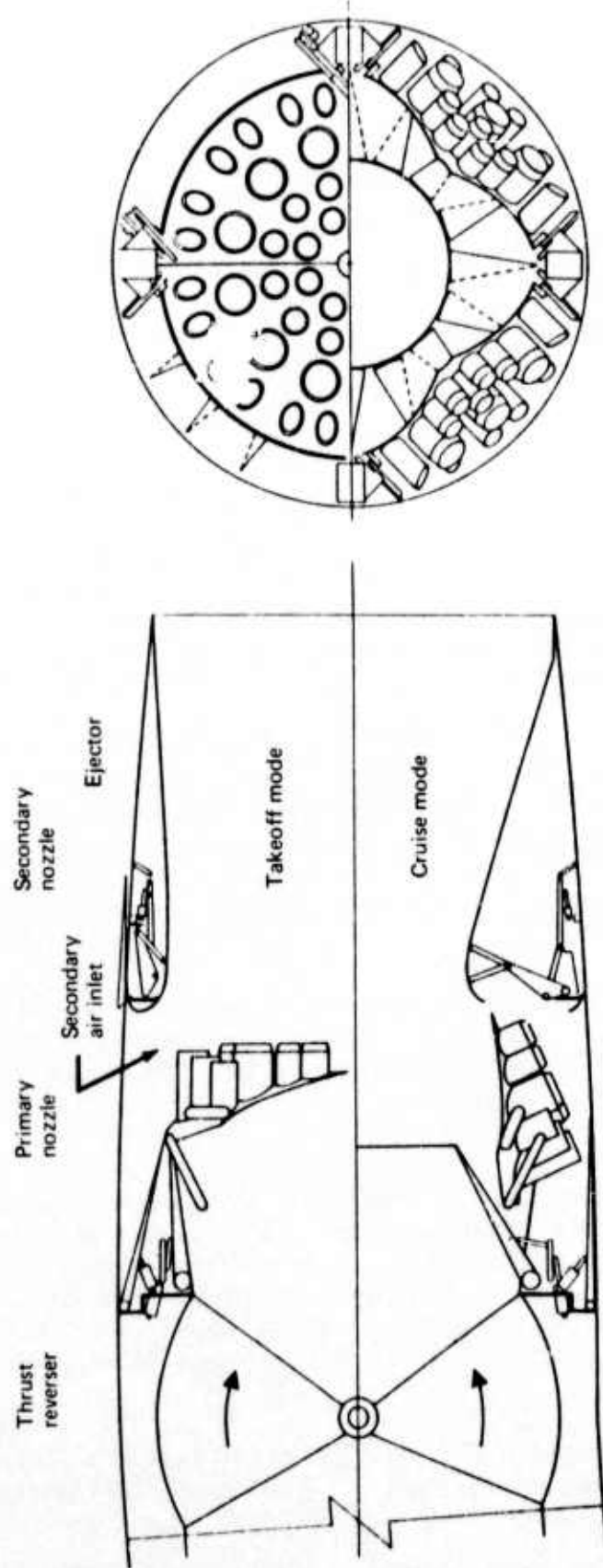


Figure 5.—Application of Stowable Suppressor to an Advanced SST Exhaust System

Model scale testing was conducted on 28 related suppressor/ejector nozzles at velocities from 0 to 167 kn and pressure ratios from 2 to 4. Families of suppressors were tested with 19 to 61 tubes. For most configurations, tube length was maintained at a length compatible with the stowable tube concept. The investigation concentrated on elliptical convergent tubes to maximize baseplate ventilation while maintaining high internal performance. For comparison, sample configurations were tested with round convergent tubes. Three ramp shapes were used, and both close-packed and radial tube arrays were incorporated. The nozzle area ratios, $NAR = 2.75-3.3$, were partially dictated by airplane installation requirements and partially by the optimums suggested in reference 1. Configuration-oriented inlet losses due to ejector mounting struts were avoided by mounting the ejector independently, but on balance, on a separate support. Each ejector tested had a constant internal area and a 2 : 1 elliptical flightlip. The ejector area ratios investigated were 2.6, 3.1, and 3.7. The largest area ratio was substantially larger than is considered practical for SST application but was used to demonstrate the effect of area ratio on performance and lapse rate.

The report will summarize the experimental results for all configurations tested on plots of performance as a function of pressure ratio and velocity. The dependence of forward velocity effects on pressure ratio will be analyzed. The importance of each of the suppressor and ejector geometric parameters will be discussed separately. Crossover velocities and the behavior of restricted inlets will be presented along with a qualitative inlet flow model. Finally, some trends will be presented for the effects of primary jet temperature on suppressor/ejector surface forces.

3.0 PARAMETERS AND DEFINITIONS

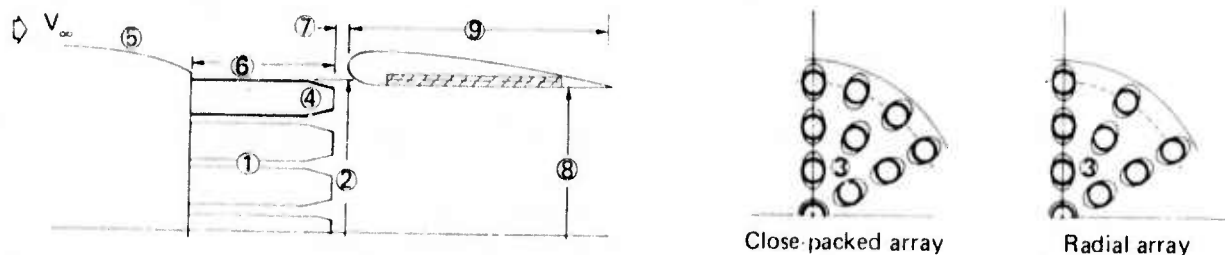
3.1 RANGE OF VARIABLES

3.1.1 FLOW VARIABLES

- Pressure ratio: 2-4
- Primary temperature ambient and 1150°F
- Velocity (V_∞) 0-167 kn (0-283 ft/sec)

3.1.2 SUPPRESSOR AND EJECTOR VARIABLES

The suppressor variables and constraints for this investigation are the same as those discussed in detail in reference 1. The suppressor area ratios were limited to 2.75 and 3.3 as a result of the performance optimum discovered in reference 1 and in order to be compatible with supersonic transport constraints. Figure 6 shows the suppressor and ejector variables.



Suppressor Variables

- 1 Tube number: 19-61
- 2 Area ratio: 2.75 and 3.3
($\pi R_D^2 / \text{geometric flow exit area}$)
- 3 Tube array: close-packed and radial
- 4 Tube shape: round convergent and elliptical convergent (both converging to round exits)
- 5 Ramp shape: elliptical, circular arc and contoured
- 6 Tube length: $L_T / D_{eq} = 0.50 - 0.75^*$

* $D_{eq} = 4$ in. throughout experimental work

Ejector Variables

- 7 Setback: $(SB / D_{eq} = 0 - 0.25)$
- 8 Ejector area ratio: 2.6 - 3.7
- 9 Ejector length: $L_E / D_{eq} = 2 - 6$

Figure 6.—Suppressor/Ejector—Schematic

3.2 CONSTRAINTS

3.2.1 SUPPRESSOR CONSTRAINTS

- Total effective exit area: 13.2 in^2 (geometric exit area $\approx 13.6 \text{ in}^2$ for convergent tubes, or approximately 1/10 scale SST)
- Approximately 0.5 internal Mach number for convergent tubes
- Coplanar tube exits
- Flat baseplate (except contoured ramp configuration)
- All tubes within an array the same (e.g., a 37-tube array has 37 tubes, each with 0.36 in^2 of effective flow area)
- Outside nacelle diameter held constant (8.89 in. to be representative of a scale SST nacelle)

3.2.2 EJECTOR CONSTRAINTS

- 8 in. long, $L_E/D_{eq} = 2.0$ (unless otherwise stated)
- Flightlip profile constant (2:1 ellipse)
- Ejector thickness approximately constant
- No suppressor/ejector mounting struts (i.e., no inlet losses due to installation)
- Constant internal area (constant geometric mixing area)
- For a given setback, axial distance from tube exit plane to the ejector throat approximately the same for all configurations

For most configurations, the ejector length was fixed at the maximum allowed on the SST at the termination of the aircraft project (8 in. model scale). To better understand the degree of mixing that was occurring in the fixed length, the constraint was relaxed for a few configurations.

3.3 DEFINITIONS FOR NOZZLE AREA RATIO, EJECTOR AREA RATIO, AND SETBACK

The various area ratios used within this investigation are defined with the aid of figure 7.

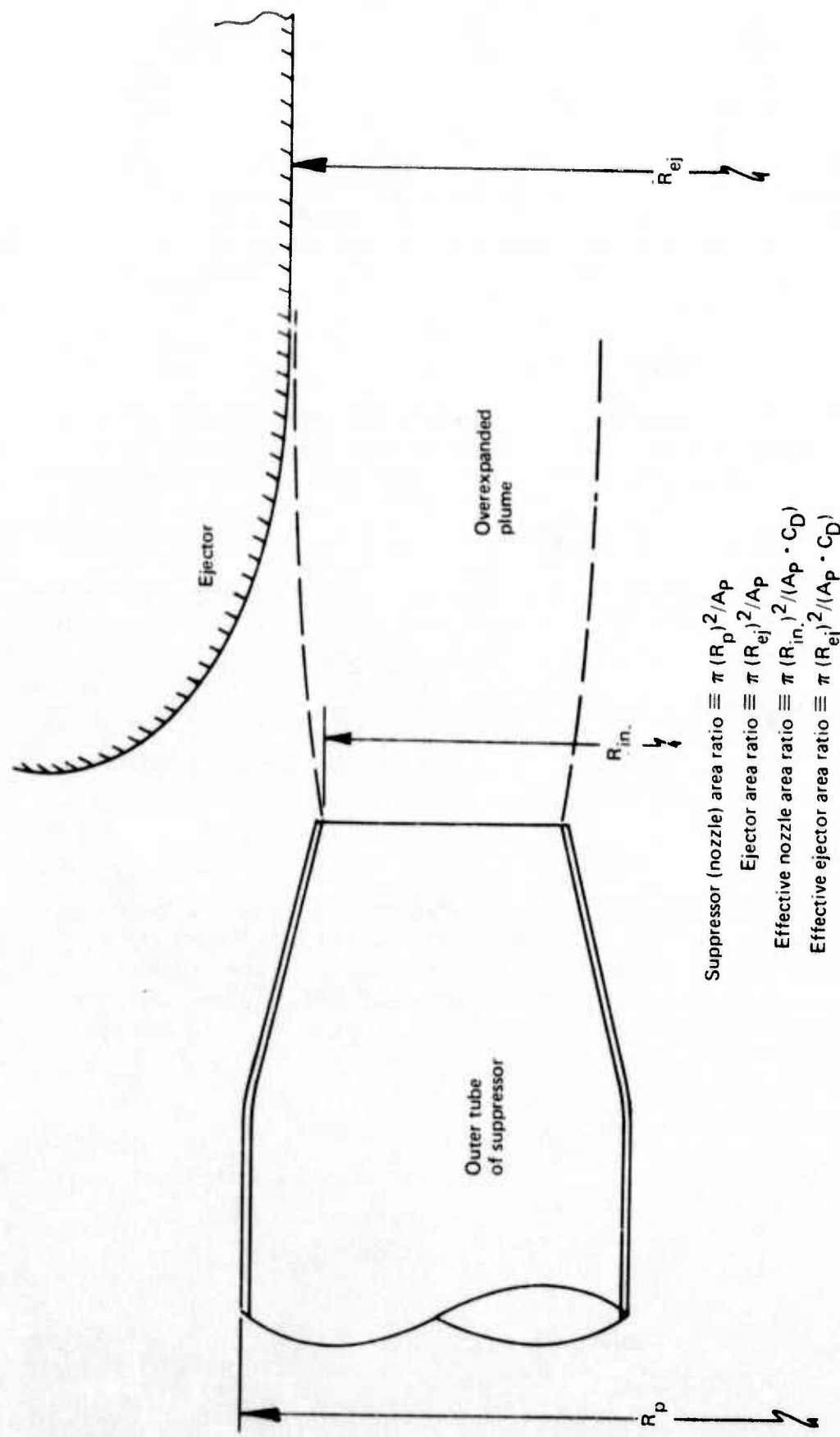


Figure 7.--Definition of Suppressor and Ejector Area Ratio

3.3.1 NOZZLE AREA RATIO (NAR)

Throughout this study the suppressor area ratio or nozzle area ratio (NAR) refers to the total area within a circle tangent to the outermost portion of the outside tubes divided by the geometric primary flow area. This definition was chosen to be representative of the physical area required to install the suppressor. Notice that configurations with convergent tubes can have nozzle area ratios larger than ejector area ratios without implying jet scrubbing on the ejectors.

3.3.2 EFFECTIVE NOZZLE AREA RATIO

The effective nozzle area ratio is defined as the area within a circle tangent to the outside of the outer jets, at the nozzle exit plane, divided by the effective primary flow area ($C_D \cdot A_p$). This area ratio is representative of the jet that must be contained by the ejector.

3.3.3 EJECTOR AREA RATIO (EAR)

Throughout the present investigation, constant mixing area ejectors are used. The ejector area ratio is defined as the geometric ejector flow area divided by the primary nozzle geometric flow area (A_p).

3.3.4 EFFECTIVE EJECTOR AREA RATIO

The effective ejector area ratio is defined as the geometric ejector flow area divided by the primary nozzle effective flow area ($C_D \cdot A_p$).

3.3.5 SETBACK

All nozzles in the present investigation have coplanar tube ends. The axial distance downstream from the tube exit plane to the ejector hilite is defined as the setback. For all ejectors the lip shape is a 2:1 ellipse segment, and the ejector thickness is maintained approximately constant, resulting in nearly the same axial distance to the ejector throat for all ejectors (for a fixed setback).

4.0 TEST DESCRIPTION

4.1 FACILITY DESCRIPTION AND DATA ACQUISITION

The test was conducted in the Boeing Propulsion/Noise laboratory's low-speed wind tunnel (A). The facility, shown in figure 8, is an open-circuit tunnel with a 9- by 9-ft test section. Driven by a gas generator and variable pitch propeller, the tunnel velocity can be varied from 30 to 167 kn.*

The multitube suppressors were installed on a forebody as shown in figure 8 and detailed in figure 9. The dual-flow forebody, enclosing a variable-slot burner, was mounted on a six-component wind tunnel balance located beneath the tunnel floor. The suppressor air flow rate was measured with an A.S.M.E. long-radius flow nozzle.

The boundary layer thickness at the ejector inlet was representative of that developed on a model SST nacelle. To provide the appropriate inlet flow on a forebody long enough to incorporate the burner, it was necessary to use boundary layer suction. The location of the boundary layer suction ports is shown in figure 9, and a detailed view of the ports is shown in figure 10. Figure 10 also shows the results of the oil-flow run used to verify that there were no separation regions on the forebody.

Ejectors are mounted on balance using a separate stand (fig. 9) to avoid configuration-oriented ejector inlet strut losses. Aerodynamic forces on the ejector stand, like those of the forebody, are removed from the force data and treated as tares.

The temperature and total pressure profiles shown in figure 11 are typical of the experimental values measured at the instrumentation cruciform (14 total pressure and 14 thermocouples) for nominal 1150° F test conditions.

4.2 DESCRIPTION OF NOZZLES

4.2.1 GENERAL

All multitube nozzles share the following characteristics:

- Total effective flow area $\approx 13.2 \text{ in.}^2$
- All tubes within a given suppressor are the same size
- All tube exits are coplanar
- All tubes are convergent, having round exits, internal Mach number = 0.5 and entrance-radius-to-tube diameter > 0.1
- Nozzle ramp and baseplate areas were instrumented with area-weighted static pressure taps

*The same model hardware was used on the Boeing Hot Nozzle Test facility to acquire the static data. Details of the static testing are presented in reference 2.

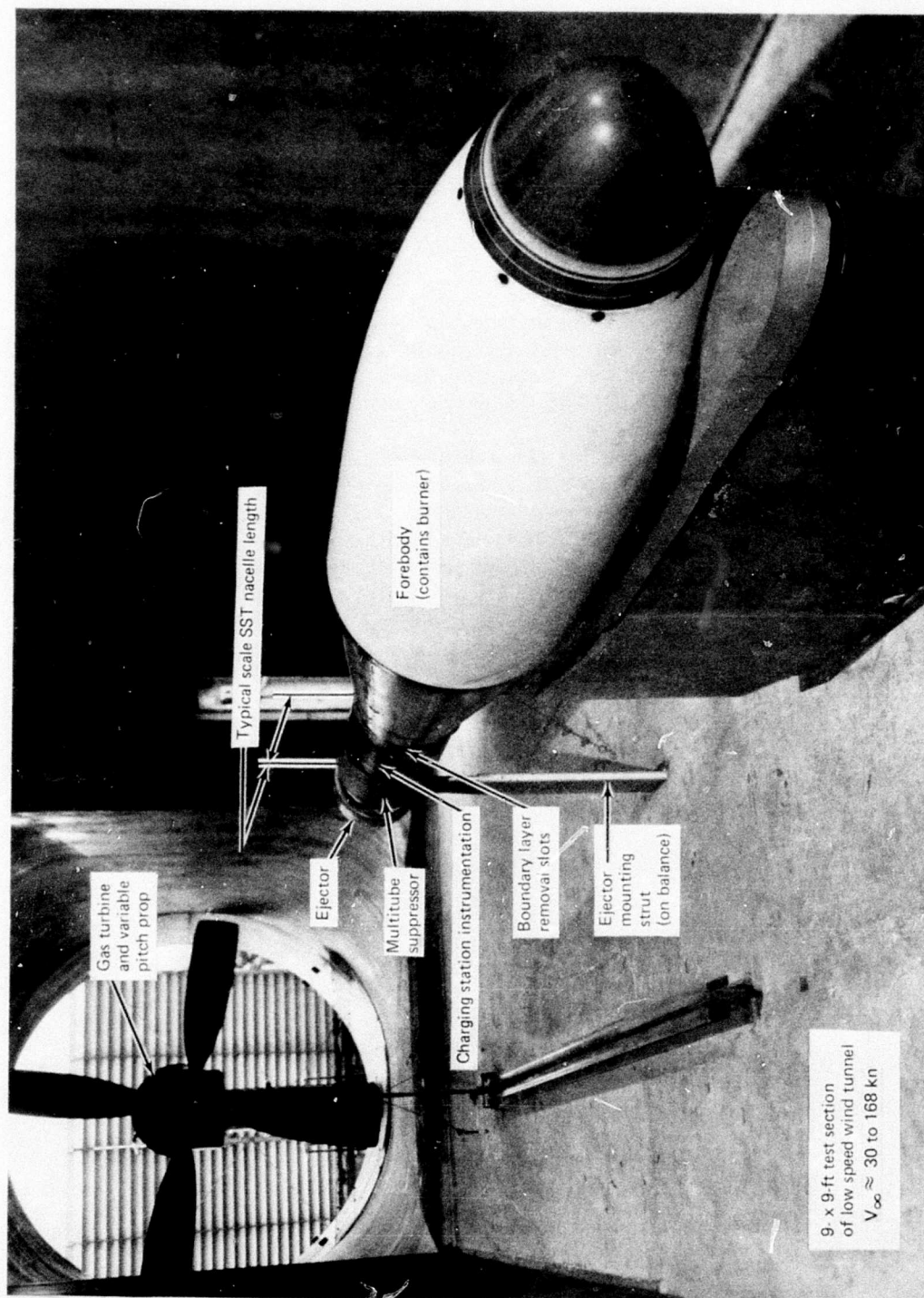


Figure 8.—Test Installation

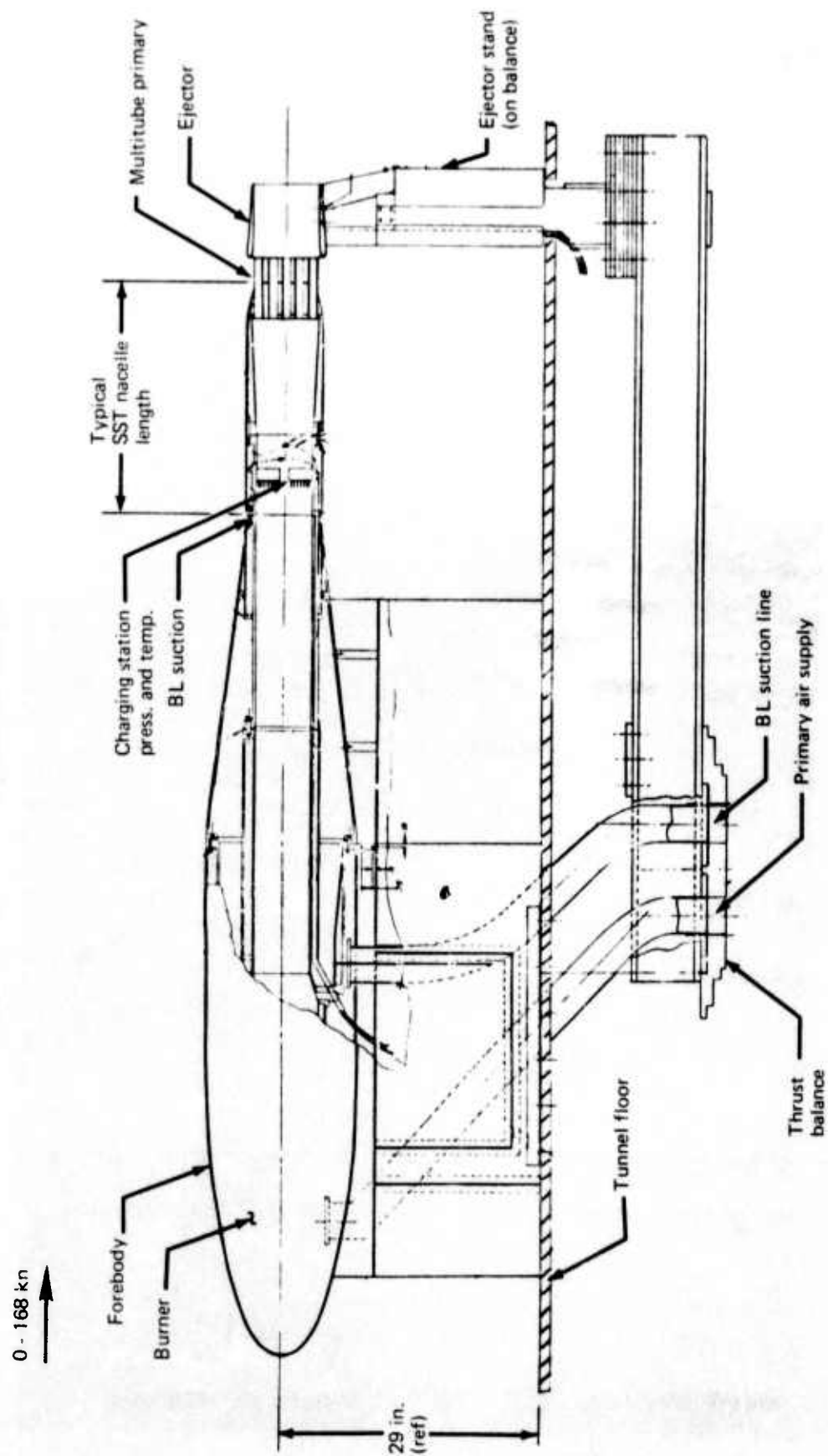


Figure 9.—Forward Velocity Effects—9- by 9-ft Wind Tunnel Test



Figure 10.—Oil Flow on Forebody and Boundary Layer Suction

Run 21 10/4/73

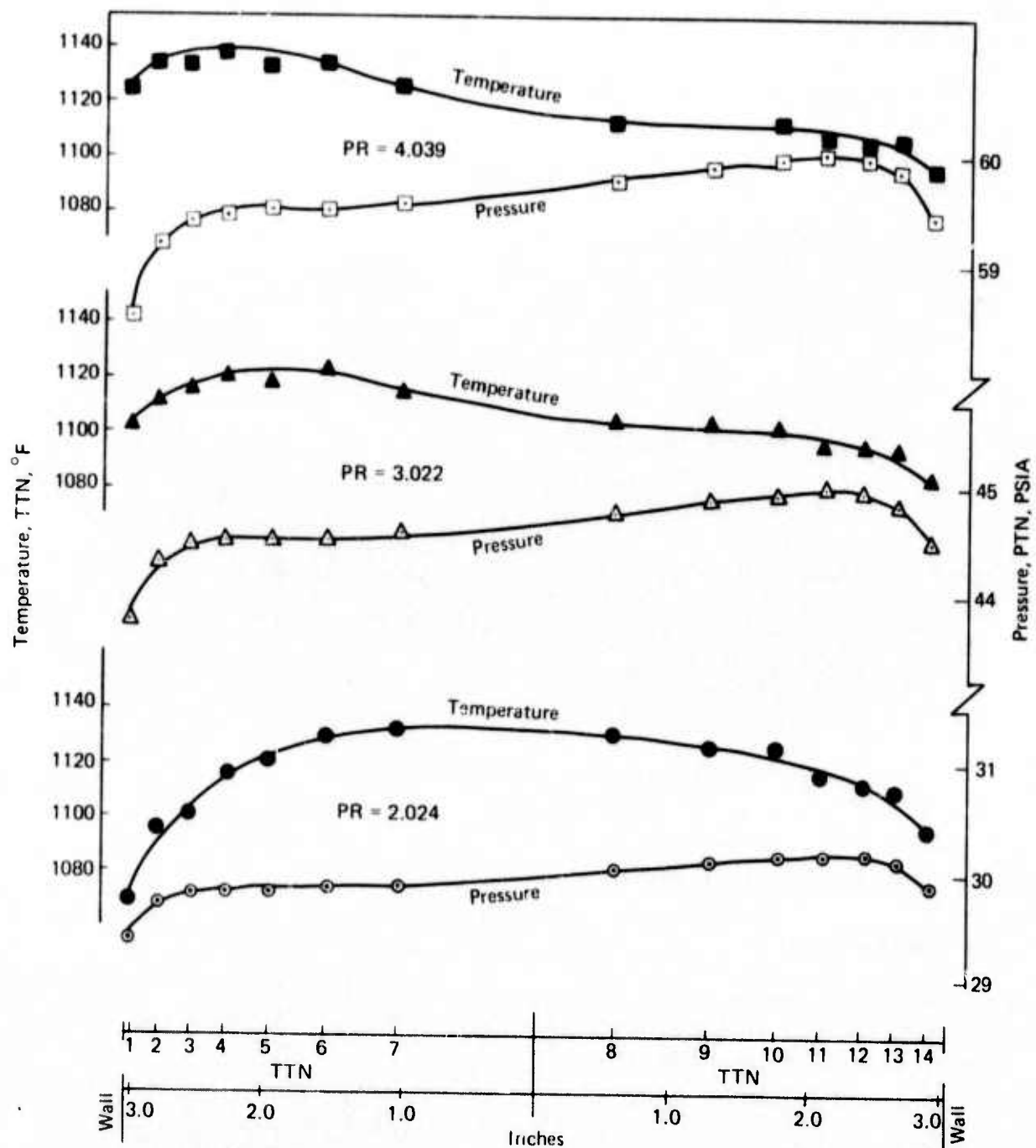


Figure 11.—Temperature and Pressure Profile at Charging Station

4.2.2 ROUND CONVERGENT REFERENCE NOZZLE (R/C)

The R/C, a 10° half-angle, round convergent nozzle (fig. 12), was used as a noise and performance referee. The nozzle has an upstream-to-exit diameter ratio (D/d) of 1.44 and a geometric exit area of 13.825 in^2 . The external contour consists of a 12° half-angle boattail, tangent to a 35.5-in.-radius arc which, in turn, is tangent to the 8.89-in. nacelle diameter upstream.

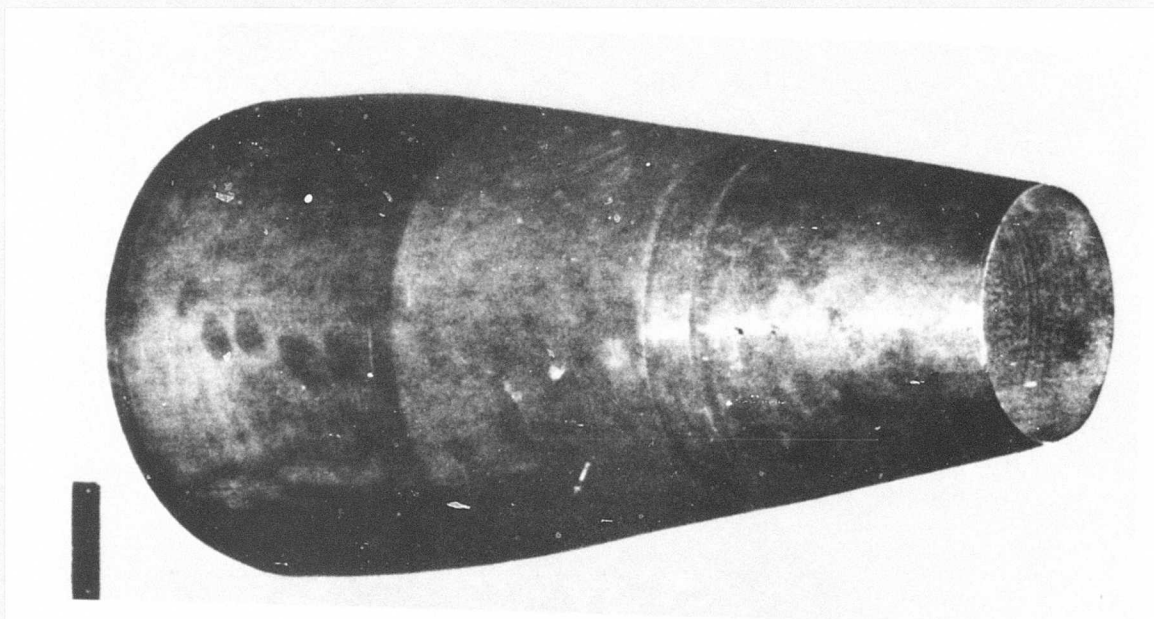


Figure 12.—Round-Convergent Reference Nozzle

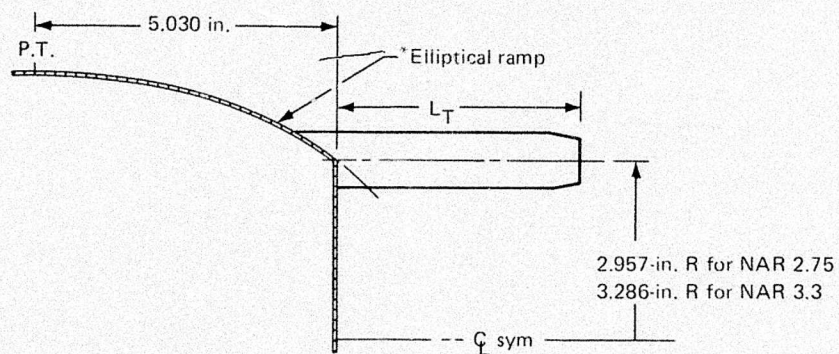
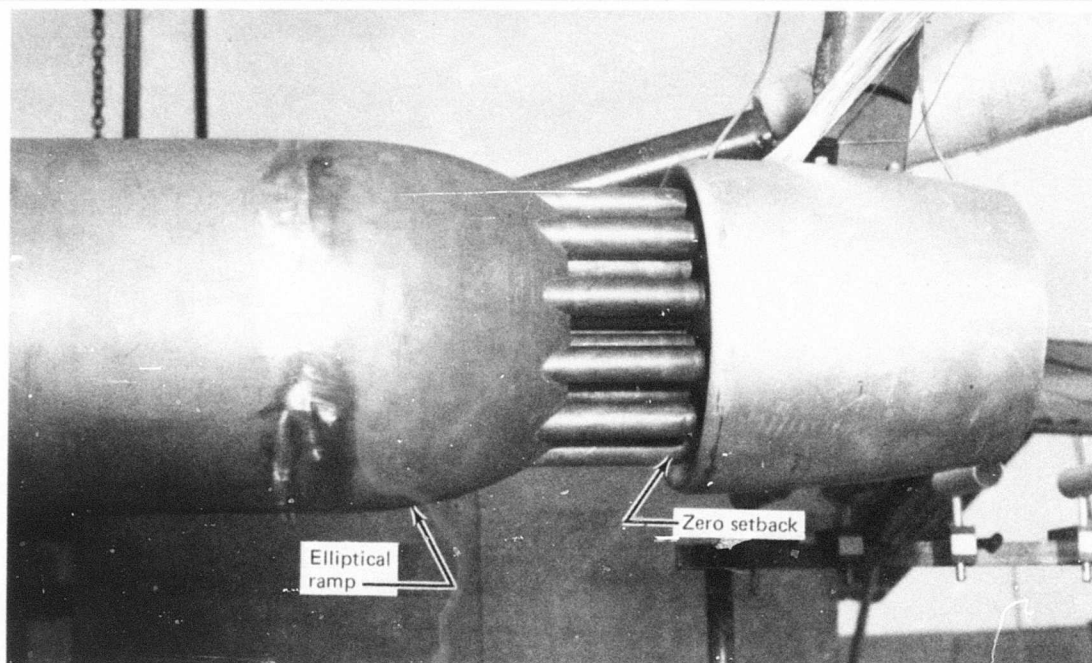
4.2.3 SUPPRESSOR RAMP SHAPES

4.2.3.1 Elliptical Ramp

Used in the majority of configurations, the elliptical ramp (fig. 13) consists of a segment of an ellipse with foci on the nozzle centerline. The segment is tangent to the nacelle and extends to the center of the outer tube row.

4.2.3.2 Circular Arc Ramp

The circular arc ramp (fig. 14) consists of a 35.5-in.-radius, circular arc that is tangent to the nacelle and intersects the baseplate just outside of the outer tubes.



*Elliptical ramp (NAR = 2.75)

$$\frac{x^2}{45.394} + \frac{y^2}{19.758} = 1.0$$

Major axis = 6.7375 in.
Minor axis = 4.445 in.

*Elliptical ramp (NAR = 3.3)

$$\frac{x^2}{31.909} + \frac{y^2}{19.758} = 1.0$$

Major axis = 5.6488 in.
Minor axis = 4.445 in.

Figure 13.—Elliptical Ramps

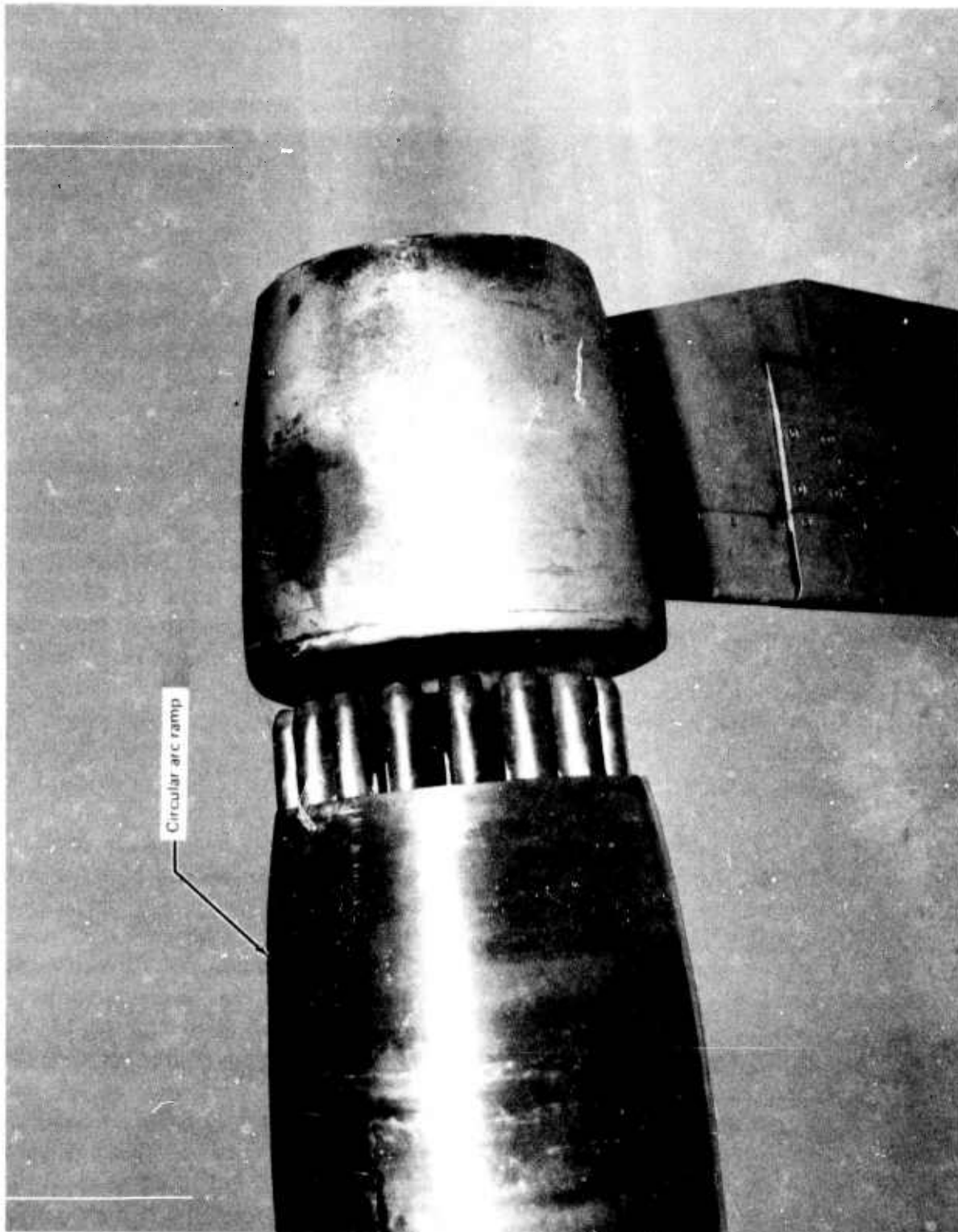


Figure 14.—37-Tube, NAR-3.3, Close-Packed Array With Circular ARC Ramp;
EAR = 3.1 and $SB/D_{eq} = 0.25$

4.2.3.3 Contoured Ramp

The contoured ramp (actually, ramp and base combined) consists of a 40-in. boattail-radius tangent to the 8.89 nacelle diameter and terminating in a central hole coplanar with the tube exits. Though incompatible with the stowable tube concept, the contoured base was intended to provide maximum ventilation and ejector inlet area and to minimize the separation region on the base.

The contoured base was tested only on the 37-tube, area-ratio-3.3, close-packed suppressor with round convergent tubes (R/37) as shown in figure 15.

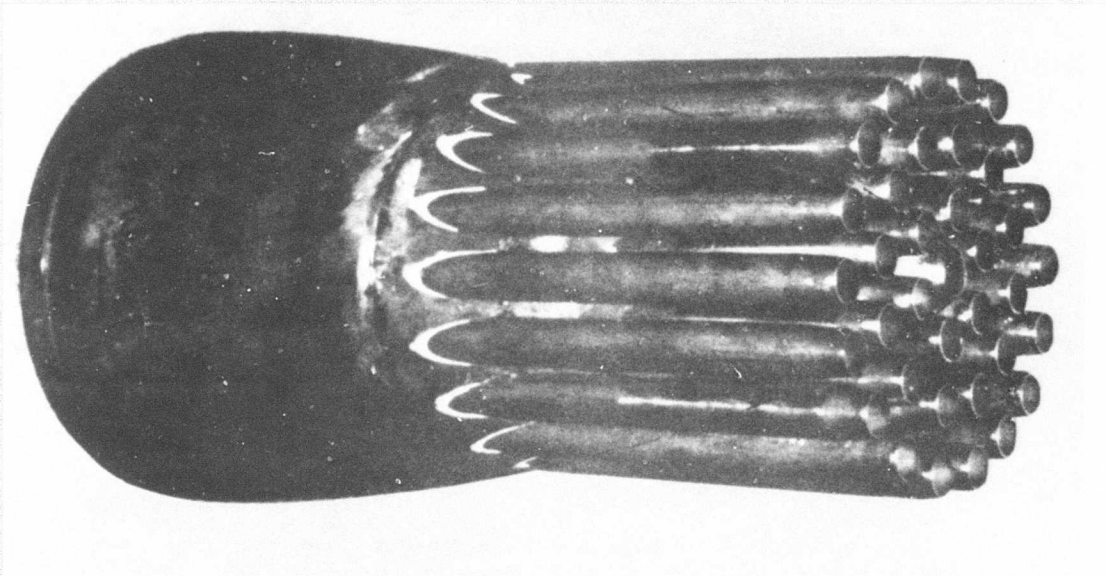


Figure 15.—Contoured Ramp

4.2.4 TUBE LENGTH

The stowable tube concept, as shown in figure 1, requires that the tubes be short enough to fold into the void left as the internal ejector wall moves inward to form the divergent portion of the con-di transonic acceleration and supersonic cruise nozzle. Present installation constraints require that the tube length nondimensionalized by the equivalent round convergent jet diameter (L_T/D_{eq}) be approximately 0.4 for stowable tubes. The constraint was relaxed slightly, and most configurations were tested with $L_T/D_{eq} = 0.5$. The constraint was further relaxed for a few configurations to establish the effects of tube length on lapse rate.

4.2.5 CLOSE-PACKED ARRAYS (FOUR) WITH ELLIPTICAL RAMPS AND TUBES: 19, 37, AND 61 TUBES

Tests of 19-, 37-, and 61-tube, 13.6-in^2 , area ratio (NAR) 3.3 suppressors were made to investigate the natural progression of nozzles with approximately equal spacing between all tubes in the array. Figures 16 and 17 show key dimensions for each nozzle. All tubes are elliptical converging to round coplanar exits.

A 37-tube, area-ratio-2.75 nozzle was built. This nozzle is similar to the 37-tube, area-ratio-3.3 nozzle shown on figure 17 in all respects other than NAR.

4.2.6 R/37: 37-TUBE, NAR-3.3 SUPPRESSOR WITH CONTOURED RAMP

The R/37 configuration (fig. 15) is a 13.695-in^2 , nozzle-area-ratio-3.3, close-packed suppressor using 37 round convergent tubes of equal diameter and varying length, and a contoured ramp. The average length of the internal constant area portion of the tubes is 4.4 in. The nozzle was used repeatedly during the investigation as a noise and performance referee.

4.2.7 37-TUBE, NAR-3.3, CLOSE-PACKED ARRAY WITH ELLIPTICAL RAMP AND R/C TUBES

To establish the effect of varying only tube shape, the R/37 nozzle was fitted with an elliptical ramp to produce a 37-tube, NAR-3.3, close-packed array with round convergent tubes. To provide a ventilation parameter ⁽¹⁾ similar to the 37-tube, NAR-3.3 suppressor with elliptical convergent tubes, $L_T/D_{eq} = 0.75$ was used. Variations in tube shape and ramp shape for 37-tube, area-ratio-3.3 nozzles are shown in figures 18 and 19.

4.2.8 RADIAL ARRAY SUPPRESSOR

The 31-tube nozzle, constructed to minimize the base ventilation by placing all tubes in radial lines, had an area ratio of 2.75 and used elliptical convergent tubes (fig. 20).

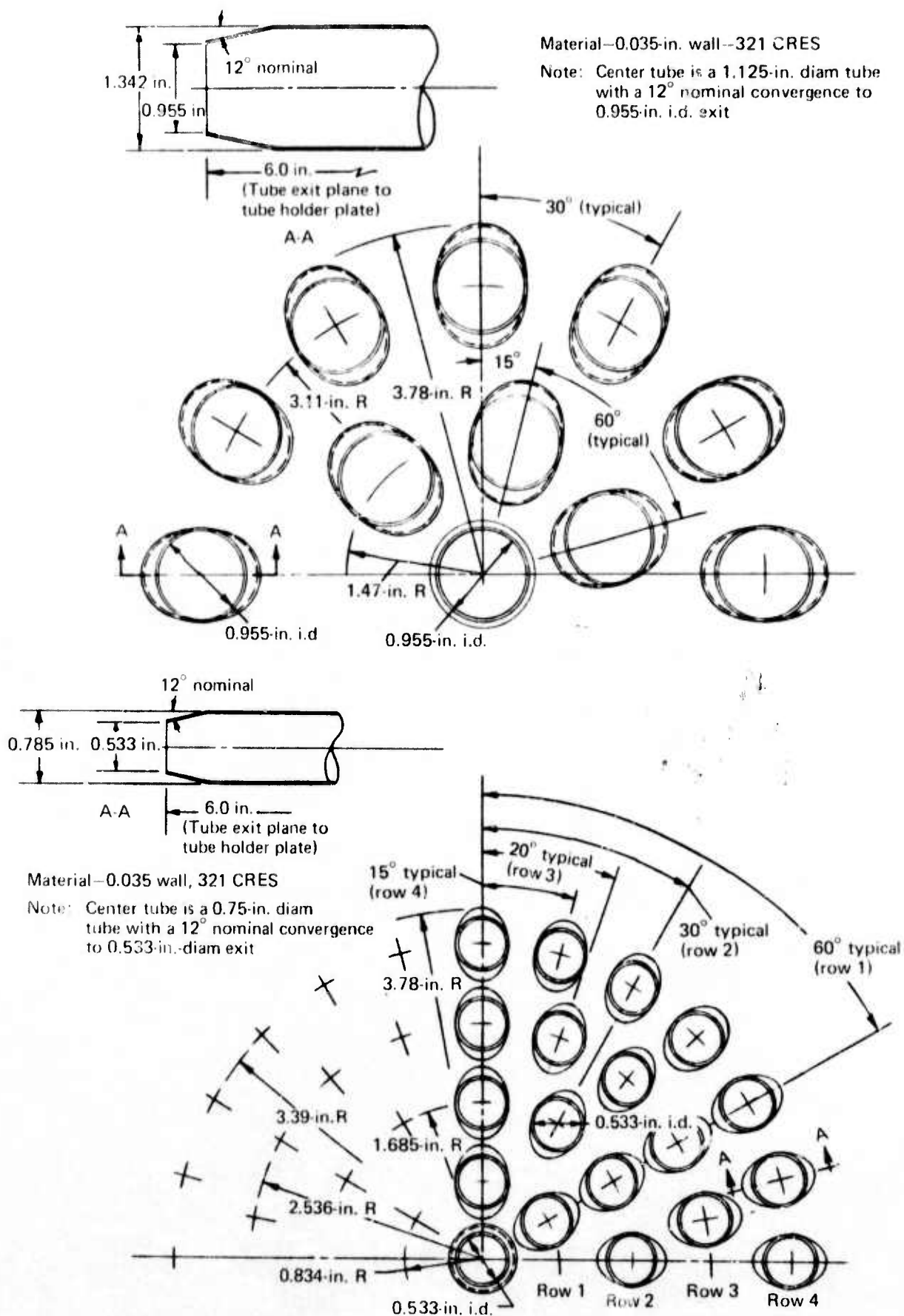
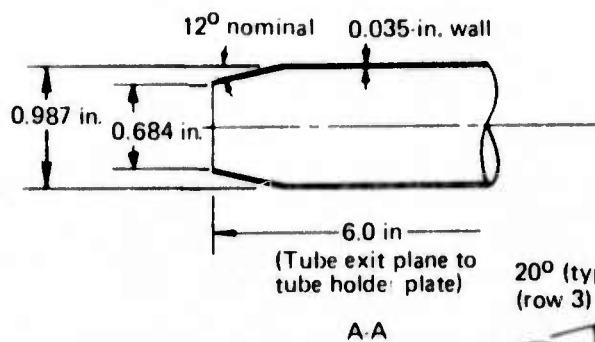
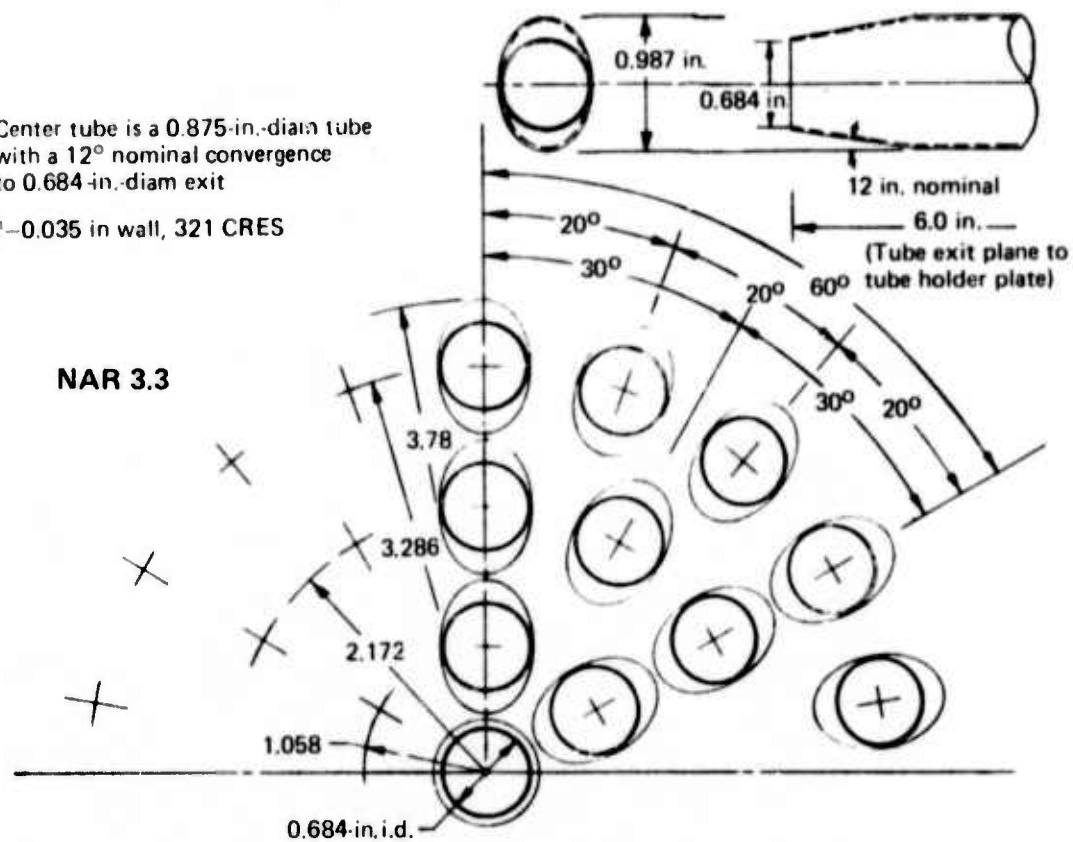


Figure 16.—19- and 61-Tube Area-Ratio-3.3 Suppressors

Note: Center tube is a 0.875-in.-diam tube with a 12° nominal convergence to 0.684-in.-diam exit

Material—0.035 in wall, 321 CRES



Material—321 CRES

Note: Center tube is a 0.75-in.-diam tube with 0.020 in. wall (0.71 in.-i.d.) with a 12° nominal convergence to 0.684-in.-diam exit

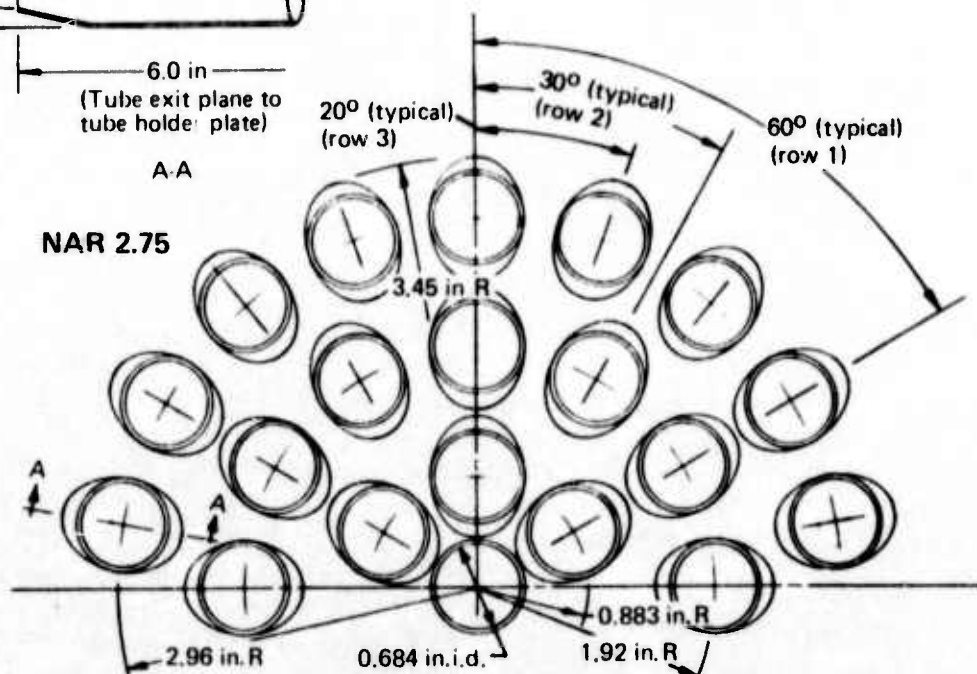


Figure 17.—37-Tube, Close-Packed Suppressors NAR = 2.75 and 3.3

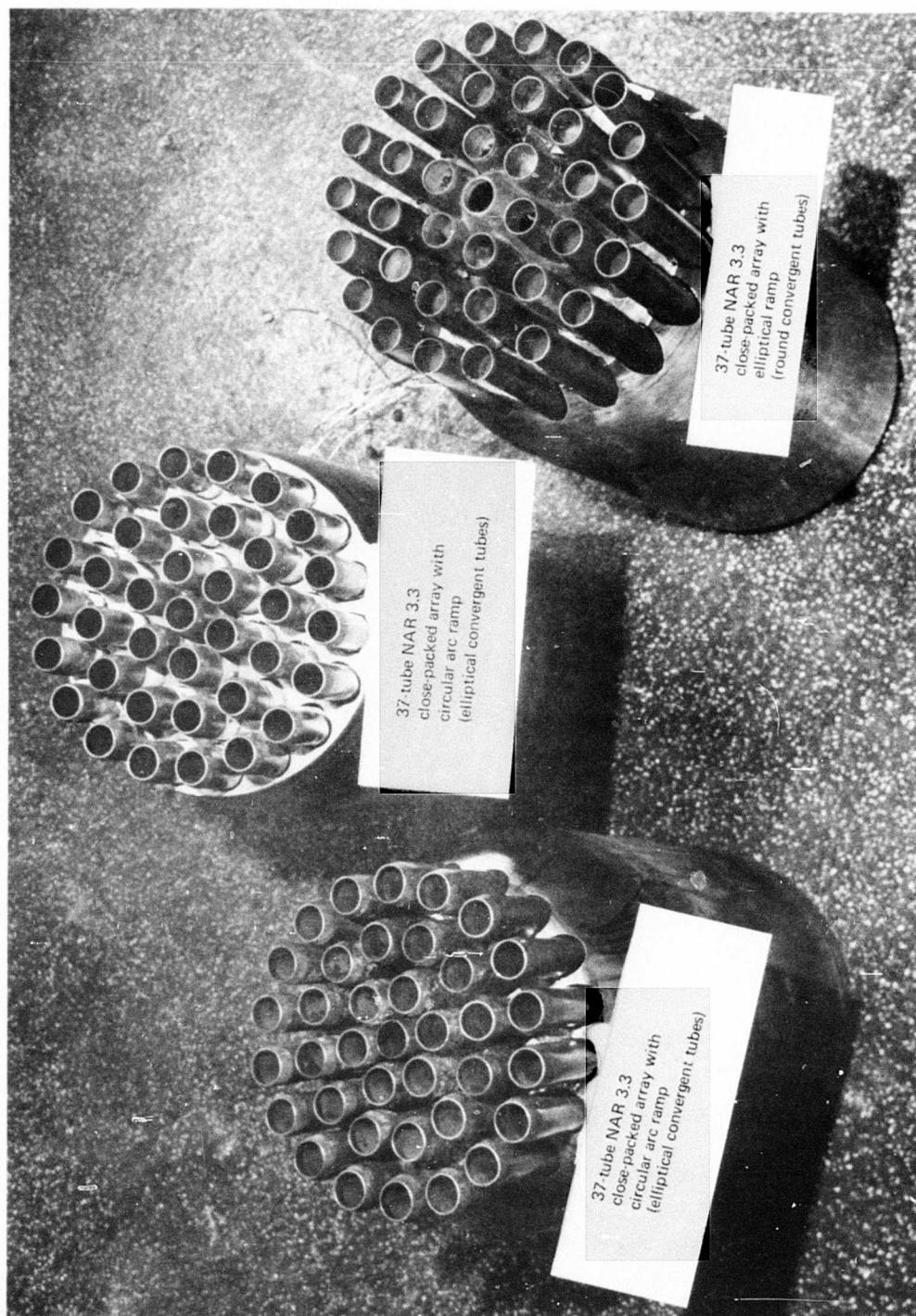


Figure 18.—Comparison of 37-Tube Area Ratio 3.3 Nozzles

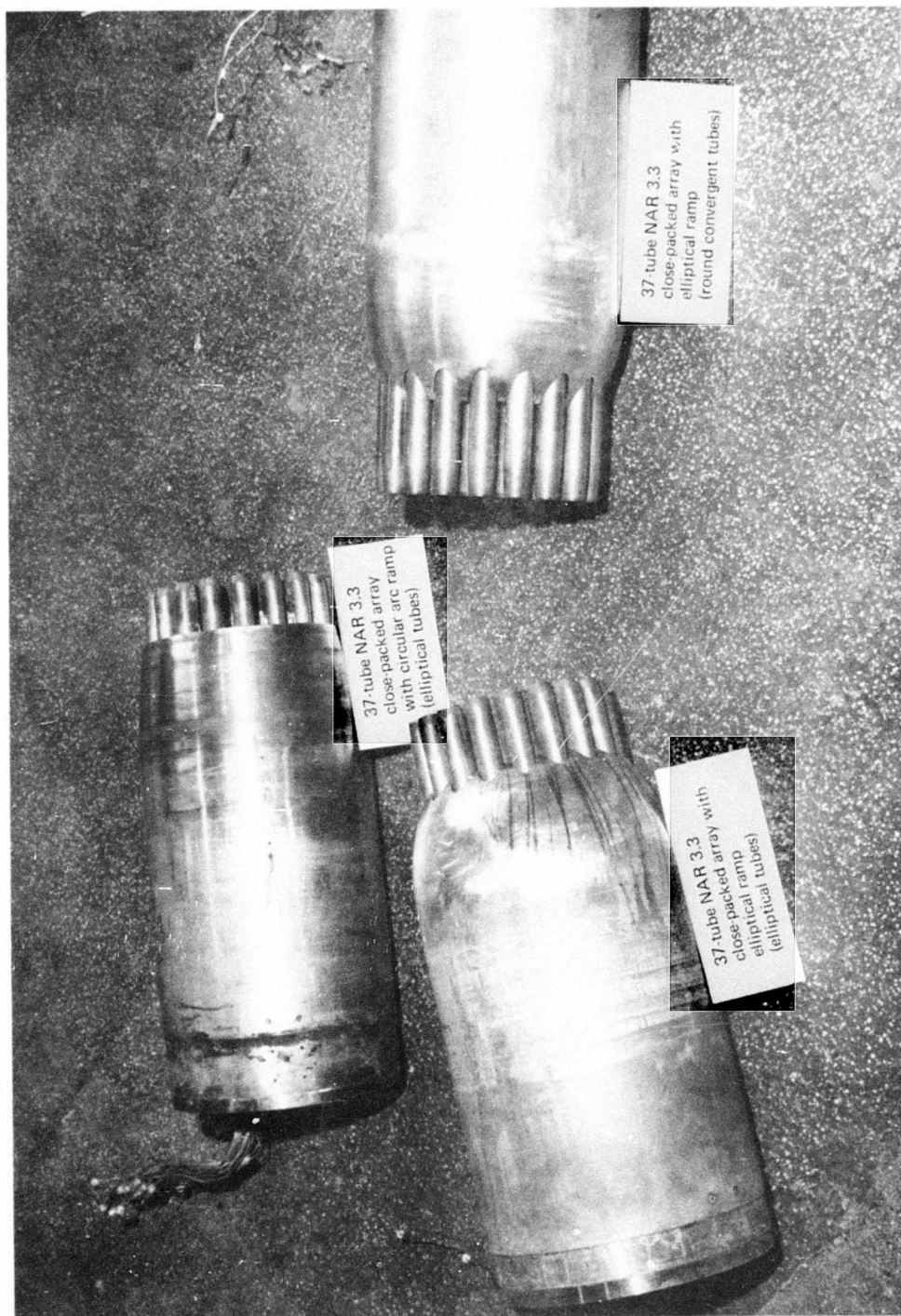
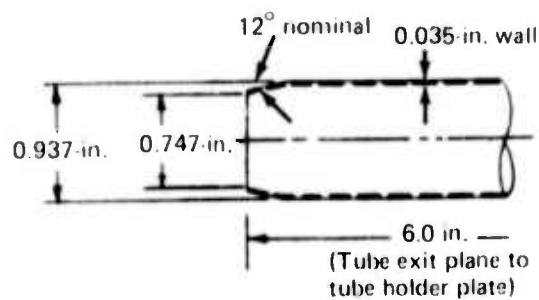


Figure 19.—37-Tube, Area-Ratio-3.3, Close-Packed Arrays With Various Ramps and Tube Shapes



Material—321 CRES
 Note: Center tube is a 0.875-in.-diam tube with 0.020-in. wall (0.835-in. i.d.) with a 12° nominal convergence to 0.747-in.-diam exit

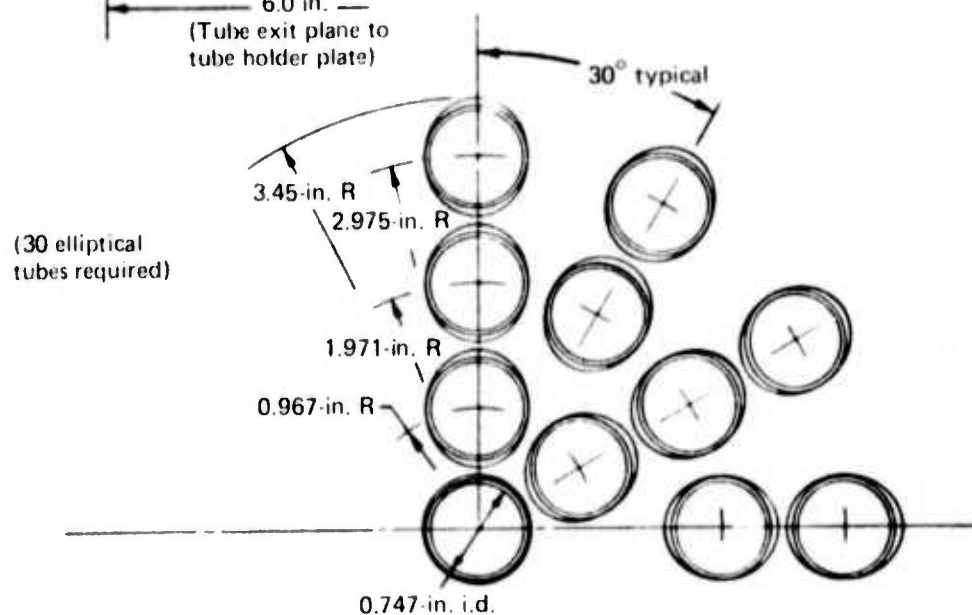


Figure 20. Radial Array Nozzles

4.2.9 SUMMARY OF SUPPRESSOR SPECIFICATIONS

Number of Tubes	Area Ratio	Effective Area Ratio	Array Type	A_p -in ²	A_S /1-in.	Type of Tube*	C_D^{**}	Mean diam to outside of outer jet
1 (R/C)	-	-		13.825		-	0.980	4.186 in.
19-Tube	3.3	3.1	Close-Packed	13.610	5.979	E.C.	0.983	7.262 in.
37-Tube	3.3	3.1	Close-Packed	13.543	6.197	E.C.	0.968	7.243 in.
37-Tube (R/37)	3.3	3.1	Close-Packed	13.695	5.269	R.C.	0.956	7.432 in.
61-Tube	3.3	3.1	Close-Packed	13.616	6.064	E.C.	0.969	7.257 in.
37-Tube	2.75	2.7	Close-Packed	13.432	4.369	E.C.	0.983	6.703 in.
31-Tube	1.75	2.7	Radial Array	13.610		E.C. (M=0.65)	0.970	6.703 in.

Percent of total flow exiting from outer row: 63%, 48%, and 38% for the 19-, 37-, and 61-tube, close-packed arrays, respectively; 38% for the 31-tube radial array

*E.C. elliptical converging to round exit (M=0.5)

R.C. round converging to round exit (M=0.5)

**Using C_D from reference 1

Detailed dimensions available for all configurations on Boeing drawing number 5457-0 through -8 and -10, -11 and -27

4.3 EJECTORS

4.3.1 GENERAL

Each ejector in the present investigation has a constant internal area. Tests were made over a range of effective ejector area ratios divided by effective nozzle area ratios from 1.0 to 1.4 ($R_{ej}^2/R_{in}^2 = 1.0$ to 1.4). Ejector area ratios (EAR) investigated were 2.6, 3.1, and 3.7. For most configurations, the tightest possible ejector was designed so that the wall of the ejector would coincide with the outermost boundary of the over-expanded plume of a jet issuing from the outer tube row at the highest pressure ratio (4.0, see fig. 3). Although the largest area ratio (3.7) was considered too large to be practical for SST application, it was used to demonstrate the effect of area ratio on lapse rate and performance.

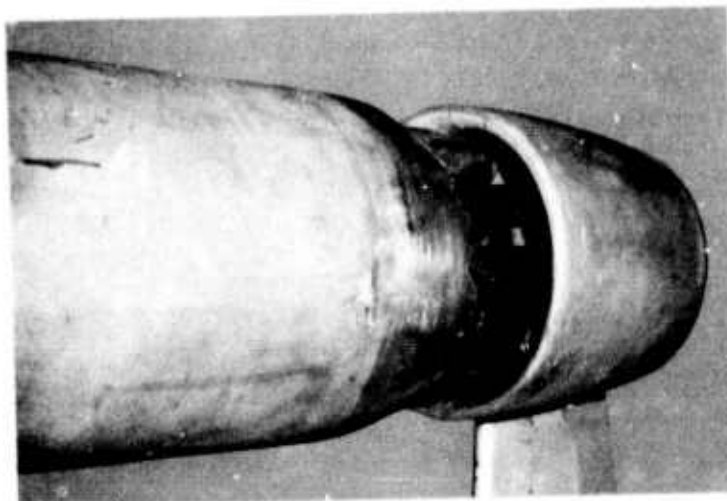


Figure 22.—View of Ejector Inlet: 19-Tube, NAR-3.3, Close-Packed Array With Elliptical Ramp; EAR 3.1 Ejector, Zero Setback

4.3.2 SUMMARY OF EJECTOR SPECIFICATIONS (See figs. 21, 23 and 24)

Ejector Area Ratio	Effective Ejector Area Ratio	Mean Re_j	R_H	R_O	L_E^* (in.)	L_A	L_B	Ejector Area (in ²)
2.6	2.7	3.33	3.74	4.09	8	6.83	1.17	34.9
3.1	3.2	3.678	4.28	4.45	8	6.83	1.17	42.5
3.7	3.8	3.99	4.67	5.00	8	6.67	1.33	50.1
3.7	3.8	3.990	4.67	5.00	24	22.67	1.33	50.0

*Length of ejector measured axially in inches from the ejector hilite to the ejector exit plane

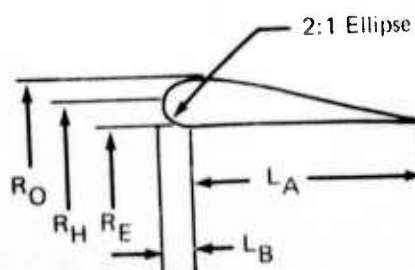


Figure 23.—Ejector Dimension Definition Sketch

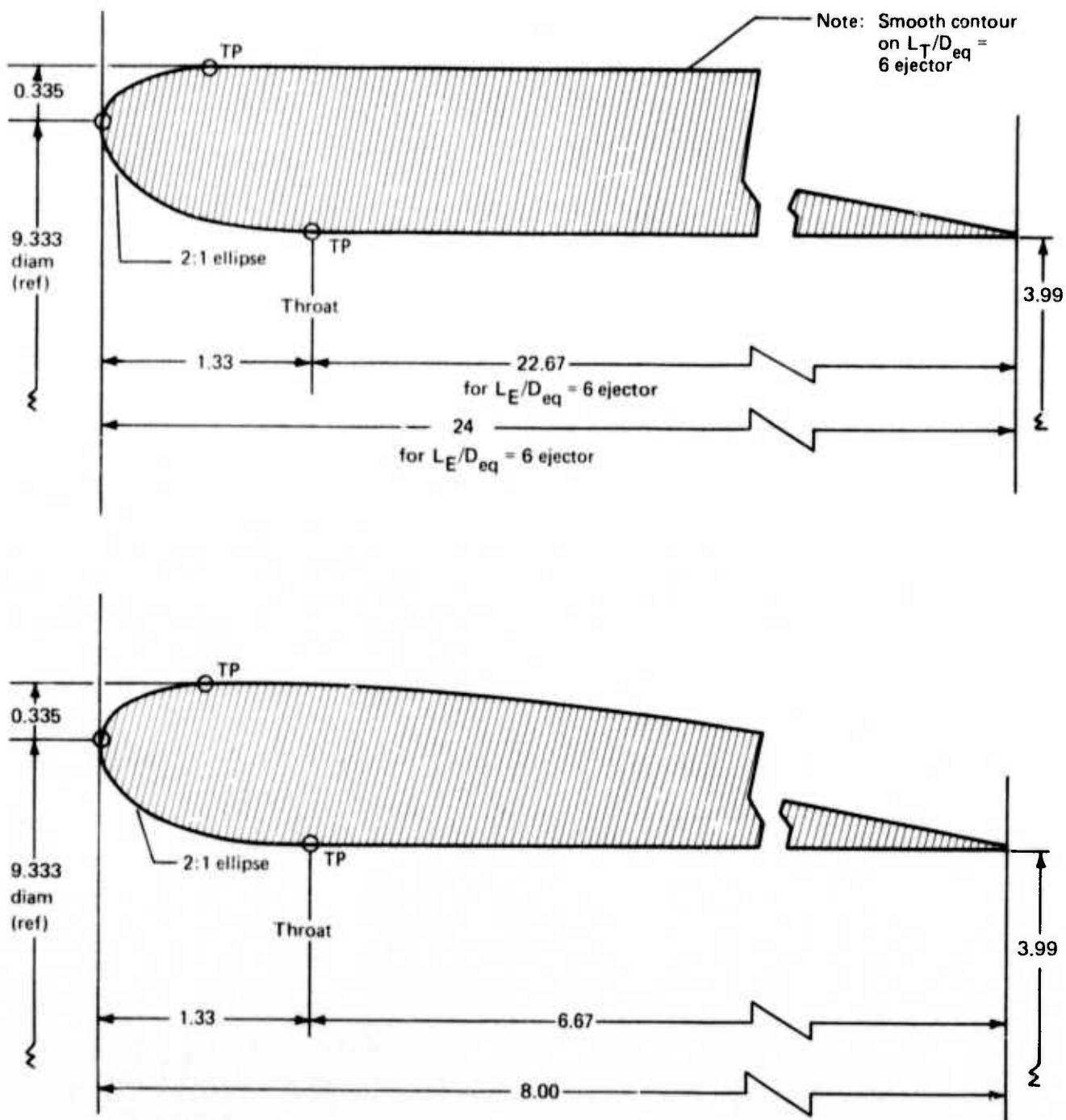


Figure 24.—Area Ratio (EAR) 3.7 Flight Ejectors $L_E/D_{eq} = 2$ and 6

5.0 EXPERIMENTAL PERFORMANCE RESULTS

5.1 INTRODUCTION

Gross thrust coefficient as a function of pressure ratio and velocity are summarized in this chapter for each of the suppressor/ejector configurations investigated. Carpet plots are used to allow determination of performance at intermediate pressure ratio and/or velocity points.

Although the values of C_{fg} change with configuration, the general shape of all bare suppressor performance curves is that shown on figure 25.

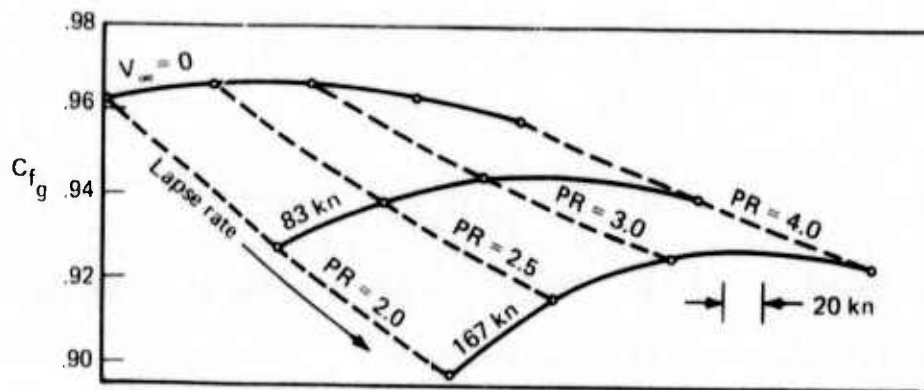


Figure 25.—General Form of Performance Carpet Plots for Bare Suppressors

Typical trends for multitube bare nozzles are:

- Maximum static performance occurs between pressure ratio 2.5 and 3.0.
- Lapse rate, $|\Delta C_{fg}| @ \Delta V_{\infty}$, decreases as pressure ratio increases.
- Thus, peak performance decreases and shifts to a higher pressure ratio as velocity increases.

The general shape of the suppressor/ejector performance curves is shown in figure 26.

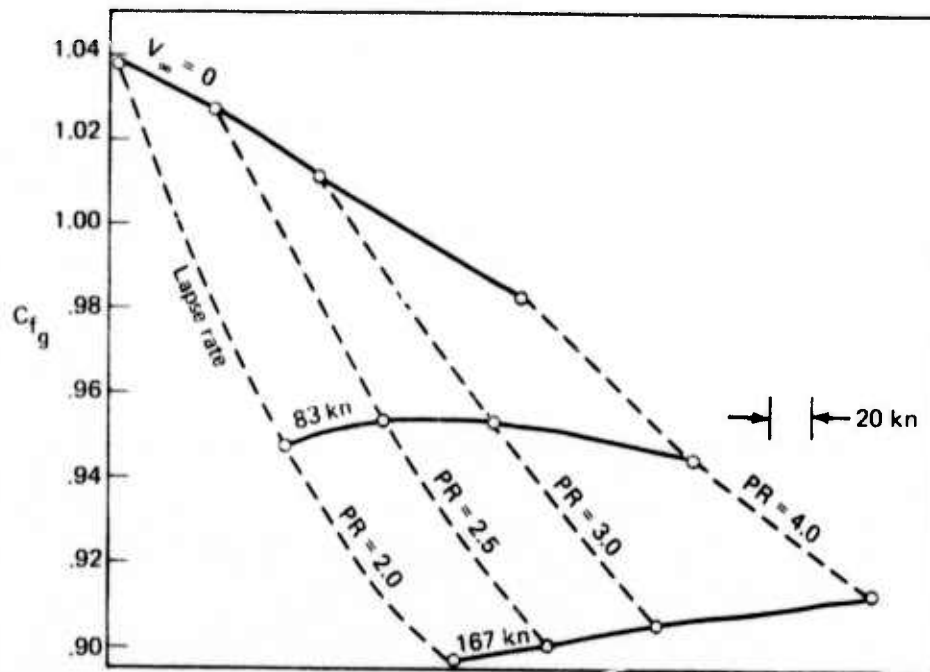


Figure 26.—General Form of Carpet Plots for Suppressor/Ejector Performance

Typical trends for suppressor/ejector nozzles are:

- Over the range of pressure ratios investigated (2-4), the maximum static performance occurs at or near pressure ratio = 2.
- The lapse rate, while still decreasing with increasing pressure ratio, is much larger (steeper) for ejectors than for similar bare suppressor cases.
- Thus, relative to a bare suppressor, as the velocity increases, the rate of performance decrease is greater and the pressure ratio at which the peak performance occurs moves to a higher value for the ejector case.

5.2 LIST OF PERFORMANCE CURVES

The following list indexes the summary performance (gross thrust coefficient) plots versus pressure ratio and velocity. Unless otherwise indicated, the configurations incorporate $L_T/D_{eq} = 0.5$, $L_E/D_{eq} = 2.0$, elliptical ramps, elliptical convergent tubes, and ambient jet temperature (figs. 27 through 60).

Configuration Versus Figure Number

Configuration					Figure Number
No. of tubes	NAR	EAR	SB/D _{eq}	Array	
1	-	-	-	Reference nozzle	27
19	3.3	none	-	C.P.	28
19	3.3	3.1	0.25	C.P.	29
19	3.3	3.7	0	C.P.	30
19	3.3	3.7	0.25	C.P.	31
37	2.75	2.6	0.25	C.P.	32
37	2.75	3.1	0	C.P.	33
37	2.75	3.1	0.25	C.P.	34
37	2.75	3.7	0	C.P.	35
37	2.75	3.7	0.25	C.P.	36
37	2.75	3.7	0	C.P.	37
37	3.3	none	-	C.P.	38
37	3.3	3.1	0	C.P.	39
37	3.3	3.1	0.25	C.P.	40
37	3.3	3.7	0	C.P.	41
37	3.3	3.1	0	C.P.	42
37	3.3	3.1	0.125	C.P.	43
37	3.3	3.1	0.25	C.P.	44
37	3.3	none	-	C.P.	45
37	3.3	3.1	0.25	C.P.	46
37	3.3	none	-	C.P.	47
37	3.3	3.1	0.25	C.P.	48
37	3.3	3.1	0	C.P.	49
37	3.3	3.7	0	C.P.	50
61	3.3	none	-	C.P.	51
61	3.3	3.1	0	C.P.	52
61	3.3	3.1	0.25	C.P.	53
31	2.75	none	-	Radial	54
31	2.75	2.6	0	Radial	55
31	2.75	2.6	0.25	Radial	56
31	2.75	3.1	0	Radial	57
31	2.75	3.1	0.25	Radial	58
31	2.75	3.7	0	Radial	59
31	2.75	3.1	0	Radial	60

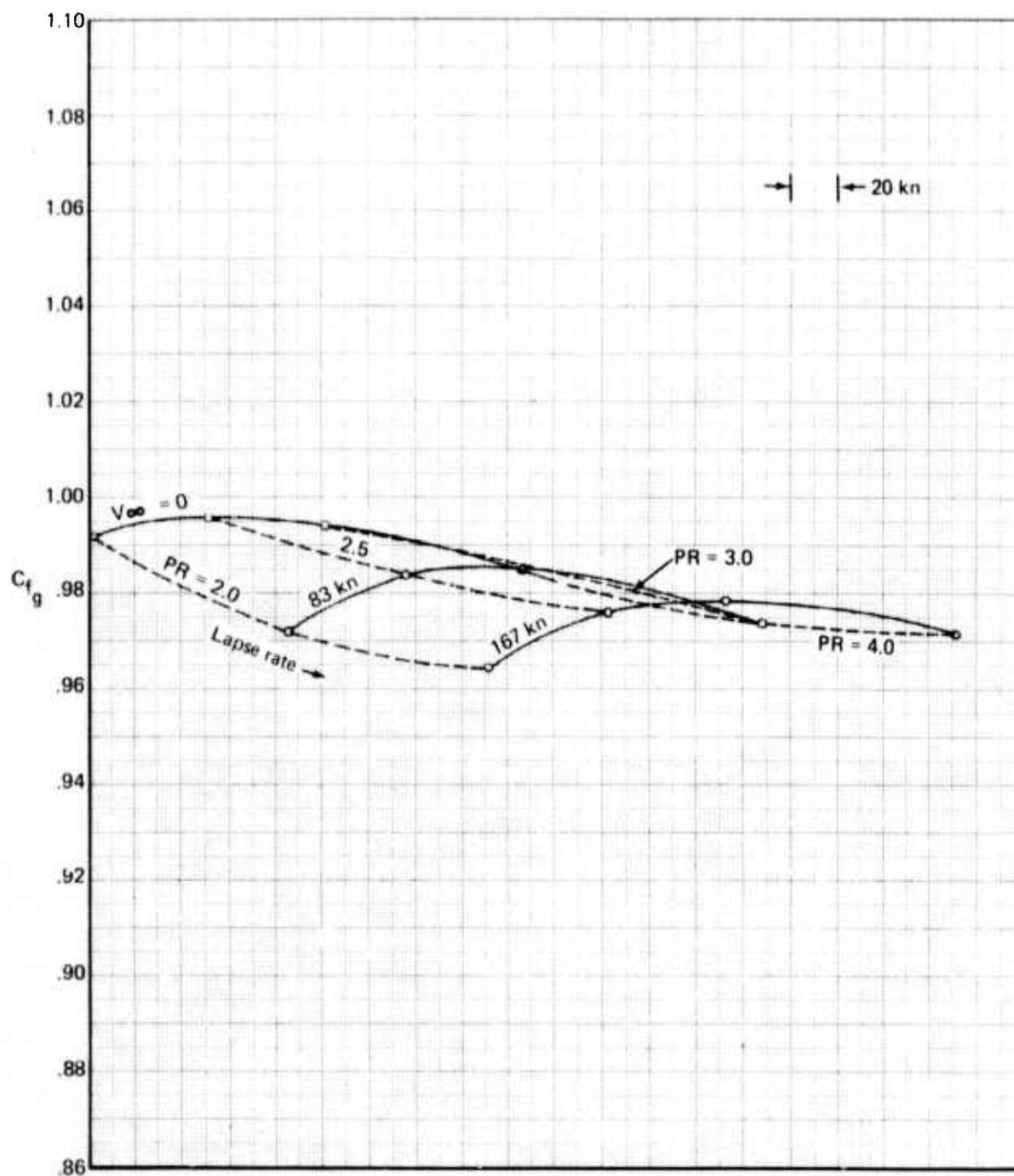


Figure 27.—Gross Thrust Coefficient for the Round Convergent Reference Nozzle, No Ejector

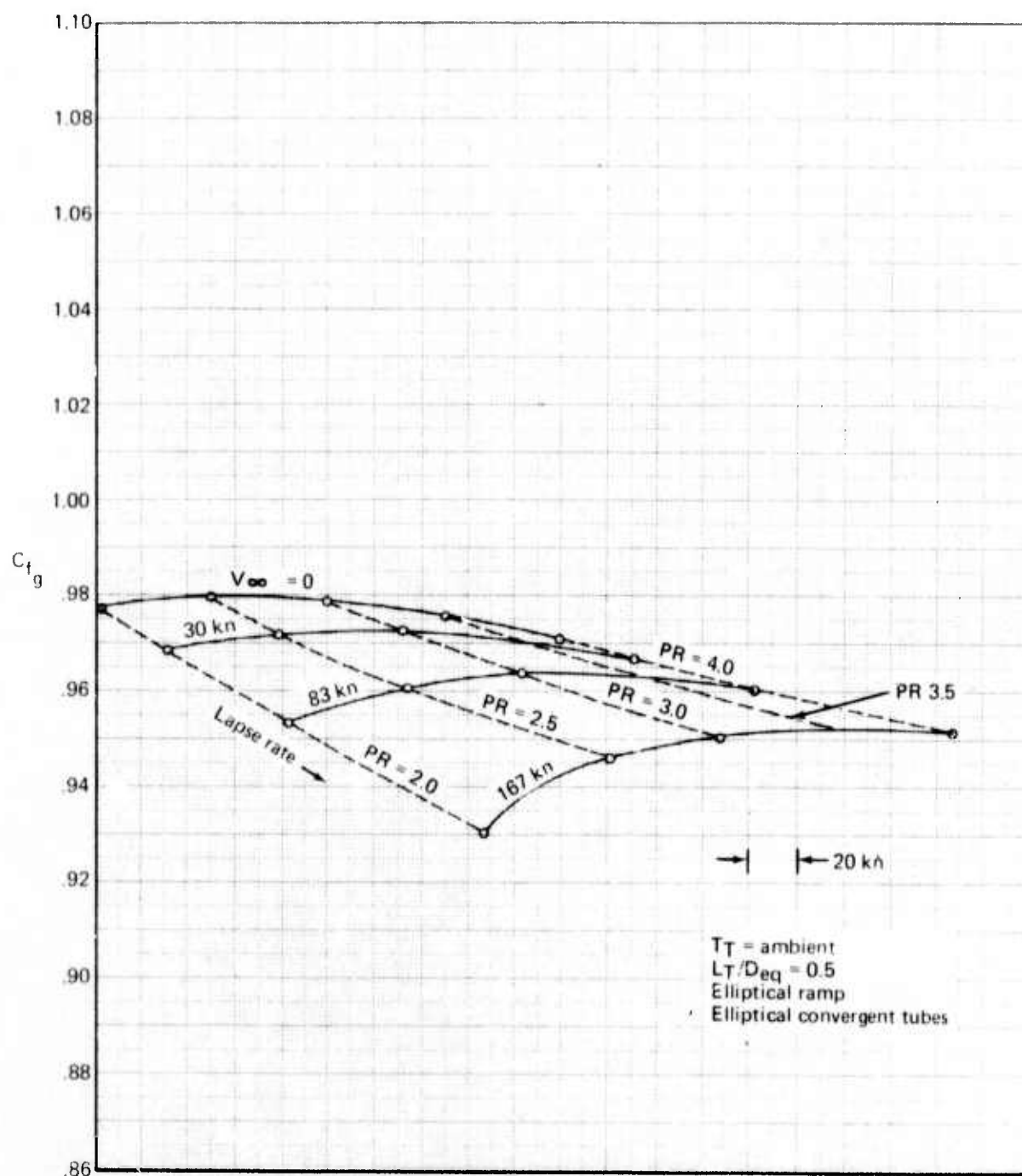


Figure 28.—Gross Thrust Coefficient for 19-Tube, $NAR = 3.3$, Close-Packed Array Without Ejector

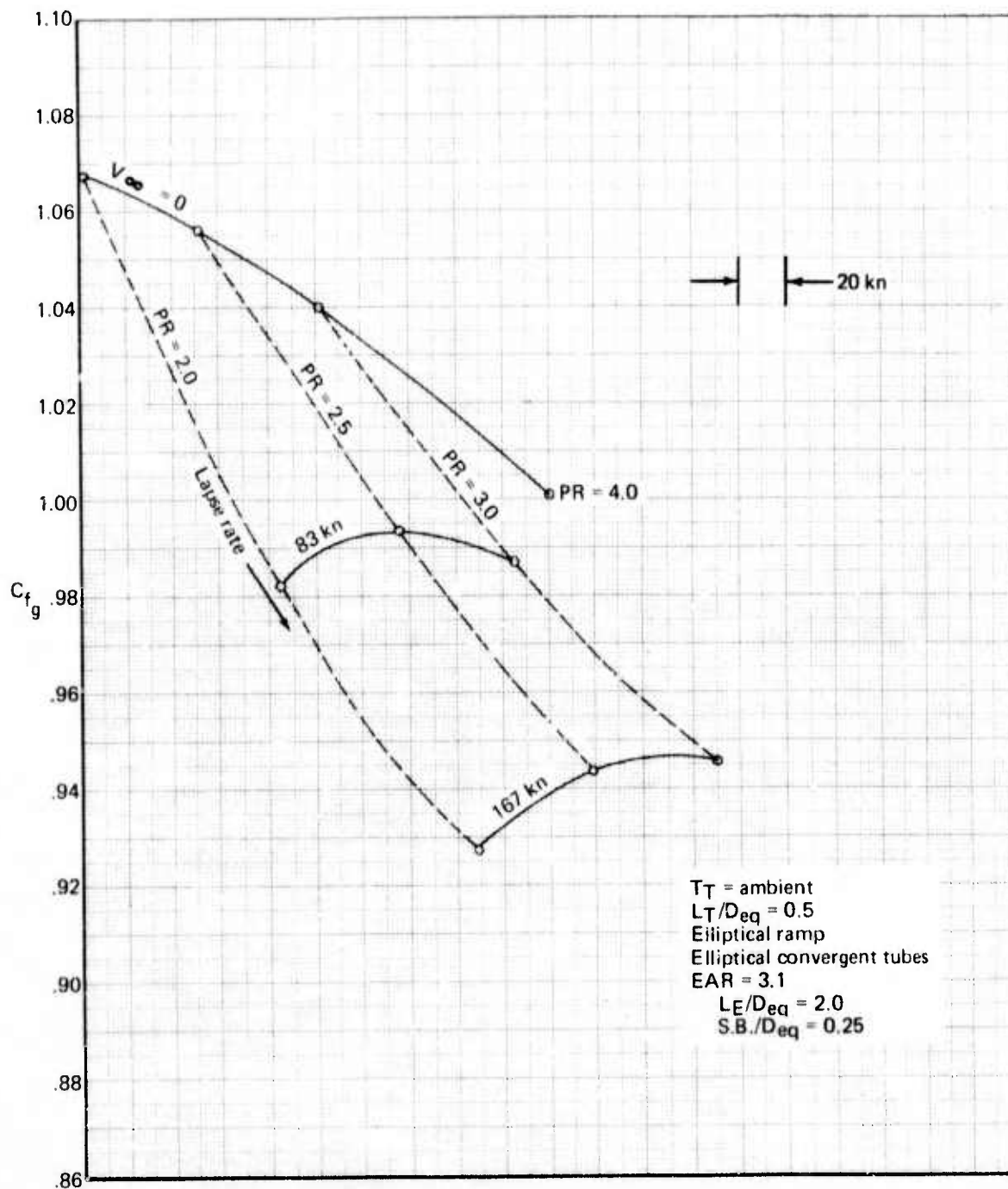


Figure 29.—Gross Thrust Coefficient for 19-Tube, NAR-3.3, Close-Packed Array With $EAR = 3.1$ Ejector (Setback 0.25)

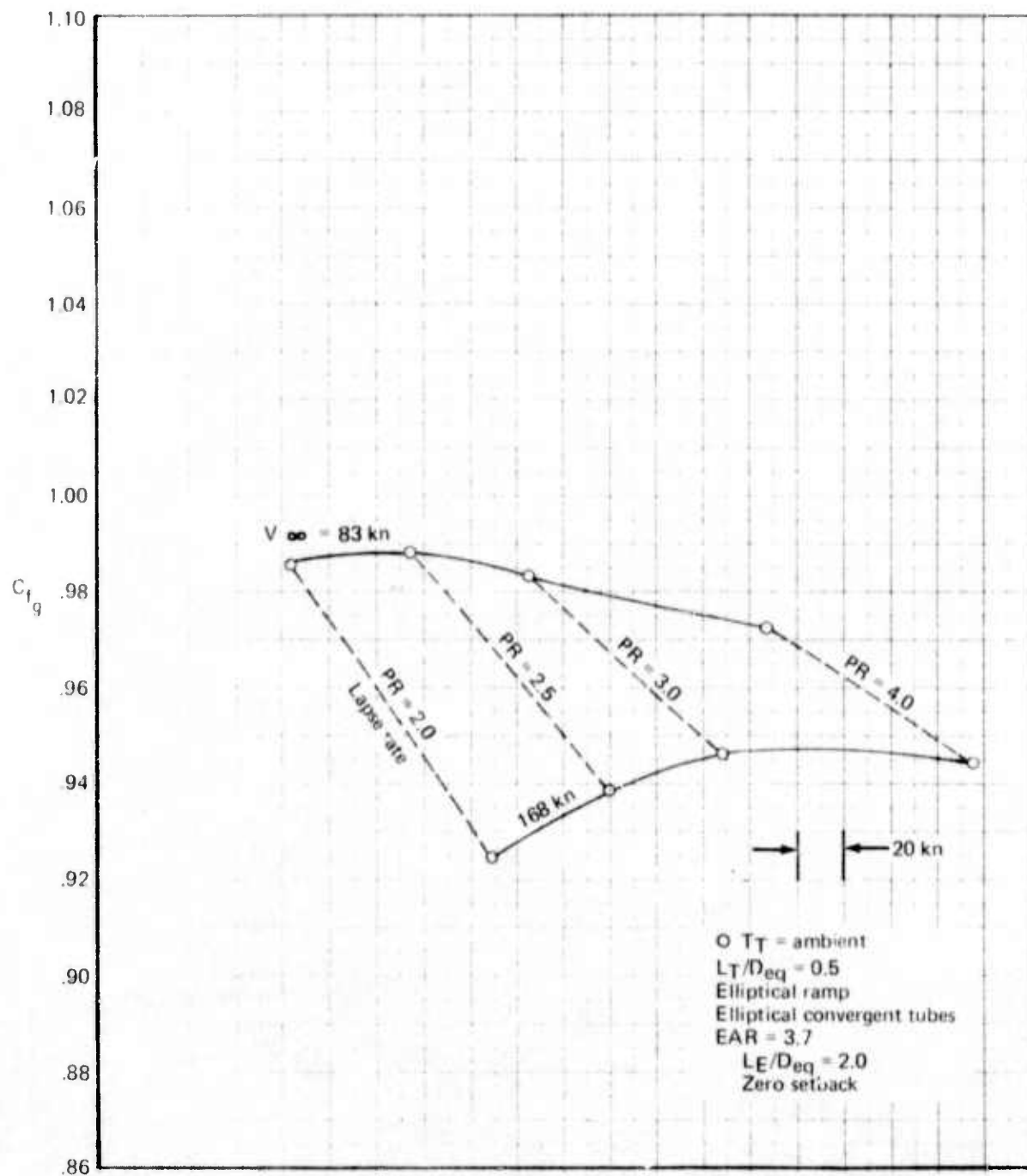


Figure 30.—Gross Thrust Coefficient for 19-Tube, NAR = 3.3, Close-Packed Array With EAR = 3.7 Ejector

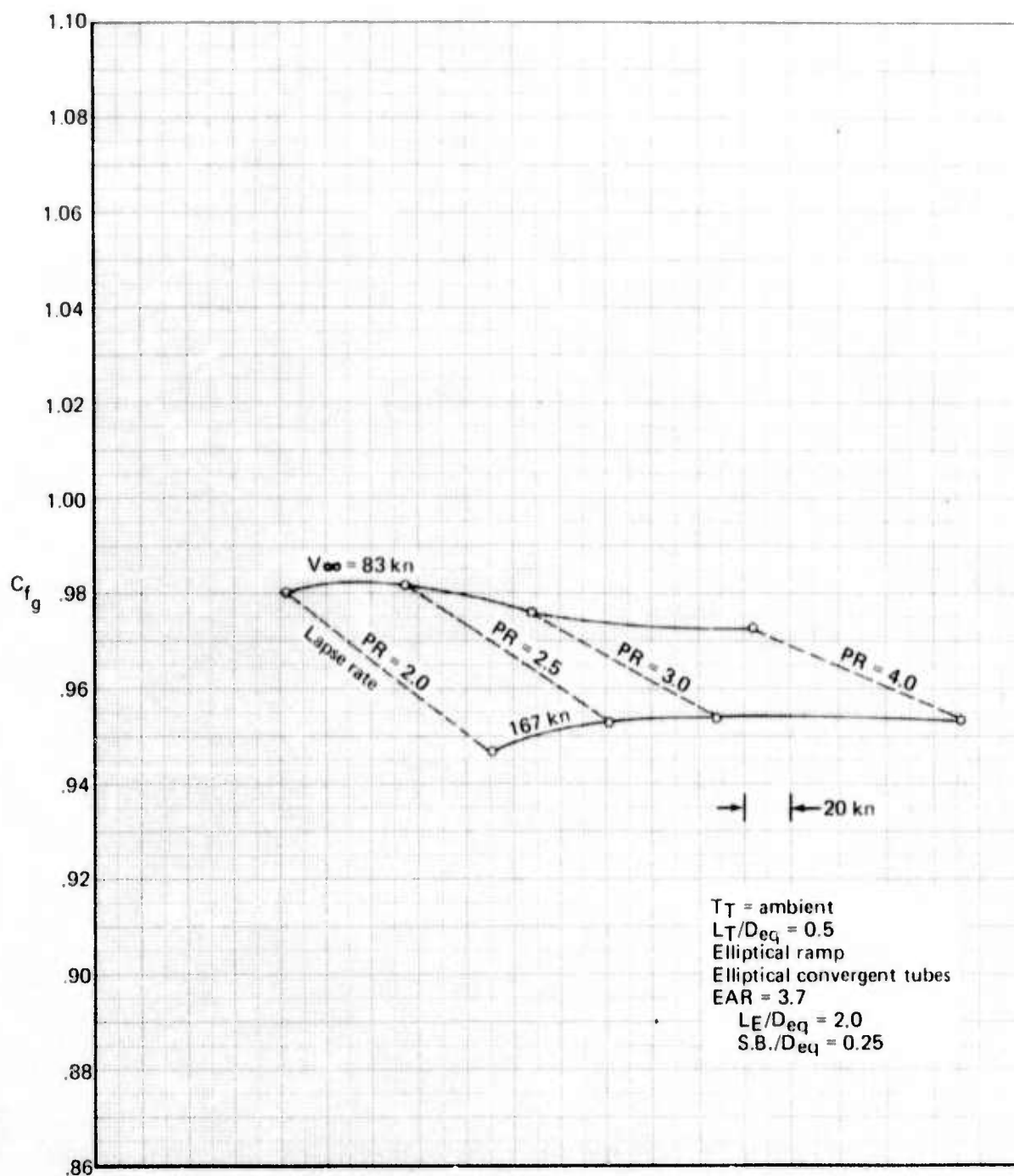


Figure 31.—Gross Thrust Coefficient for 19-Tube, NAR-3.3, Close-Packed Array With $EAR = 3.7$ Ejector (Setback 0.25)

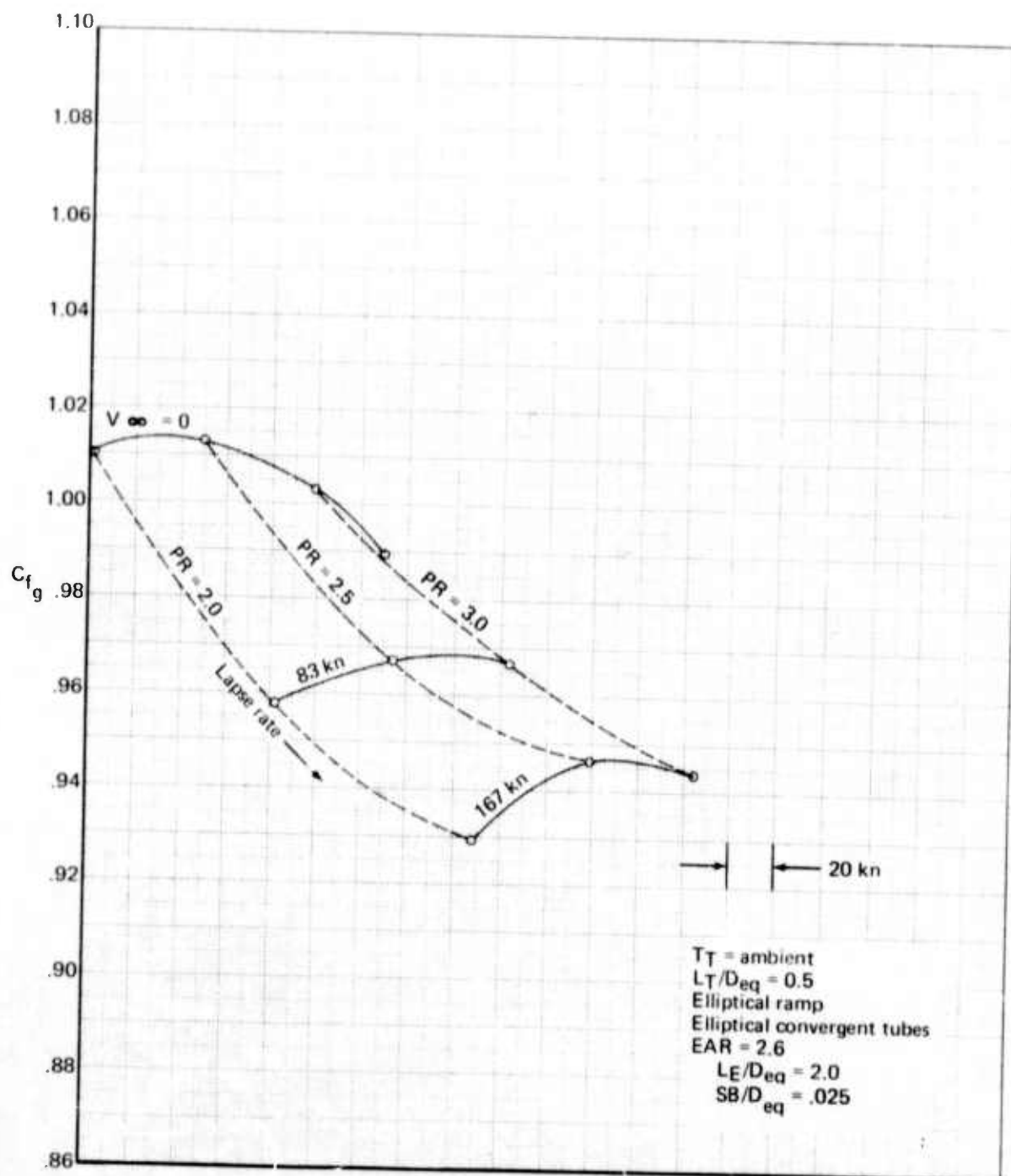


Figure 32.—Gross Thrust Coefficient for 37-Tube, $NAR = 2.75$, Close-Packed Array With $EAR = 2.6$ Ejector (Setback 0.25)

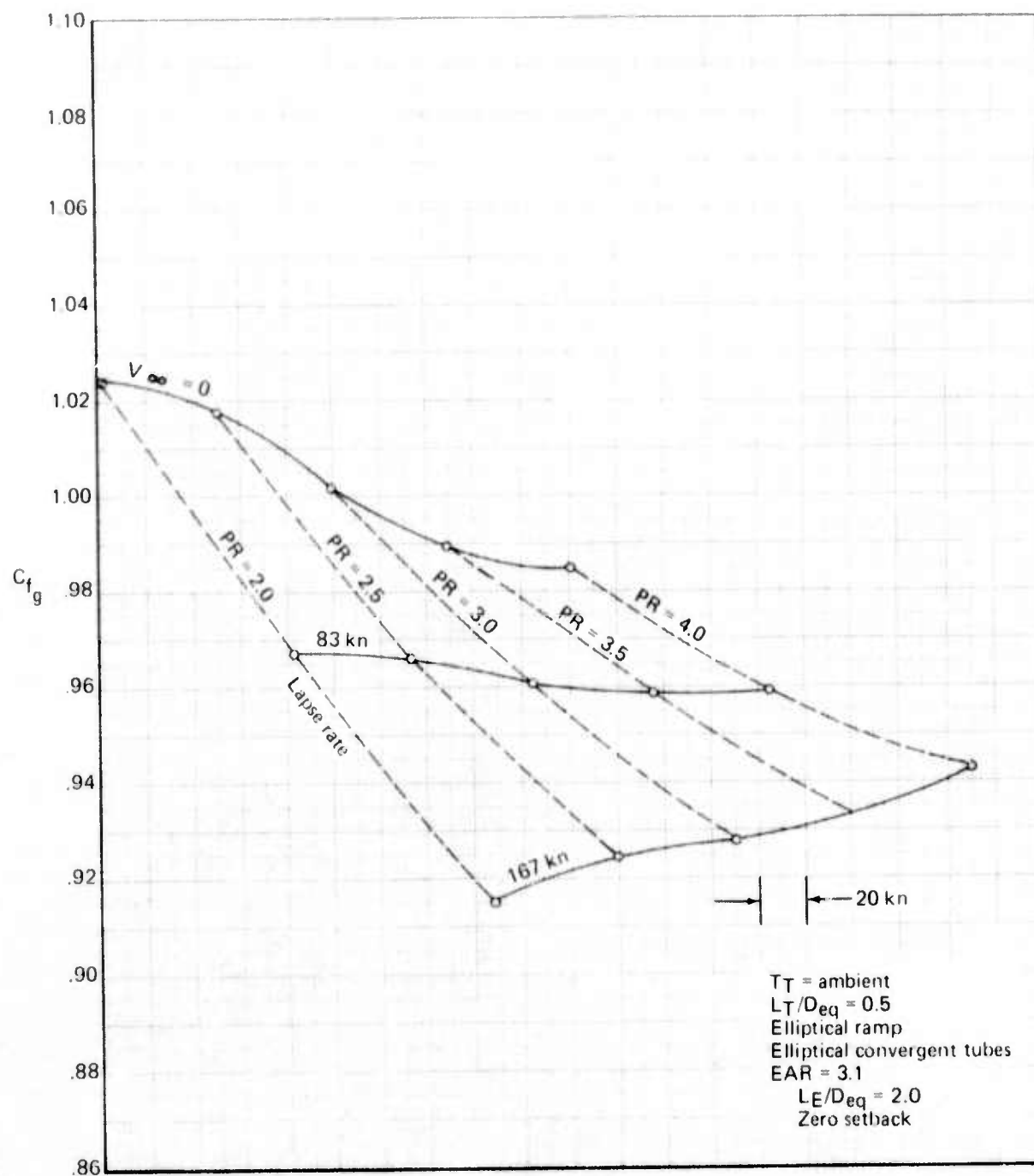


Figure 33.—Gross Thrust Coefficient for 37-Tube, $NAR = 2.75$, Close-Packed Array With $EAR = 3.1$ Ejector

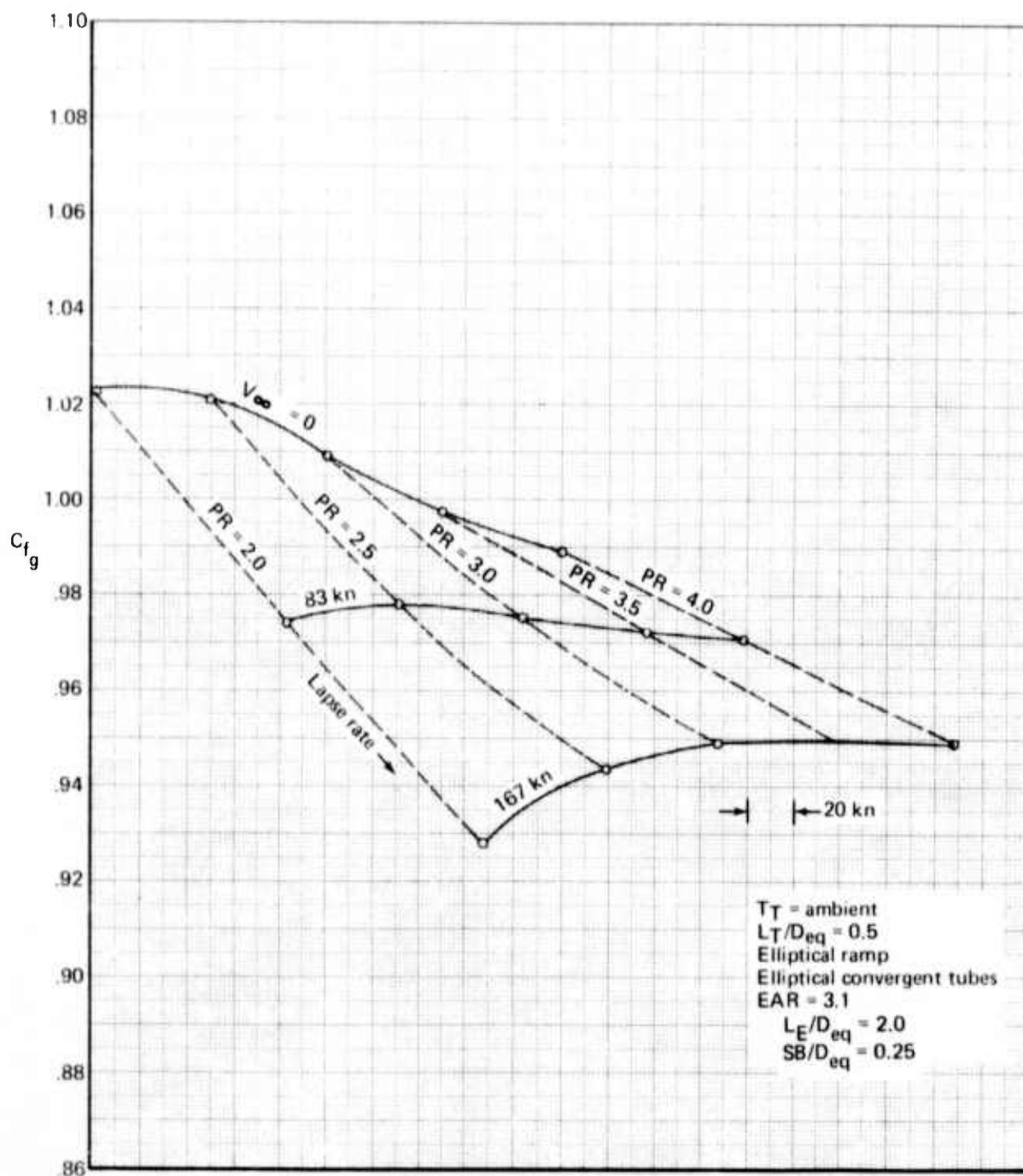


Figure 34.—Gross Thrust Coefficient for 37-Tube, $NAR = 2.75$, Close-Packed Array With $EAR = 3.1$ Ejector (Setback 0.25)

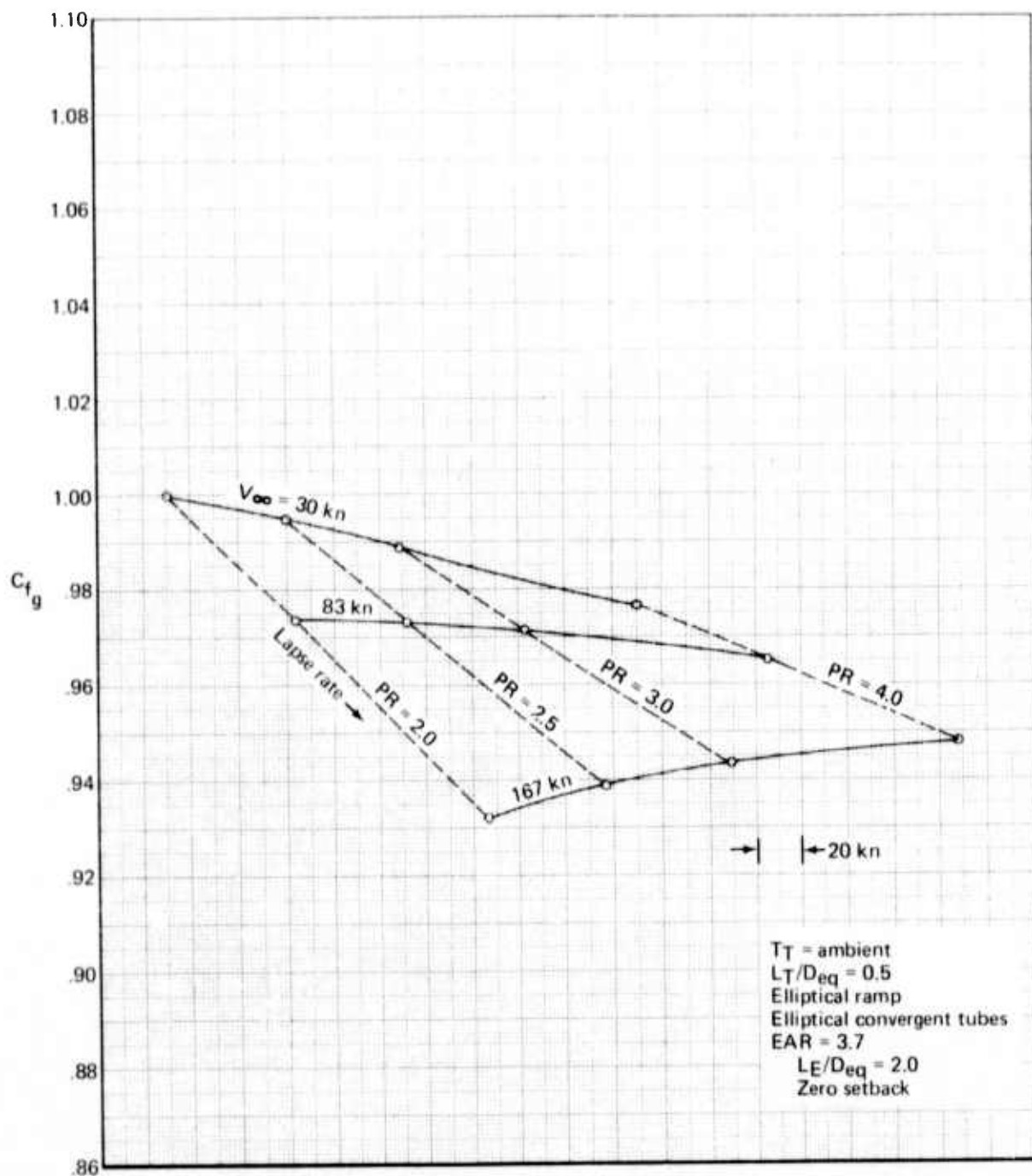


Figure 35.—Gross Thrust Coefficient for 37-Tube, $NAR = 2.75$, Close-Packed Array With $EAR = 3.7$ Ejector

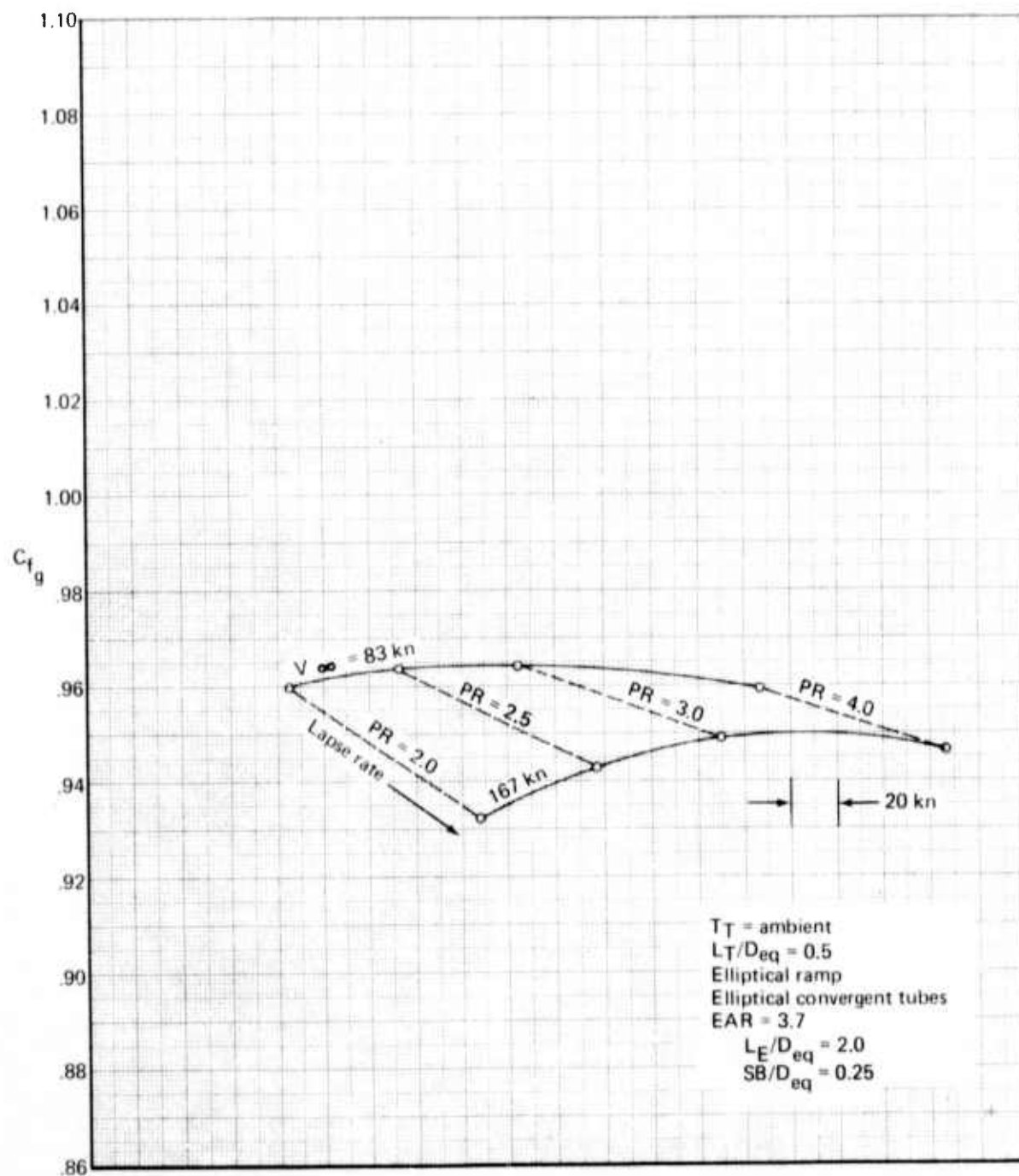


Figure 36.—Gross Thrust Coefficient for 37-Tube, $NAR = 2.75$, Close-Packed Array With $EAR = 3.7$ Ejector (Setback 0.25)

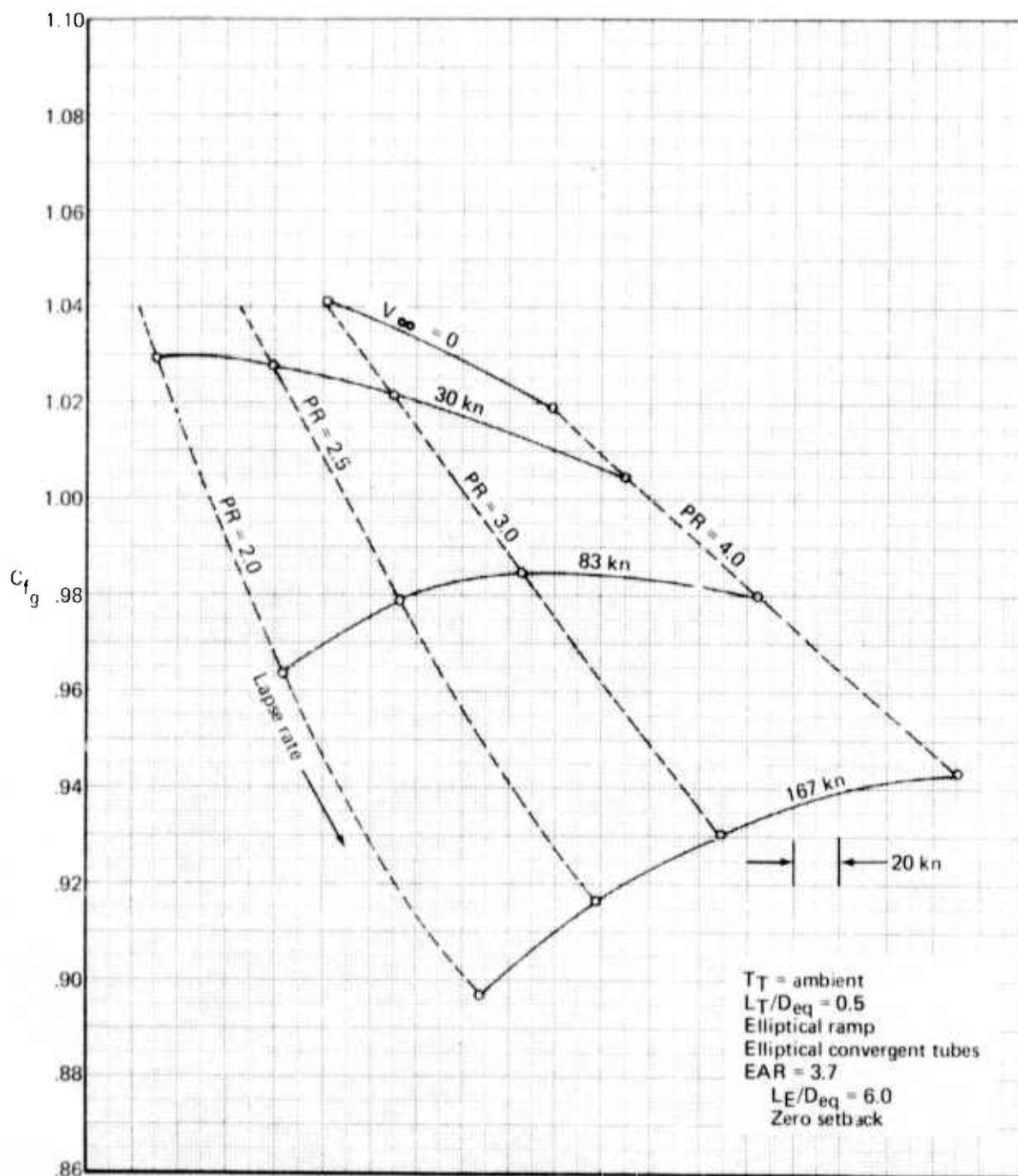


Figure 37.—Gross Thrust Coefficient for 37-Tube, $NAR = 2.75$, Close-Packed Array With $EAR = 3.7$ Ejector (Length $L_E/D_{eq} = 6.0$)

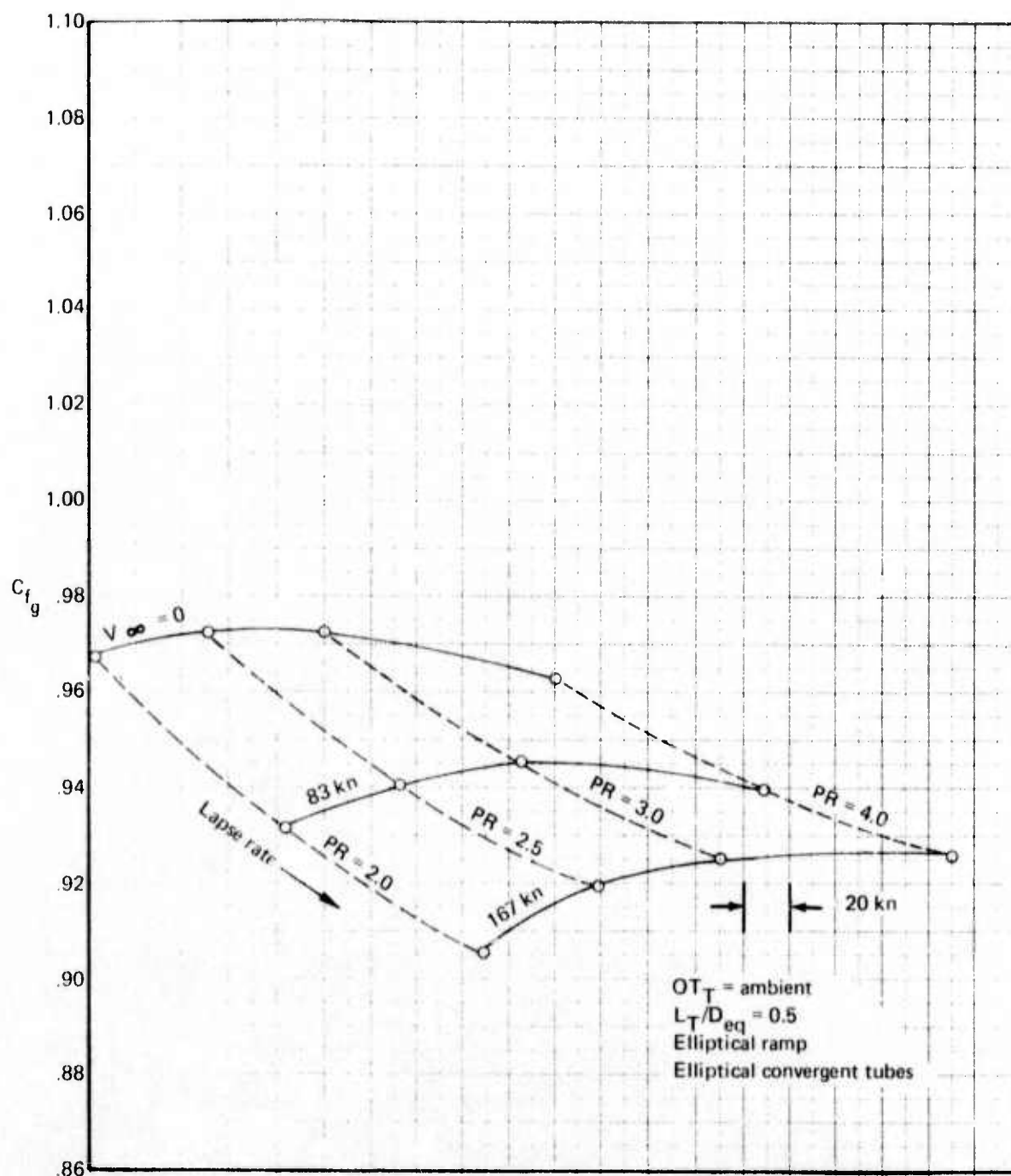


Figure 38.—Gross Thrust Coefficient for 37-Tube, $NAR = 3.3$, Close-Packed Array Without Ejector

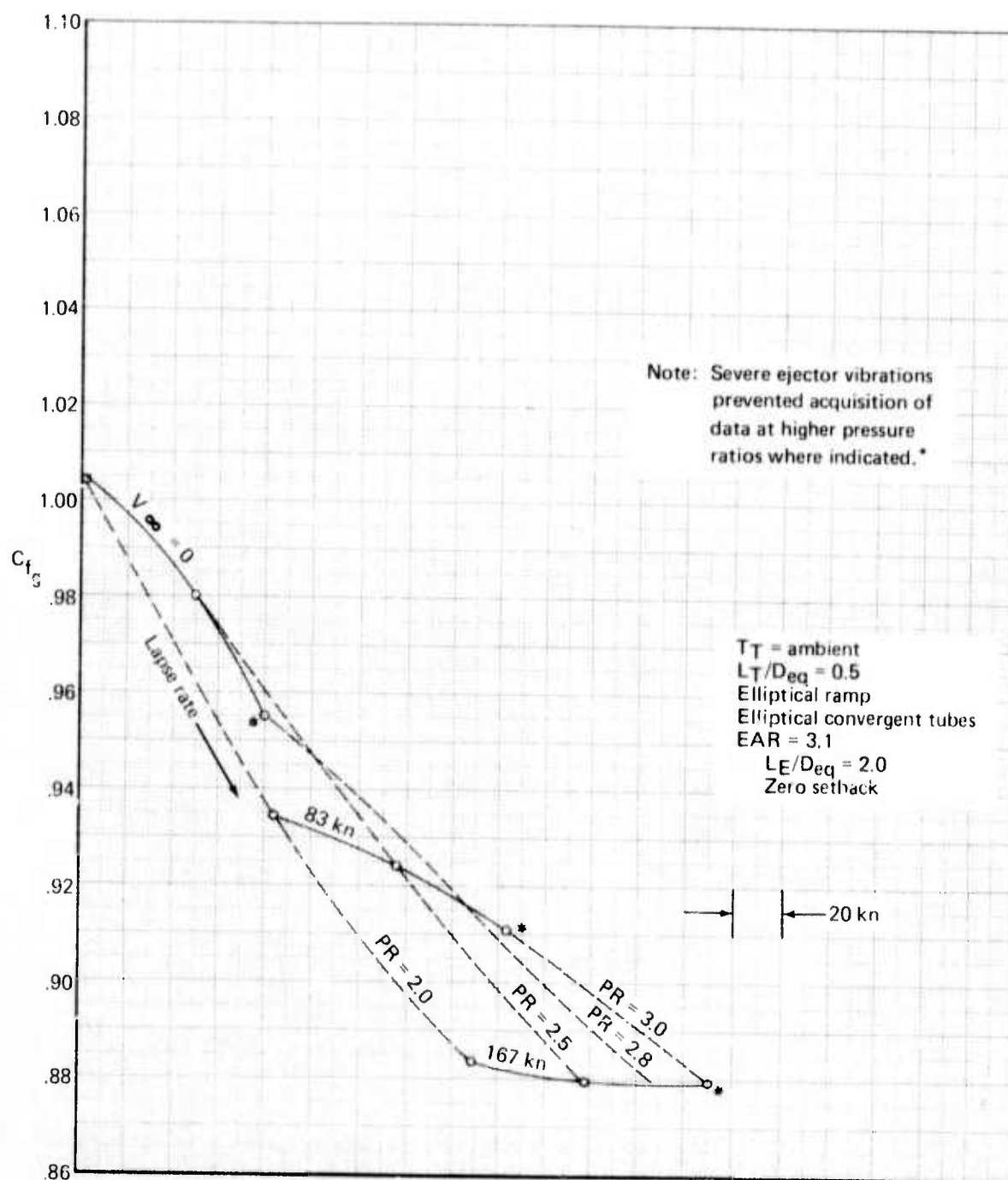


Figure 39.—Gross Thrust Coefficient for 37-Tube, $NAR = 3.3$, Close-Packed Array With $EAR = 3.1$ Ejector

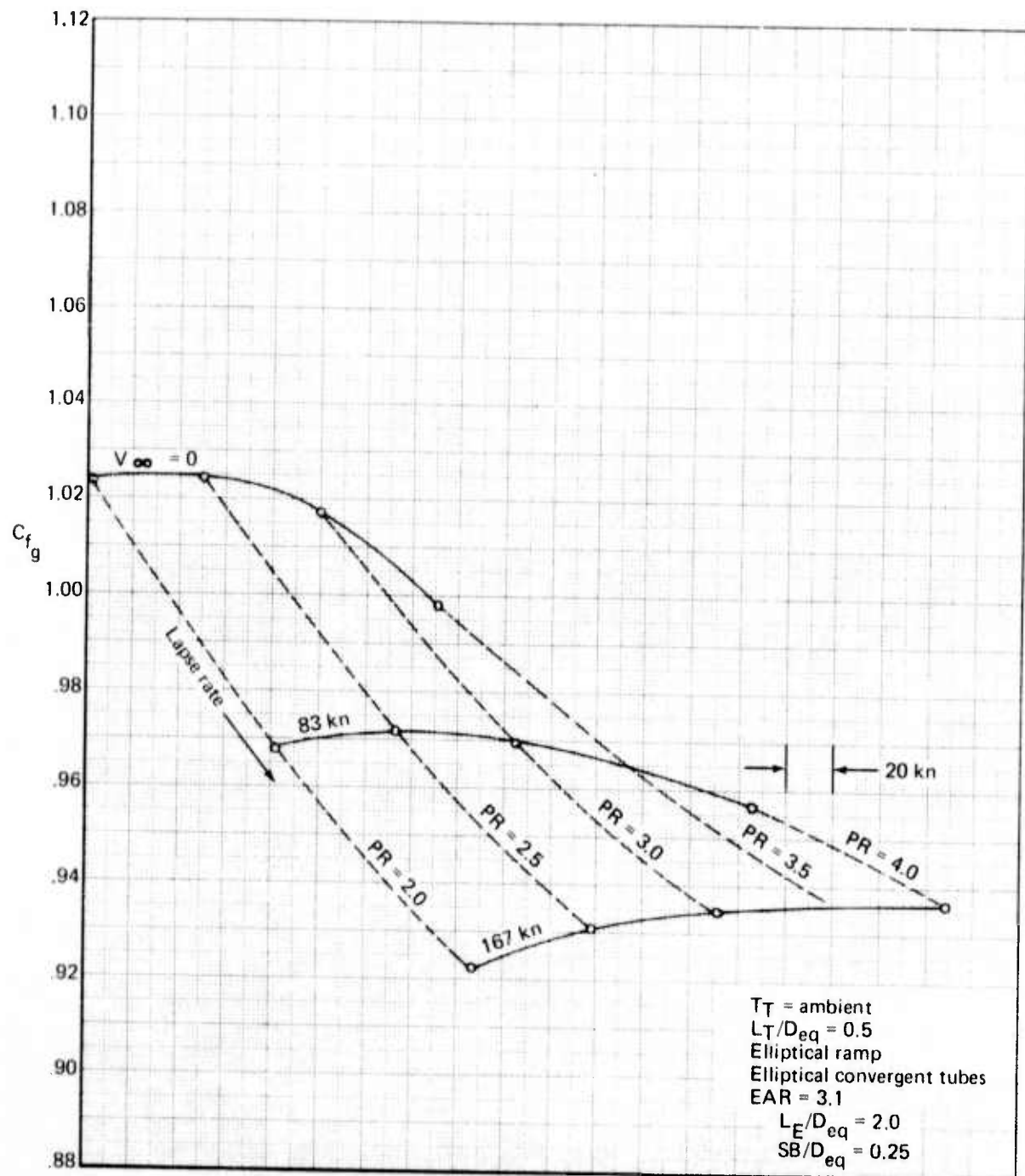


Figure 40.—Gross Thrust Coefficient for 37-Tube, $NAR = 3.3$, Close-Packed Array With $EAR = 3.1$ Ejector (Setback 0.25)

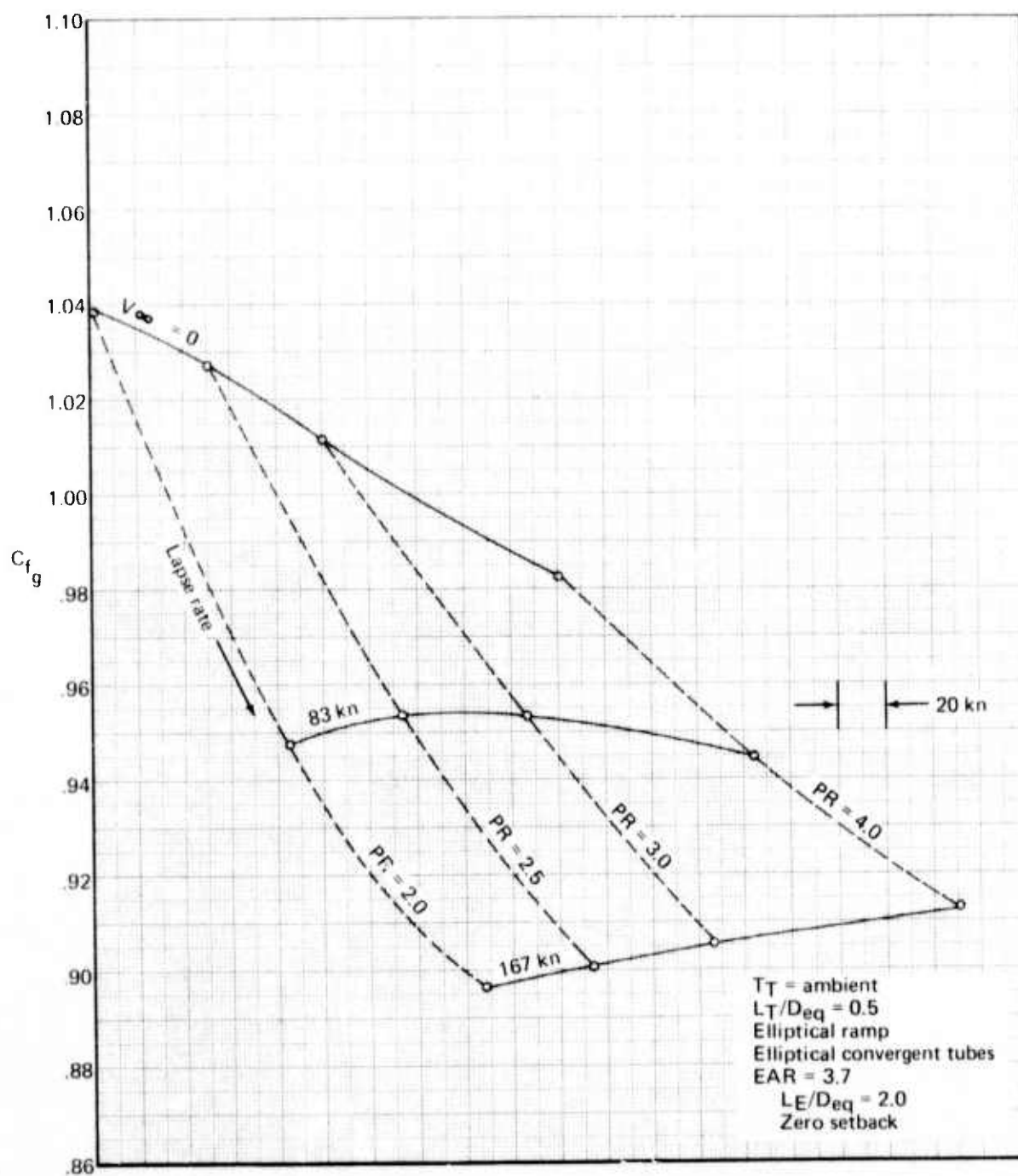


Figure 41.—Gross Thrust Coefficient for 37-Tube, $NAR = 3.3$, Close-Packed Array With $EAR = 3.7$ Ejector

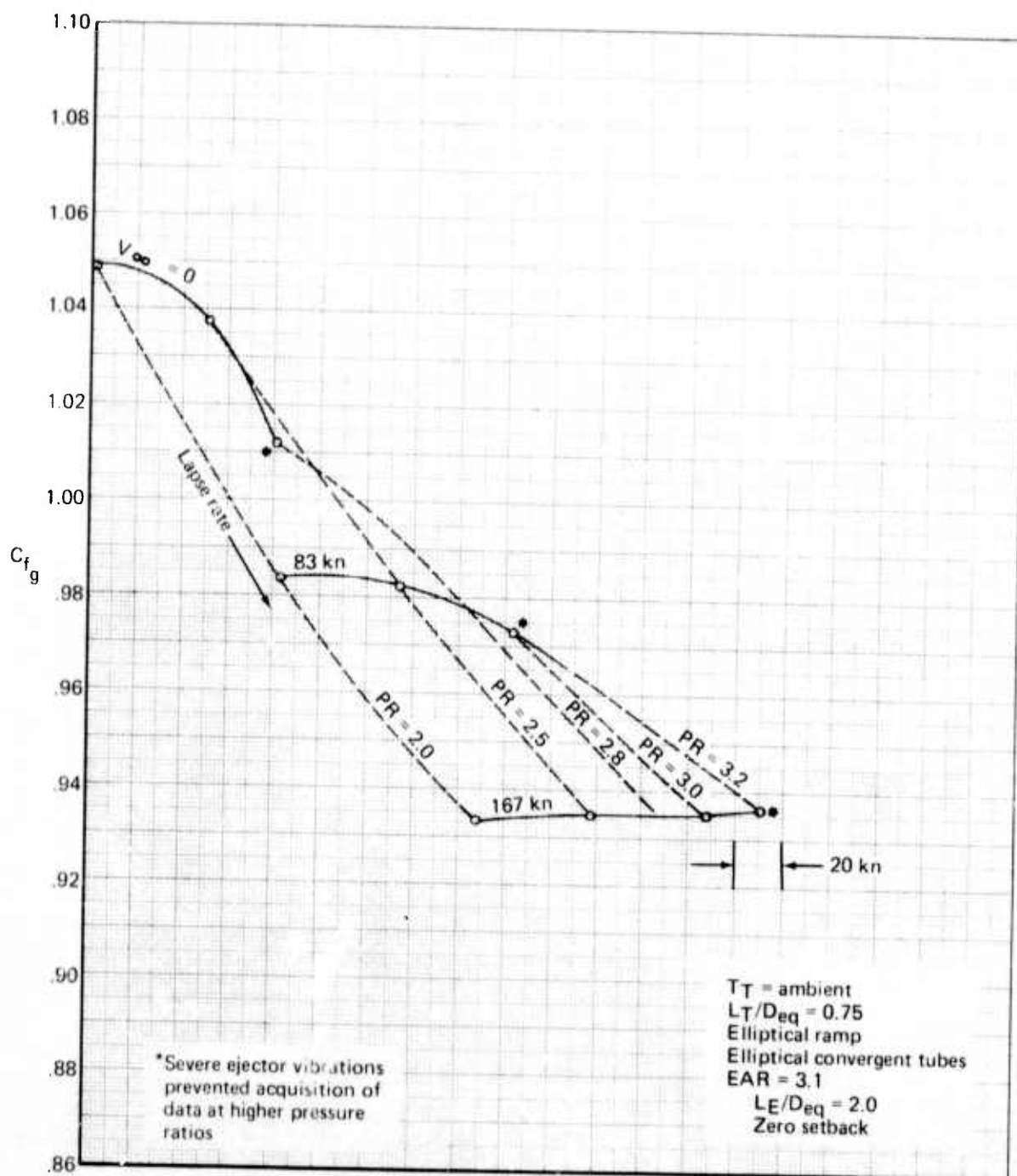


Figure 42.—Gross Thrust Coefficient for 37-Tube, NAR = 3.3, Close-Packed Array (L_T/D_{eq} = 0.75) With EAR = 3.1 Ejector

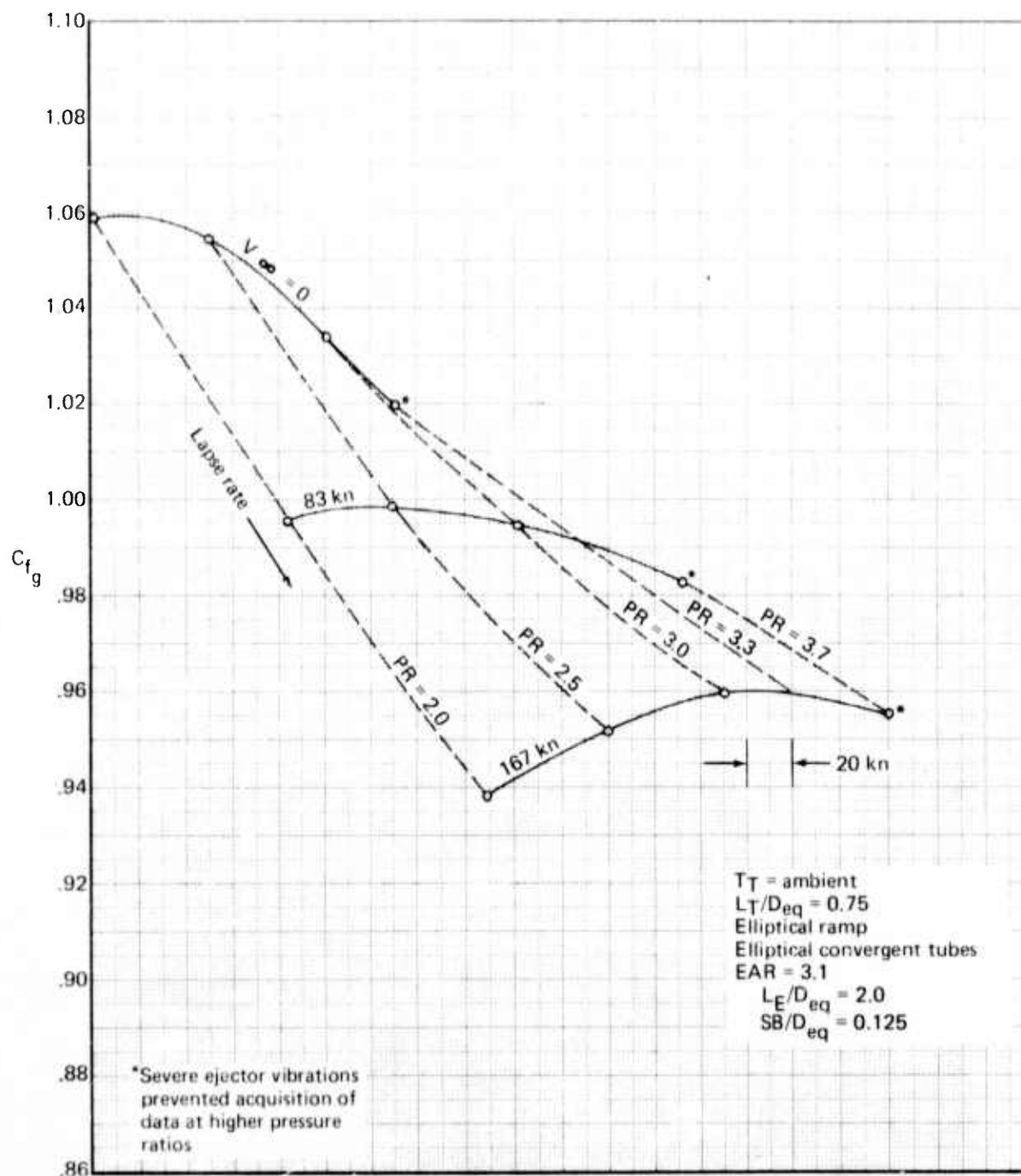


Figure 43.—Gross Thrust Coefficient for 37-Tube, NAR = 3.3, Close-Packed Array ($L_T/D_{eq} = 0.75$) With $EAR = 3.1$ Ejector (Setback 0.125)

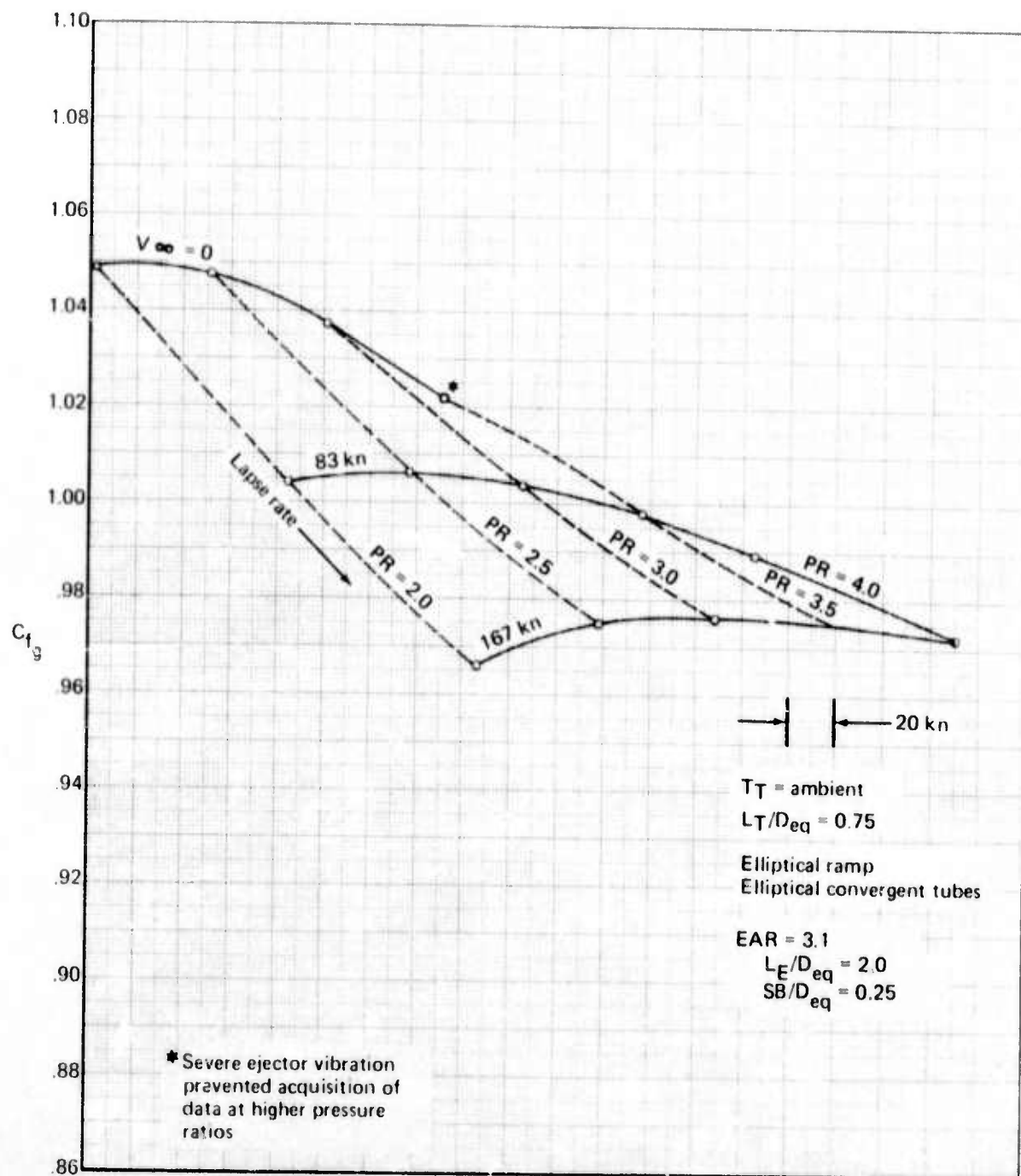


Figure 44.—Gross Thrust Coefficient for 37-Tube, $NAR = 3.3$, Close-Packed Array ($L_T/D_{eq} = 0.75$) With $EAR = 3.1$ Ejector (Setback 0.250)

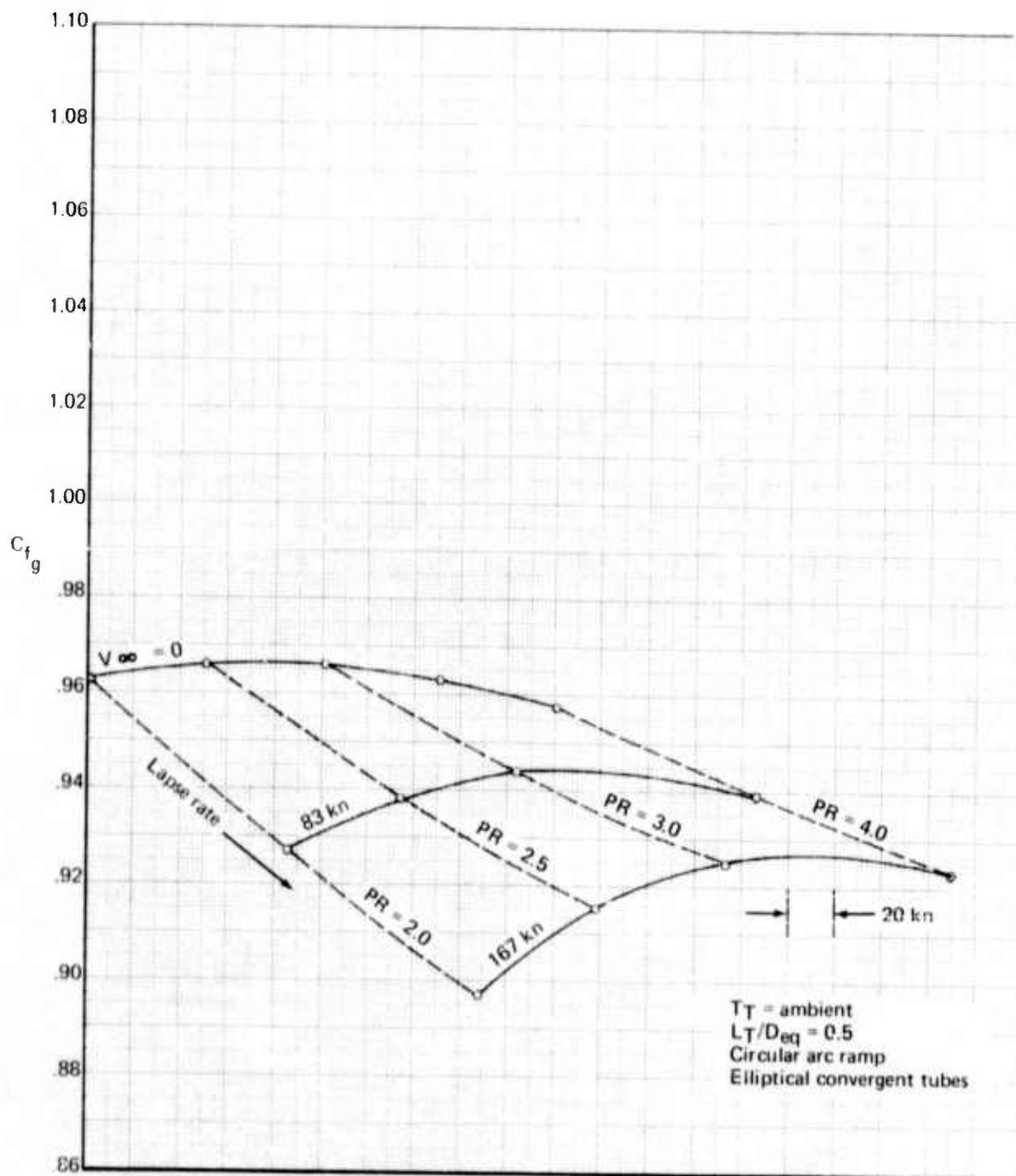


Figure 45.—Gross Thrust Coefficient for 37-Tube, $NAR = 3.3$, Close-Packed Array, Circular Arc Ramp Without Ejector

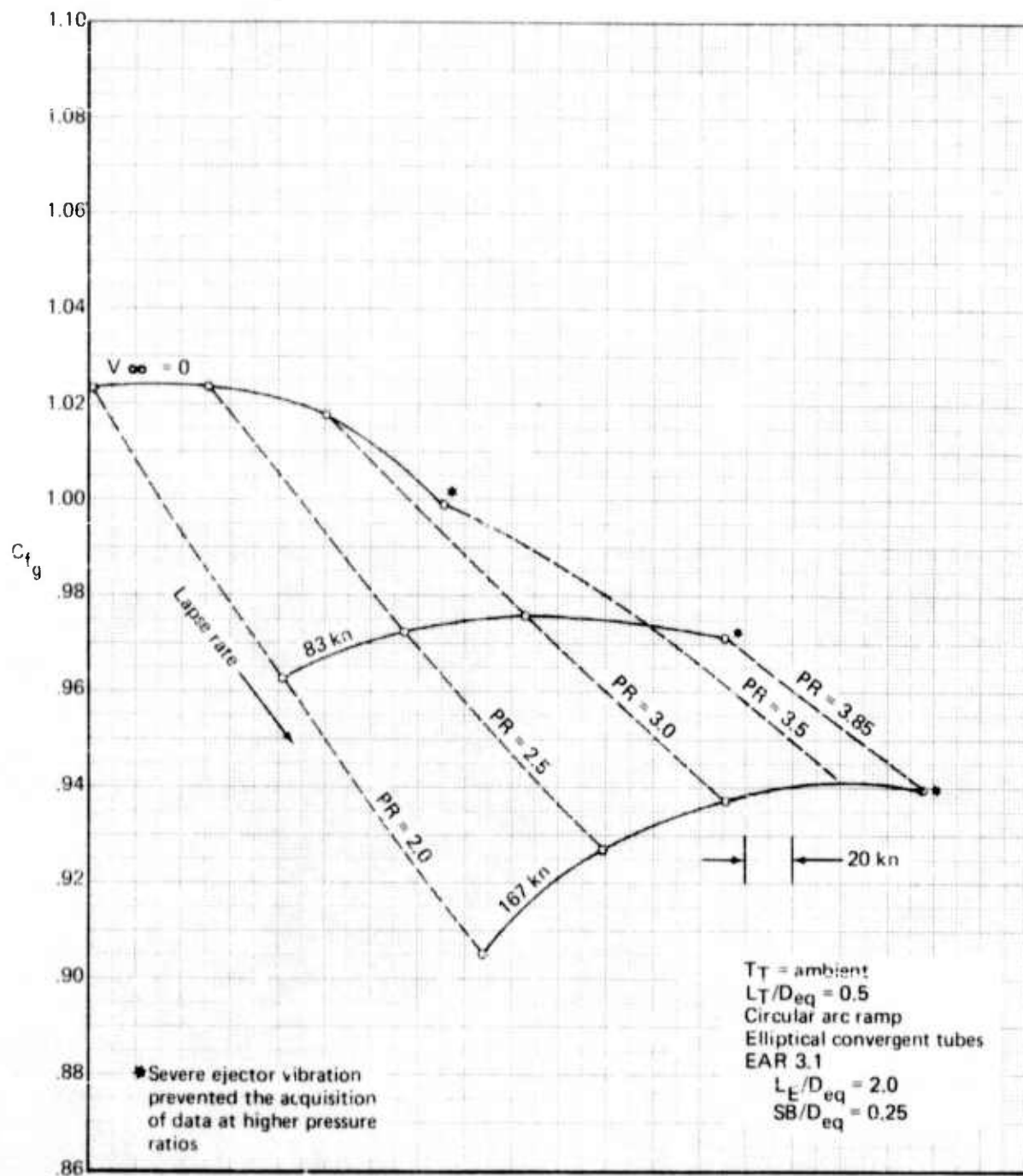


Figure 46.—Gross Thrust Coefficient for 37-Tube, NAR 3.3, Close-Packed Array, Circular Arc Ramp With $EAR = 3.1$ Ejector (Setback 0.25)

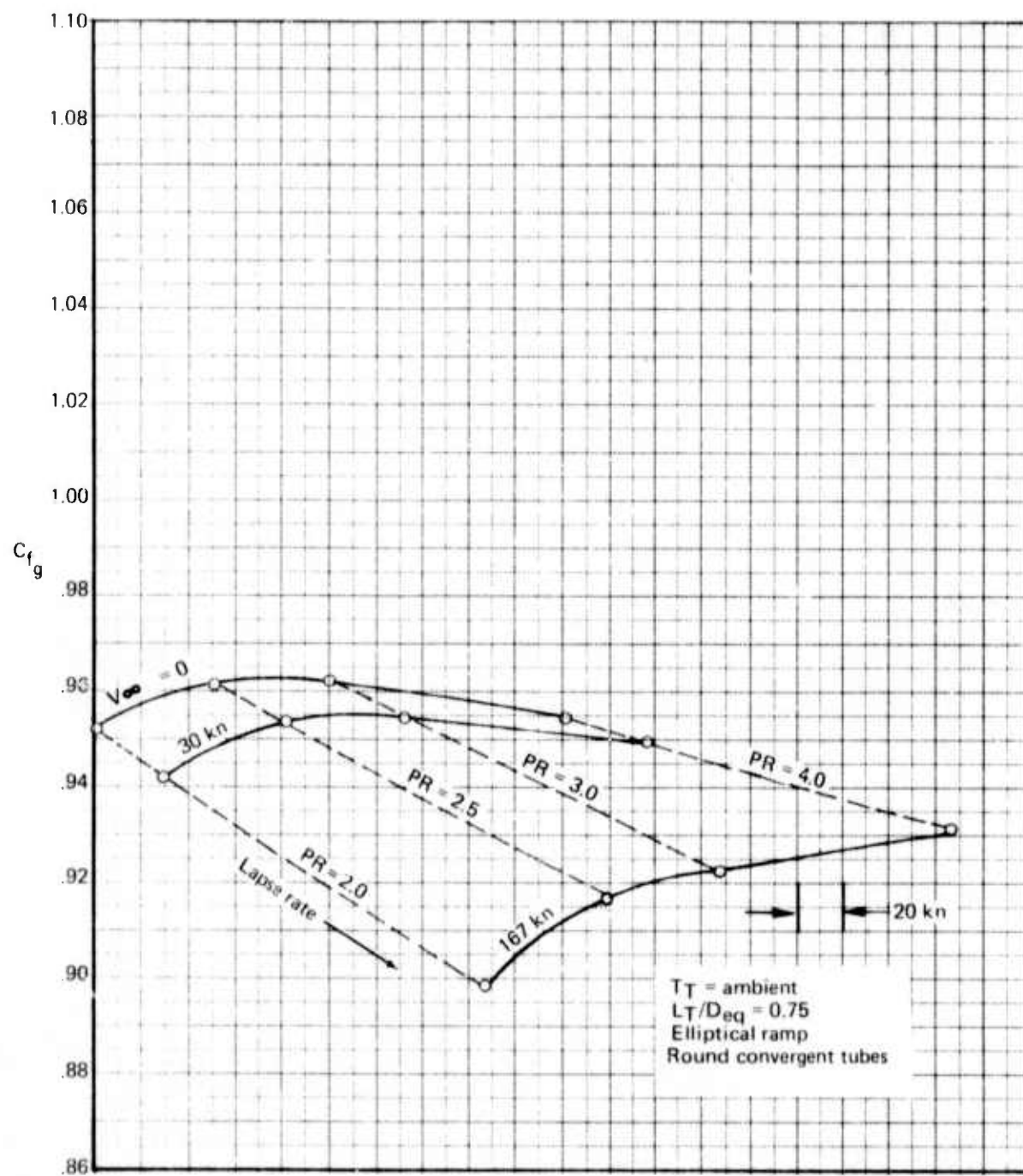


Figure 47.—Gross Thrust Coefficient for 37-Tube, NAR = 3.3, Close-Packed Array With $L_T/D_{eq} = 0.75$ Round Convergent Tubes Without Ejector

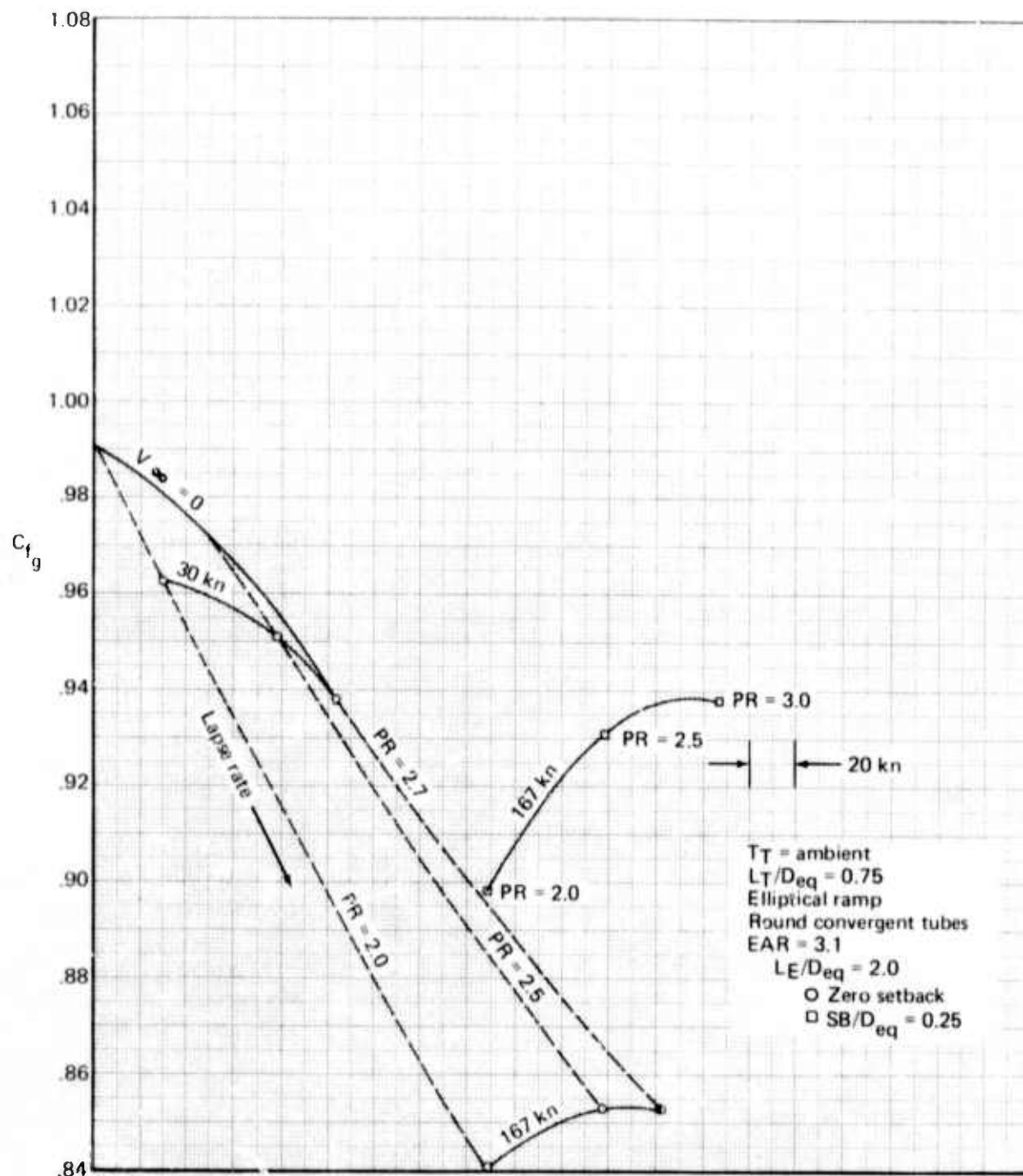


Figure 48.—Gross Thrust Coefficient for 37-Tube, NAR = 3.3, Close-Packed Array With $L_T/D_{eq} = 0.75$, Round Convergent Tubes With EAR = 3.1 Ejector (Zero and 0.25 Setback)

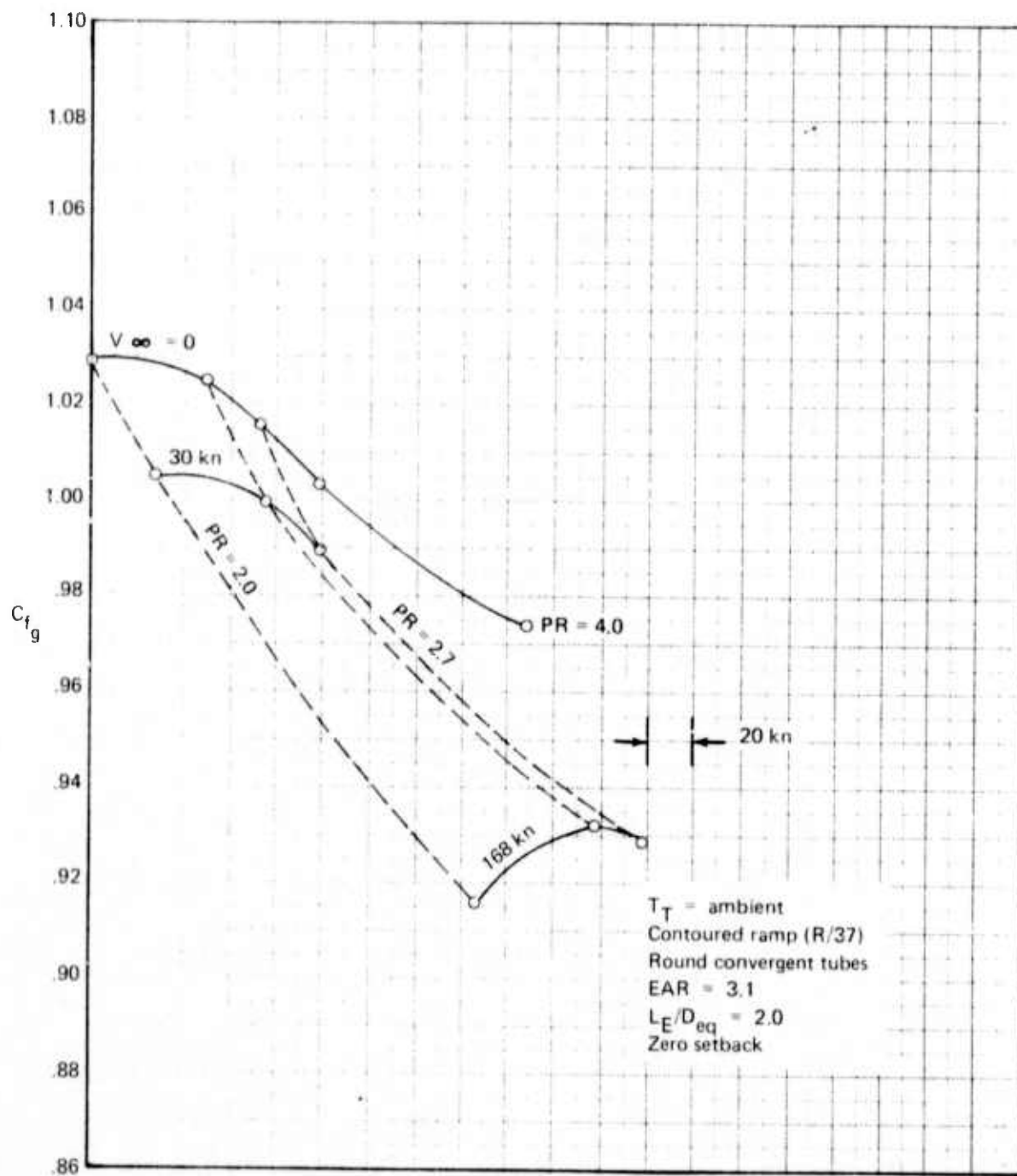


Figure 49.—Gross Thrust Coefficient for 37-Tube, $NAR = 3.3$, Close-Packed Array: Round Convergent Tubes, Contoured Ramp With $EAR = 3.1$ Ejector

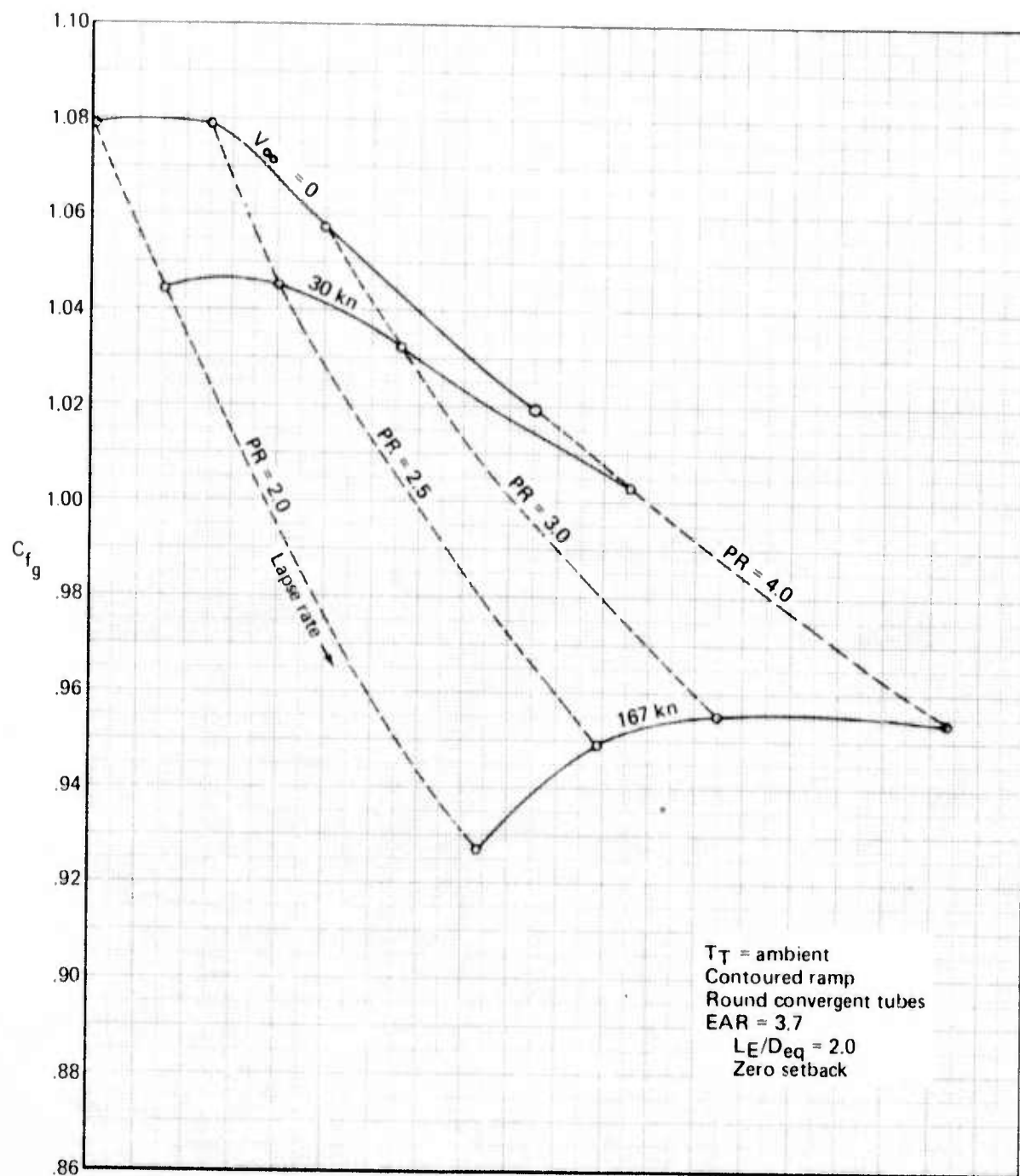


Figure 50.—Gross Thrust Coefficient for 37-Tube, $NAR = 3.3$, Close-Packed Array: Round Convergent Tubes, Contoured Ramp With $EAR = 3.7$ Ejector

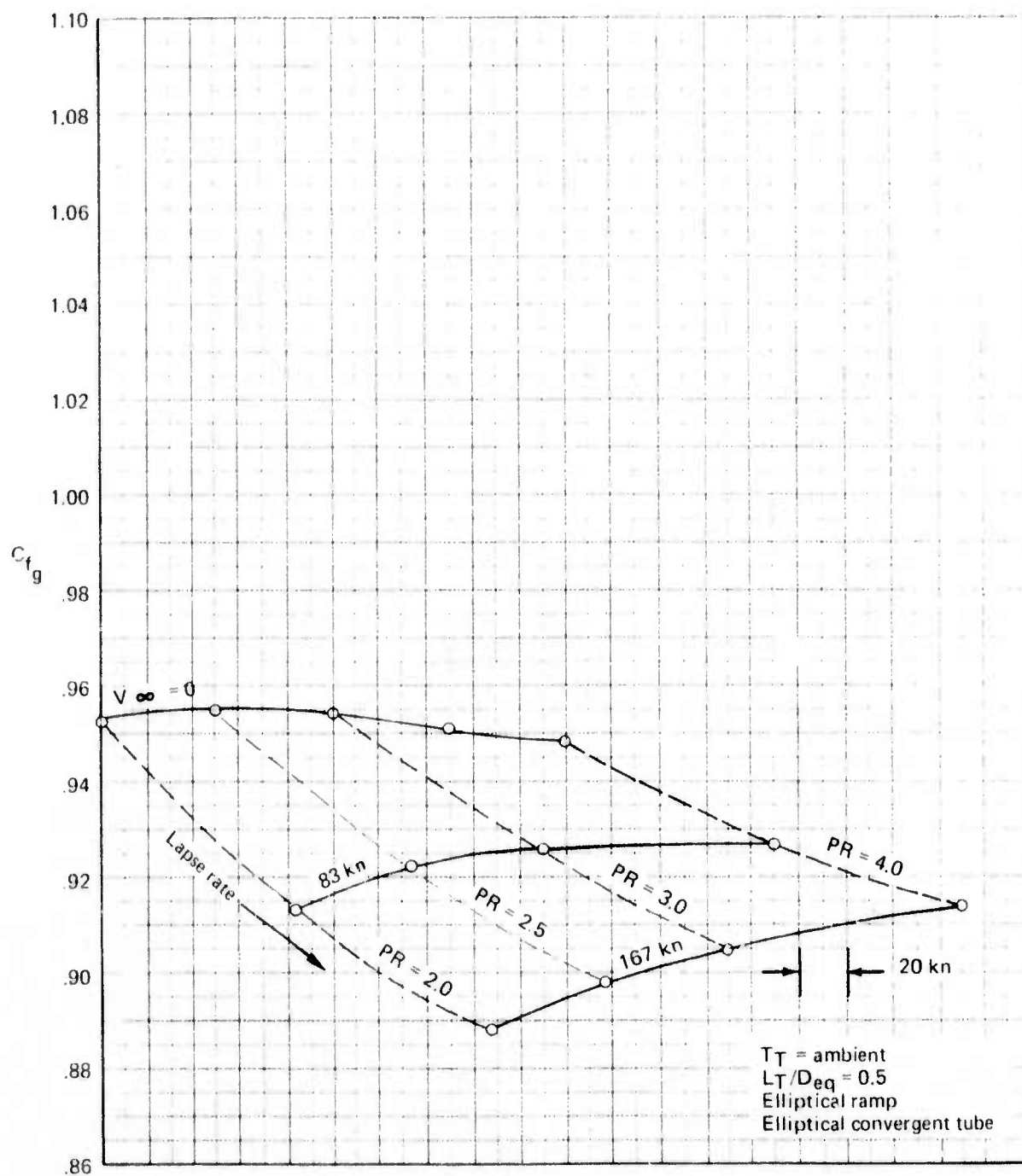


Figure 51.—Gross Thrust Coefficient for 61-Tube, $NAR = 3.3$, Close-Packed Array Without Ejector

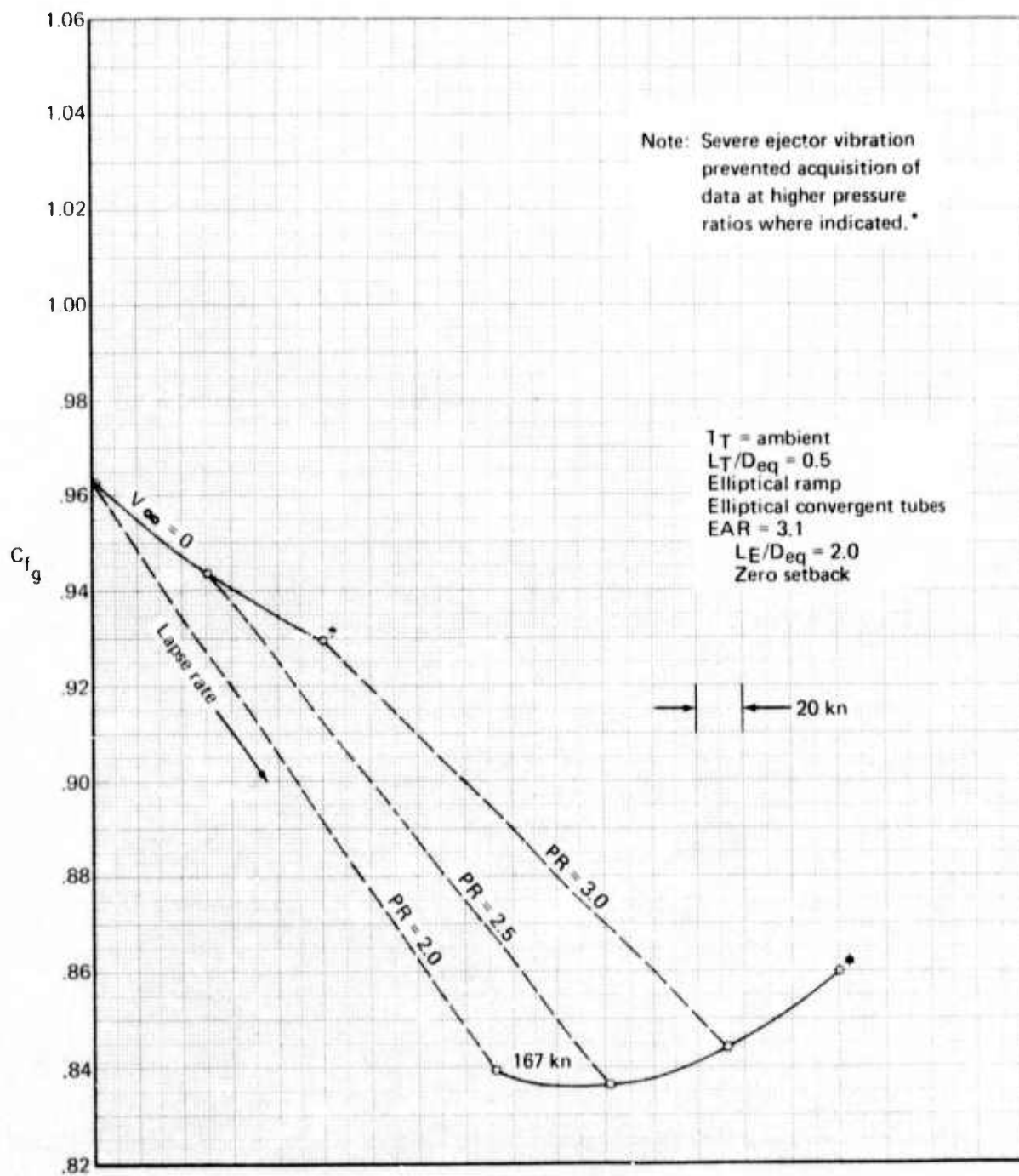


Figure 52.—Gross Thrust Coefficient for 61-Tube, $NAR = 3.3$, Close-Packed Array With $EAR = 3.1$ Ejector

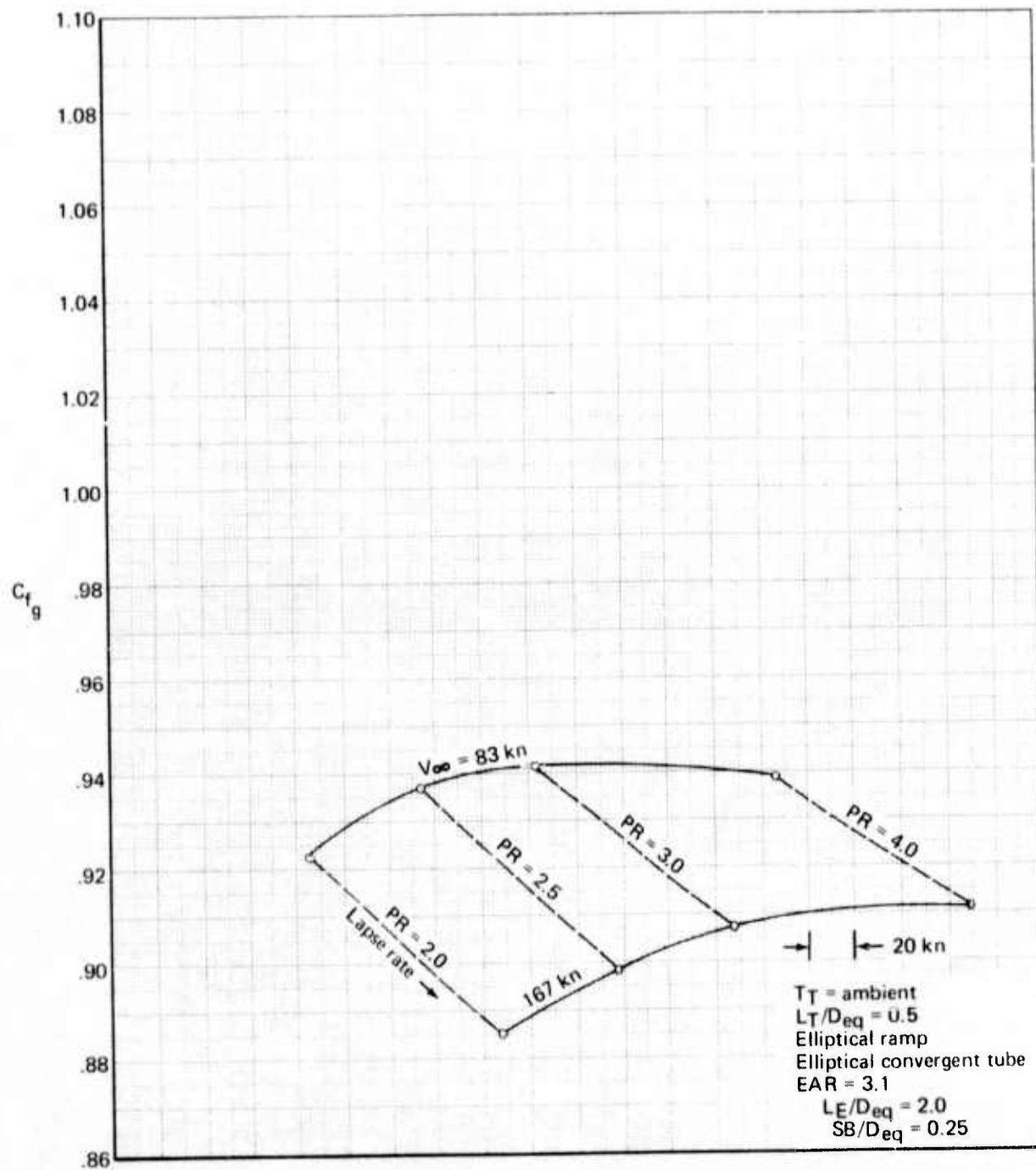


Figure 53.—Gross Thrust Coefficient for 61-Tube, NAR = 3.3, Close-Packed Array With EAR = 3.1 Ejector (Setback 0.25)

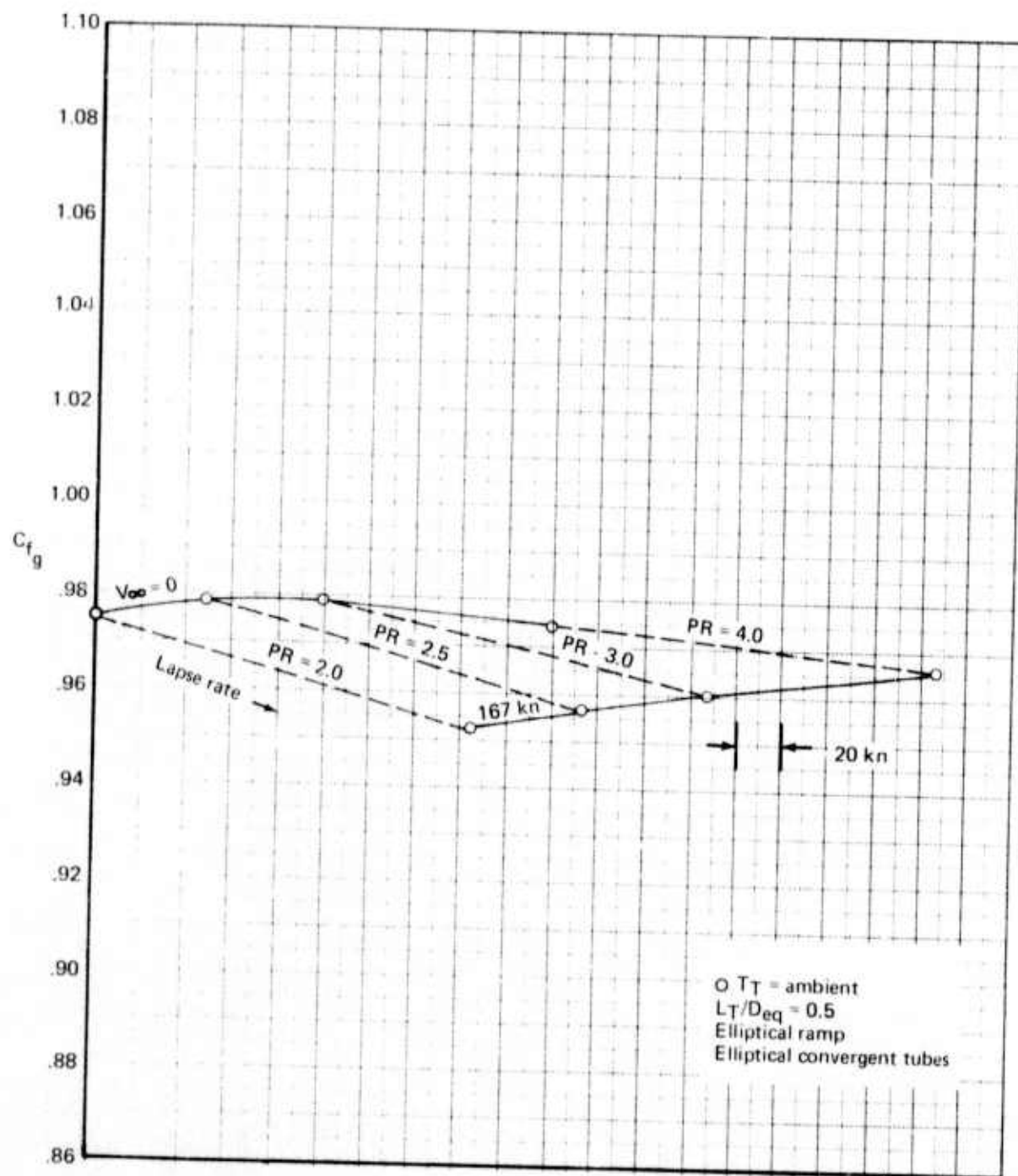


Figure 54.—Gross Thrust Coefficient for 31-Tube, $NAR = 2.75$ Radial Array Without Ejector

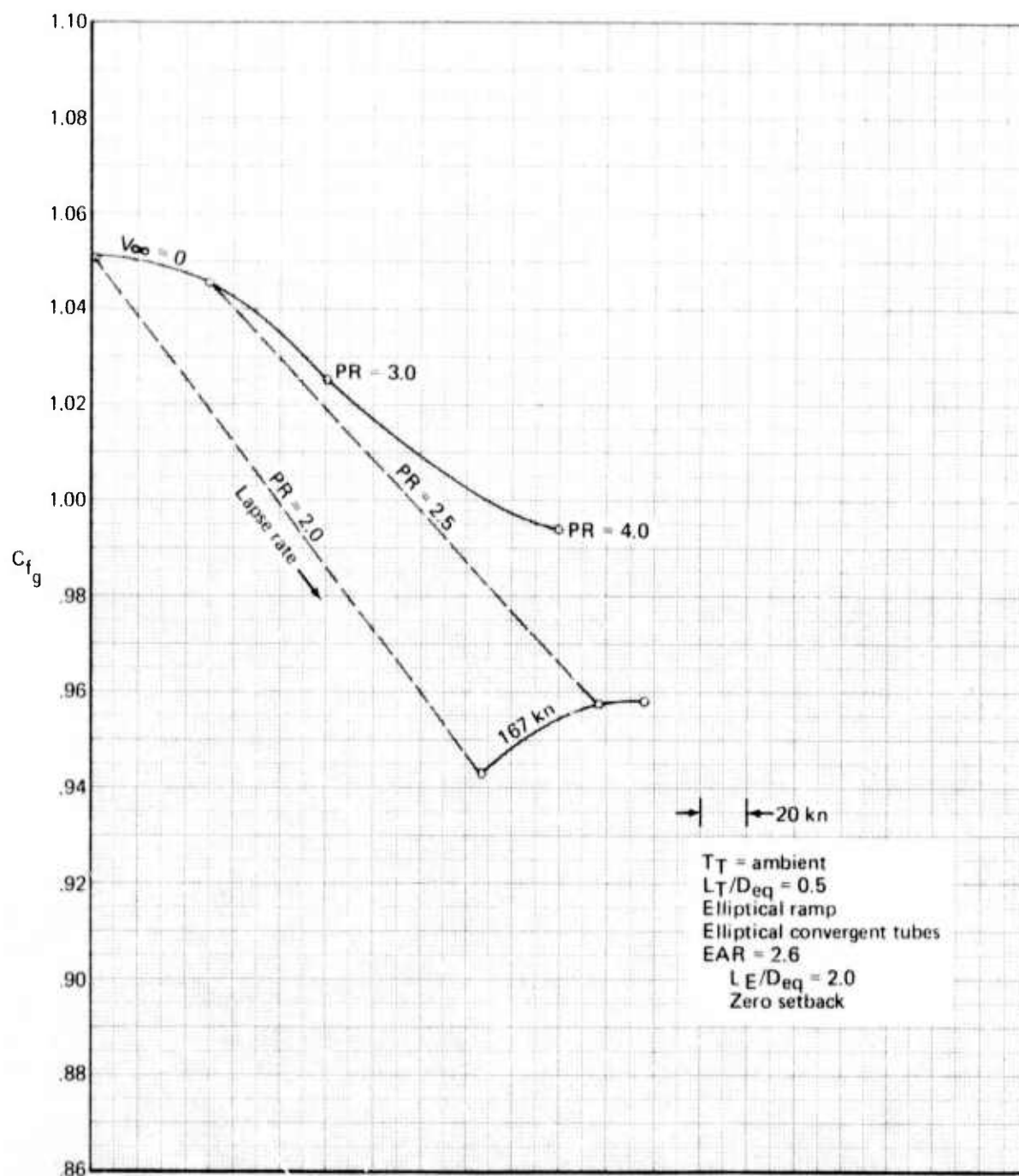


Figure 55.—Gross Thrust Coefficient for 31-Tube, $NAR = 2.75$ Radial Array
With $EAR = 2.6$ Ejector

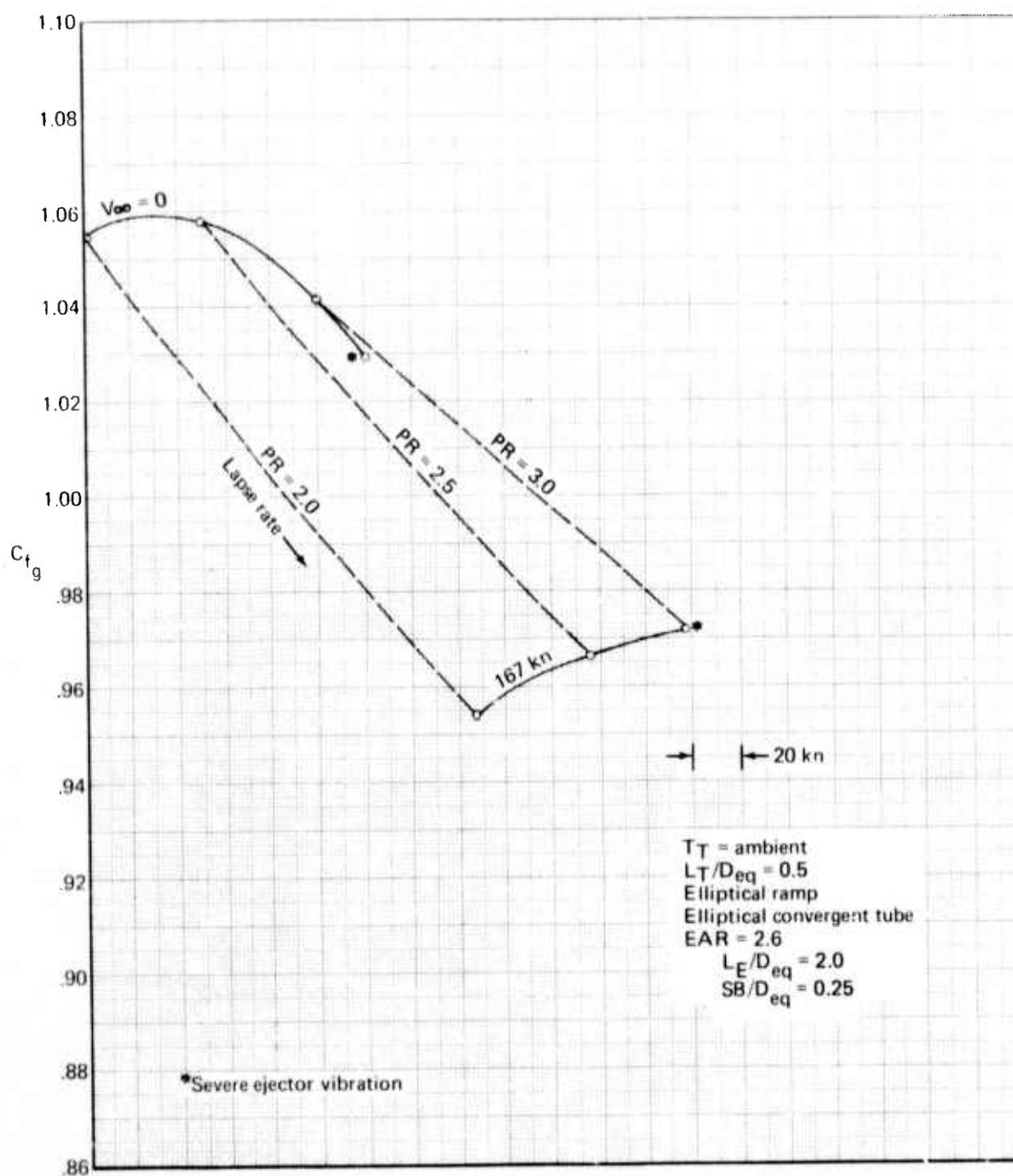


Figure 56.—Gross Thrust Coefficient for 31-Tube, NAR = 2.75 Radial Array
With EAR = 2.6 Ejector (Setback 0.25)

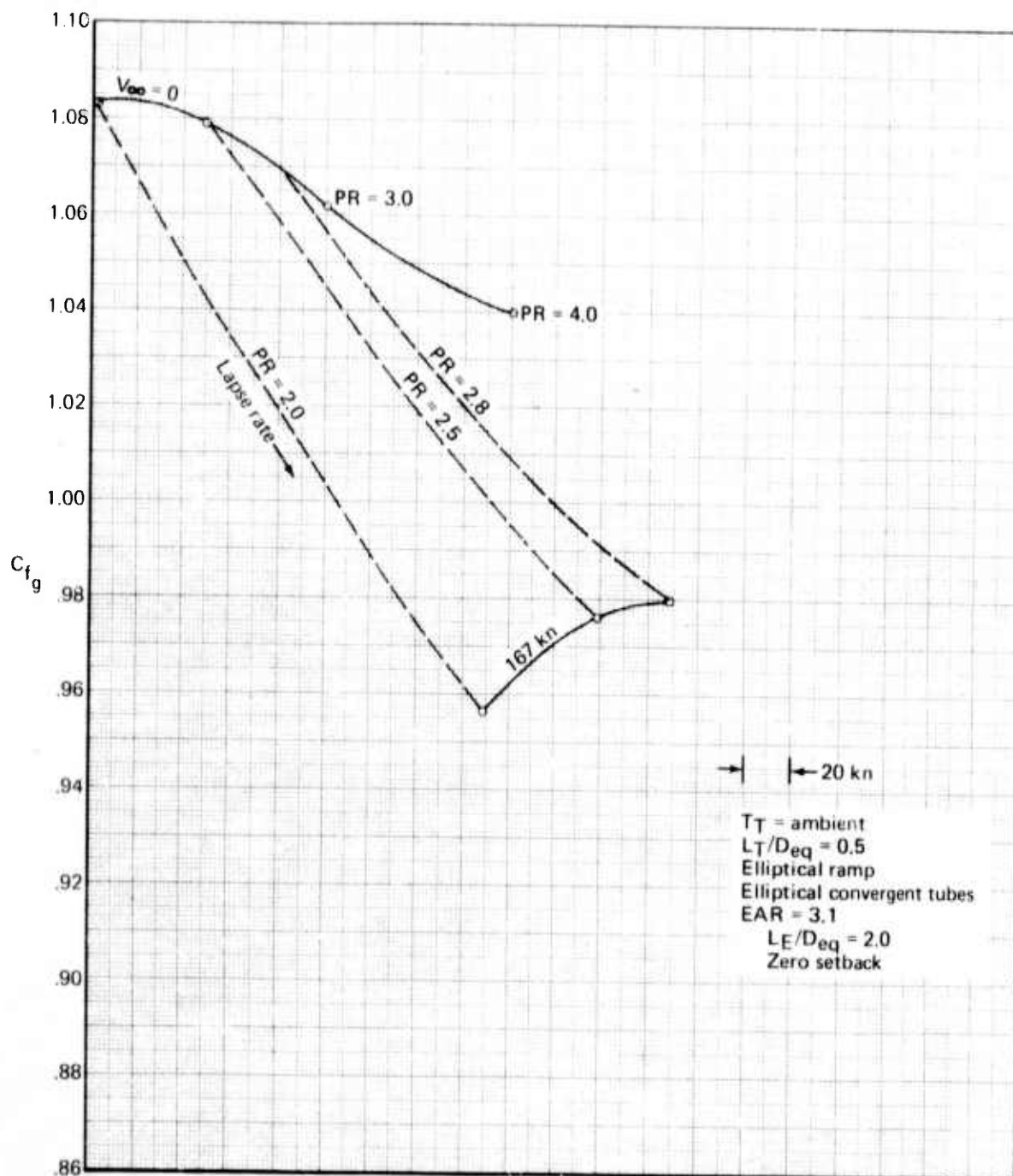


Figure 57.—Gross Thrust Coefficient for 31-Tube, NAR = 2.75 Radial Array
With EAR = 3.1 Ejector

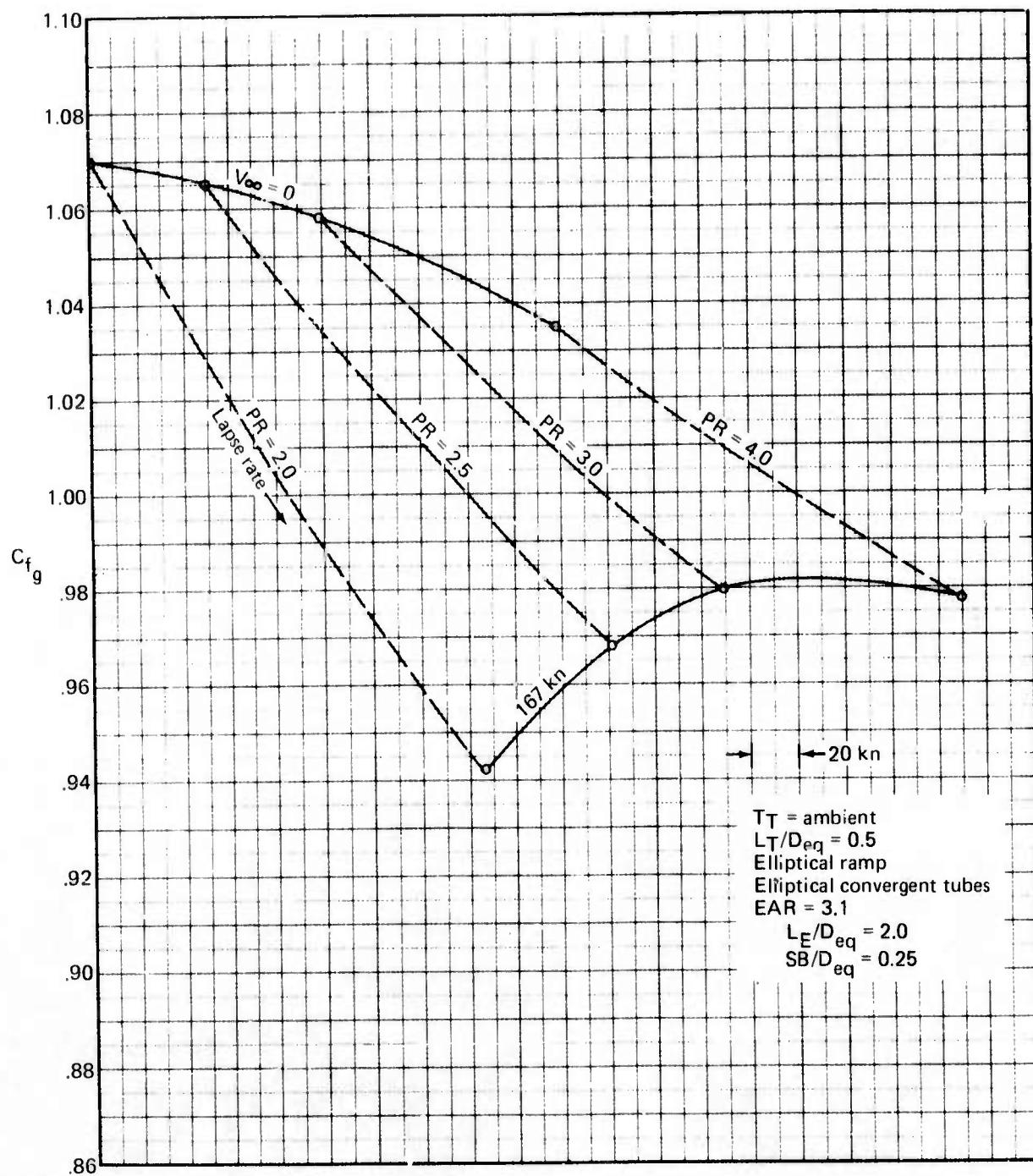


Figure 58.—Gross Thrust Coefficient for 31-Tube, $NAR = 2.75$ Radial Array
With $EAR = 3.1$ Ejector (Setback 0.25)

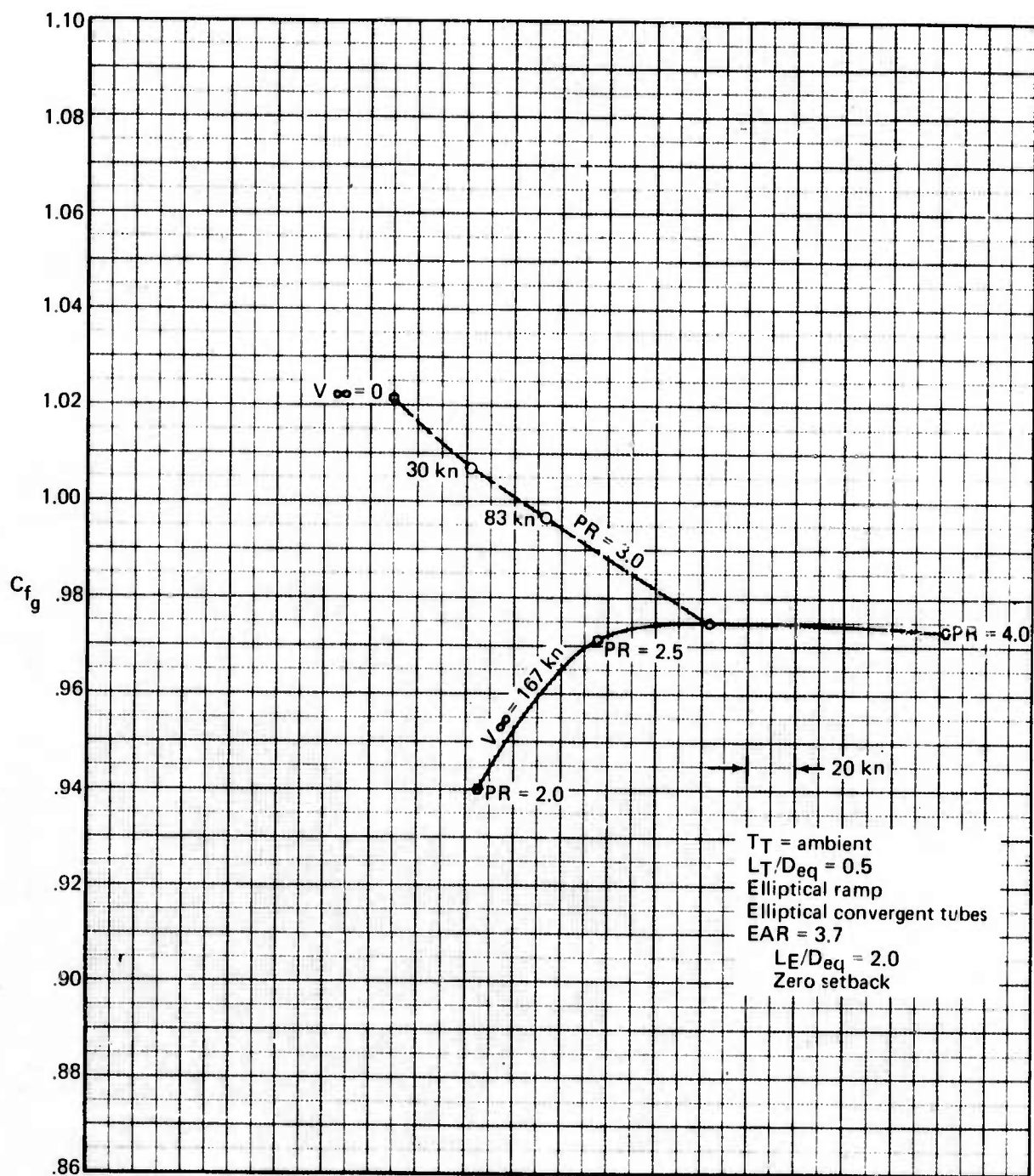


Figure 59.—Gross Thrust Coefficient for 31-Tube, NAR = 2.75 Radial Array With EAR = 3.7 Ejector

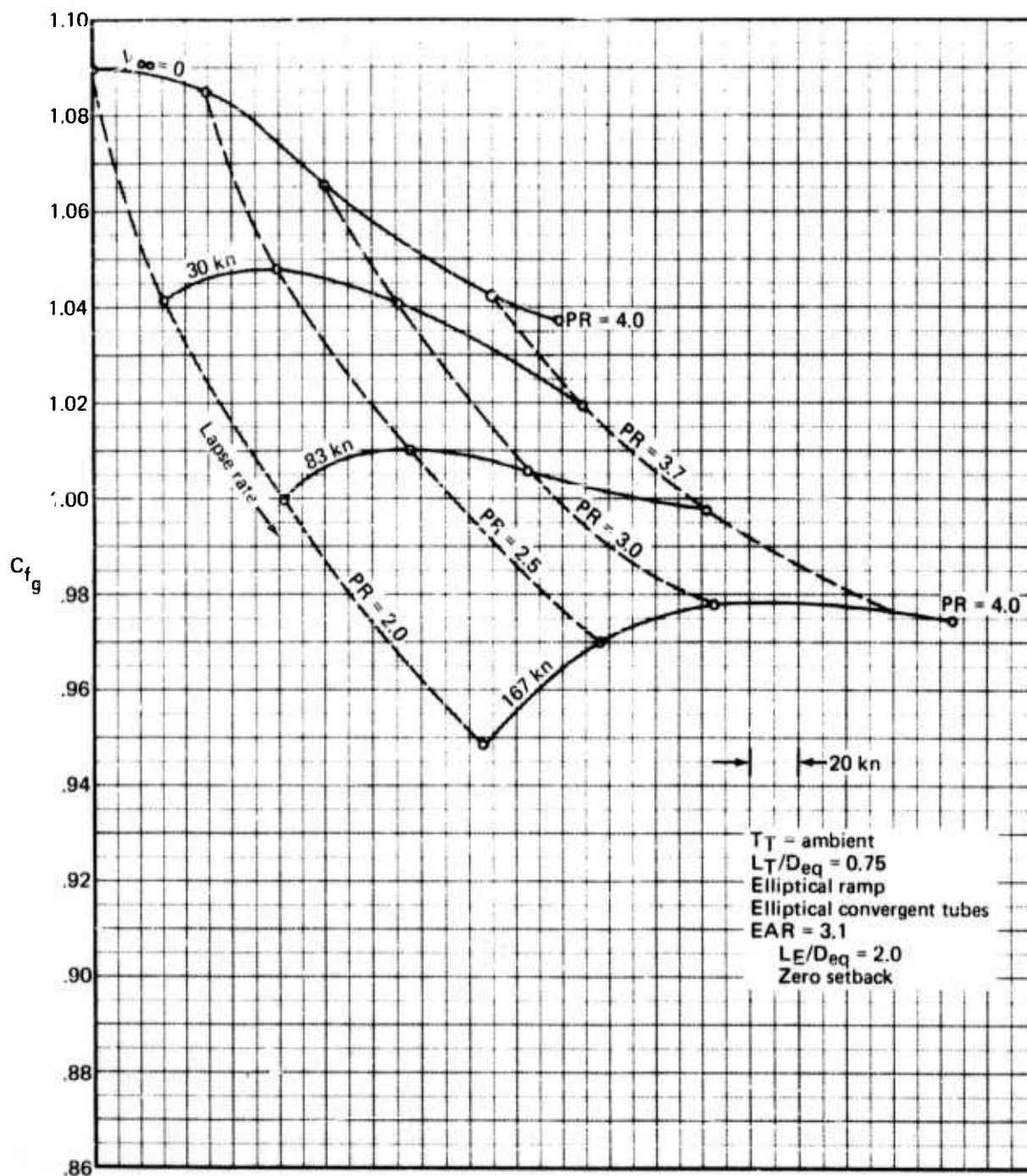


Figure 60.—Gross Thrust Coefficient for 31-Tube, $NAR = 2.75$ Radial Array ($L_T/D_{eq} = 0.75$) With $EAR = 3.1$ Ejector

6.0 ANALYSIS

6.1 INTRODUCTION

This section analyzes the experimental results (sec. 5) and establishes trends by comparing performance and surface forces for the various parameters investigated.

The dependence of forward velocity effects on pressure ratio is discussed first. The section includes bare-nozzle and suppressor/ejector descriptions of the effects of pressure ratio and velocity on suppressors with and without ejectors. The "cross-over" velocity (maximum velocity at which an ejector is beneficial to performance) is considered as well as the behavior of restricted ejector inlets.

The pressure ratio is then fixed; and variations in performance with velocity, due only to changes in geometry, are considered. An example suppressor with various ejectors is considered in detail. Then the general suppressor geometry effects are discussed, following which there is a discussion of the ejector including the description of qualitative inlet flow model and performance effects due to ejector geometry. Finally, a brief discussion of the effects of temperature on the surface forces is presented.

6.2 THE PRESSURE RATIO DEPENDENCE OF FORWARD VELOCITY EFFECTS

6.2.1 BARE SUPPRESSOR PERFORMANCE

At any fixed velocity, afterbody drag always becomes a decreasing percentage of ideal primary thrust as pressure ratio increases. The decrease is not usually linear. Reference 2 shows details of these effects statically.

For a fixed pressure ratio, the base drag linearly increases with velocity.

For a fixed pressure ratio, the ramp drag increases in proportion to velocity squared. Thus, for a fixed pressure ratio, the afterbody drag (the sum of the base and ramp drags) has a slightly non-linear increase with velocity. The static performance of multitube nozzle without ejectors has been shown to be optimum at pressure ratios between 2 and 3 (ref. 1). The combination of the above effects results in a typical behavior of bare multitube nozzles as shown in figure 61.

6.2.2 SUPPRESSOR/EJECTOR PERFORMANCE

6.2.2.1 Preamble

The additional of an ejector to an exhaust system subjected to forward velocity creates these additional concerns:

- Ejector lip suction
- Increased suppressor afterbody drag
- Ejector pressure drag (constant area)
- Skin friction losses
- Ram drag penalty

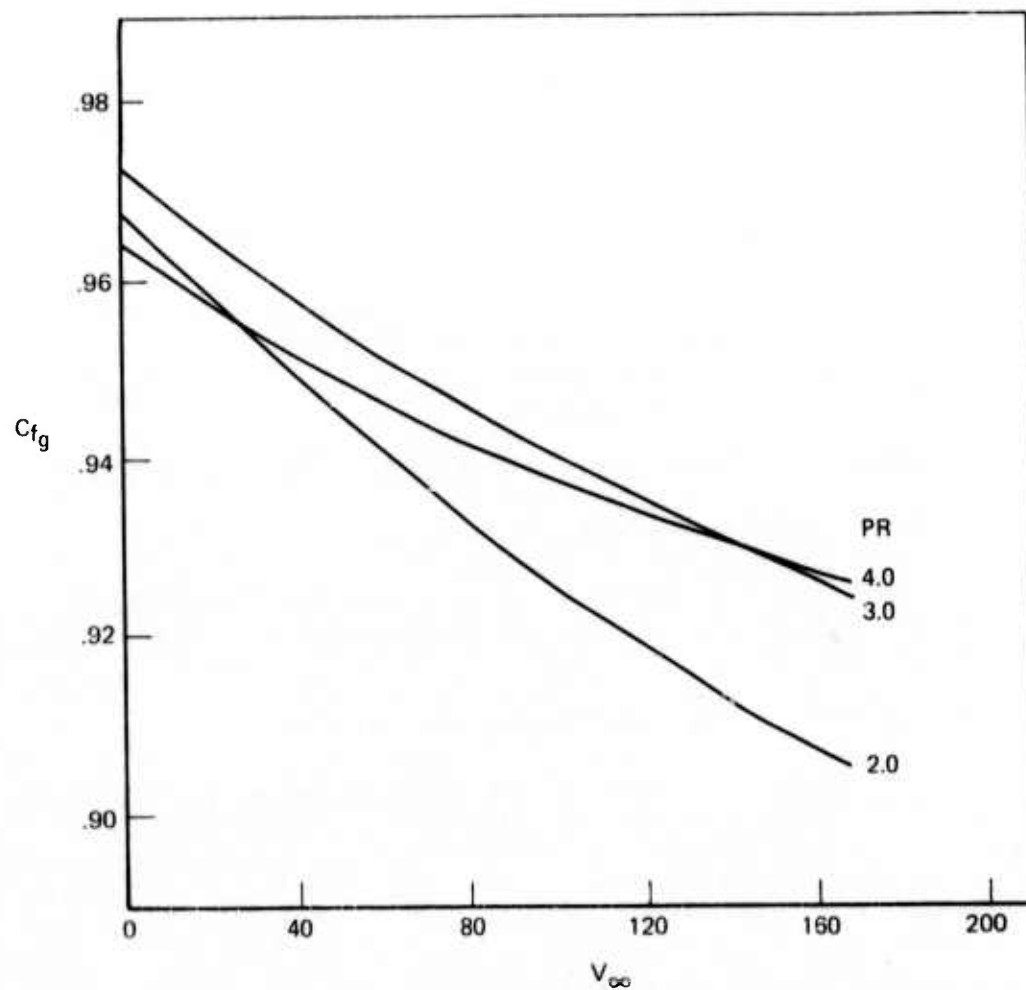


Figure 61.—General Behavior of Bare Suppressor Performance as a Function of Pressure Ratio and Velocity

6.2.2.2 Ejector Lip Suction

As the suppressor jets mix with surrounding air, flow is entrained by the jets. Ambient air moves into the regions of pressure depression created by the entrained air. When an ejector is installed, this replacement air must flow into the ejector through the complex inlet provided between the outer row suppressor tubes, A_S , and through the annular opening between the outer tube row and the ejector lip, A_A , (see fig. 62). This inlet flow affects ejector lip suction and suppressor afterbody drag. The lip suction, a result of the pressure reduction caused by the high velocity flow entering the inlet, becomes a decreasing percentage of ideal primary thrust as pressure ratio increases (i.e., the lip force increases by a smaller amount than the ideal thrust).

6.2.2.3 Suppressor Afterbody Drag

Countering the performance benefit of the lip suction is the increased level of afterbody drag resulting from the presence of an ejector. At any fixed velocity the afterbody drag becomes a decreasing percentage of the ideal primary thrust as pressure ratio increases. The result is the same as for the suppressor without ejector, except the absolute levels are higher. At any fixed pressure ratio both the afterbody drag and lip suction become decreasing percentages of the ideal primary thrust as velocity increases. (These subjects are treated in detail later.)

6.2.2.4 Ejector Drag

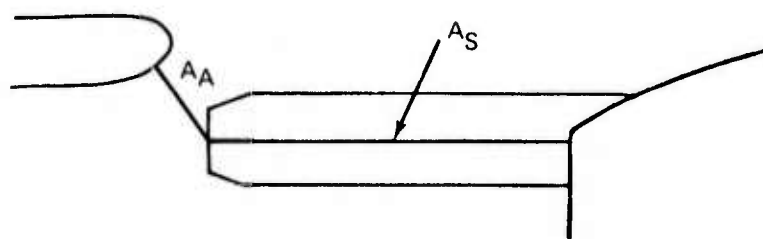
The present investigation considers only constant area mixers; thus, the only ejector pressure drag to consider is the ejector boattail drag, which is independent of pressure ratio. The dependence of ejector pressure drag on velocity is covered in section 6.3.7.1.

6.2.2.5 Ram Drag Penalty

At a fixed velocity the amount of secondary air increases as pressure ratio increases (unless the inlet flow is choked). Therefore, by definition, the amount of ram drag increases with increasing pressure ratio. Though it is a real component in the momentum equation, the ram drag physically manifests itself as a change in lip suction. The effect of pressure ratio on ram drag is a secondary concern compared to the velocity effects on lip suction due to ram drag.

6.2.2.6 Resulting Performance

The net result of the above parameters is a pressure ratio dependence of overall performance which is similar to that of the bare suppressor case but with steeper lapse rates. Figure 41 shows the performance of the suppressor (shown bare in fig. 38) with an area ratio EAR 3.1 ejector installed. The skin friction, ram drag, afterbody drag, and ejector pressure drag all increase with velocity and thus increase the lapse rate for the ejector configuration. Since increasing pressure ratio decreases both afterbody drag and lip suction with velocity (either one of which can be dominant), the lapse rate dependence on pressure ratio for these components can go either way. At a fixed velocity both the lip suction and base drag become



Detail A-A

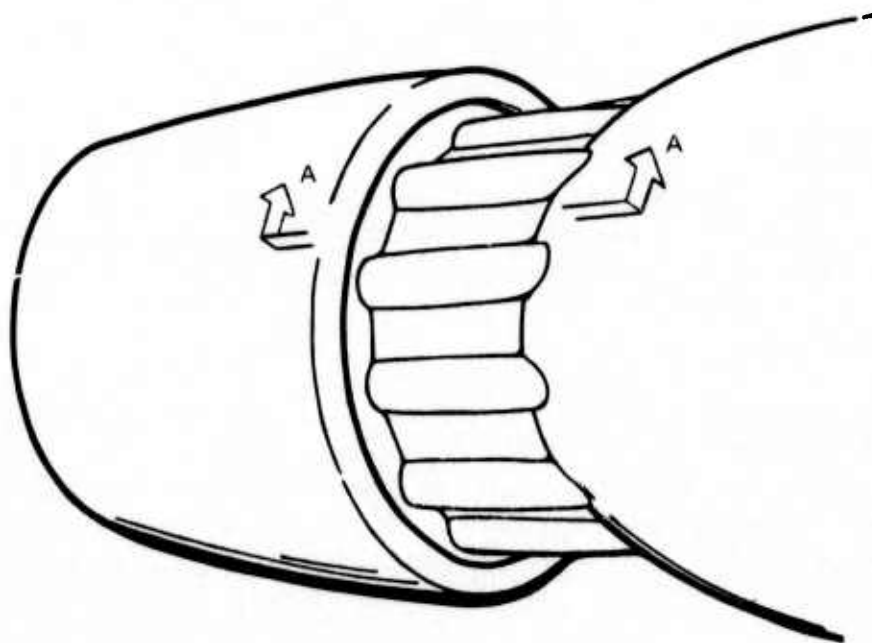


Figure 62.—Ejector Inlet Area A_A and A_S

decreasing percentages of the ideal thrust as the pressure ratio increases. The lip suction has a stronger dependence on pressure ratio than does the base drag. Thus, over the range of pressure ratios investigated (2-4), the static gross thrust coefficient for suppressor/ejector nozzles is always at or near the maximum value at pressure ratio 2.0.* (See ref. 2.) The lip suction decreases with forward velocity due to the ram drag penalty. The net result is a decrease in performance with increasing velocity and an upward shift in the pressure ratio at which maximum performance occurs. These performance effects are readily apparent on the summary plots of gross thrust coefficient versus velocity and pressure ratio shown in section 5.

6.2.2.7 Crossover Velocity

A typical comparison of lapse rates for the ejector and bare suppressor configurations is shown on Figure 63. The figure shows the performance crossover velocity (i.e., the velocity above which the ejector becomes a performance handicap) at each pressure ratio. The crossover velocity decreases slightly with increasing pressure ratio and approaches a constant value. This trend held true for all configurations investigated where the inlet was not restricted.

6.2.2.8 Behavior of Restricted Inlet

If the crossover velocity is strongly dependent on pressure ratio, it is due to a restricted inlet. In these cases, as the pressure ratio increases, the ejector demands more air than can be brought through the inlet. At low pressure ratios this is manifested as increasing inlet losses, resulting in a crossover at a lower velocity as pressure ratio increases. As the pressure ratio continues to increase, the demand for secondary air increases until supersonic flow occurs at the ejector throat (monitored on static wall taps). This situation arises on "tight" ejectors without sufficient setback (such as the configuration in figures 39 and 42 in section 5). As the pressure ratio producing the inlet choking is approached, a steeper decrease in performance usually occurs. The experimental technique of mounting the ejector separate from the suppressor provided insight into another characteristic of the ejector behavior as inlet choking occurs. When the pressure ratio is sufficient to produce static pressures at the ejector throat indicating supersonic flow, the ejector begins to vibrate so violently that the flow must be shut down. The severe vibration and additional performance losses are attributed to shock-induced flow separations. (The vibration is low frequency, < 200 Hz, and produces excursions greater than can be produced by manually pushing on the side of the ejector.)

The pressure ratio at which this phenomenon occurs is dependent upon the effective inlet area of the ejector. The effective inlet area is not presently a quantitative item; rather, one can only observe its effects by looking at curves presented in section 5 and noting the configurations where data could not be acquired over the entire pressure ratio range.

*The actual peak static C_{f_g} occurs at a pressure ratio < 2.0 for most configurations.

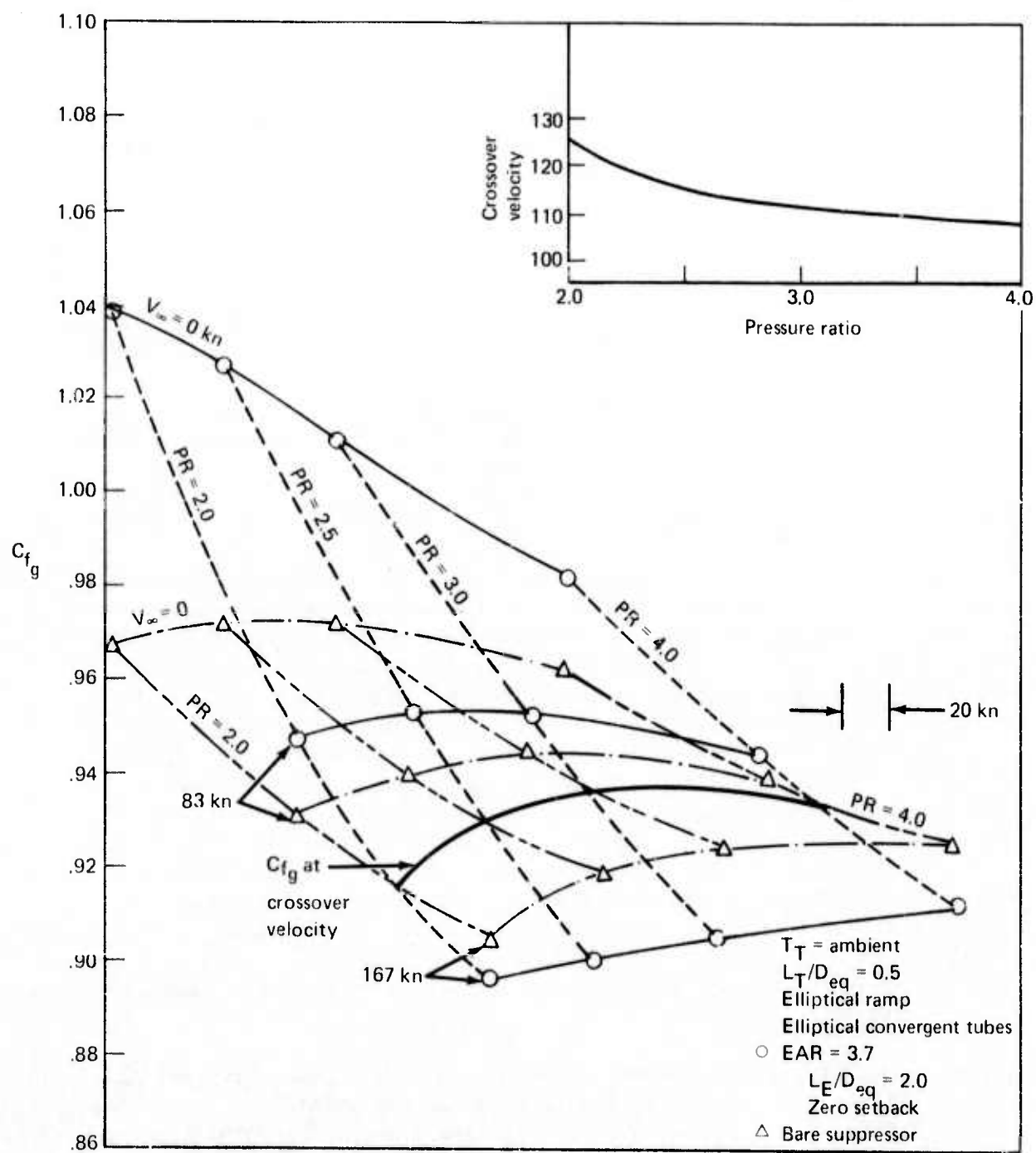


Figure 63.—Comparison of Performance and Lapse Rate and Crossover Velocity for 37-Tube, NAR-3.3, Close-Packed Array, Bare and With EAR-3.7 Ejector

As the EAR/NAR and setback increase, the occurrence of inlet choking moves to higher pressure ratios. The effect of inlet area on the pressure ratio at which supersonic flow occurs at the ejector throat is shown on figure 64. The only difference in configurations is that the upper carpet has 50% longer tubes. In both configurations, the ejector hilite is coplanar with the tube exit plane. The major effect on the additional tube lengths is the displacement of the entire carpet to a higher performance. The lapse rates are nearly the same and the onset of ejector vibration occurs at only a slightly higher pressure ratio. This behavior suggests that the amounts of secondary airflow going between the tubes is a small percentage of the total secondary mass flow (i.e., most of the air enters the ejector in the annulus, A_A , between the outer tubes and the ejector lip). The shift to higher performance is primarily due to a large decrease in base drag provided by the small increase in ventilating flow going between the tubes and the increased static pressure gradient between the lip and baseplate.

Reference 2 shows the static lip suction for these two cases to be the same at pressure ratio 2.8, for example, while the afterbody drag/FID is 9% less for the longer tubes. Now consider the same ejector and suppressor except with the short ($L_T/D_{eq} = 0.5$) tubes and a setback ($L_E/D_{eq} = 0.25$). Thus, the total axial distance from the baseplate to the ejector hilite is the same as that for the long tube case just considered, but the annulus area A_A has been substantially increased. The carpet for this configuration is shown in figure 65 (along with a repeat of the carpet for the same tube length but zero setback from figure 64). The performance of this configuration at pressure ratio 2 is between that of the other configurations considered above. As pressure ratio increases (requiring more secondary air), the configuration with short tubes and setback not only out-performs the other two, but it continues to operate statically at a pressure ratio up to 3.5 while the others begin to vibrate at 2.8.

There are several reasons for this behavior. The afterbody drag for the short tube configuration with setback is only 0.5% greater than for the long tubes without setback (compared to the 9% penalty of the short tubes without setback). The larger annular opening on the setback case allows the secondary air to enter the ejector at a lower velocity than it did for zero setback. The reduced velocity decreases the lip suction and this, combined with the afterbody drag relationship, results in the overall performance difference between the two no-setback cases at low pressure ratio. As the pressure ratio increases, the restricted inlets cannot pass any more air, while the setback case benefits from: (1) a nearly constant lip suction/FID until pressure ratio = 3.0 and (2) a continued increase in secondary airflow until pressure ratio = 3.5.

Setback provides a mechanism for obtaining the appropriate inlet area necessary to optimize the performance at any given pressure ratio. The amount of setback required for peak performance increases as pressure ratio increases because of the increased demand for secondary air. At a fixed pressure ratio there is an optimum setback for each suppressor-ejector combination. If the setback is too small, supersonic flow can occur. For small increases in setback, the lip velocity (hence lip suction) decreases but the base drag benefit increases substantially. The sketches in figure 66 show typical performance.

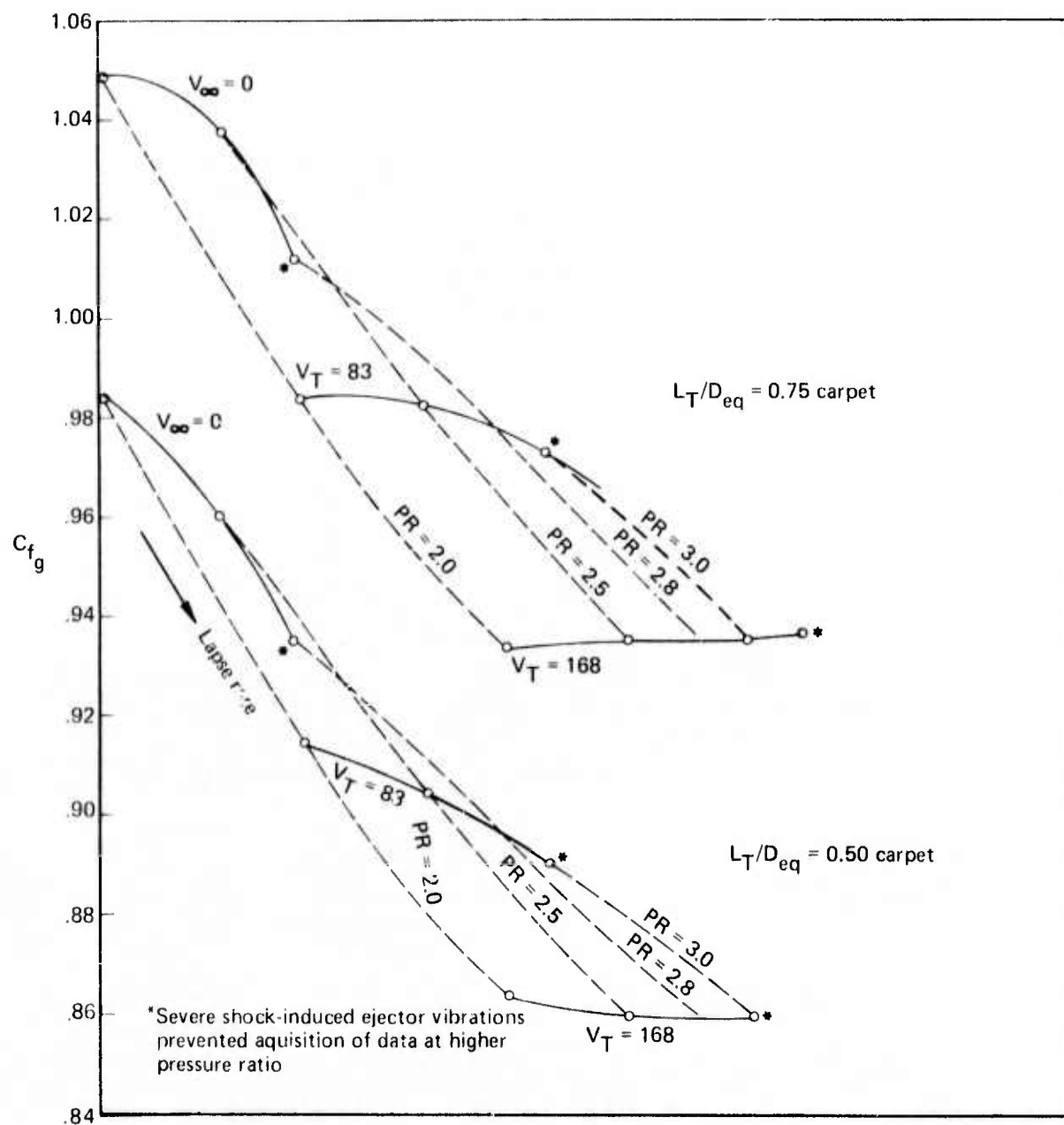
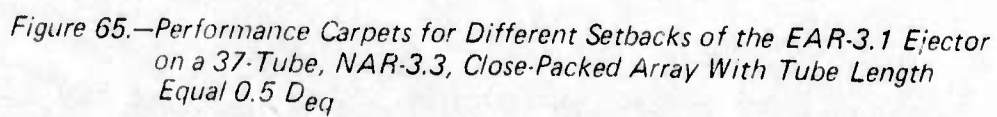


Figure 64. — 37-Tube, $NAR = 3.3$, Close-Packed
 $EAR = 3.1$ Ejector With Zero Setback



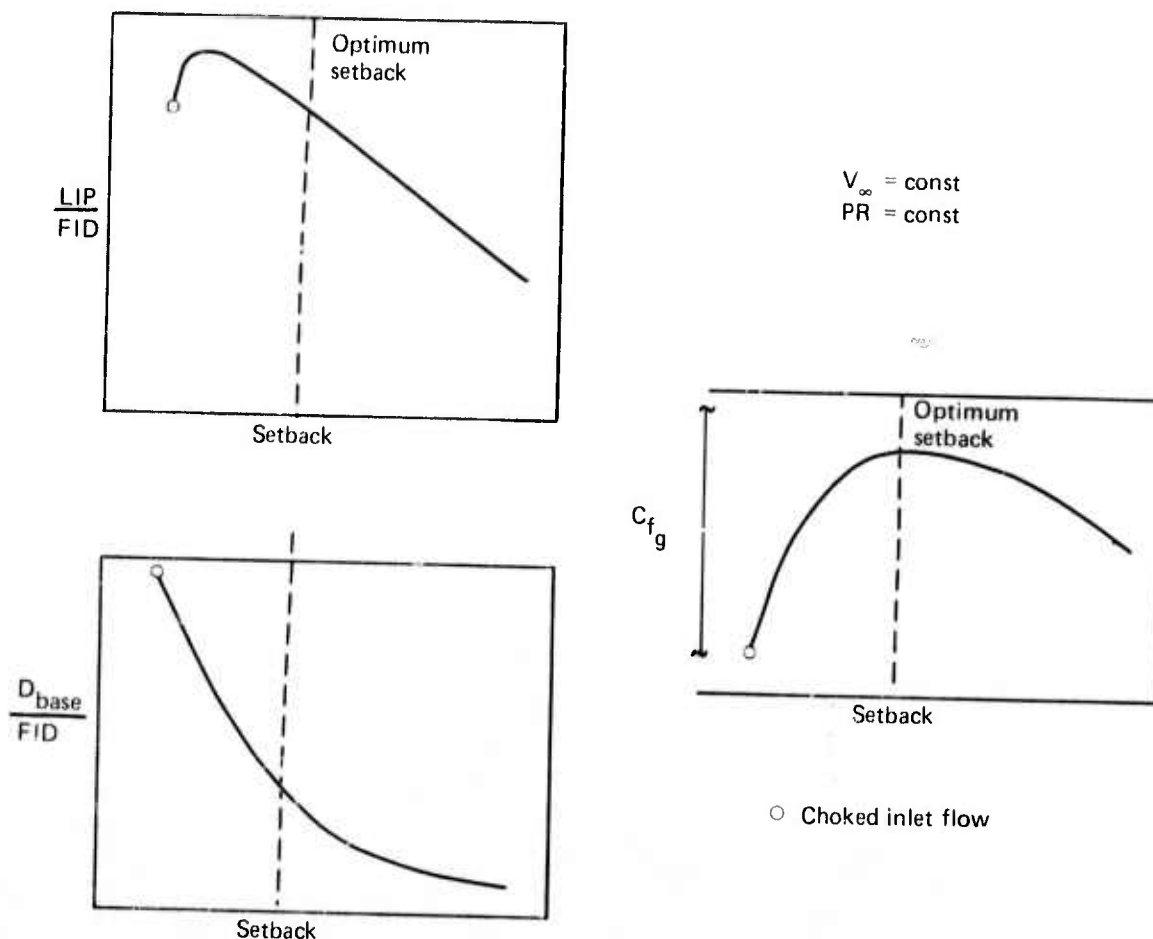


Figure 66.—Schematic of Performance Versus Setback

Reference 2 covers the details of the required setback statically. Forward velocity requires increasing setback (at a fixed pressure ratio) to produce peak performance and minimum lapse rate. (See sec. 6.3.)

The occurrence of the ejector vibration moves to slightly higher pressure ratios as velocity increases for a fixed geometry because of the inlet ram effects.* If static tests do not monitor supersonic flow at the ejector throat over the desired pressure ratio range, one can be confident that the low-speed performance will not be affected by this problem. Some available information suggests that a vibrating ejector stabilizes and the rate of performance

* P_T freestream increases relative to P_{Tp} as velocity increases and the pressure ratio is held constant.

loss decreases if the system is driven to even higher pressure ratios. This situation is shown in figure 55 where the static run could be pushed on to stable performance at pressure ratio 4 while the vibration first occurred at pressure 2.6. (Concern for the turboprop at the exit of the tunnel in the event of hardware failure precluded such attempts during wind tunnel testing.)

Within the present context, presumed inlet choking associated with the ejector vibration means only that supersonic flow was monitored by wall static pressure taps at the ejector throat. The ejector instrumentation included pressure taps in line with as well as in between outer row jets. The supersonic flow is noted at the tangent point between the lip and constant area portion of the ejector and occurs around the entire circumference of the ejector (not just in line with the jets).

6.3 FORWARD VELOCITY EFFECTS (CONSTANT PRESSURE RATIO)

6.3.1 INTRODUCTION

Section 6.3 discusses the effects of velocity on performance as the geometric parameters are varied while maintaining a constant pressure ratio of three. The trends apply to other pressure ratios as well and quantitative values at pressure ratios from 2 to 4 can be obtained from the performance curves presented in section 5.

6.3.2 IDEAL THRUST

Increasing wind tunnel velocity, produced by a turboprop at the tunnel exit, is accompanied by a decrease in freestream static pressure P_∞ , while the freestream total pressure, P_{T_∞} , remains constant (neglecting tunnel inlet losses). Actual forward velocity produces a constant freestream static pressure while the freestream total pressure increases. In the wind tunnel, if nozzle pressure ratio (P_{Tp}/P_∞) is held constant, the ideal thrust decreases with increasing velocity. If P_{Tp}/P_{T_∞} is held constant in the tunnel, the ideal thrust increases with velocity. For convenience and consistency in data presentation, nozzle pressure ratio is held constant throughout the present investigation.

In airplane evaluation it is necessary to account for the changes in pressure ratio with velocity due to the ram effect and engine power settings. The performance for any required combination of pressure ratios and velocity can be constructed using the carpet plots presented in section 5.

6.3.3 DISCHARGE COEFFICIENT

Discharge coefficient is defined as the measured primary flow rate divided by the ideal weight flow rate of a jet expanded to ambient conditions. Below nozzle choke pressure ratio, the ideal weight flow is a function of pressure ratio, while above the choke pressure ratio, the ideal weight flow is a function only of the stagnation conditions. The presence of an ejector reduces the actual static pressure to which the primary nozzle expands. Thus, below primary choke the discharge coefficient is affected by the presence of the ejector. Above choke the discharge coefficient should not be affected by the ejector presence.

All experimental data acquired during the present investigations were above pressure ratio = 2.0. For all these configurations the discharge coefficient was completely independent of all ejector parameters ($\pm 0.25\%$). The discharge coefficient was also independent of forward velocity. Reference 1 presents the C_D values for the various suppressors. The calculated primary nozzle exit area increase, assuming a linear nozzle perimeter growth with increased jet temperature, resulted in discharge coefficients that were independent of jet temperature.

6.3.4 BARE SUPPRESSOR PERFORMANCE

The low-speed performances of various suppressors are shown in figure 67.

The following trends occur:

- For a constant nozzle area ratio the lapse rate is nearly constant. Comparison of the 19-, 37-, and 61-tube, NAR-3.3 suppressors with elliptical ramps and elliptical convergent tubes shows a 2.8% variation in the static performance due to a combination of increasing internal losses and increased base drag resulting from the ventilation as the number of tubes increases. Because of the lapse rate to 167 kn, a reduction in C_{f_g} of 3.4%, 4.8%, and 4.9% occurs for the 19-, 37-, and 61-tube configurations, respectively. The 19-tube nozzle benefits from significantly better ventilation paths than the other nozzles.
- The base drag increases linearly with velocity as shown on figure 68. Though the static level of base drag is strongly dependent on ventilation, the rate of change of drag with velocity shows only a second order influence of ventilation (i.e., the static base drag of the 61-tube suppressor is 2.8% greater than that of the 19-tube nozzle, yet the increase in the difference in drags at 167 kn for the two configurations is only 0.75%). For all three configurations the ramp drag was less than 2% of the ideal thrust at 167 kn and the variation in ramp drag was at most 0.3% (greatest ramp drag being on the 61-tube nozzle). The ramp drag increases behaved in proportion to the square of the velocity. It is this ramp drag which produces the slight nonlinearity in the performance lapse rates shown on figure 67.

Figure 67 also shows the effects of these parameters on lapse rate. The 31-tube, NAR-2.75 radial array demonstrates the smallest lapse rate of the multitube nozzles investigated. Its shallow lapse rate is due to its lower nozzle area ratio and good base ventilation. At 167 kn the ramp drag for the configuration was 2% of the ideal thrust (which is nominally the same value as for NAR 3.3 suppressors with elliptical ramps). The base drag/FID was only 1.4% at 167 kn for the 31-tube radial array compared to 5.5% for the 37-tube, NAR-3.3, close-packed array. At 1150°F the value of ramp and base drag decreased slightly (1.9% and 1.4% of ideal thrust, respectively, for the 31-tube nozzle at 167 kn). Figure 67 also demonstrates that, for suppressors with constant nozzle area ratio and ventilation, the lapse rate is nearly independent of ramp shape and tube shape.

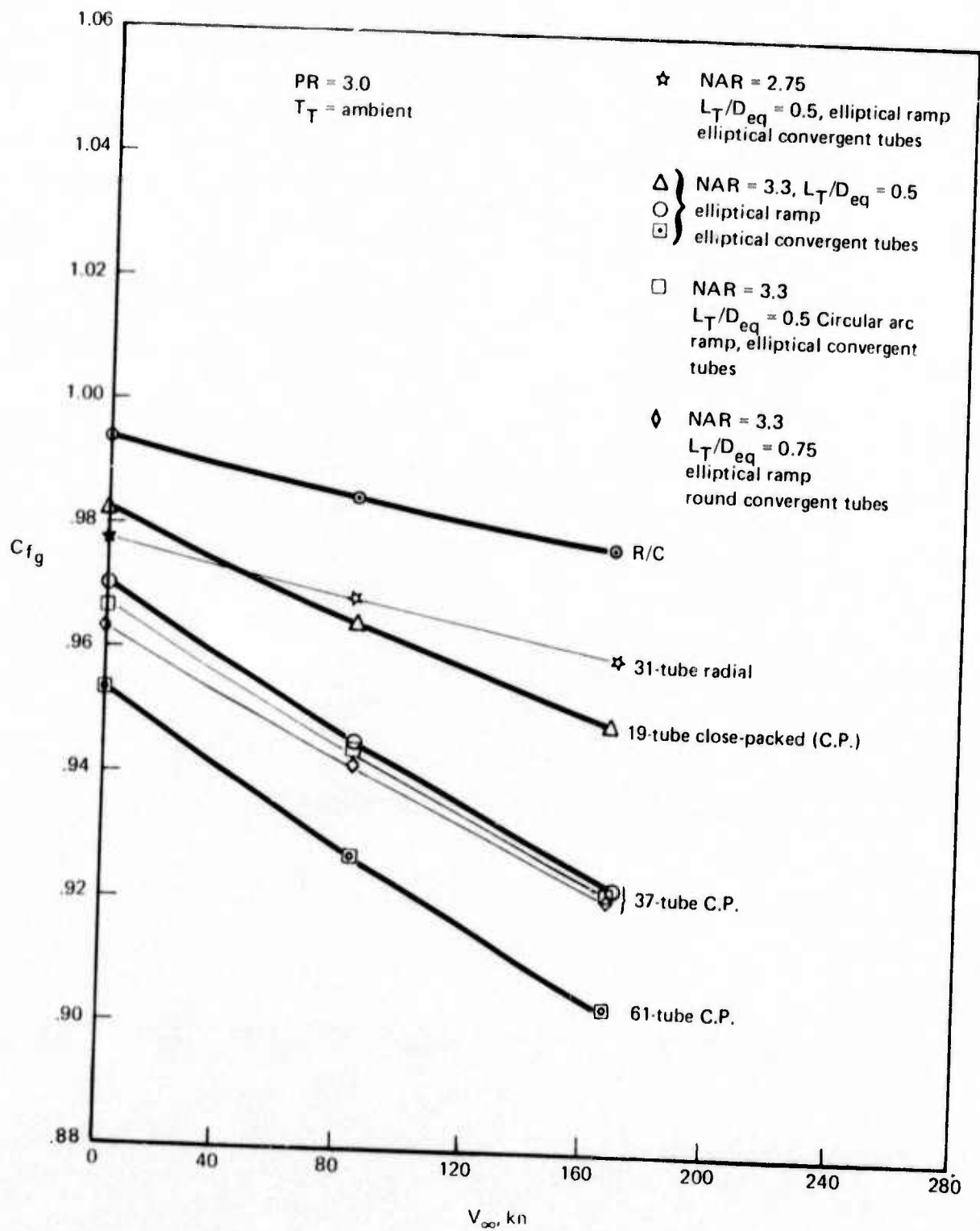


Figure 67.—Effect of Velocity on the Performance of Suppressors Without Ejectors

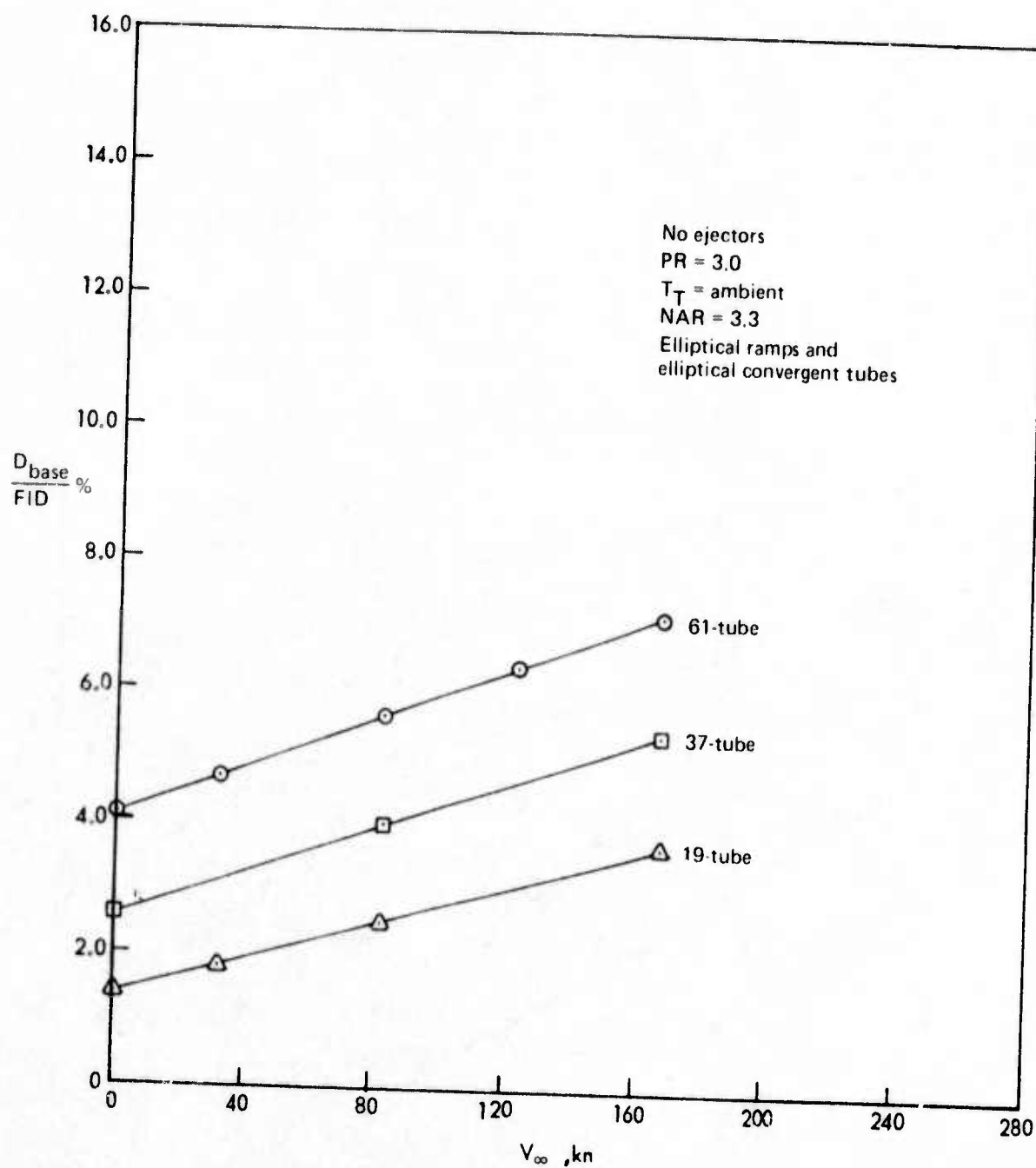


Figure 68.—Effect of Velocity on Base Drag as a Percentage of Ideal Thrust for NAR 3.3
 Suppressor With Various Numbers of Tubes (No Ejectors)

6.3.5 SUPPRESSOR/EJECTOR PERFORMANCE: AN EXAMPLE SUPPRESSOR WITH VARIOUS AREA RATIO EJECTORS

Ejector/suppressor interactions are first examined using various ejectors on a particular suppressor. The 3I-tube, NAR-2.75 radial suppressor was fitted with various ejectors of constant length, $L_E/D_{eq} = 2.0$. Ejector area ratios (EAR) cover the useful range from EAR = 2.6, where the outermost jet plumes nearly impinge on the ejector, up to EAR = 3.7, the limit of sufficient ejector length for mixing.

The various performance components are discussed separately below. The principal trends and tradeoffs also apply to all other configurations investigated, though levels of performance will vary from one suppressor to another.

6.3.5.1 Base Drag

The drag on the flat baseplate increases linearly with velocity for configurations tested. The 3I-tube nozzle has good ventilation and a small nozzle area ratio resulting in relatively small values of base drag. Figure 69 shows the base drag of this nozzle as a function of velocity for various ejector area ratios. The trends shown display the fundamental reaction of base drag to the presence of an ejector with forward velocity. The dominant effect of the ejector on base drag is to alter the level and not the rate of change of base drag with freestream velocity.

The pressure near the outside of the baseplate produced by the velocity of the air entering the ejector causes large changes in the base pressure and, hence, drag. Figure 69 shows that the base drag with the ejector having the most restricted inlet is nearly five times as great as that with the no-ejector. Using setback to increase the annular inlet to the ejector and lower the velocity of the inlet air results in a substantial reduction in base drag.

As forward velocity increases, the momentum of the secondary air resists turning to enter the recirculation region between the tubes near the baseplate. The related reduction in pressure on the boundary of the recirculation region results in an increase in drag with velocity. The base drag increases linearly with velocity and, to a first order, the rate of change is independent of the ejector area ratio and setback. A second order effect causes an additional increase in the rate of changes in base drag with velocity as ejector area ratio increases.

Summarizing, base drag has the following characteristics:

- It is primarily dependent on the suppressor ventilation and effective ejector inlet area, which causes large changes in the level of performance.
- Increases linearly with velocity.
- Rate of change in base drag with velocity is nearly independent of ejector geometry or setback and has nearly the slope of the no-ejector case.

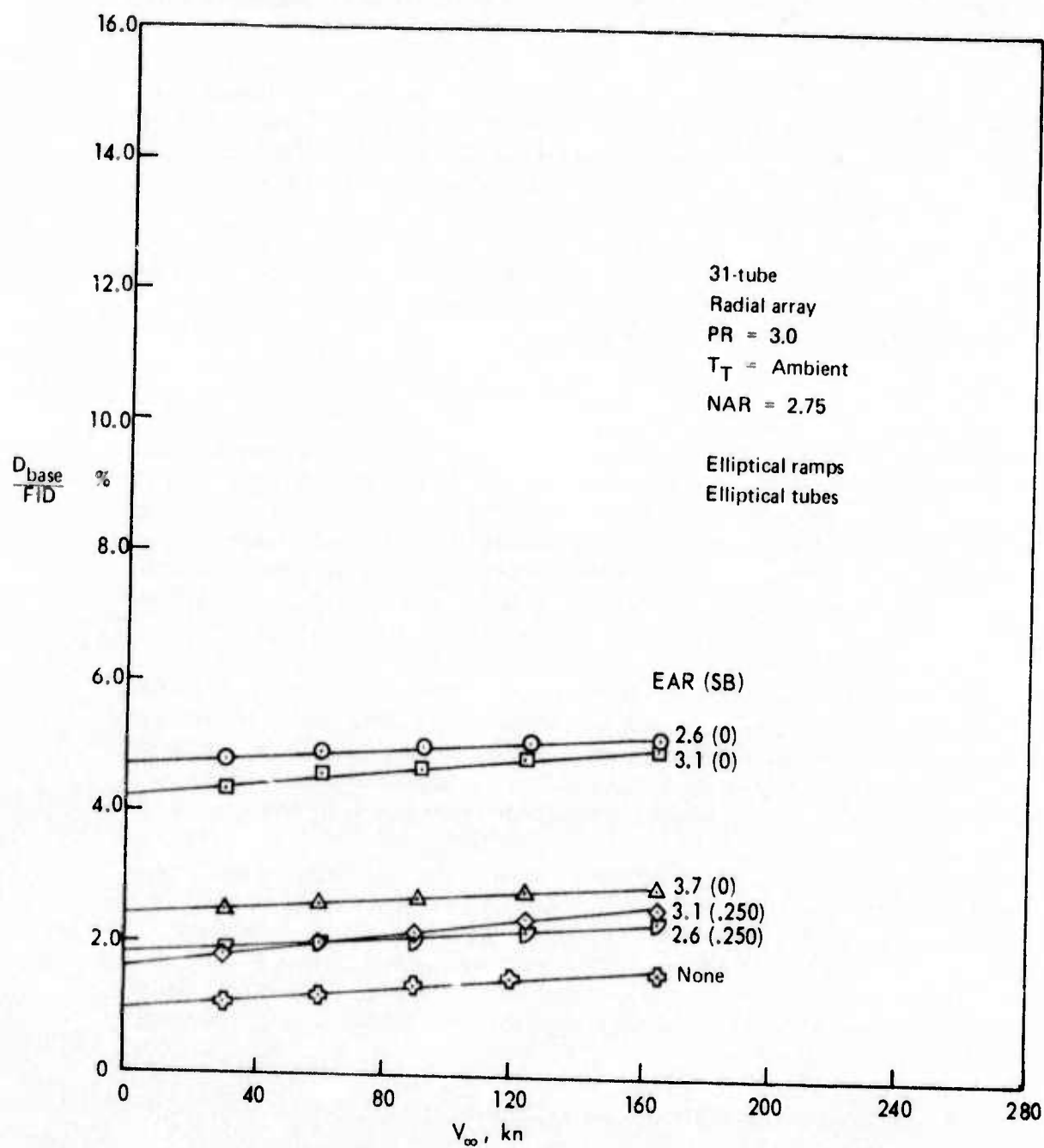


Figure 69.—Base Drag as a Percentage of Ideal Thrust for Various Ejectors on the 31-Tube, NAR 2.75 Radial Array Suppressor

- As a second order effect, the rate of change of base drag with velocity increases as the ejector area ratio increases.

6.3.5.2 Ramp Drag

The ramp drag (detailed in sec. 6.3.6.2) is a function of the square of the velocity. The presence of an ejector affects the level of the ramp drag statically but does not affect the rate of change of ramp drag with velocity.

6.3.5.3 Afterbody Drag

The sum of the linear base drag and nonlinear ramp drag is shown in figure 70 as a function of the velocity for the 31-tube suppressor and various ejectors.

6.3.5.4 Ejector Lip Suction

Ejector lip suction decreases with increasing velocity. Over the range of ejector area ratios investigated, the level of lip suction is primarily determined by the static performance because the rate of change of lip suction with velocity is reasonably independent of configuration for ejectors with sufficient length and unrestricted inlets*. The nonlinear decrease in lip suction with velocity is due to the movement of the stagnation point on the lip and the decrease in secondary air handling due to the ramp drag penalty and possible decreased inlet recovery.

Figure 71 demonstrates lip force as a percentage of ideal thrust versus velocity for various ejectors fitted to the 31-tube, NAR-2.75 suppressor. Notice that the 3.7% decrease in lip suction/FID from static to 167 kn holds even though the level of the EAR-3.1 with zero setback configuration is 5% higher than the EAR-2.6 configuration with setback. Two exceptions are shown in the figure. The EAR 2.6 ejector without setback has an inlet that is so restricted that the secondary air is supersonic at the throat at pressure ratio = 2.7. Severe ejector vibrations due to the shock-induced flow instabilities prevent the acquisition of data at pressure ratio 3.0. As mentioned in the discussion of pressure ratio effects, performance decreases rapidly (with increasing pressure ratio) just prior to the onset of ejector vibration. It was also noted that the pressure ratio at which supersonic throat flow occurs moves to slightly higher values as the velocity increases.** The combination of these effects produces the decreased lapse rate noted for the restricted inlet of the EAR-2.6 ejector with zero setback (shown at PR = 2.7). The implication is that, had the ejector inlet been slightly larger, the lip suction at low velocity would have increased to result in a lapse rate of nearly the 3.7% noted for the other configurations. The other exception noted in figure 71 demonstrates the dependence of ejector performance on ejector length. As the ratio of the ejector-to-suppressor area ratios (EAR/NAR) increases, more ejector length is required

*Theoretically (ref. 6), lip suction increases as ejector area ratio increases.

**Probably a ram effect due to increased P_T freestream (relative to P_{Tp})

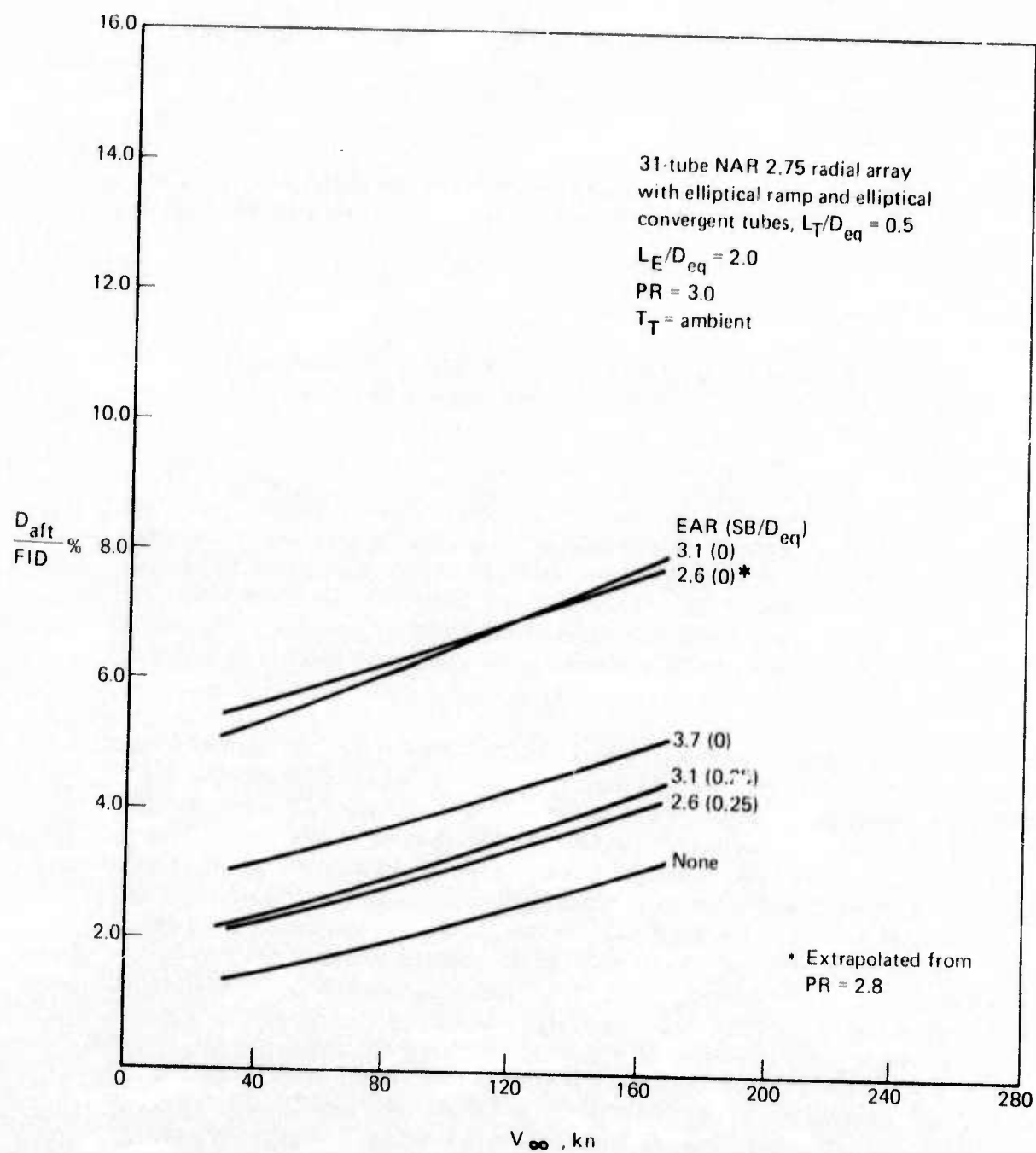


Figure 70.—Afterbody Drag Versus Velocity for a 31-Tube, NAR = 2.75, Radial Array With Various Ejectors

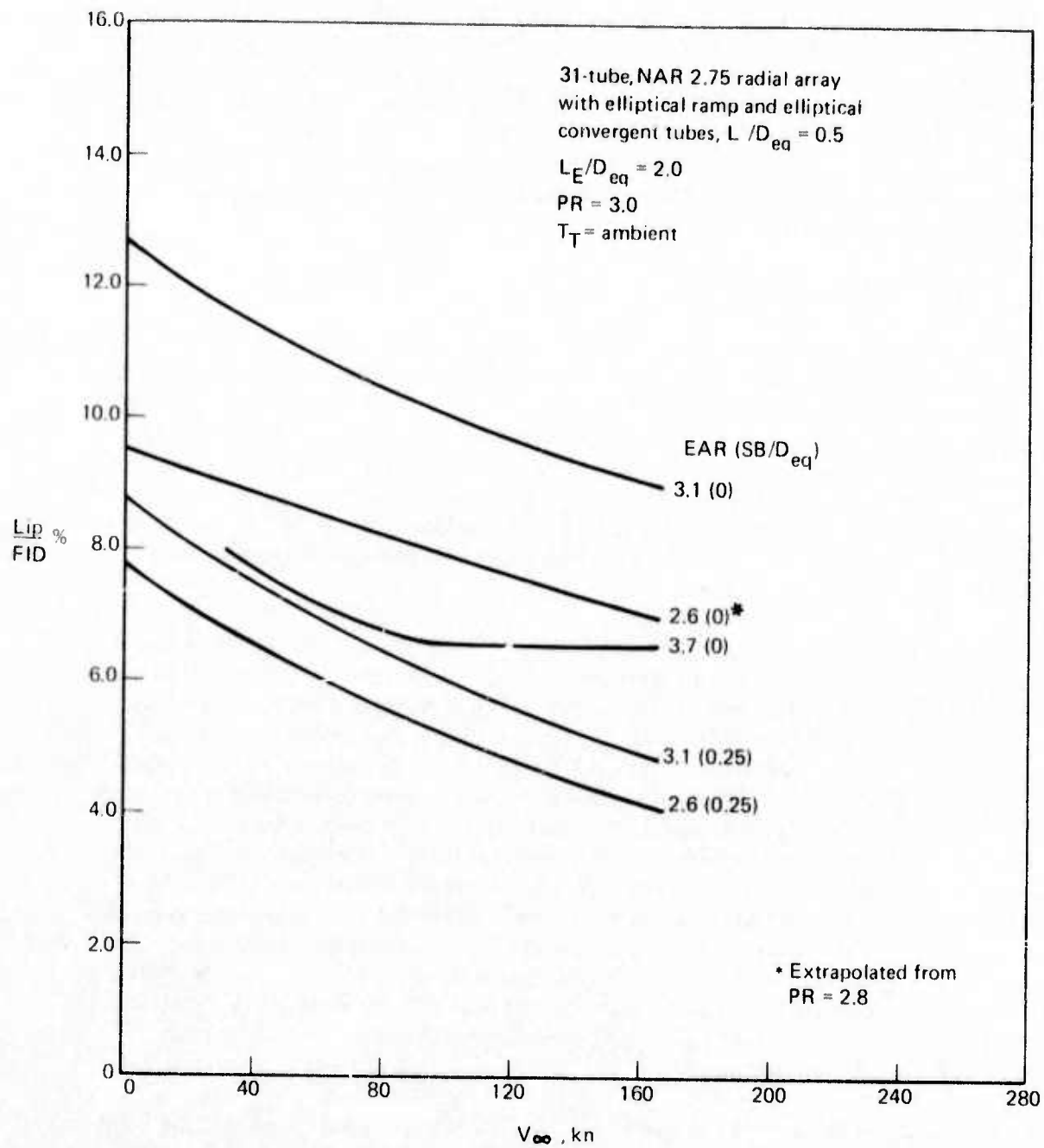


Figure 71.—Lip Suction Versus Velocity for 31-Tube, NAR = 2.75 Radial Array
With Various Ejectors

to produce optimum mixing. Though the subject of ejector length is treated separately (sec. 6.3.7.5), it is instructive to note that, on the chosen NAR-2.75 suppressor fitted with various area ratio ejectors of constant length ($L_E/D_{eq} = 2.0$), the EAR 3.7 ejector is not long enough to provide sufficient mixing. The result is a decrease in entrained secondary air and, in turn, a decrease in the velocity of the air entering the inlet. Thus, the lip suction did not change as much with forward velocity as it did in the other configurations. The short ($L_E/D_{eq} = 2.0$), EAR-3.7 ejector fitted to the NAR-2.75 suppressor shows no decrease in lip suction/FID above 90 kn.

6.3.5.5 Gross Thrust Coefficient

The gross thrust coefficients for the various ejectors fitted to the 31-tube, NAR-2.75 suppressor are shown in figure 72 as a function of forward velocity. The primary components affecting the lapse rate are the surface forces shown in figures 70 and 71. One-dimensional ejector theory (ref. 6) requires an increase in secondary air handling and lapse rate with increasing ejector area ratio. For the EAR 2.6 and 3.1 ejector area ratios investigated, the dominant effect of the ejector is to shift the level of performance and not to produce a large change in lapse rate. Thus, the primary effect of the changes in EAR and setback for these configurations is to alter the effective ejector inlet area into which a nearly fixed amount of secondary air must flow.

The EAR 2.6 ejector provides such a restricted inlet that supersonic inlet flow occurred at a pressure ratio of 2.8. By increasing the setback (SB/D_{eq}) to 0.25, the effective inlet was increased sufficiently to eliminate the supersonic flow problem and produce substantial reductions in both lip suction and afterbody drag, resulting in a favorable tradeoff for a net increase of 1.2% at all velocities. The EAR 3.1 ejector, on the other hand, has enough inlet area ($EAR/NAR = 1.13$) that zero setback produces slightly better performance than the $SB/D_{eq} = 0.25$. (The actual peak performance occurs at an intermediate setback.) Notice that the small change in performance ($< 0.5\%$) at these two setbacks is a result of more than 3.5% change in lip suction and base drag. The EAR 3.7 ejector of the same physical length as the others has insufficient mixing length to entrain the required amount of secondary air. The effects of the decreased secondary air handling is twofold; the static performance is less than the EAR 3.1 ejector because of insufficient lip suction, but lapse rate is also less, suggesting higher crossover velocity. The crossover velocities are greater than 167 kn for all ejectors used with the 31-tube suppressor except the restricted inlet case of EAR 2.6 without setback.

The performance of the same set of ejectors on a different suppressor (37-tube, NAR-2.75, close-packed) is shown in figure 73 for comparison. The performance levels are lower than those for the 31-tube, NAR-2.75 radial (fig. 72) due to the decrease in ventilation on the close-packed array. The lapse rates are similar for the EAR 2.6 and 3.1 ejectors with $SB/D_{eq} = 0.25$ and the EAR 3.7 ejector without setback. The EAR 3.7 ejector ($EAR/NAR = 1.13$) has an ejector-length-to-individual-jet diameter ratio (L_E/d) of 11.7, which appears to have been sufficient to provide approximately the same secondary air handling as the EAR 2.6 and 3.1 ejectors.* Because the effective inlet area is more restricted on the 37-tube,

*Recall from figure 72 that the same ejector on the 31-tube suppressor, $L_E/d = 10.7$, did not have a sufficient number of tube diameters to entrain the amount of air handled by the EAR 3.1 ejector.

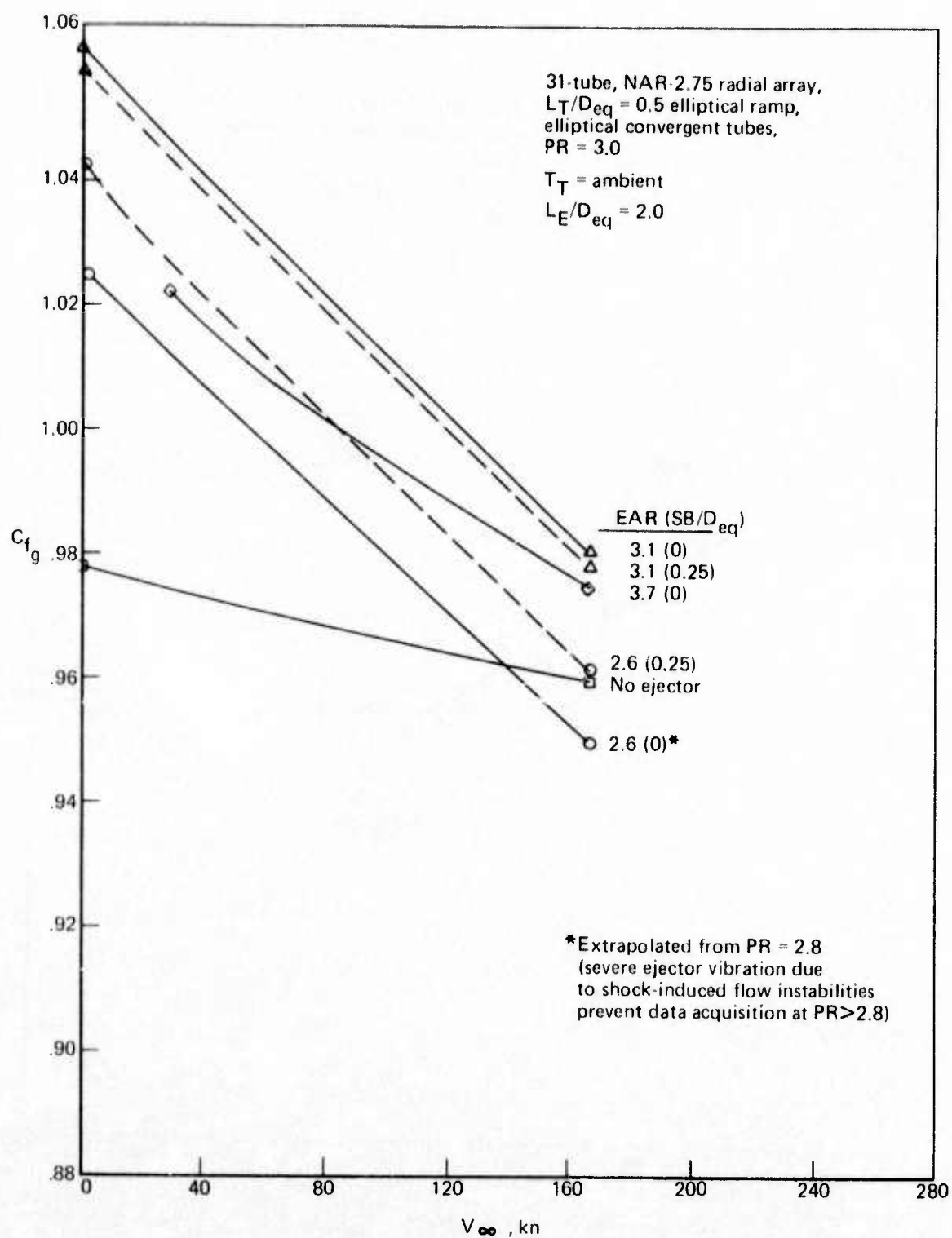


Figure 72.—Effect of Ejector Area Ratio on Performance at Forward Velocity

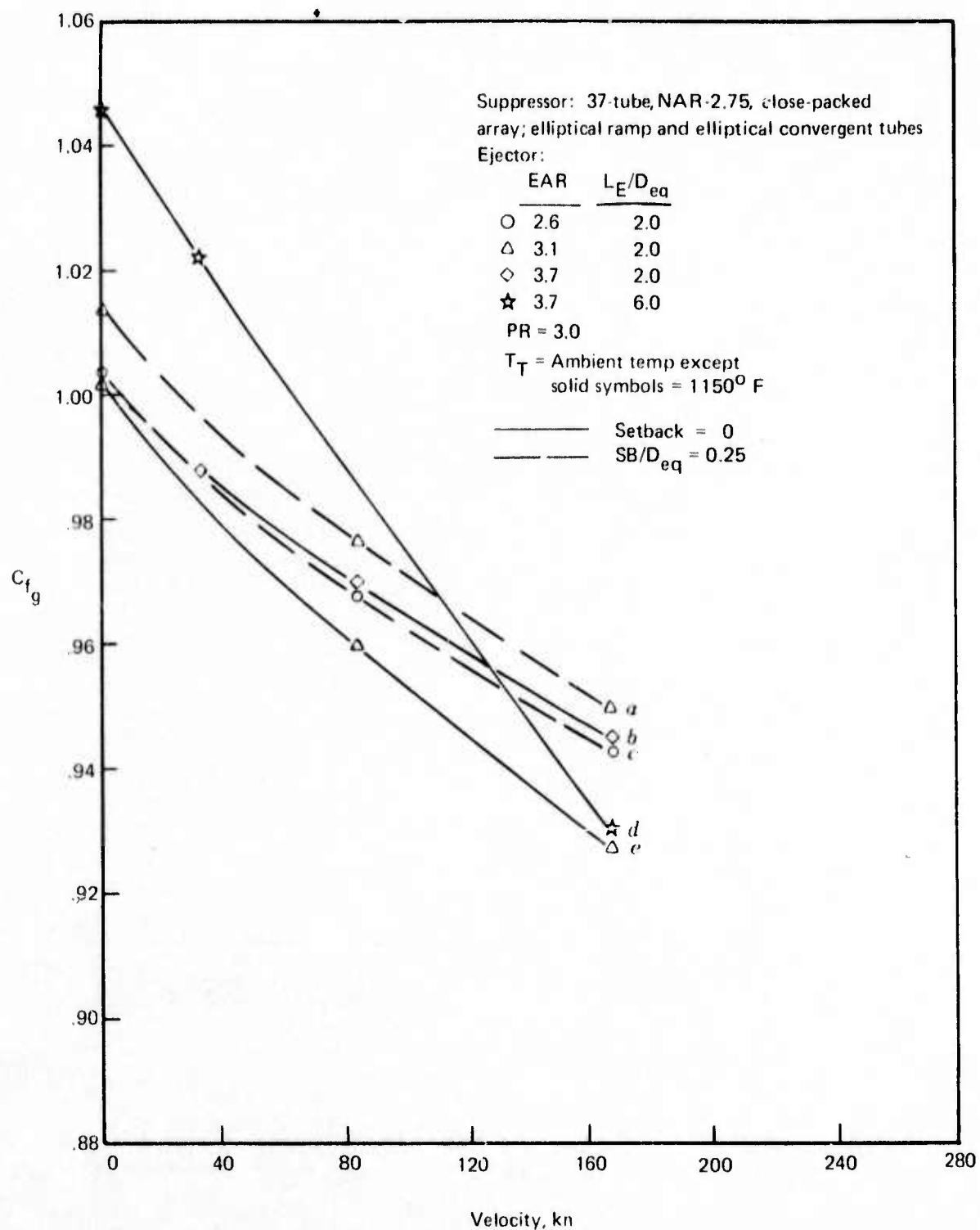


Figure 73.—Effect of Velocity on the Performance of Constant Suppressor With Various Ejectors

close-packed nozzle than the 31-tube radial, more setback is required to obtain optimum performance. Thus the EAR 3.1 ejector with setback (SB/D_{eq}) 0.25 has higher performance than the no-setback case for the close-packed array while the same amount of setback was more than was needed for the well-ventilated radial array.

The reasons for the occurrence of both increased performance and decreased lapse rate due to setback for the EAR 3.1 ejector (lines a and e in fig. 73) are discussed in section 6.3.7.4. Lines b and d in figure 73 demonstrate the effect of ejector length when all other parameters are held constant. The high static performance and sharp increase in lapse rate for the longer ejector imply that substantially more ejector length than 12 individual jet diameters is necessary to entrain the maximum amount of secondary air when $EAR/NAR = 1.3$. Even though the static performance of the long ejector is about 4.5% higher than that of the short ejector, the combination of the ram drag penalty due to the increased secondary air handling and the friction drag on the increased wetted area produces a greater lapse rate for the long ejector, and thus the short ejector performs better at velocities above 130 kn. The example points out the general trend that if—and only if—enough ejector inlet area and ejector length are provided, the effect of increasing ejector area ratio results in increased static performance and an increased lapse rate which causes a performance deficit at takeoff velocities.

Having examined particular suppressors with various ejectors, the effects of varying other parameters can now be examined.

6.3.6 SUPPRESSOR GEOMETRY EFFECTS

6.3.6.1 Nozzle Area Ratio

The effect of varying only suppressor area ratio on a suppressor with a fixed ejector size is demonstrated on figure 74. For the fixed EAR of 3.1, the NAR-3.3 suppressor is the largest nozzle area ratio that can be used without jet impingement on the ejector. This "tight" ejector configuration produces such a restricted effective inlet area (without setback) that supersonic flow is monitored at the ejector throat. By increasing the setback to 0.25 SB/D_{eq} , the base drag is reduced enough to produce a 7.5% increase in performance (C_{fg}). Notice that the lapse rate remains approximately the same for these configurations, suggesting that they handled similar amounts of air and that the dominant feature of the restricted inlet was to produce large values of base drag. The performance of the nozzle area ratio 2.75 suppressor with the same ejector benefits from the larger annular opening, AA . Its zero setback performance is nearly 7% above that of the NAR-3.3 suppressor. The performance level of the NAR-2.75 suppressor without setback is within 1% of the NAR-3.3 suppressor with setback at 167 kn, and the lapse rate of the two curves is within 0.75%.

The change in lapse rate with setback for the NAR-2.75 nozzle is explained in part in section 6.3.7.4. Because the ejector is at the limit of sufficient mixing, some of the change in lapse rate may be due to secondary air-handling variations caused by setback. (There is insufficient data to verify or contradict this.)

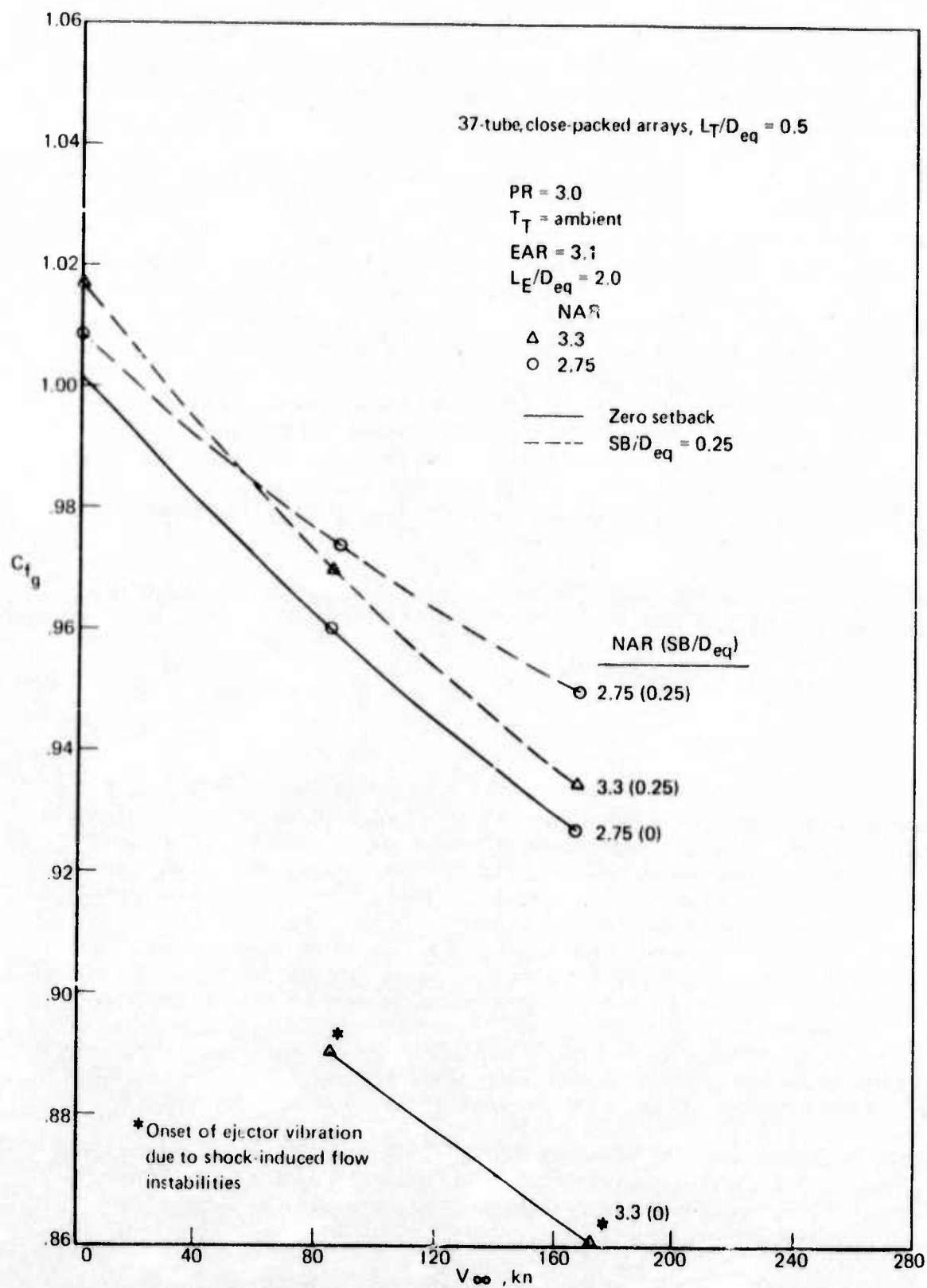


Figure 74.—Effect of Suppressor Nozzle Area Ratio on Performance With Forward Velocity

6.3.6.2 Ramp Shape

Reference 4 indicated a performance gain due to the use of a ramp rather than allowing a separated region to exist between the outer tubes and the nacelle o.d. as shown below.

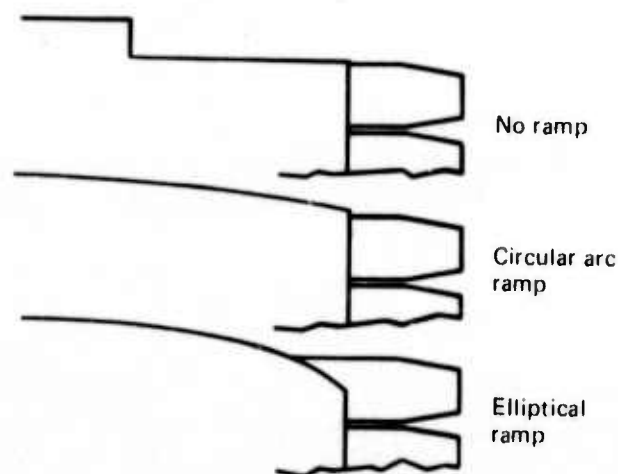


Figure 75.—Ramp Shapes

Ramps were always used in the present investigation to minimize the separated base region. Two ramp shapes were used: a circular arc ramp terminating at the outside of the outer tubes and an elliptical ramp extending to the center of the outer row tubes (fig. 75). The total projected area of the sum of the ramp and base are the same for the two configurations. It was assumed at the outset that the increase in minimum dimensions from the base-plate to the ejector provided by the elliptical ramp would result in improved mass flow into the ejector and the radial location of the separated flow should be less.

Minimizing the separate region by using a ramp is important, but experimental results show that the shape of the ramp is unimportant to the overall performance of the ejector suppressors in the range of tube lengths pressures and velocities tested. Figure 76 shows the ramps superimposed on a 37-tube, NAR-3.3 suppressor with an EAR-3.1 ejector.

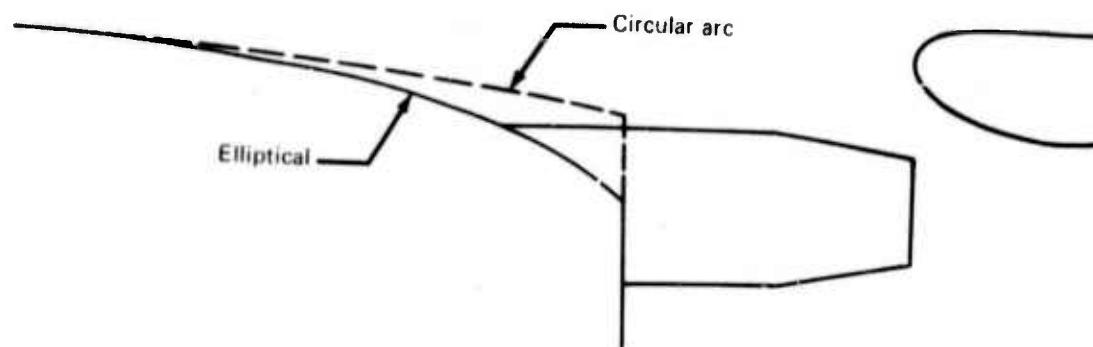


Figure 76.—Superposition of Circular Arc and Elliptical Ramps on a 37-Tube, NAR-3.3 Suppressor With EAR-3.1 Ejector (Zero Setback)

The performance of this suppressor/ejector combination with the two ramps is shown on figure 77. With or without the ejector the performance change due to ramp shape is less than 0.5% over the entire velocity range tested. At 167 kn the ramp drag was 1% higher for the elliptical ramp than the circular arc ramp ($D_{aft}/FID = 2.1\%$ instead of 1.07%) for both the ejector and no-ejector cases. Of course, the elliptical ramp also has nearly twice the projected area. The effect of base drag almost completely compensates for the ramp drag. Afterbody drag, the sum of ramp and base drags, is nearly identical for the two cases.*

The lip suction does not "know" which ramp is being used. At 167 kn the lip suction as a percentage of ideal thrust equals 5.33 and 5.32 for the circular arc ramp and elliptical ramp, respectively. This implies that the majority of the flow into the ejector enters through the annular region between the outer row tubes and the ejector lip and that only a small percentage of the secondary mass flow "turns" down between the tubes near the baseplate.

To a first order approximation, the change in suppressor ramp drag due to forward velocity is not affected by the presence of the ejector. Figure 78 shows that for all combinations of ejectors and setback on the 31-tube, NAR-2.75 radial suppressor, the value of the ramp drag as a percentage of ideal primary thrust at pressure ratio 3.0 can be written as

$$\left. \frac{D_{\text{ramp}}}{FID} \right|_{\text{at } V_{\infty}} = \left. \frac{D_{\text{ramp}}}{FID} \right|_{\text{static}} + (6.7 \times 10^{-5}) V_{\infty}^2 \quad (1)$$

*At 167 kn, the no-ejector case has $D_{aft}/FID = 7.43\%$ for the circular arc and 7.45% for the elliptical ramp.

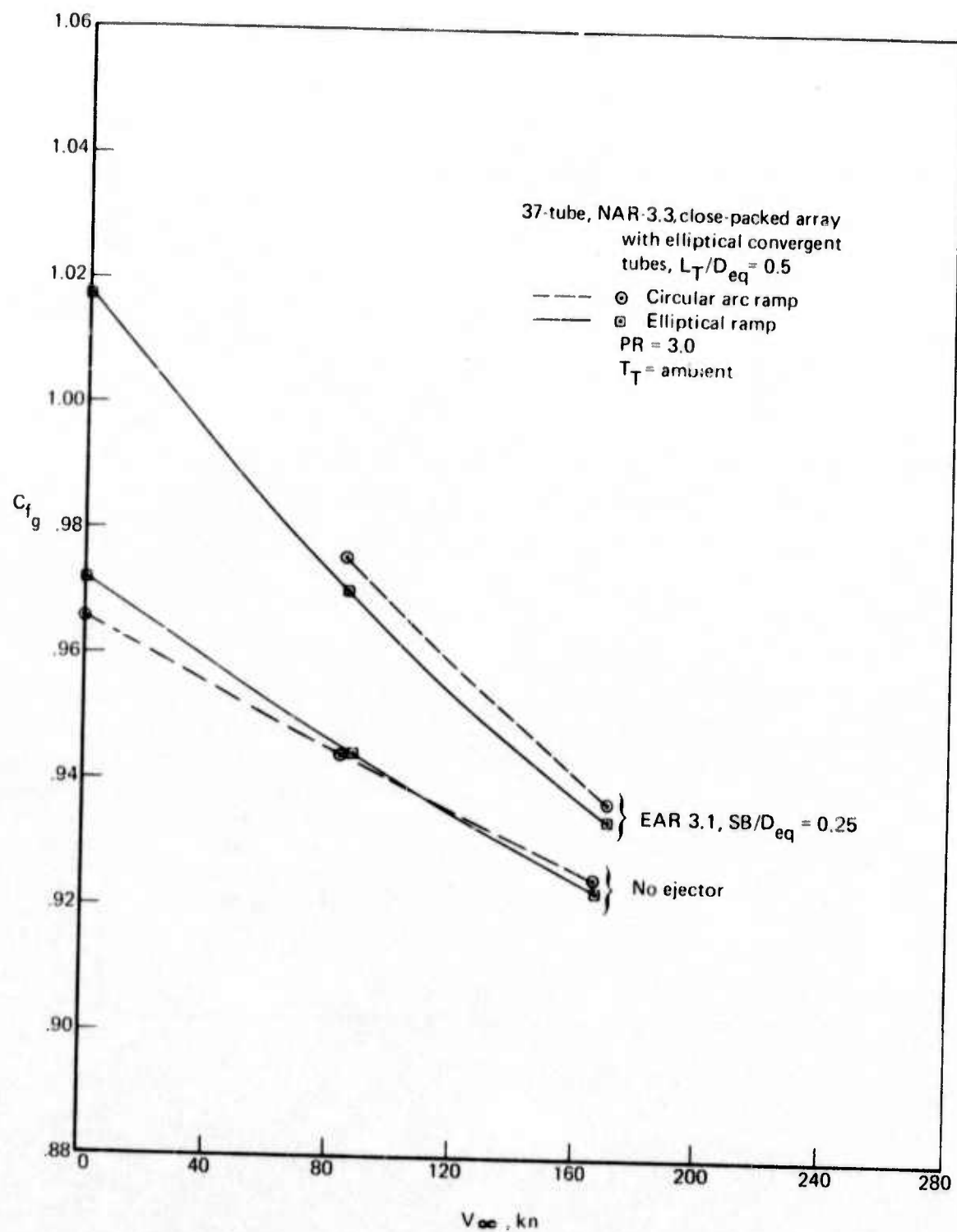


Figure 77.—Effect of Ramp Shape on Performance With Forward Velocity

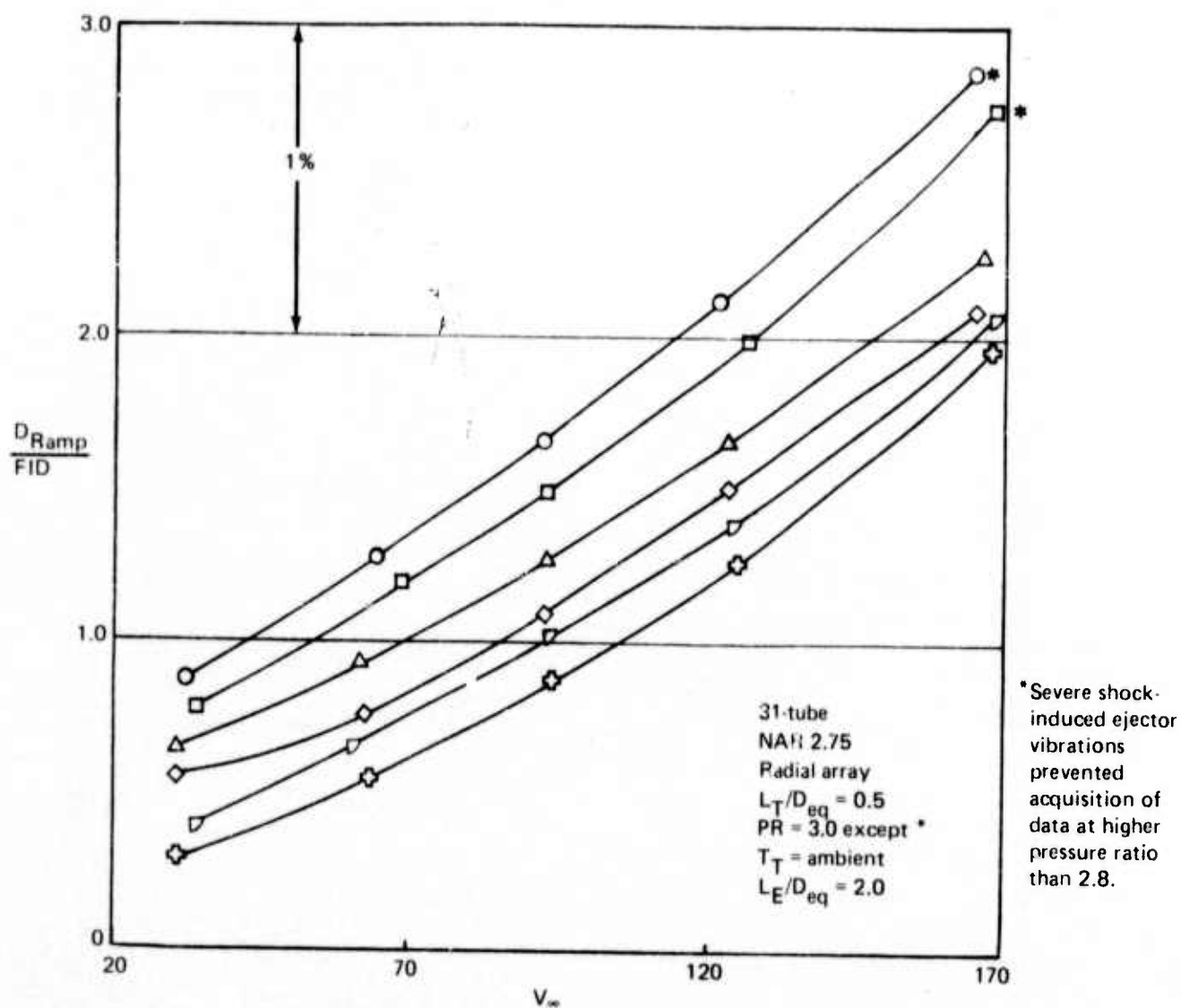


Figure 78.—Ramp Drag as a Percentage of Ideal Thrust Versus Velocity for the 31-Tube, NAR-2.75 Radial Array With Various Ejectors

Notice that the zero velocity intercept is affected by the presence of the ejector but that most ejector cases have exactly the same rate of change of ramp drag with velocity as the no-ejector case. The exceptions are the extremely restricted inlets produced by the zero setback cases of the EAR 2.6 and 3.1 ejectors. These two cases are so restricted on inlet area that severe ejector vibrations due to shock-induced flow instabilities prevented the data from being taken at pressure ratio = 3.0. Instead the values are taken at $PR = 2.8$.*

The consistency of the rate of change of drag with velocity for the various configurations suggests a flow-field near the ramp extending from the outside of the nacelle aft to and including the outside of the outer row tubes (at the baseplate) that does not "know" of the presence of the ejector. Any flow-field changes occurring near the suppressor must occur aft of the baseplate along the tubes.

The above statements were based on the 31-tube, NAR-2.75 radial array which is a very well-ventilated suppressor. For comparison examine the suppressor with the poorest ventilation, the 61-tube close-packed nozzle with elliptical ramp and $NAR = 3.3$. Figure 79 shows identical characteristics to those of the 31-tube array, i.e., the rate of change of ramp drag with velocity is independent of the presence of an ejector. Also notice that the same equation is adequate to quantify the amount of drag. The constant in equation 1 should change as ramp shape changes. For the single round convergent nozzle, the rate of change in ramp drag from 0 to 167 kn as a percentage of ideal thrust is 1.9, 1.3, 1.0, and 0.7 for pressure ratios of 2, 2.5, 3.0, and 4.0, respectively. For the circular arc ramp which extends only to the outside of the outer row tubes, the amount of increase in ramp drag from static to 167 kn is only 0.92% of ideal thrust at pressure ratio 3. Again, the behavior with velocity is that described by equation 1 where the constant for this small ramp is 3.3×10^{-5} . (Remember that differences in ramp drag between the circular arc and elliptical ramps are nearly counteracted by the changes in base drag.)

6.3.6.3 Tube Number

Changes in lapse rate due to tube number are insignificant. References 1 and 2 demonstrate a strong dependence of the static performance level on the base ventilation restrictions produced by tube number and nozzle array. Changing only the number of tubes in a suppressor/ejector configuration (with constant suppressor and ejector area ratio) results in a family of performance curves which are parallel, decreasing with velocity, and have levels governed by the static ventilation. Figure 80 presents these effects for 19-, 37-, and 61-tube, NAR-3.3 suppressors with a constant EAR 3.1 ejector using setback ($SB/D_{eq} = 0.25$) to assure adequate secondary inlet area to prevent supersonic flow at the ejector throat.**

*Since the rate of change of drag with velocity becomes an increasing percentage of FID as pressure ratio decreases, the amount of difference in the rate of change of drag on the ramp due solely to the presence of the ejector is 0.2% even for these very restricted "choked" inlets at $PR = 2.8$.

**The occurrence of supersonic flow at the ejector throat is observed for "tight" ejectors ($EAR/NAR \approx 1$) as the suppressor ventilation decreases due to insufficient setback.

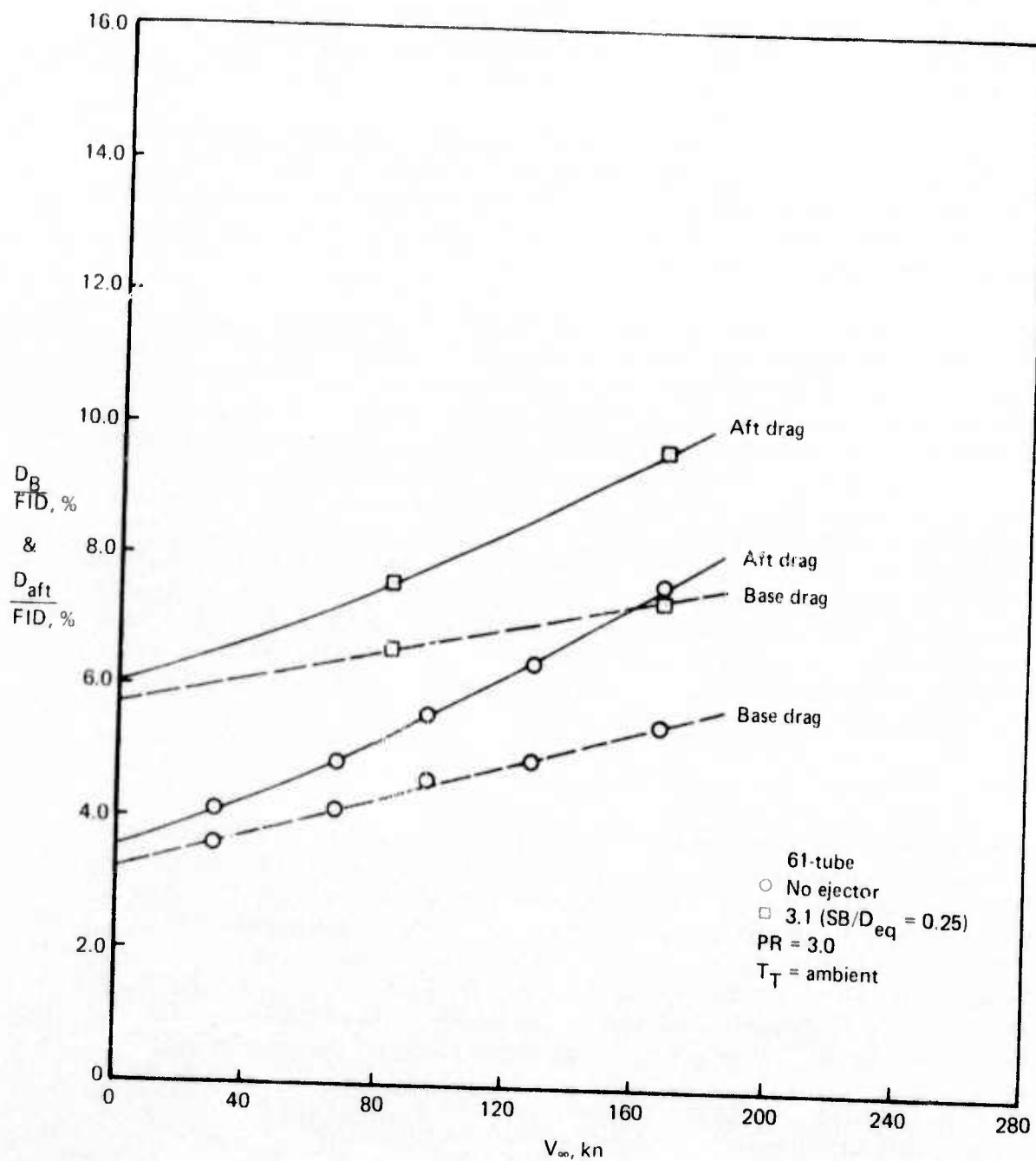


Figure 79.—Base and Afterbody Drags as a Function of Velocity for the 61-Tube, NAR-3.3 Close-Packed Suppressor With and Without Ejector

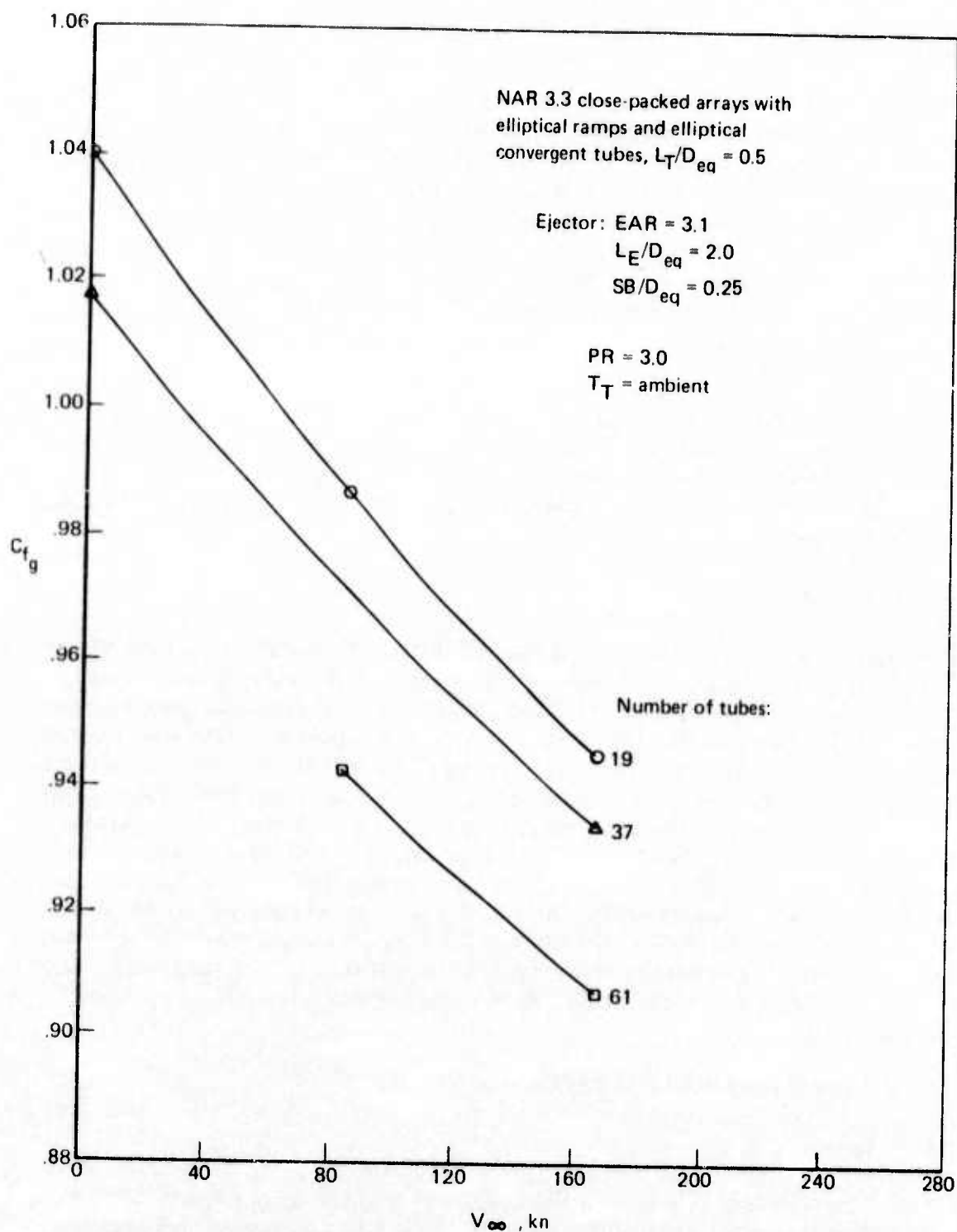


Figure 80.—Effect of Suppressor Tube Number on Performance With Forward Velocity

6.3.6.4 Tube Shape

Reference 1 established the importance of the shape of the individual tubes on the base drag and internal performance of multitube suppressors. The level of base drag is a strong function of the ventilation area between the outer row tubes. Use of elliptical convergent tubes was recommended because they provide large ventilation areas without sacrificing internal performance. The present investigation, while concentrating on elliptical convergent tubes, also sampled the lapse rate of configurations with round convergent tubes. Figure 81 suggests that, while the level of performance is sensitive to the ventilation resulting from the tube shape, the lapse rate is reasonably independent of tube shape.

6.3.6.5 Tube Length

The tube length behaves like the other geometric parameters affecting ventilation (i.e., the level of performance is a function of tube length, but the lapse rate is reasonably independent of tube length). References 1 and 2 discuss the importance of tube length on the static performance of multitube nozzles. Figure 82 demonstrates the lack of dependence of lapse rate on tube length.

6.3.6.6 Tube Array

Tube array, another parameter affecting base ventilation, does not affect the lapse rate of suppressor/ejector nozzles. References 1 and 2 demonstrate the strong increase in static performance due to the increased ventilation provided by radial arrays compared to close-packed arrays. Figure 83 shows the performance of close-packed and radial array suppressors, each having nozzle area ratio = 2.75 and each fitted with the same ejector (EAR 3.1) and no setback. The lapse rate of the two configurations is nearly identical. This behavior suggests that they handled the same amount of secondary air. The difference in performance level can be attributed to the small base drag resulting from good ventilation in the radial array. Notice that the radial array nozzle has the same performance at 115 kn that the close-packed array has statically. The lack of dependence of lapse rate on ventilation supports the flow model presented in section 6.3.7.3. In summary, the last four sections have shown that the geometric suppressor parameters that greatly affect static performance do not contribute substantially to the rate of change in performance due to forward velocity.

6.3.7 EJECTOR GEOMETRY EFFECTS

6.3.7.1 Ejector Drag

6.3.7.1.1 Pressure Drag.—As velocity increases, an increasing drag force is measured on the ejector boattail. For the constant area mixers of this investigation the boattail drag is the only ejector pressure force countering the ejector lip suction. Figure 84 shows the ejector drag (exclusive of skin friction drag) as a percentage of ideal thrust for various ejector area ratios, and the curves for both the EAR 2.6 and 3.1 ejectors can be expressed as

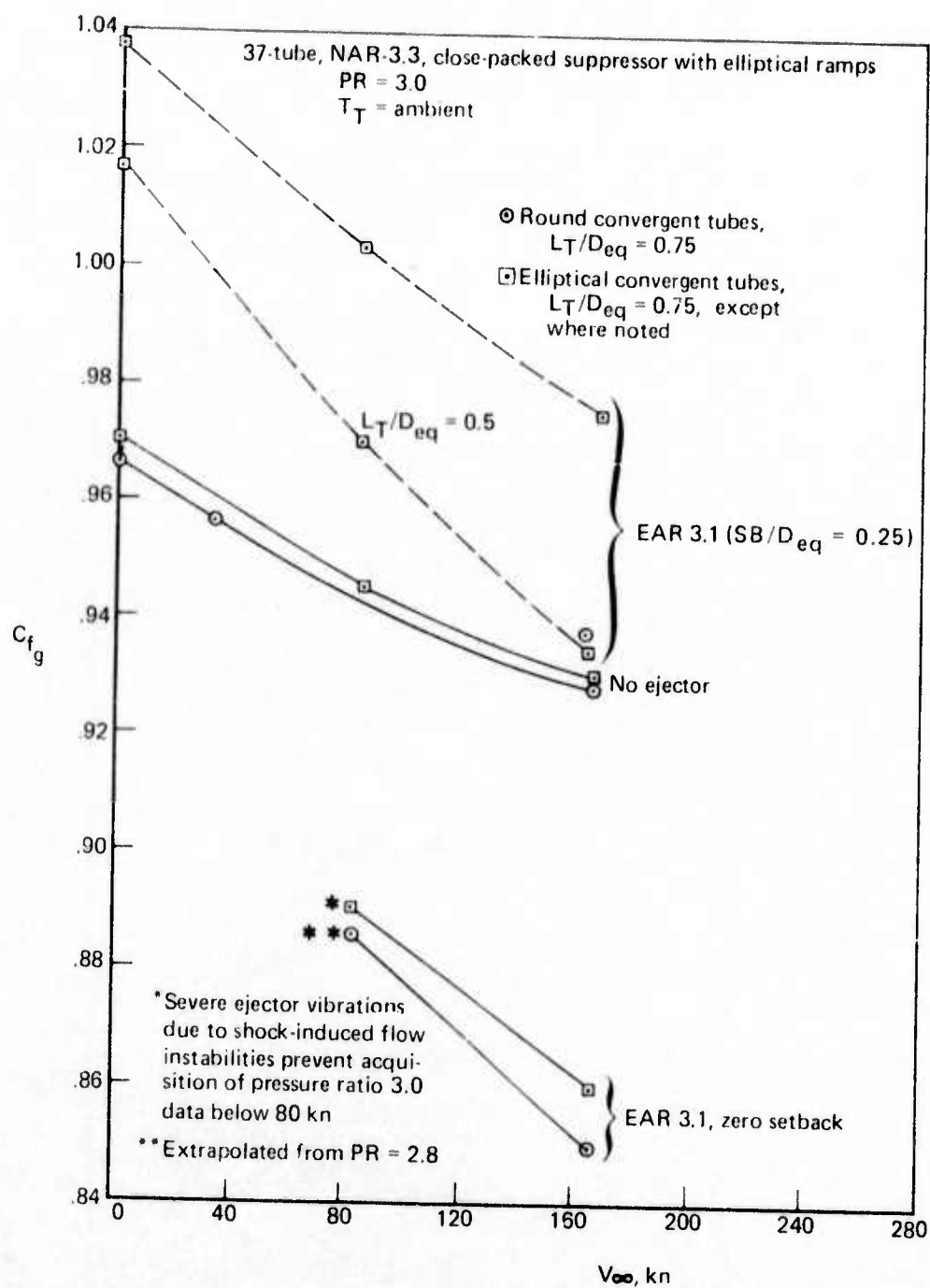


Figure 81.—Effect of Tube Shape on Performance With Forward Velocity

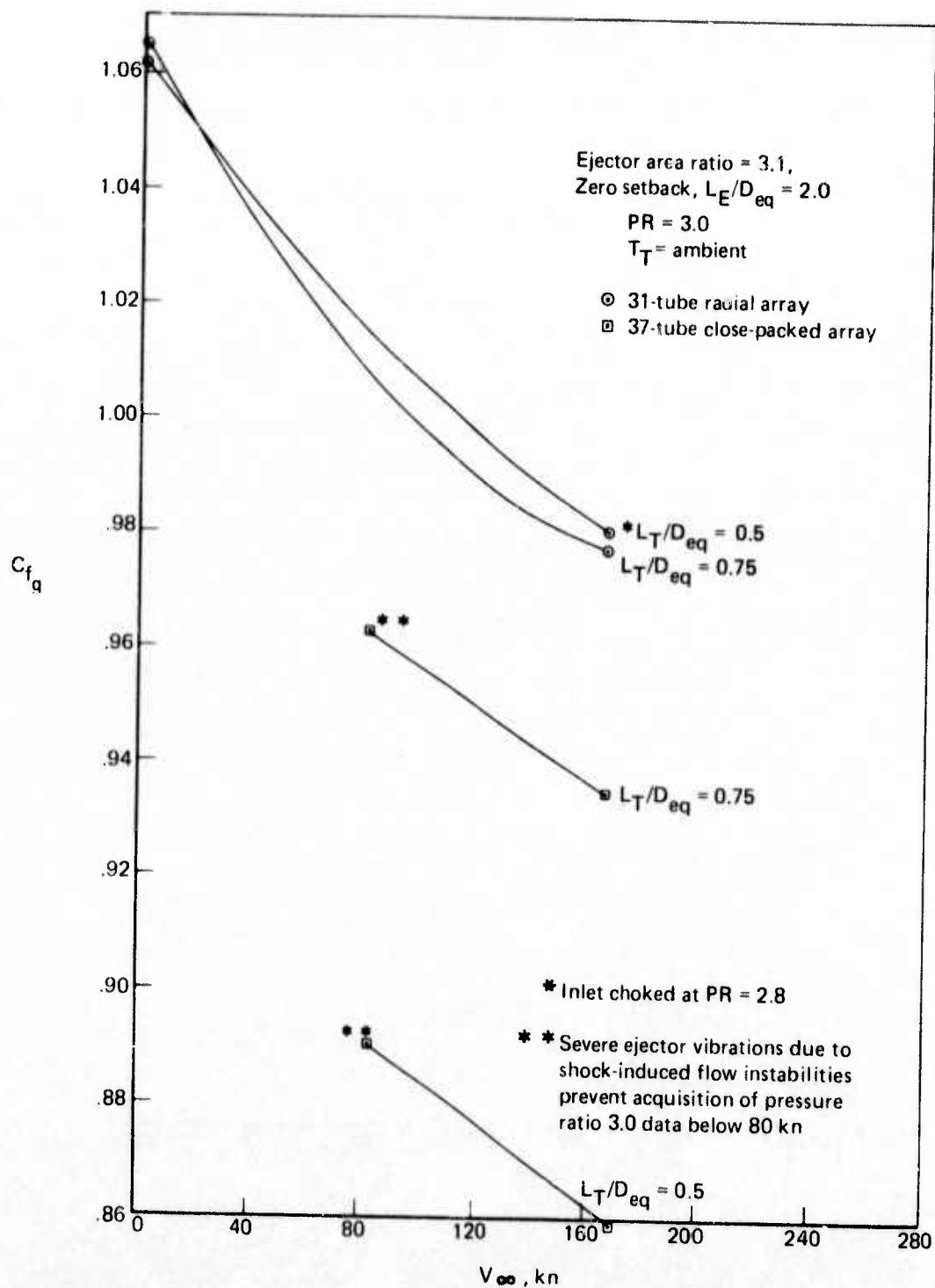


Figure 82.—Effect of Tube Length on Performance With Forward Velocity

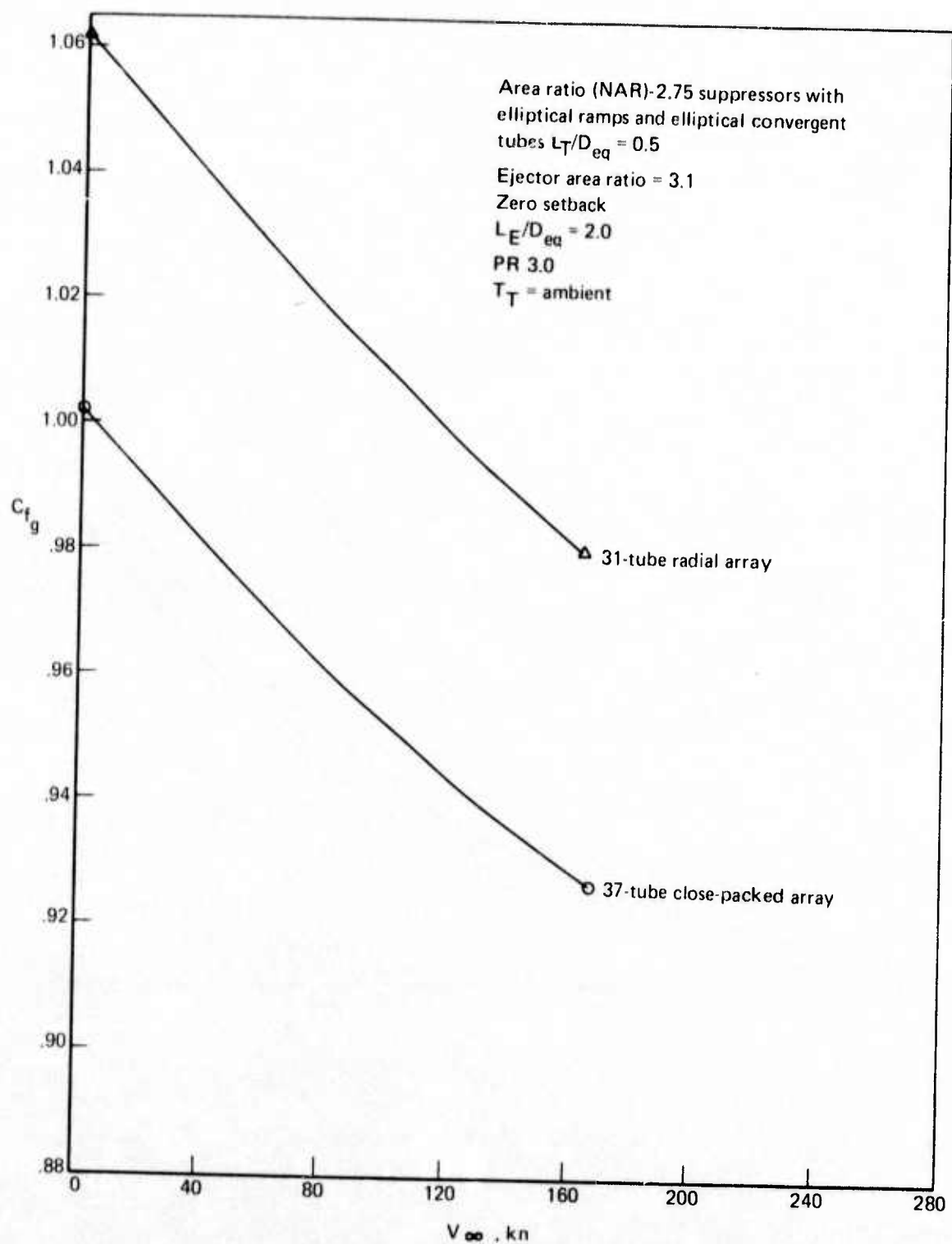


Figure 83.—Effect of Tube Array on Performance With Velocity

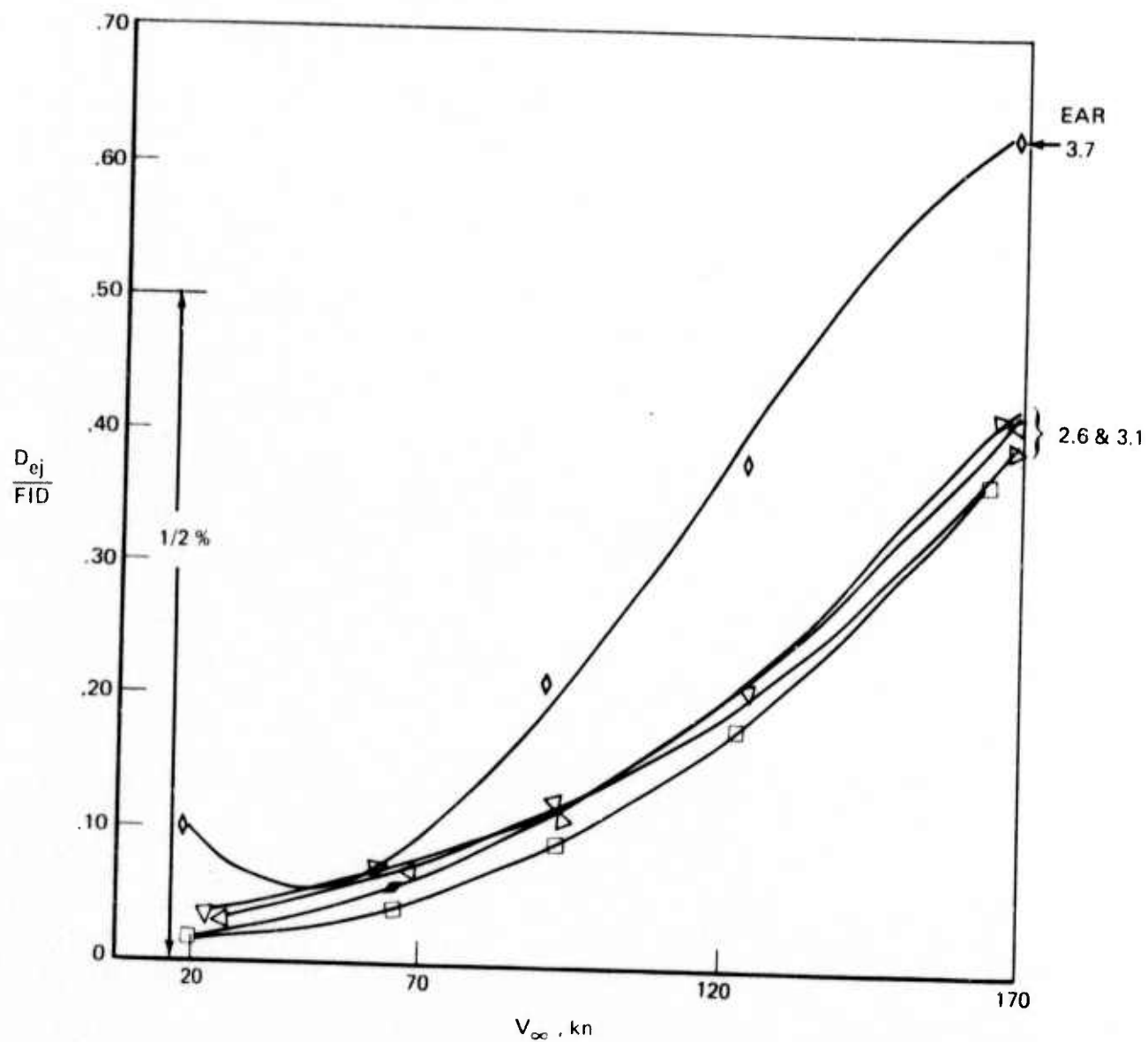


Figure 84. — Ejector Pressure Drag

$$\frac{D_{\text{ejector}}}{FID} = (1.43 \times 10^{-5}) V_{\infty}^2 \quad (2)$$

where the velocity, V_{∞} , is expressed in kn and D_{ejector}/FID is in percent. At a pressure ratio 3.0, the ejector pressure drag amounts to 0.4% of the ideal thrust at 167 kn. To hold a constant lip shape and thickness, the EAR 3.7 ejector has a diameter 12% larger than the suppressor nacelle diameter. Figure 84 shows the ejector boattail drag of the EAR 3.7 ejector (at $PR = 3.0$) to be

$$\frac{D_{\text{ejector}}}{FID} \text{ (for EAR 3.7)} = (2.2 \times 10^{-5}) V_{\infty}^2 \quad (3)$$

6.3.7.1.2 *Skin Friction Losses.* – Skin friction losses are not analyzed during the present investigation.

6.3.7.2 Secondary Air Handling

The effect of forward velocity in the tunnel results in the following relationships:

- If pressure ratio, P_{Tp}/P_{∞} is held constant, the effect of increasing velocity is a reduction in P_{Tp} , WP , and hence ideal primary thrust, FID , decreases.
- If $P_{Tp}/P_{T\infty}$ is held constant as velocity increases, the results are:
 1. Constant, P_{Tp} , and primary weight flow, WP .
 2. The pressure ratio P_{Tp}/P_{∞} increases. (For $P_{Tp}/P_{T\infty} = 3.0$, FID increases 1.7% from static to 167 kn for standard day, ambient conditions and 2.0% for 1150° F.)

Consider the following relationship where velocity is varied but $P_{Tp}/P_{T\infty}$ is held constant. The primary mass flow is independent of velocity as shown in figure 85.

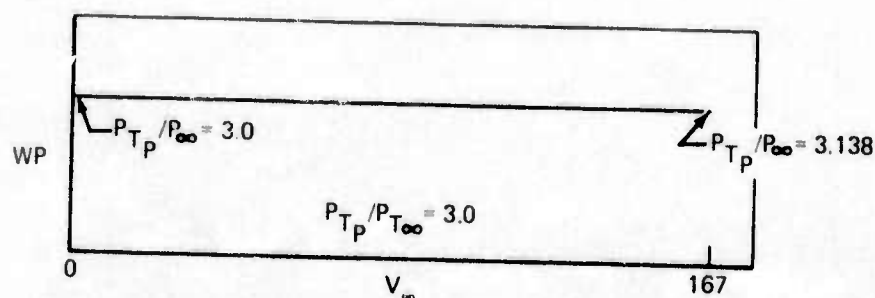


Figure 85.—Primary Weight Flow as a Function of Velocity (Constant $P_{Tp}/P_{T\infty}$)

Notice the pressure ratio must rise from 3.0 to 3.138 to produce a constant $P_{TP}/P_{T\infty} = 3.0$ at 167 kn ($M = 0.253$, standard day). Reference 7 provides measurements for secondary/primary weight flow ratios $W_S \sqrt{T_{TS}} / W_P \sqrt{T_{TP}}$ vs P_{TP}/P_{∞} statically for ejectors with large bellmouths and ejector area ratio = 3.1. These curves can be used to establish the trend for $W_S \sqrt{T_{TS}} / W_P \sqrt{T_{TP}}$ as a function of P_{TP}/P_{∞} , which is required to establish $W_S \sqrt{T_{TS}} / W_P \sqrt{T_{TP}}$ as a function of V_{∞} assuming the inlet recovery is approximately constant. Cross-plotting from reference 7 at the required pressure ratio yields the results shown on figure 86.

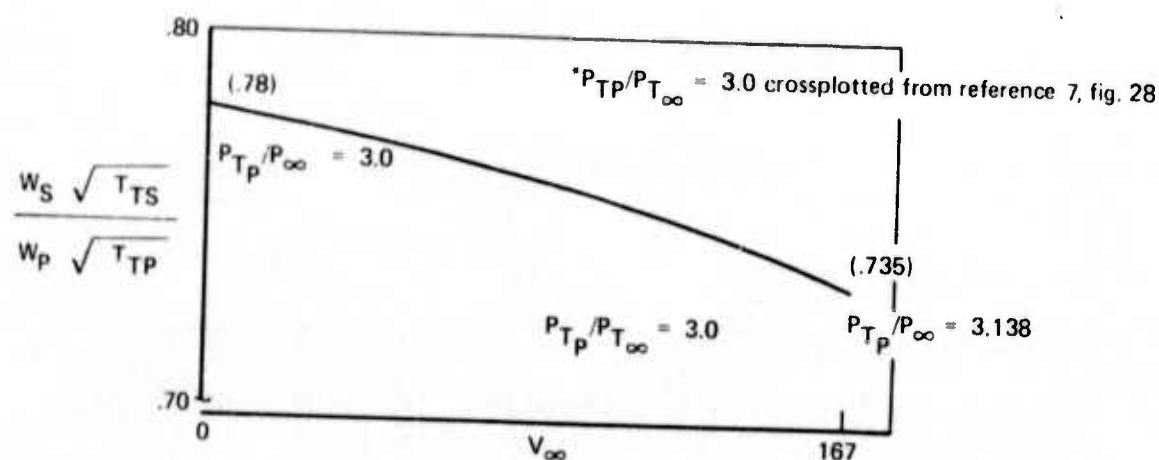


Figure 86.— $W_S \sqrt{T_{TS}} / W_P \sqrt{T_{TP}}$ Versus Velocity, for Constant $P_{TP}/P_{T\infty}^*$

As the secondary mass flow into the ejector decreases with velocity at constant $P_{TP}/P_{T\infty}$, the ejector lip suction should also decrease. The corresponding change in lip force for this configuration is shown in figure 87 to reflect a 9% change in lip suction for the above 5.7% decrease in secondary weight flow.

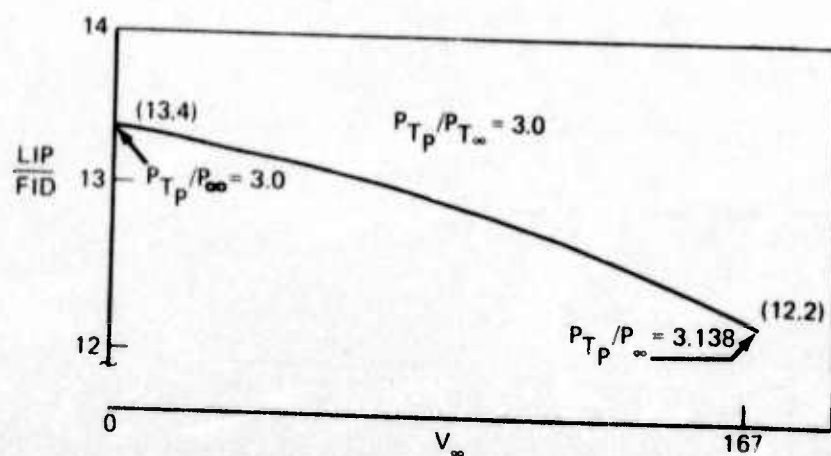


Figure 87.—Lip Suction Versus Velocity for Constant $P_{TP}/P_{T\infty}$

The 31-tube radial array with EAR-3.1 ejector and setback is studied in detail throughout this investigation. Plotting the lip force in pounds as a function of $P_{Tp}/P_{T\infty}$ results in figure 88.

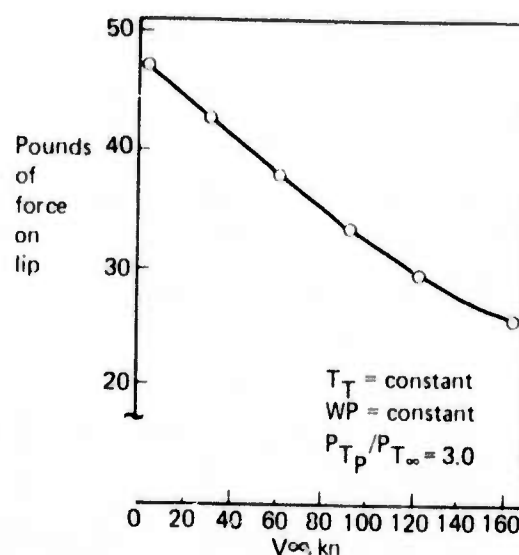


Figure 88.—Lip Force Versus Velocity for the 31-Tube NAR 2.75 Radial Array With EAR 3.1 Ejector (Zero Setback)

The lip force is shown to decrease by 4.6% from static to 167 kn (lip force/FID decreases by 47.7% from $LIP/FID = 8.73\%$ to $LIP/FID = 4.57\%$ at $P_{Tp}/P_{T\infty} = 3.0$). The comparison of this configuration with that discussed above from reference 7 suggests a much larger decrease in secondary air handling with velocity for the 31-tube configuration. If the ratio of weight-flow change to lip-suction change due to velocity were the same for the two configurations (it may not be), then the amount of secondary air handled by the 31-tube nozzle with EAR-3.1 ejector and setback would decrease by 30.2% as velocity increases from static to 167 kn.

From the above discussion we can establish some general qualitative results:

- Even with the two-to-one ellipse inlet chosen for the present investigation, the inlet recovery decreases substantially with forward velocities.
- The decrease in secondary air handling results in a decrease in the ram drag penalty, which in turn diminishes the rate of decrease in performance (i.e., improved lapse rate) with increasing velocity.

6.3.7.3 Inlet Flow Model

Secondary air entering the ejector to mix with the primary flow must pass through either the area between the outer tubes, A_S , or the annular area, A_A (fig. 89).

An effective inlet area can be defined by assigning discharge coefficients to the two geometric flow areas

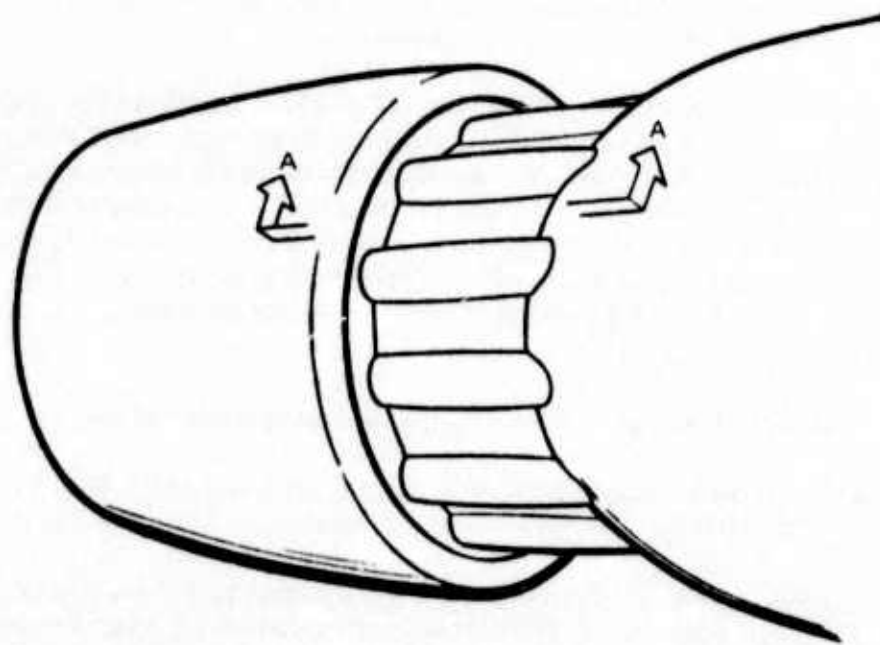
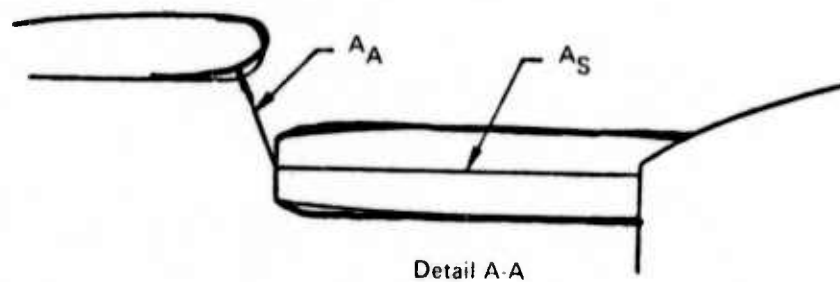


Figure 89.—Ejector Inlet Area A_A and A_S

$$A_{eff} = C_{DS}AS + C_{DA}AA,$$

where: A_{eff} is the effective ejector inlet area.

C_{DS} is the discharge coefficient of the flow passing between the outer row tubes.

C_{DA} is the discharge coefficient of the minimum annular area between the outer row tubes and the ejector lip.

The present investigation did not measure secondary mass flow rate and thus, does not quantify the values of C_{DS} and C_{DA} . On the other hand, the results and analysis presented in this chapter give a qualitative understanding of the relative importance of C_{DS} and C_{DA} .

For a fixed primary geometry, constant primary gas conditions, and constant ejector area ratio and length, a given primary nozzle tends to entrain a constant amount of secondary air; thus, any changes in the secondary air handling must be due to ejector inlet losses.

Experimental results suggest a flow field as shown in figure 90.

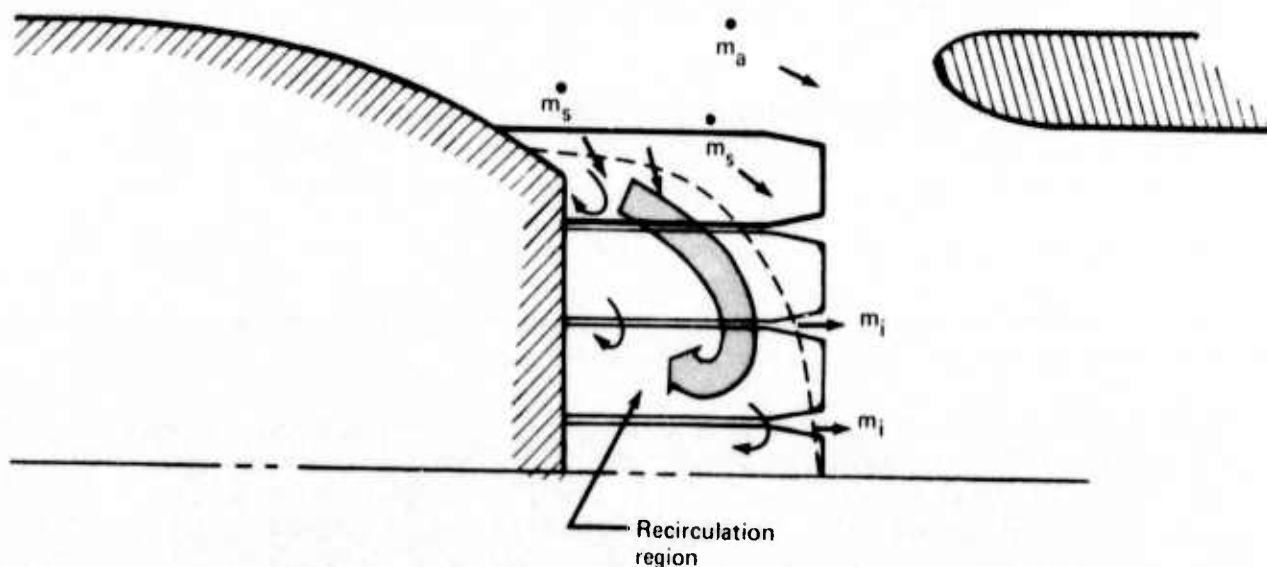


Figure 90.—Schematic for Suppressor/Ejector Inlet Flow Field

A large recirculation region exists aft of the base plate. The jets exiting the central tubes entrain air from the recirculation region, which must be replaced by air having a radial component, crossing A_S . The remainder of the secondary air goes directly into the ejector through A_A and a small portion of A_S . Statically, as the annulus area, A_A is reduced by decreasing setback (constant suppressor and ejector geometry and gas conditions), the velocity of the secondary mass flow must increase, resulting in a static pressure depression at the outside of the recirculating region. The demand for mass flow into the recirculating region remains similar because the suppressor jets tend to entrain a quantity of mixing air that is independent of the inlet size. The pressure near the outside of the baseplate produced by the velocity of the air entering the ejector produces large changes in the base pressure and hence the level of drag. Using setback as a technique to increase the annular inlet to the ejector and lower the velocity of the inlet air results in a substantial reduction in base drag.

The drag on the flat baseplate linearly increases with freestream velocity for configurations tested. The dominant effect of the ejector on base drag is to increase base drag. As forward (freestream) velocity increases, the momentum of the secondary air resists turning to enter the recirculating region between the tubes near the baseplate. The related reduction in pressure on the boundary of the recirculating region results in an increased drag with velocity. If the quantity of air entrained from the recirculating region were dependent upon the inlet area, then the slope of the base drag curve would be dependent on inlet area. However, this is not the case. The slope of drag increase with velocity is independent of ejector size or inlet area. (There is a second order effect of an additional increase in base drag due to increasing ejector area ratio). The fact that the increase in drag is also small compared to the value of the static drag implies that a relatively small percentage of the secondary air passes into the recirculating region. For the configurations investigated this requires that CD_D be small compared to CD_A .

Over the range of variables investigated, changes in inlet geometry produce large variations in surface pressure forces while creating relatively small variations in secondary mass flow. As a result, changes in performance level are large in comparison to changes in lapse rate.

6.3.7.4 Inlet Geometry

Reference 2 shows that ejector setback is a useful mechanism to provide optimum performance through the tradeoff between base drag and lip suction.

Figure 91 shows the effects of setback on the performance of a constant suppressor/ejector as a function of forward velocity. At any fixed velocity, performance is a nonlinear function of setback as demonstrated in figure 92. Base drag decreases asymptotically with increasing setback while the lip suction has a peak value at the minimum effective inlet area that provides the amount of secondary air that can be entrained by the primary jets.

For "tight" ejectors ($EAR/NAR \approx 1$), the annular secondary flow area A_A is inherently small, and setback must be used to optimize the performance. Figures 91 and 93 show the increase in performance due to increasing the inlet area with setback for two configurations

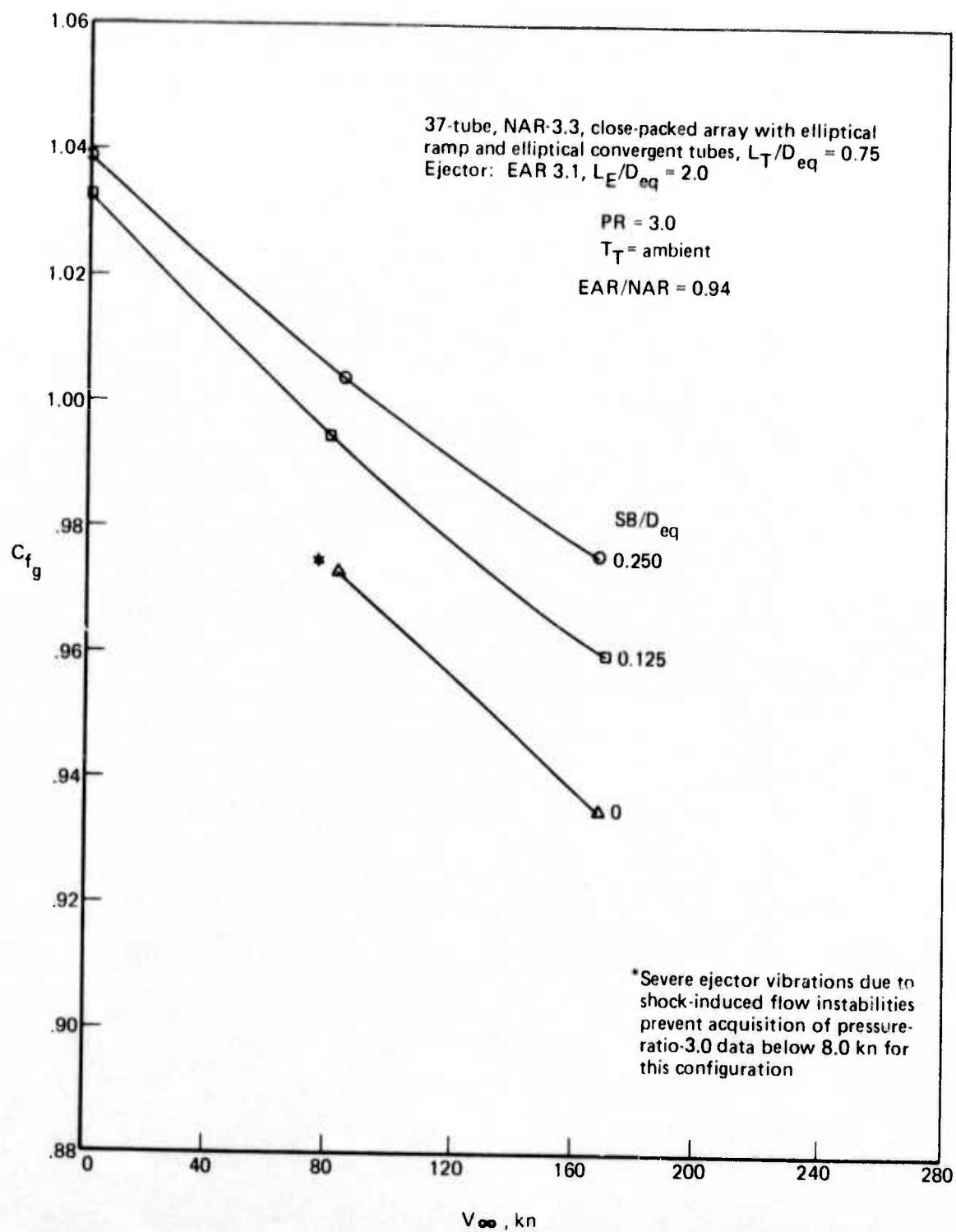


Figure 91.—Effect of Setback and Velocity on Performance (Other Parameters Constant)

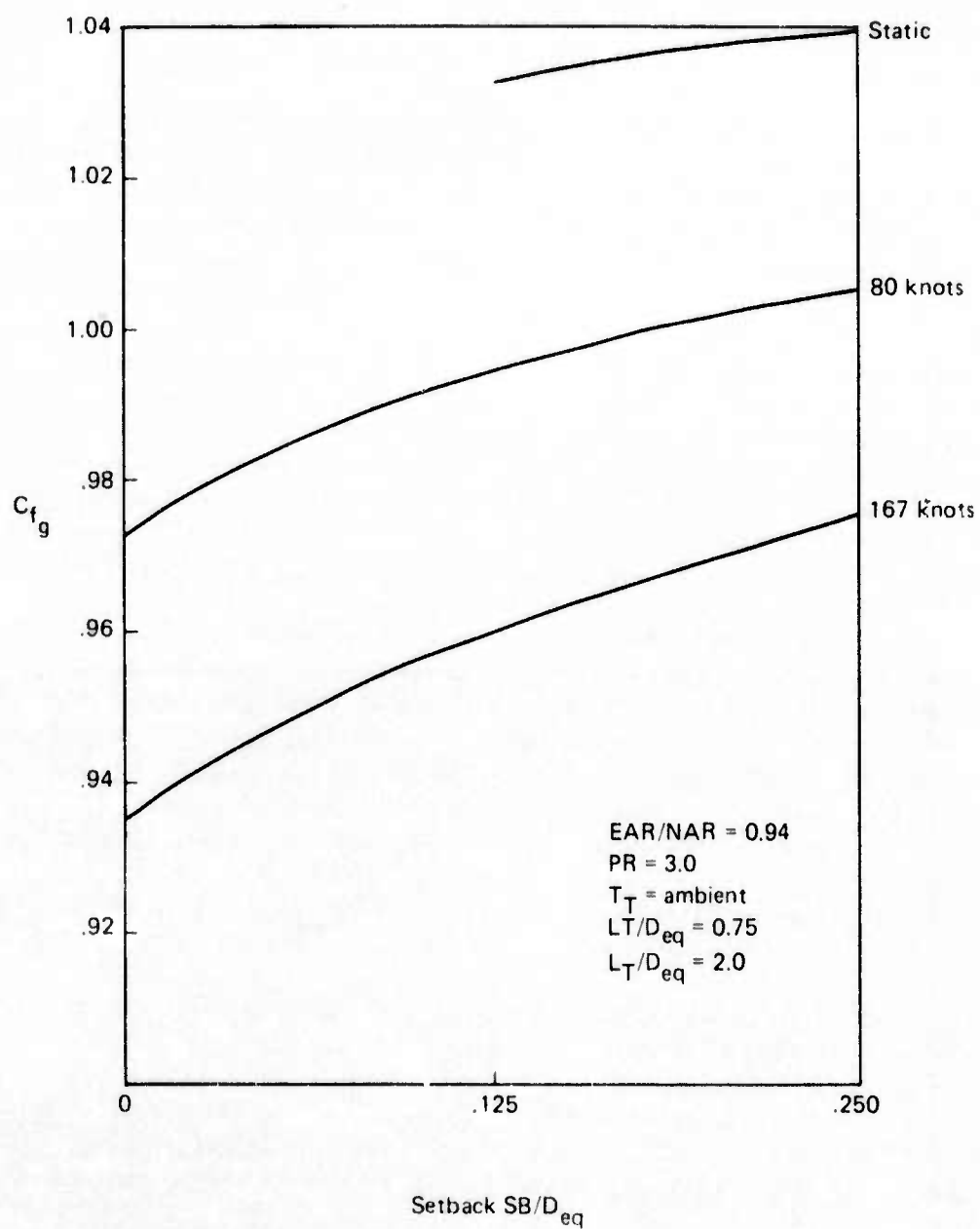


Figure 92.—Variation of Performance as a Function of Setback and Velocity for the
 37-Tube, NAR-3.3 Close-Packed Array With EAR = 3.1 (EAR/NAR = 0.94)

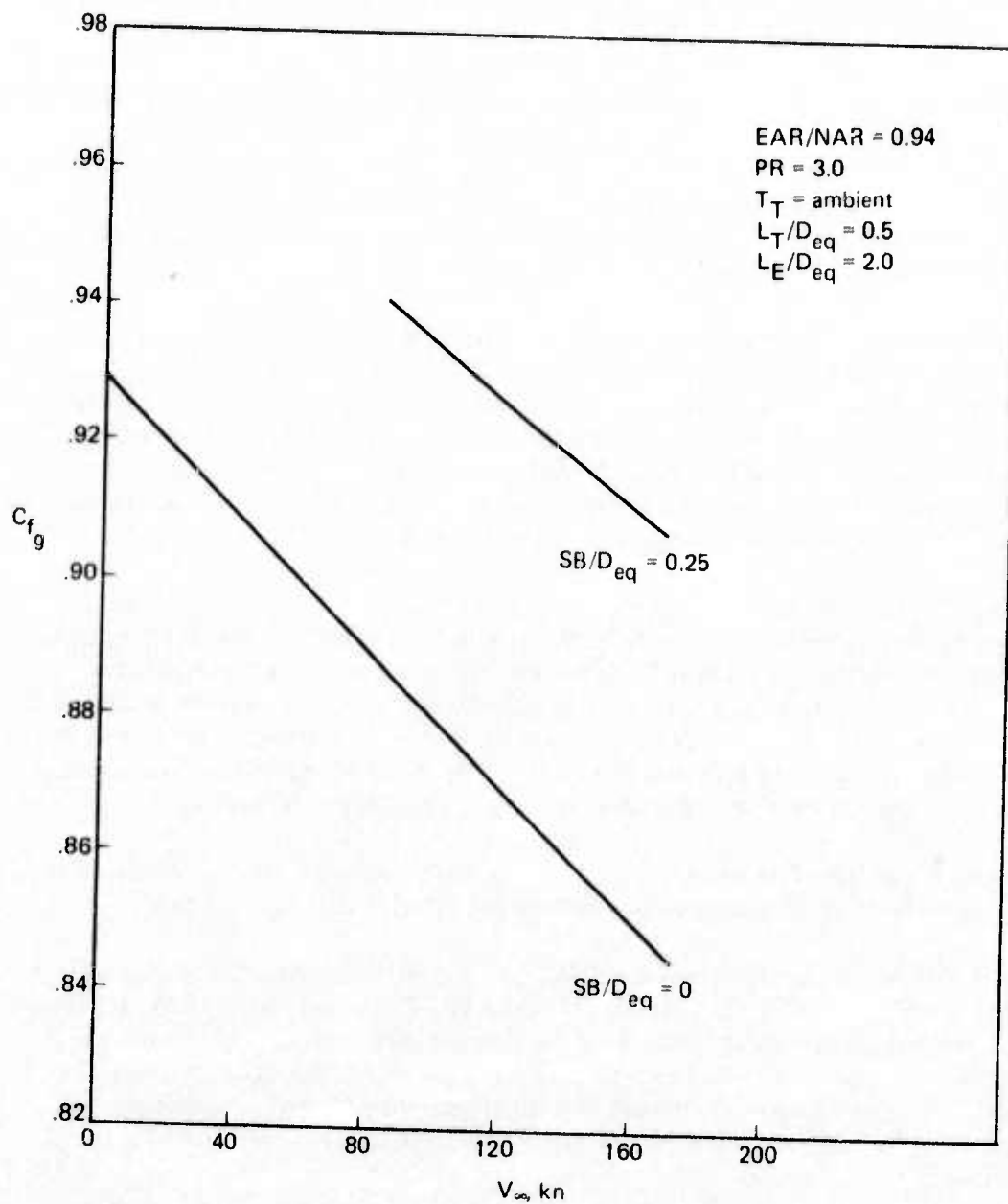


Figure 93.—Performance as a Function of Setback and Velocity for a 61-Tube, NAR-3.3 Suppressor With EAR = 3.1 Ejector (EAR/NAR = 0.94)

with $\text{EAR}/\text{NAR} = 0.94$. * The performance gain due to setback becomes increasingly favorable as velocity increases. At all velocities the tight ejectors require a setback greater than 0.25 (SB/D_{eq}) to produce optimum performance.

Figure 94 shows the effect of using setback to increase the inlet area on a $\text{EAR}/\text{NAR} = 1.12$ configuration. The annulus A_A is inherently larger than on the tight ejectors. Therefore, the improvement in performance with setback is less. The performance level improves and the lapse rate is less for the setback configuration. Figure 95 shows another $\text{EAR}/\text{NAR} = 1.12$ ejector. Though the ejector length was too short (sec. 6.3.7.5) to provide enough mixing, the lapse rate was still less for the setback case.

When EAR/NAR is large, the peak static performance is obtained with zero setback because the annular inlet area, A_A , is sufficiently large to provide the amount of secondary air necessary to mix with the primary jets. Increasing setback statically reduces the inlet velocity, and hence the lip suction, while the base drag remains nearly constant. Figure 96 demonstrates the effect of setback on an $\text{EAR}/\text{NAR} = 1.34$ configuration. Again, the lapse rate is less for the setback case, resulting in a performance crossover where the setback case outperforms the no-setback at velocities above 120 kn.

In all cases investigated, the lapse rate was less than the lapse rate at smaller setbacks. Therefore, setback, unlike ejector area ratio and length, provides a mechanism for optimizing performance without increasing the lapse rate. The effect of setback on lapse rate should be viewed as "fine tuning" because the changes in lapse rate with setback are second order compared to the changes in performance level. These characteristics are consistent with the flow model that suggests that geometry changes produce much larger changes in the surface pressure forces than in the lapse rate due to secondary air handling.

Though changes in lapse rate due to setback are relatively small, the experimental results suggest a behavior of performance versus setback and velocity as shown in figure 97.

Notice that the percentage of performance decrease due to increasing velocity (lapse rate) is less as setback increases. From the above behavior and that shown in figure 91 an important performance consideration is evident. The optimum ejector setback allows both high static performance and minimum ram drag penalty. The setback should be optimized at the takeoff condition. This will automatically minimize lapse rate and still produce nearly optimum static performance. (The setback will be slightly larger than optimum for static performance.)

*Note that $\text{EAR}/\text{NAR} < 1$ does not imply jet scrubbing. (See sec. 3.3.3.)

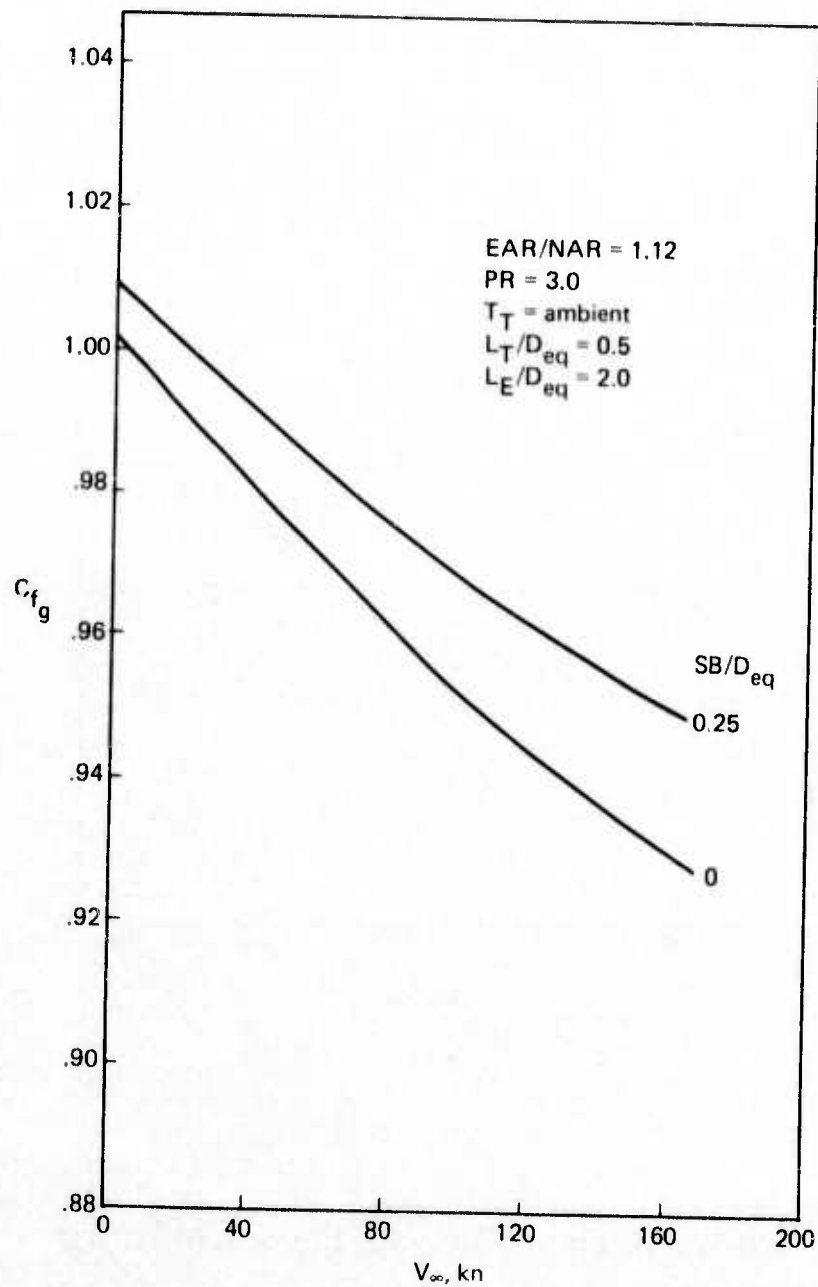


Figure 94.—Performance as a Function of Setback and Velocity for the 37-Tube, NAR 2.75 Suppressor With EAR 3.1 Ejector ($E_{AR}/N_{AR} = 1.12$)

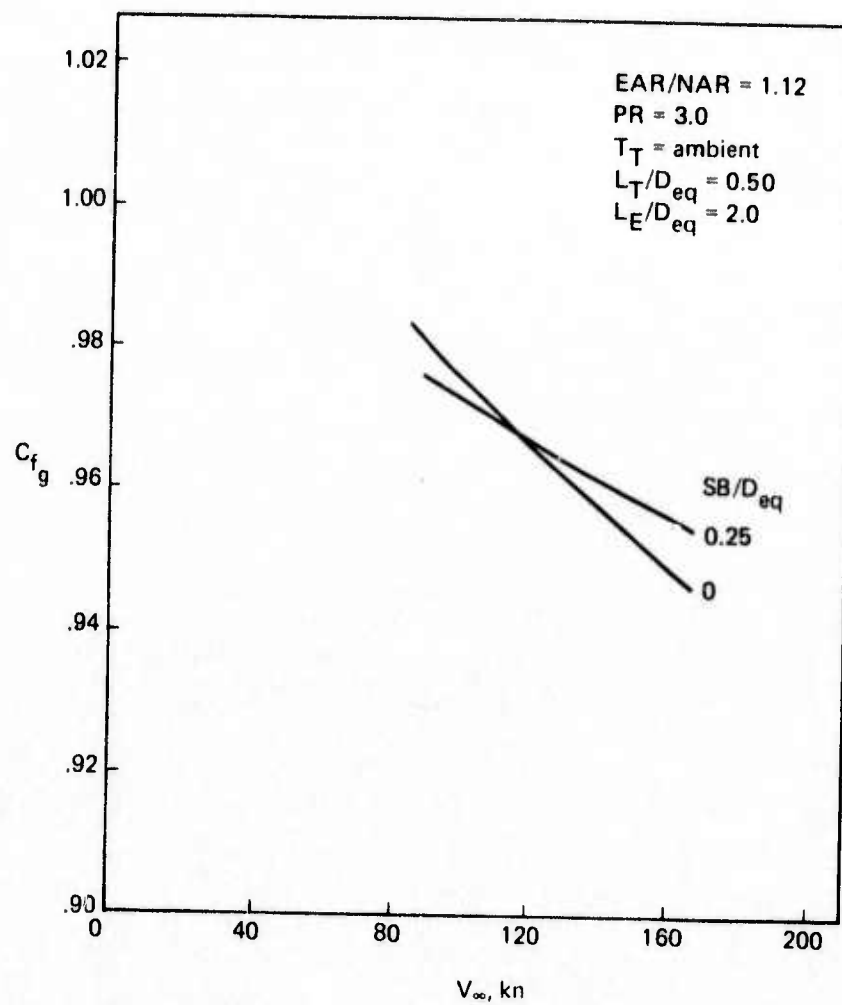


Figure 95.—Performance as a Function of Setback and Velocity for the 19-Tube, NAR-3.3 Suppressor With $EAR = 3.7$ Ejector ($EAR/NAR = 1.12$)

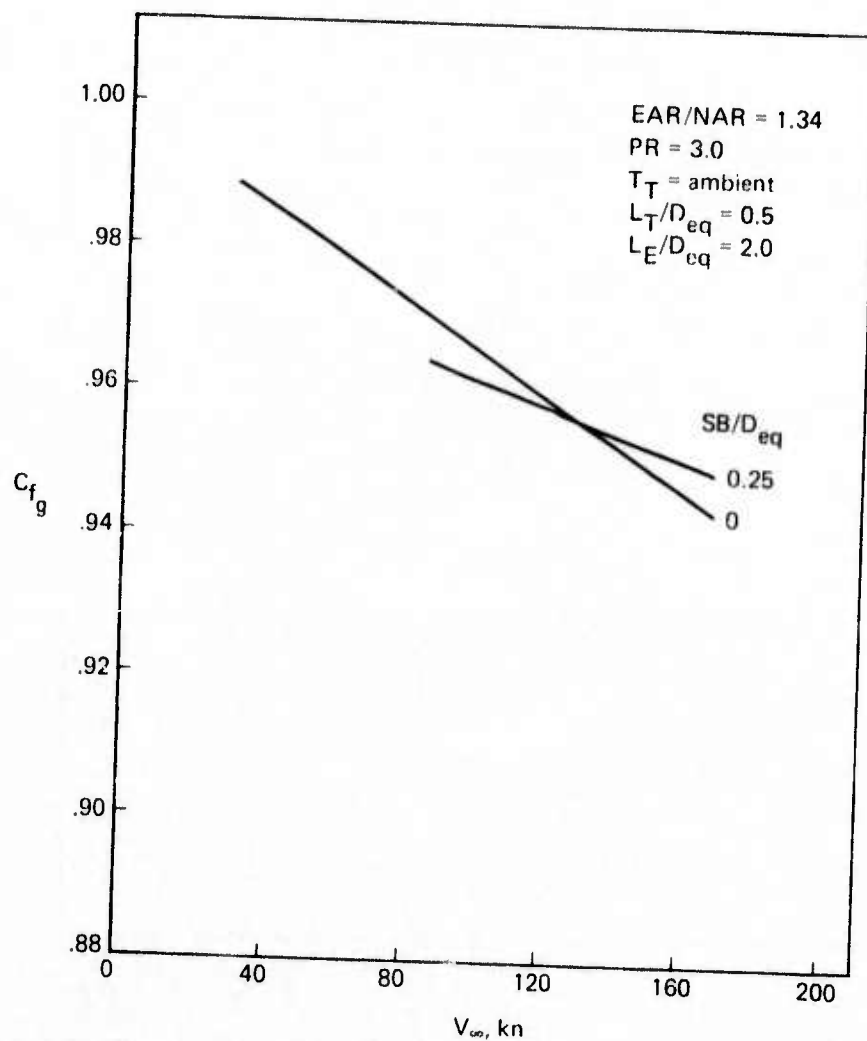


Figure 96.—Performance as a Function of Sethback and Velocity for the 37-Tube, NAR-2.75 Suppressor With EAR-3.7 Ejector ($EAR/NAR = 1.34$)

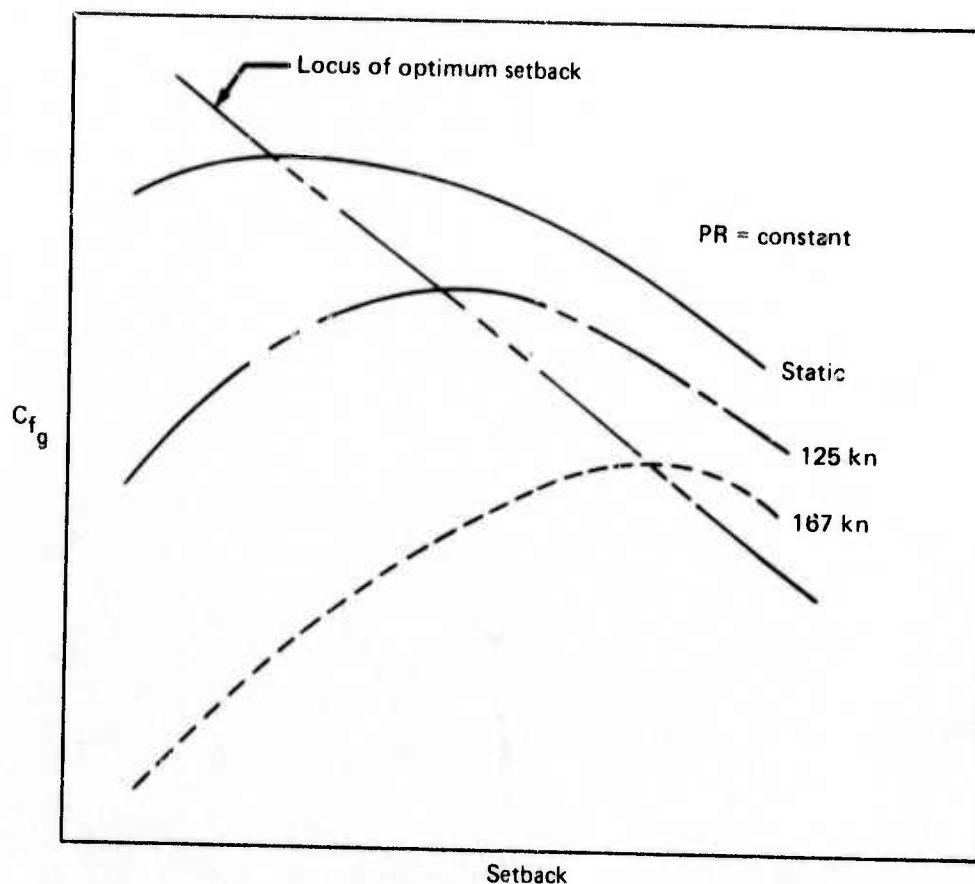


Figure 97.— C_{fg} Versus Setback Showing Optimum Setback as a Function of Velocity

6.3.7.5 Ejector Length and Area Ratio

The ejector length required to produce peak static thrust is a function of suppressor element size and the ratio of the ejector to suppressor area ratios (EAR/NAR). One-dimensional ejector flow analysis (ref. 6) demonstrates that, for constant primary gas conditions, the secondary mass flow rate increases as ejector area ratio increases. (The analysis assumes sufficient ejector length is available for mixing and does not treat the effect of length.)

The peak performance of any suppressor/ejector system occurs when the ejector length is sufficient to provide optimal mixing of the primary jets with the secondary flow. Large local peaks in the velocity profile can still be present, but their value must be slightly less than the primary core velocity. If the length increases substantially beyond this, the reduction in effective area due to boundary layer growth and drag due to increased wetted area reduces the system performance. The individual element size affects the length required to mix out the primary core. As the number of primary nozzle tubes is increased, the amount of primary jet perimeter available to induce mixing increases and the ejector length required for maximum secondary air handling decreases. For the multitube suppressor the required length is conveniently nondimensionalized by the individual tube diameter. The jet core mixes out in nominally twelve length-to-individual-jet diameters (ref. 5). Aircraft constraints required an ejector of $L_E/D_{eq} = 2.0$. This ejector length requires 37 equal-area tubes to provide 12 individual jet diameters within the $L_E/D_{eq} = 2$ ejector. As the distance between the outer jets and the ejector wall becomes greater (i.e., as EAR/NAR increases) the required ejector length increases to provide enough distance for the mixing to extend across the ejector. When the ejector length is less than required for optimum entrainment, the secondary air decreases, resulting in lower lip suction and, hence, lower static performance.

For short ejectors, which entrain less than the maximum amount of secondary air, the decrease in secondary mass flow results in less ram drag penalty. Thus, the shorter the ejector (< 12 individual jet diameters), the lower the static performance and the smaller the lapse rate with velocity. This results in a crossover velocity for performance of any suppressor/ejector with ejector length as the only variable. A performance envelope can be established where the highest static performance and maximum lapse rate are provided by the ejector of sufficient length to establish mixing across the ejector. The lowest lapse rate will be established by the no-ejector case. The static performance and ram drag penalties due to too short an ejector are much more severe than those for too long an ejector. Figure 98 dramatically illustrates these effects. The $L_E/D_{eq} = 2$ ejector is 12 individual jet diameters long for the 37-tube suppressor. The ejector area ratio is held constant at 3.7. The figure shows that the NAR-2.75 suppressor with the short $L_E/D_{eq} = 2.0$ ejector does not provide sufficient mixing length. The larger area ratio suppressor, NAR-3.3, mixes out sooner and the decreased distance to the ejector wall decreases the length required for the primary flow to spread to fill the ejector. This results in greater secondary air handling and, in turn, a steeper lapse rate. The air handling of the EAR-3.7 ejector can be substantially increased by using a long ejector. The figure shows a 4% increase in static thrust due to the larger ejector on the NAR-2.75 suppressor.

However, the increased air handling also increases the ram drag penalty and skin friction drag to the point where, above 120 kn, the shorter ejector performs better. This crossover velocity and the trade between static performance and lapse rate must be kept in mind when designing a suppressor/ejector for takeoff.

6.3.8 TEMPERATURE EFFECTS ON PERFORMANCE

- Base drag and lip suction both decrease with increasing jet temperature.
- The temperature effect is more pronounced on lip suction than it is on base drag.

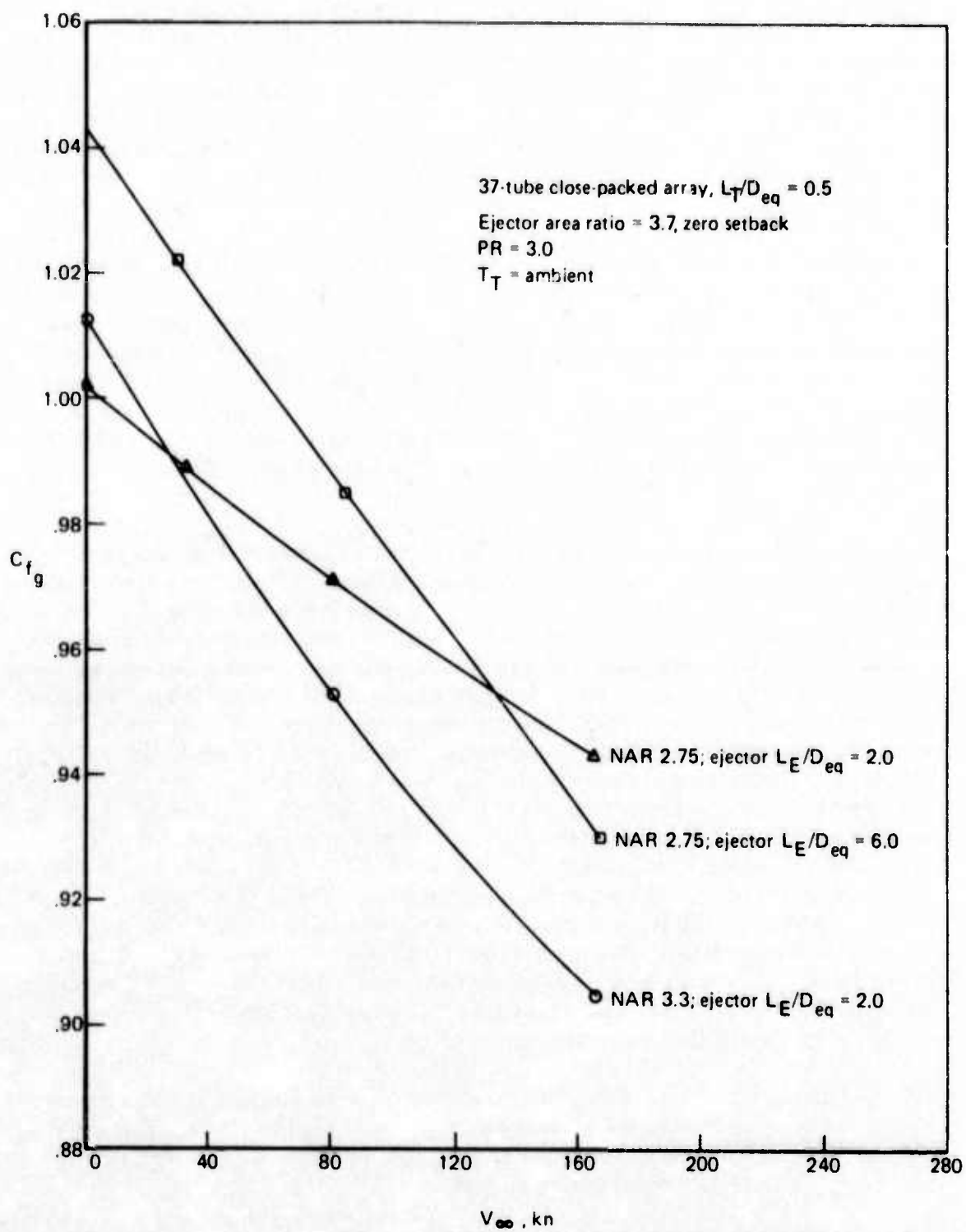


Figure 98.—Effect of NAR and Ejector Length on Performance With Forward Velocity

The observed decrease in lip suction implies a decrease in secondary air handling; thus, the ram drag penalty (i.e., decrease in lip suction with increasing velocity) decreases as jet temperature increases. Figure 99 shows this to be the case. Statically, the lip suction at 1150°F is 3.39% less than the ambient value for the configuration shown. Increasing velocity produces a decrease in lip suction for both cases. Since the ram drag is less for the hot flow, its rate of decrease is less. The difference in rate is small compared to the static difference in level; hence, the velocity required to get the same lip suction from the hot and cold cases would be nearly 300 kn for this configuration. Temperature effects on internal performance are covered by reference 1.

References 1 and 2 detail the decrease in base drag due to elevated temperature for static performance. The configurations tested at 1150°F to establish the effects of forward velocity on base drag showed that the base drag is slightly less at 1150°F jet temperature than ambient at all velocities. Insufficient data were taken to quantify the amount except to notice that the ratio of change of drag with velocity was approximately the same for hot and cold configurations. Thus, a first order approximation would suggest that the static reduction in base drag due to hot primary flow be used as the quantity of reduction at all velocities. In this manner an approximate value can be obtained by using the hot to cold changes statically from reference 2 and the rate of change of drag with velocity from the appendix of reference 10.

Unfortunately, lip suction is not as well understood as base drag. Except for the general statements about lip suction made in this section, the present investigation can only conclude that future testing must be done at the desired temperature. Performance data acquired at elevated temperatures have traditionally been much less accurate than ambient temperature data. The present program was successful in obtaining 1150°F primary flow data statically. The limited wind-on data suggests a need for substantial development prior to future wind tunnel performance tests to insure the correct temperature profiles and data levels and repeatability.

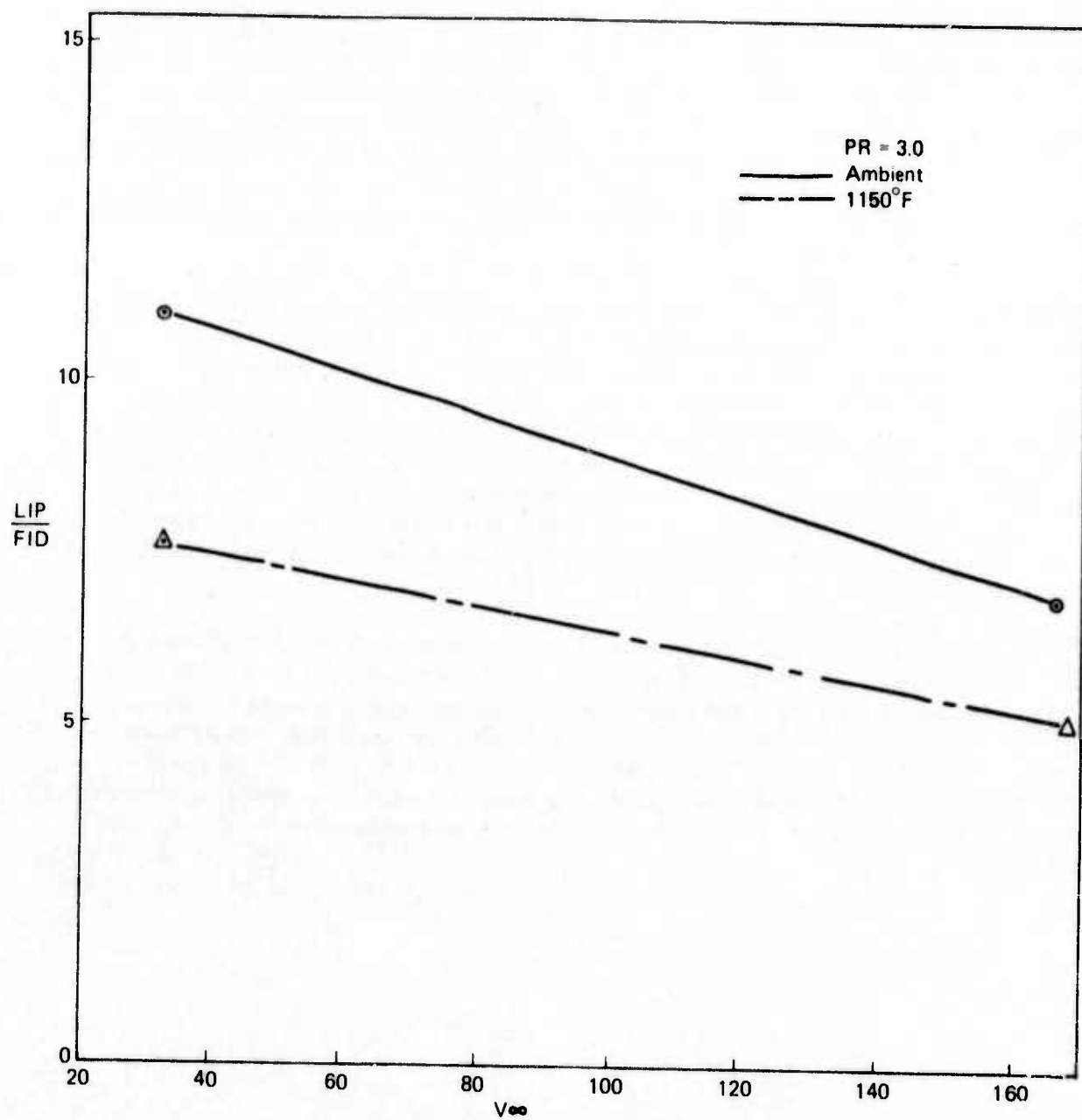


Figure 99.—Lip Suction as a Function of Forward Velocity for Ambient and 1150° F Jet Temperatures

7.0 CONCLUSIONS AND RECOMMENDATIONS

It has been demonstrated that high static performance and low lapse rates are compatible with the appropriate choices of geometry. Due to the ram drag penalty and ejector drag, the lapse rate of suppressor/ejector configurations is inherently larger (steeper) than that of the bare suppressor configuration. Though the ejectors can produce large static augmentations to offset the thrust loss of the suppressor hardware, there is always some velocity beyond which the ejector becomes a performance handicap. When considering the exhaust system of a supersonic commercial aircraft, the task is not to decide if suppressors and ejectors should be used but rather to define the geometry necessary to make the best use of them within specified constraints.

Geometry changes were shown to have a large effect on the level of performance while producing relatively small changes in the lapse rate. The maximum performance over a range of velocities is provided by the configurations which minimize the afterbody drag through the appropriate selection of suppressor variables and effective ejector inlet area rather than those which obtain high static augmentation through the use of large ejector area ratios. To minimize suppressor drag, the use of a radial tube placement and elliptical convergent tubes is recommended. The number of tubes should be held at the minimum consistent with suppression requirements and installation and weight constraints. Twelve individual jet diameters provide sufficient ejector length for optimum mixing for ejector area ratios < 3.7 and $EAR/NAR < 1.3$. The ejector length must be increased if either the ejector area ratio or the EAR/NAR ratio increases beyond these values.

The majority of the secondary air entering the ejector appears to pass through the annular area between the ejector lip and the outer row tubes. Only a small percentage of the flow passes between the tubes into the recirculation region. The annular area and hence the majority of the effective inlet area is established by the EAR/NAR ratio and the ejector setback. The effective ejector inlet area plays a major role in determining the tradeoff between lip suction and basedrag. If the inlet area is too small, the secondary air becomes supersonic at the ejector throat, producing shock-induced flow instabilities, ejector vibration, and disproportionate performance losses. This situation arises for pressure ratios above 3.0 when $EAR/NAR \approx 1$ and setback equals zero. For small increases in the inlet area the performance level increases greatly due to the strong decrease in afterbody drag. If the inlet area continues to increase, the base drag asymptotes and the lip suction dominates the performance. If the ejector inlet area increases much beyond this, the decrease in inlet velocity results in a decrease in lip suction with no further gain in base drag reduction. Thus, for each pressure ratio, ejector area, ejector length, and suppressor geometry, there exists an optimum inlet area. When $EAR/NAR \approx 1$, the setback must be greater than $0.25 D_{eq}$ to produce the peak performance. For all configurations investigated, the peak performance required that setback increase slightly with forward velocity. $EAR/NAR > 1.3$ (and $EAR < 3.7$) produces a situation where the inlet area is larger than necessary even with zero setback, and considerable forward velocity is required before any setback is advantageous. Thus, setback is an important mechanism to allow an appropriate amount of ejector inlet area. Setback, unlike ejector area ratio and length, provides a method of optimizing the performance and minimizing the lapse rate. For the type of suppressor/ejector system investigated, $EAR/NAR \approx 1.2$ and $EAR \approx 3.1$ are recommended as providing the best tradeoffs. Very little setback would

be needed for such a configuration, and the setback could be used to "fine tune" the system over the velocity range.

The use of a ramp to avoid a separation region between the baseplate and the nacelle outer diameter is recommended but the shape of ramp is unimportant.

During climbout the suppressor may still be required for noise suppression while the velocity is high enough that the ejector is producing a performance decrement due to secondary air ram drag. Closing the inlet to reduce the ram drag is not recommended because of the high suppressor afterbody drag that will occur. Instead, a series of axial slots (or the aerodynamic equipment) should be opened along the ejector to effectively reduce the length of the ejector cutting down the mixing, and hence reducing the amount of secondary air handled.

The majority of this investigation was conducted with ambient jet temperatures. The effects of elevated jet temperatures on the rate of change of afterbody drag with velocity appears minimal. Lip suction and secondary air handling appear to decrease significantly with velocity as the jet temperature increases (for a fixed geometry and pressure ratio). The amount of decrease is not well understood except to affirm that lapse rate becomes less as primary temperature increases. Future testing must be done at the desired temperature. Performance data acquired at elevated temperatures have traditionally been much less accurate than ambient temperature data. The present program was successful in obtaining 1150°F primary flow data statically. The limited wind-on data suggests a need for substantial development prior to future wind tunnel performance tests to insure the correct temperature profiles and data levels and repeatability.

More effort is also needed to quantify the effective inlet area. Enough data is provided to allow a reasonably accurate assessment of the amount of inlet area needed for nozzles similar to those tested. Though the principal flow area appears to be the outer annulus, it is not possible to nondimensionalize or generalize the required size.

REFERENCES

1. D.B. Morden and R.S. Armstrong, *SST Technology Follow-On Program—Phase II—Noise Suppressor/Nozzle Development—Volume VII—Performance Technology—Static Performance: Trends and Trades*, FAA-SS-73-11-7, March 1975.
2. D.B. Morden and R.S. Armstrong, *SST Technology Follow-On Program—Phase II—Noise Suppressor/Nozzle Development—Volume VIII—Multitube Suppressor Ejector Interaction Effects on Static Performance (Ambient and 1150°F Jet Temperatures)*, FAA-SS-73-11-8, March 1975.
3. J. Atvars, et. al, *SST Technology Follow-On Programs—Phase II—Noise Suppressor Nozzle Development—Volume II—Noise Technology*, FAA-SS-73-11-2.
4. H. Lu, D. Morden, R. Benefiel and C. Simcox, *SST Technology Follow-On Program—Phase I, Performance Evaluation of the NSC-119B Nozzle System; Volume I: Suppressed Mode*, AD-900-399L, February 1972.
5. J. Reid, *The Effects of Cylindrical Shroud on the Performance of a Stationary Convergent Nozzle*, Aeronautical Research Council Report and Memorandum No. 3320, Ministry of Aviation, London 1963.
6. P. Scoffield, *One-Dimensional Ejector Analysis*, Unpublished Boeing Document.
7. F. Pearlman and R.S. Armstrong, *SST Technology Follow-On Program—Phase II—Noise Suppressor/Nozzle Development—Volume VI—Thrust and Flow Characteristics of a Reference Multitube Nozzle With Ejector*, FAA-SS-73-11-6.